SYNTHESIS AND REACTIVITY STUDIES OF CHROMIUM

COMPLEXES SUPPORTED BY β–DIKETIMINATE LIGANDS

by

Yu-Ting Hung

A dissertation submitted to the Faculty of the University of Delaware in partial fulfillment of the requirements for the degree of Doctor of Philosophy in Chemistry and Biochemistry

Fall 2017

SYNTHESIS AND REACTIVITY STUDIES OF CHROMIUM

COMPLEXES SUPPORTED BY β–DIKETIMINATE LIGANDS

by

Yu-Ting Hung

Approved: _____
Brian J. Bahnson, Ph.D.
Chair of the Department of Chemistry and Biochemistry

Approved: _____
George H. Watson, Ph.D.
Dean of the College of Arts and Sciences

Approved: _____
Ann L. Ardis, Ph.D.
Senior Vice Provost for Graduate and Professional Education

I certify that I have read this dissertation and that in my opinion it meets the academic and professional standard required by the University as a dissertation for the degree of Doctor of Philosophy.

Signed: _____

Klaus H. Theopold, Ph.D.
Professor in charge of dissertation

I certify that I have read this dissertation and that in my opinion it meets the academic and professional standard required by the University as a dissertation for the degree of Doctor of Philosophy.

Signed: _____

Svilen Bobev, Ph.D.
Member of dissertation committee

I certify that I have read this dissertation and that in my opinion it meets the academic and professional standard required by the University as a dissertation for the degree of Doctor of Philosophy.

Signed: _____

Andrew V. Teplyakov, Ph.D.
Member of dissertation committee

I certify that I have read this dissertation and that in my opinion it meets the academic and professional standard required by the University as a dissertation for the degree of Doctor of Philosophy.

Signed: _____

Lawrence R. Sita, Ph.D.
Member of dissertation committee

ACKNOWLEDGMENTS

The most important person that I would like to express my sincere gratitude to is my research advisor, Professor Klaus Theopold. It has been an extremely great honor to work with him for the duration of my Ph.D. studies. Not only does he have a vast knowledge of chemistry, but he is also an amazing educator, greater than I could have asked for. His never-ending patience, encouragement, and supportive guidance toward my research has allowed me to expand my knowledge in chemistry. Klaus has proven himself as a role model of a chemist through his encouraging attitude these past five years. This has made my entire learning experience very rewarding. Overall, during this journey Klaus has also shown the kindness, enthusiasm, and wide wisdom of life, which are, and will always be invaluable throughout my life.

In addition to my advisor, I would like to thank the members of my dissertation committee, Professor Svilen Bobev, Professor Andrew Teplyakov, and Professor Lawrence Sita, for their involvement and comments during my Ph.D. studies. My special thanks goes to Dr. Glenn Yap for his help in X-ray crystallography throughout my time conducting research. I am also very grateful for all the facilities and staff in this department. I'm especially thankful for Dr. Steve Bai for his help in NMR techniques. I would like to thank my lab mates, both past and present, for all of their help and support. I am also very appreciative for the friendships I have created here. They have made this journey more delightful. Lastly, I would like to thank my entire family back in Taiwan for all their spiritual support, especially my parents and brothers. The special bonding in this journey will never be forgotten.

TABLE OF CONTENTS

Chapter

viii

LIST OF TABLES

LIST OF FIGURES

xiii

xvi

LIST OF SCHEMES

LIST OF ABBREVIATIONS

Et_2O = Diethylether

LIFDI = Liquid injection field desorption ionization

L^{Me} = 2,4 Pentane-N,N'-bis(2,6-dimethylphenyl) ketiminato

L^{iPr} = 2,4 Pentane-N,N'-bis(2,6-diisopropylphenyl) ketiminato

L^{Et} = 2,4 Pentane-N,N'-bis(2,6-diethylphenyl) ketiminato

*L^{Me} = 2,2,6,6-Tetramethylheptane-3,5,N,N'-bis(2,6-dimethylphenyl) ketiminato

*L^{iPr} = 2,2,6,6-Tetramethylheptane-3,5,N,N'-bis(2,6-diisopropylphenyl) ketiminato

Nacnac = 2,4-Pentane-N,N'-bis(aryl or alkyl) ketiminato

NHC = N-heterocyclic carbene

Ph = Phenyl

THF = Tetrahydrofuran

Tol = Toluene

TECHNIQUES USED IN THE DISSERTATION

Liquid injection field desorption ionization (LIFDI) is a mass spectrometry that is used in this dissertation. Field desorption is considered a soft ionization process, and this method usually causes little or no fragmentation of molecular ions.

X-ray diffraction is a crystal structure determination technique. This technique provides electron density in molecules by recording the differences between electrons of molecule and X-ray beam. The three-dimensional structures of molecules are detailed.

Nuclear magnetic resonance (NMR) is a technique that provides chemical and physical information of atomic nuclei. This dissertation is dedicated to describing paramagnetic compounds, and the paramagnetic ^{1}H NMR spectra taken were useful for characterization of complexes.

Transmission infrared spectroscopy is a technique that reveals the vibrational modes of molecule by the interaction between infrared radiation with compounds. It is particularly useful for identifying certain functional groups.

The solid-state magnetic susceptibilities were measured with Gouy balance. This technique measures the change in mass of sample when applied with external magnetic field. The solution-state magnetic moments were determined by using Evans method. This method measures the change in NMR chemical shift of the solvent caused by the presence of paramagnetic materials.

ABSTRACT

This dissertation describes research on paramagnetic chromium complexes coordinated by β-diketiminato ligands (this ligand is often referred to as *nacnac*). The motivation of this research is to explain and understand the thermally stable alkyl hydride complex, $(L^{Me}Cr)_2(\mu\text{-}CH_2SiMe_3)(\mu\text{-}H)$ (**1**), that the Theopold research group reported earlier. The thesis also presents the synthesis of a nitride complex that is an isomer of previously reported chromium dinitrogen complex, $(L^{iPr}Cr)_2(\mu_2\text{-}\eta^2\text{:}\eta^2\text{-}N_2)$ (**23**).

Chapter 1 describes the reaction of $(L^{Me}Cr)_2(\mu\text{-}H)_2$ (**2**) with 1.0 equiv. of trimethylsilyl-diazomethane, which resulted in a set of unexpected molecules. The structures of dinitrogen complexes $[L^{Me}Cr(THF)]_3(\mu\text{-}N_2)_3$ (**3**), $(L^{Me}Cr)_4(\mu\text{-}N_2)_4$ (**4**), and $(L^{Me}Cr)_3(\mu\text{-}N_2)_3(\mu\text{-}N)CrL^{Me}$ (**6**) were determined and these complexes were discussed. Complexes $(L^{Me}Cr)_2(\mu\text{-}NSiMe_3)(\mu\text{-}H)$ (**7**) and $(L^{Me}Cr)_2(\mu\text{-}NCH_2)(\mu\text{-}NH)$ (**8**) were also found in the reaction. These complexes were separated by fractional crystallization. A proposed mechanism for the formation of this variety of products is shown in **Appendix A**.

Chapter 2 starts with the synthesis of chromium(II) alkyls; an investigation of their thermal stability was conducted. Hydrogenolysis of chromium(II) alkyls led to the formation of alkyl hydride derivatives, specifically $(L^{Me}Cr)_2(\mu\text{-}CH_2SiMe_3)(\mu\text{-}H)$ (**1**), $(L^{Me}Cr)_2(\mu\text{-}CH_2CMe_3)(\mu\text{-}H)$ (**16**), and $(L^{Me}Cr)_2(\mu\text{-}CH_2C_6H_5)(\mu\text{-}H)$ (**17**). Their structures as well as the characterizations are described. Their reactivities were evaluated and $(L^{Me}Cr)_2(\mu\text{-}CH_2CMe_3)(\mu\text{-}H)$ (**16**) was found to undergo C-H bond

activation in the presence of a number of organic substrates, such as benzene, toluene and tetramethylsilane. These activations led to the transformation into $(L^{Me}Cr)_2(\mu$-$C_6H_5)(\mu$-H) (**18**), $(L^{Me}Cr)_2(\mu$-m-$CH_3C_6H_4)(\mu$-H) (**19**), and $(L^{Me}Cr)_2(\mu$-$CH_2SiMe_3)(\mu$-H) (**1**), respectively. Labeling experiments of **16** with labeled benzene (C_6D_6) and **16-d_1** with benzene (C_6H_6), were carried out and the outcomes were examined by mass spectrometry. The results suggested that the bridging hydride or deuteride of the reactants were preserved in the products. Finally, a mechanism for the transformation of alkyl hydrides was proposed based on all the experimental observations.

Chapter 3 reports on the studies of isomeric chromium complexes coordinated only by nitrogen atoms. Side-on bridged dinitrogen complex $(L^{iPr}Cr)_2(\mu_2$-η^2:η^2-$N_2)$ (**23**) was previously reported. This chapter describes the discovery of an isomer of **23**, namely $(L^{iPr}Cr)_2(\mu$-$N)_2$ (**25**). **25** was originally found in the irradiation reaction of a chromium azido complex. The isolation of **25** was difficult due to its subsequent transformation into the final product, **23**. In this vein, chromium azido complexes supported by variously substituted nacnac ligands were prepared and the irradiation reactions were studied. The bis(μ-nitrido) complexes $(L^{Me}Cr)_2(\mu$-$N)_2$ (**30**), $(L^{Et}Cr)_2(\mu$-$N)_2$ (**32**), and $(*L^{iPr}Cr)_2(\mu$-$N)_2$ (**34**) were structurally characterized. Another side-on bridged dinitrogen complex, $(L^{Et}Cr)_2(\mu_2$-η^2:η^2-$N_2)$ (**33**), was found along the way. A number of attempts at clean formation of **25** were carried out, but failed to produce **25**. Finally, a successful synthesis for **25** was developed, which involved the irradiation of $(L^{iPr}CrCl)_2(THF)(\mu$-$N_3)_2$ (**37**), followed by reductive dehalogenation of $(L^{iPr}CrN)_2(\mu$-$Cl)_2$ (**38**). The conversion of bis(μ-nitrido) **25** into its isomeric dinitrogen complex **23** was successfully achieved by photolysis.

Chapter 1

USE OF DIAZOALKANES IN CHROMIUM ORGANOMETALLIC CHEMISTRY

1.1   Introduction

Inorganic and organometallic compounds supported by β-diketiminato ligands (the ligand is usually referred to as *nacnac*) have been widely studied. Nacnac ligands have been shown to support a large number of main group elements, transition metals and even lanthanide and actinide metals.[1, 2] As shown in Scheme 1.1, nacnac ligands are useful due to their tunable steric and electronic demands, through the variation of R_1, R_2 and R_3.
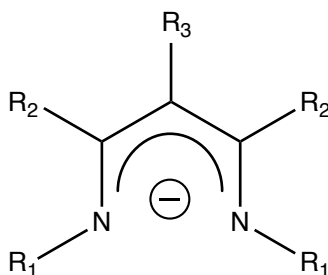
Scheme 1.1 β-diketiminato ligand

Among the various nacnac complexes reported by the Theopold research group, a thermally stable binuclear chromium bridging alkyl and hydride complex has caught attention, which is $(L^{Me}Cr)_2(\mu\text{-}CH_2SiMe_3)(\mu\text{-}H)$ (**1**) (L^{Me} = 2,4 Pentane-N,N'-bis(2,6-dimethylphenyl) ketiminato).[3] **1** is composed of two nacnac chromium fragments

bridged by a hydride and a trimethylsilylmethyl ligand. Scheme 1.2 shows the synthesis of the complex. Structure determination revealed a butterfly configuration of **1**. **1** was found to be stable at 100°C over several days in toluene-d^8. In general, organometallic complexes containing both an alkyl and a hydride in adjacent positions are unstable. Especially those of the first row of the transition metals, which decompose by facile reductive elimination of alkane.[4]

Ar = 2,6-dimethylphenyl
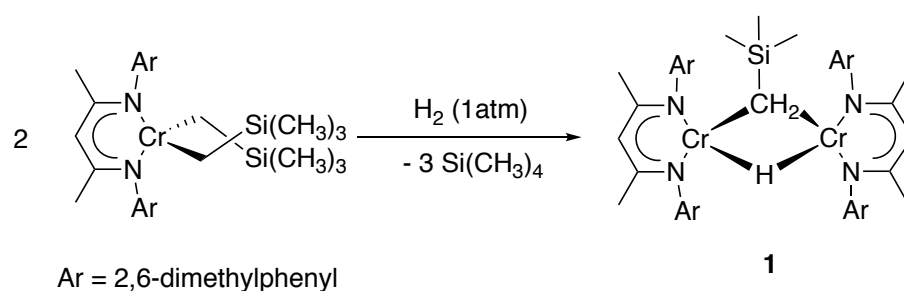
Scheme 1.2 Synthesis of nacnac chromium alkyl hydride

To explore the nature of this unusual molecule **1**, it may be helpful to synthesize analogs with different alkyl ligands. These types of molecules may share some common general properties, which may help in understanding the thermal stability of **1**. Conventional synthetic strategies were considered, including hydrogenolysis of alkyl complexes (this will be discussed in **Chapter 2**); C-H bond activation of alkane substrates;[5, 6] and alkylidene insertion into metal hydrides. This chapter will focus on the last reaction type. Alkylidene insertion has been proved to be a successful way to prepare metal alkyl complexes. Herrmann et. al. have demonstrated the carbene insertion into metal hydride bonds, with the liberation of N$_2$ and the formation of corresponding alkyl derivatives (Scheme 1.3).[7-9]
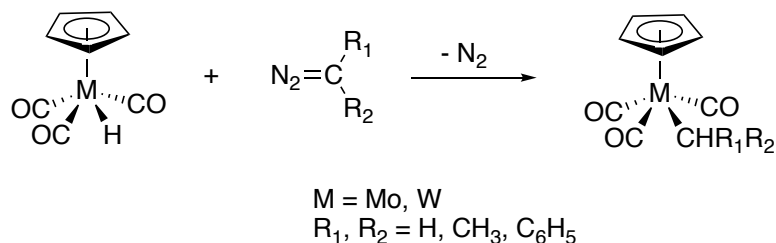
Scheme 1.3   Alkylidene insertion into a metal hydride

Carlucci et. al. observed the unsaturated hydrido-carbonyl rhenium compound reacted with diphenyldiazomethane.[10] This reaction is shown in Scheme 1.4. The authors suggested that in this reaction, the generated bridging hydrazonato ligand was by 1,1-insertion of the diazo group into Re-H-Re bond.
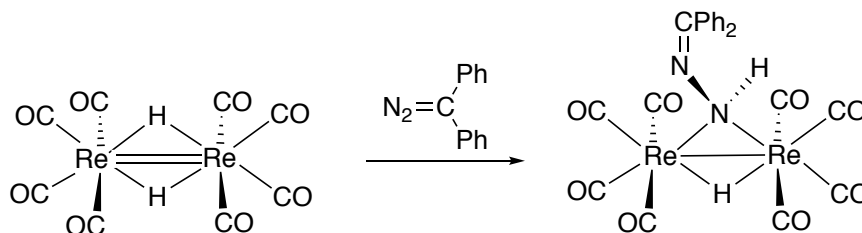
Scheme 1.4   Results of rhenium hydrido carbonyl complex with
             diphenyldiazomethane

Hillhouse et. al. showed a carbene group-transfer reaction from a diazoalkane.[11] (dtbpe)Ni(cod) (dtbpe = 1,2-bis(di-*tert*-butylphosphino)-ethane; cod = 1,5-cyclooctadiene) was treated with 1 equiv. of diphenyldiazomethane to result in the formation of diphenyldiazomethane complex. They found out when this complex was heated in the presence of catalytic amount of anhydrous Sm(OTf)$_3$ (OTf =

trifluoromethanesulfonate), a nickel diphenylcarbene complex was formed by the extrusion of N_2. This reaction is illustrated in Scheme 1.5.
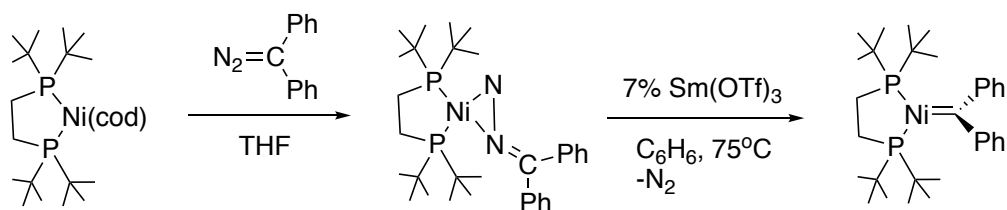
Scheme 1.5   The synthesis of nickel diphenylcarbene complex

Applying this strategy, by treating the dinuclear chromium hydride $(L^{Me}Cr)_2(\mu-H)_2$ (**2**) [12] with 1.0 equiv. of diazoalkane reagent would ideally result in a chromium bridging alkyl hydride complex. In a proof of principle, we first tried the reaction with trimethylsilyl-diazomethane. The known alkyl hydride **1** was expected to be formed with the liberation of N_2 (Scheme 1.6). However, instead of forming **1**, this reaction yielded a set of unexpected products, including novel dinitrogen complexes. This chapter is dedicated to the description of these unexpected reaction products.

2, Ar = 2,6-dimethylphenyl   **1**
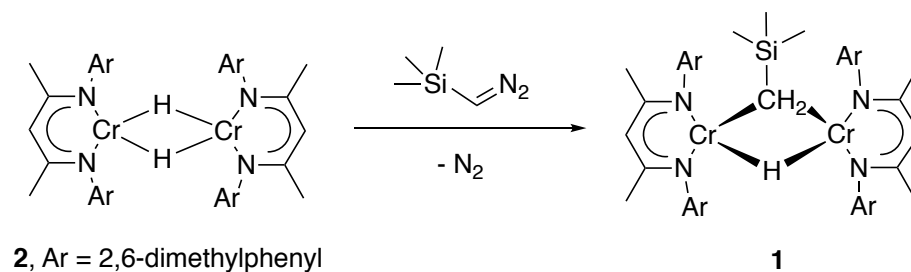
Scheme 1.6   Prediction of the formation of alkyl hydride complex by alkylidene insertion reaction

1.2 Results and Discussion

Reaction of $(L^{Me}Cr)_2(\mu-H)_2$ (**2**) with 1.0 equiv. of trimethylsilyl-diazomethane in THF, while stirring for 12 hours at room temperature under nitrogen atmosphere, resulted in a color change from orange-red to emerald-green. The THF was then removed in vacuo and the residue was extracted with Et_2O. An Et_2O insoluble orange powder was filtered off and collected. After redissolving the orange powder in THF, this solution was cooled to low temperature (-30°C) overnight to yield dark red crystals. Determination of the structure by X-ray crystallography revealed it to be a trinuclear end-on bridged dinitrogen complex, i.e. $\mu\text{-}\kappa^1$, $\kappa^1\text{-}N_2$., or $[L^{Me}Cr(THF)]_3(\mu\text{-}N_2)_3$ (**3**). The molecular structure of **3** is depicted in Figure 1.1, while the corresponding interatomic distances and angles are listed in Table 1.1.
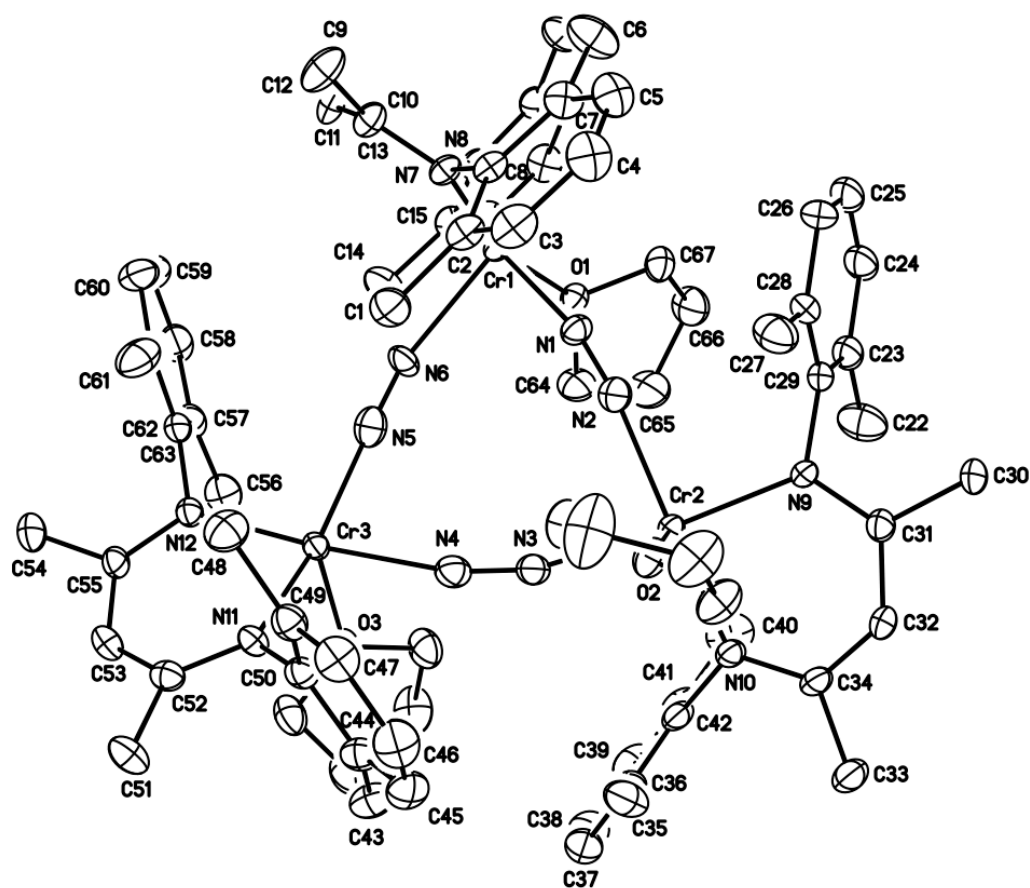
Figure 1.1   Molecular structure of [L^{Me}Cr(THF)]$_3$(μ-N$_2$)$_3$ (**3**). Ellipsoids are drawn at the 30% probability level. Hydrogen atoms and two THF molecules that are not bonded to chromium have been omitted for clarity.

Table 1.1   Interatomic distances (Å) and angles (°) for [L^{Me}Cr(THF)]$_3$(μ-N$_2$)$_3$ (**3**)

Distances (Å)			
Cr(1)-N(7)	2.047(3)	C(24)-C(25)	1.349(7)
Cr(1)-N(8)	2.074(3)	C(25)-C(26)	1.386(7)
Cr(1)-N(1)	2.081(3)	C(26)-C(28)	1.402(6)
Cr(1)-O(1)	2.098(3)	C(27)-C(28)	1.484(7)
Cr(1)-N(6)	2.235(4)	C(28)-C(29)	1.399(6)
Cr(2)-N(9)	2.075(3)	C(30)-C(31)	1.511(6)
Cr(2)-N(10)	2.080(3)	C(31)-C(32)	1.391(6)
Cr(2)-N(2)	2.113(4)	C(32)-C(34)	1.401(6)
Cr(2)-N(3)	2.117(4)	C(33)-C(34)	1.504(6)
Cr(2)-O(2)	2.369(3)	C(35)-C(36)	1.491(7)
Cr(3)-N(11)	2.073(3)	C(36)-C(42)	1.398(6)
Cr(3)-N(12)	2.081(3)	C(36)-C(37)	1.407(7)
Cr(3)-N(5)	2.116(4)	C(37)-C(38)	1.391(8)
Cr(3)-N(4)	2.131(4)	C(38)-C(39)	1.351(8)
Cr(3)-O(3)	2.379(3)	C(39)-C(41)	1.381(7)
N(1)-N(2)	1.158(4)	C(40)-C(41)	1.508(7)
N(3)-N(4)	1.168(4)	C(41)-C(42)	1.401(6)
N(5)-N(6)	1.158(4)	C(43)-C(44)	1.485(6)
N(7)-C(13)	1.332(5)	C(44)-C(45)	1.399(6)
N(7)-C(21)	1.436(5)	C(44)-C(50)	1.402(6)
N(8)-C(10)	1.326(5)	C(45)-C(46)	1.377(7)
N(8)-C(8)	1.443(5)	C(46)-C(47)	1.372(7)
N(9)-C(31)	1.336(5)	C(47)-C(49)	1.395(6)
N(9)-C(29)	1.443(5)	C(48)-C(49)	1.502(6)
N(10)-C(34)	1.332(5)	C(49)-C(50)	1.390(6)
N(10)-C(42)	1.448(5)	C(51)-C(52)	1.523(6)
N(11)-C(52)	1.335(5)	C(52)-C(53)	1.388(6)
N(11)-C(50)	1.443(5)	C(53)-C(55)	1.396(6)
N(12)-C(55)	1.331(5)	C(54)-C(55)	1.522(6)
N(12)-C(63)	1.447(5)	C(56)-C(57)	1.493(7)
C(1)-C(2)	1.511(6)	C(57)-C(58)	1.392(6)
C(2)-C(3)	1.390(6)	C(57)-C(63)	1.392(6)
C(2)-C(8)	1.407(6)	C(58)-C(59)	1.359(8)
C(3)-C(4)	1.367(7)	C(59)-C(60)	1.386(8)

C(4)-C(5)	1.374(7)	C(60)-C(62)	1.380(7)
C(5)-C(7)	1.391(6)	C(61)-C(62)	1.495(7)
C(6)-C(7)	1.513(6)	C(62)-C(63)	1.401(6)
C(7)-C(8)	1.408(6)	O(1)-C(67)	1.444(5)
C(9)-C(10)	1.506(5)	O(1)-C(64)	1.449(5)
C(10)-C(11)	1.401(6)	C(64)-C(65)	1.486(7)
C(11)-C(13)	1.384(6)	C(65)-C(66)	1.499(7)
C(12)-C(13)	1.527(6)	C(66)-C(67)	1.486(6)
C(14)-C(15)	1.502(6)	O(2)-C(71)	1.421(5)
C(15)-C(16)	1.387(6)	O(2)-C(68)	1.422(5)
C(15)-C(21)	1.397(6)	C(68)-C(69)	1.494(7)
C(16)-C(17)	1.383(7)	C(69)-C(70)	1.434(8)
C(17)-C(18)	1.365(7)	C(70)-C(71)	1.505(7)
C(18)-C(20)	1.377(6)	O(3)-C(72)	1.440(5)
C(19)-C(20)	1.517(6)	O(3)-C(75)	1.448(5)
C(20)-C(21)	1.407(6)	C(72)-C(73)	1.502(7)
C(22)-C(23)	1.487(7)	C(73)-C(74)	1.505(8)
C(23)-C(24)	1.398(6)	C(74)-C(75)	1.489(7)
C(23)-C(29)	1.395(6)		

Angles (°)

N(7)-Cr(1)-N(8)	89.89(13)	C(20)-C(21)-N(7)	118.8(4)
N(7)-Cr(1)-N(1)	94.96(13)	C(24)-C(23)-C(29)	118.7(5)
N(8)-Cr(1)-N(1)	171.01(14)	C(24)-C(23)-C(22)	120.4(5)
N(7)-Cr(1)-O(1)	163.94(12)	C(29)-C(23)-C(22)	121.0(4)
N(8)-Cr(1)-O(1)	89.18(12)	C(25)-C(24)-C(23)	120.9(5)
N(1)-Cr(1)-O(1)	84.06(12)	C(24)-C(25)-C(26)	120.3(5)
N(7)-Cr(1)-N(6)	104.78(14)	C(25)-C(26)-C(28)	121.4(5)
N(8)-Cr(1)-N(6)	98.20(13)	C(29)-C(28)-C(26)	117.0(5)
N(1)-Cr(1)-N(6)	87.89(13)	C(29)-C(28)-C(27)	121.8(4)
O(1)-Cr(1)-N(6)	91.21(13)	C(26)-C(28)-C(27)	121.2(5)
N(9)-Cr(2)-N(10)	88.56(13)	C(23)-C(29)-C(28)	121.6(4)
N(9)-Cr(2)-N(2)	91.57(13)	C(23)-C(29)-N(9)	118.3(4)
N(10)-Cr(2)-N(2)	162.10(14)	C(28)-C(29)-N(9)	120.1(4)
N(9)-Cr(2)-N(3)	174.58(13)	N(9)-C(31)-C(32)	124.0(4)
N(10)-Cr(2)-N(3)	96.84(13)	N(9)-C(31)-C(30)	119.3(4)

N(2)-Cr(2)-N(3)	83.42(13)	C(32)-C(31)-C(30)	116.7(4)
N(9)-Cr(2)-O(2)	93.47(12)	C(31)-C(32)-C(34)	128.3(4)
N(10)-Cr(2)-O(2)	96.54(12)	N(10)-C(34)-C(32)	123.1(4)
N(2)-Cr(2)-O(2)	101.32(13)	N(10)-C(34)-C(33)	121.3(4)
N(3)-Cr(2)-O(2)	85.53(12)	C(32)-C(34)-C(33)	115.6(4)
N(11)-Cr(3)-N(12)	88.61(13)	C(42)-C(36)-C(37)	117.5(5)
N(11)-Cr(3)-N(5)	161.96(14)	C(42)-C(36)-C(35)	120.9(4)
N(12)-Cr(3)-N(5)	91.14(13)	C(37)-C(36)-C(35)	121.6(5)
N(11)-Cr(3)-N(4)	96.39(14)	C(38)-C(37)-C(36)	120.5(5)
N(12)-Cr(3)-N(4)	174.95(14)	C(39)-C(38)-C(37)	119.9(5)
N(5)-Cr(3)-N(4)	83.88(14)	C(38)-C(39)-C(41)	122.6(6)
N(11)-Cr(3)-O(3)	96.87(12)	C(39)-C(41)-C(42)	117.7(5)
N(12)-Cr(3)-O(3)	94.44(12)	C(39)-C(41)-C(40)	121.6(5)
N(5)-Cr(3)-O(3)	101.13(13)	C(42)-C(41)-C(40)	120.7(4)
N(4)-Cr(3)-O(3)	85.74(12)	C(36)-C(42)-C(41)	121.8(4)
N(2)-N(1)-Cr(1)	160.9(3)	C(36)-C(42)-N(10)	119.0(4)
N(1)-N(2)-Cr(2)	167.3(3)	C(41)-C(42)-N(10)	119.2(4)
N(4)-N(3)-Cr(2)	164.3(3)	C(45)-C(44)-C(50)	118.1(4)
N(3)-N(4)-Cr(3)	165.0(3)	C(45)-C(44)-C(43)	121.9(4)
N(6)-N(5)-Cr(3)	170.0(4)	C(50)-C(44)-C(43)	120.0(4)
N(5)-N(6)-Cr(1)	153.2(3)	C(46)-C(45)-C(44)	121.5(5)
C(13)-N(7)-C(21)	117.9(3)	C(47)-C(46)-C(45)	119.1(5)
C(13)-N(7)-Cr(1)	122.7(3)	C(46)-C(47)-C(49)	121.9(5)
C(21)-N(7)-Cr(1)	119.4(2)	C(50)-C(49)-C(47)	118.3(4)
C(10)-N(8)-C(8)	117.8(3)	C(50)-C(49)-C(48)	120.9(4)
C(10)-N(8)-Cr(1)	122.5(3)	C(47)-C(49)-C(48)	120.7(4)
C(8)-N(8)-Cr(1)	119.6(2)	C(49)-C(50)-C(44)	121.0(4)
C(31)-N(9)-C(29)	115.9(3)	C(49)-C(50)-N(11)	119.3(4)
C(31)-N(9)-Cr(2)	123.9(3)	C(44)-C(50)-N(11)	119.7(4)
C(29)-N(9)-Cr(2)	120.2(2)	N(11)-C(52)-C(53)	124.2(4)
C(34)-N(10)-C(42)	116.1(3)	N(11)-C(52)-C(51)	119.6(4)
C(34)-N(10)-Cr(2)	125.1(3)	C(53)-C(52)-C(51)	116.1(4)
C(42)-N(10)-Cr(2)	118.9(2)	C(52)-C(53)-C(55)	127.2(4)
C(52)-N(11)-C(50)	115.3(3)	N(12)-C(55)-C(53)	124.8(4)
C(52)-N(11)-Cr(3)	125.3(3)	N(12)-C(55)-C(54)	119.3(4)
C(50)-N(11)-Cr(3)	119.3(2)	C(53)-C(55)-C(54)	115.9(4)
C(55)-N(12)-C(63)	115.6(3)	C(58)-C(57)-C(63)	118.4(5)

C(55)-N(12)-Cr(3)	124.7(3)	C(58)-C(57)-C(56)	120.4(5)
C(63)-N(12)-Cr(3)	119.6(2)	C(63)-C(57)-C(56)	121.2(4)
C(3)-C(2)-C(8)	118.5(4)	C(59)-C(58)-C(57)	121.1(5)
C(3)-C(2)-C(1)	120.8(4)	C(58)-C(59)-C(60)	120.1(5)
C(8)-C(2)-C(1)	120.6(4)	C(59)-C(60)-C(62)	121.0(5)
C(4)-C(3)-C(2)	121.7(5)	C(60)-C(62)-C(63)	118.2(5)
C(3)-C(4)-C(5)	119.8(4)	C(60)-C(62)-C(61)	120.5(5)
C(4)-C(5)-C(7)	121.2(4)	C(63)-C(62)-C(61)	121.3(4)
C(5)-C(7)-C(8)	118.8(4)	C(57)-C(63)-C(62)	121.1(4)
C(5)-C(7)-C(6)	120.9(4)	C(57)-C(63)-N(12)	121.0(4)
C(8)-C(7)-C(6)	120.3(4)	C(62)-C(63)-N(12)	118.0(4)
C(7)-C(8)-C(2)	120.0(4)	C(67)-O(1)-C(64)	107.0(3)
C(7)-C(8)-N(8)	119.1(4)	C(67)-O(1)-Cr(1)	117.2(2)
C(2)-C(8)-N(8)	120.9(4)	C(64)-O(1)-Cr(1)	126.4(3)
N(8)-C(10)-C(11)	123.3(4)	O(1)-C(64)-C(65)	106.2(4)
N(8)-C(10)-C(9)	120.4(4)	C(64)-C(65)-C(66)	106.3(4)
C(11)-C(10)-C(9)	116.2(4)	C(67)-C(66)-C(65)	104.3(4)
C(13)-C(11)-C(10)	128.7(4)	O(1)-C(67)-C(66)	104.4(4)
N(7)-C(13)-C(11)	124.2(4)	C(71)-O(2)-C(68)	109.6(3)
N(7)-C(13)-C(12)	119.4(4)	C(71)-O(2)-Cr(2)	121.9(3)
C(11)-C(13)-C(12)	116.3(4)	C(68)-O(2)-Cr(2)	128.1(3)
C(16)-C(15)-C(21)	117.7(4)	O(2)-C(68)-C(69)	105.9(4)
C(16)-C(15)-C(14)	120.9(4)	C(70)-C(69)-C(68)	104.8(5)
C(21)-C(15)-C(14)	121.4(4)	C(69)-C(70)-C(71)	107.6(5)
C(17)-C(16)-C(15)	122.3(4)	O(2)-C(71)-C(70)	105.6(4)
C(18)-C(17)-C(16)	118.8(5)	C(72)-O(3)-C(75)	108.9(3)
C(17)-C(18)-C(20)	121.7(5)	C(72)-O(3)-Cr(3)	127.5(3)
C(18)-C(20)-C(21)	119.0(4)	C(75)-O(3)-Cr(3)	123.3(3)
C(18)-C(20)-C(19)	119.9(4)	O(3)-C(72)-C(73)	105.2(4)
C(21)-C(20)-C(19)	121.1(4)	C(72)-C(73)-C(74)	103.3(5)
C(15)-C(21)-C(20)	120.4(4)	C(75)-C(74)-C(73)	102.3(4)
C(15)-C(21)-N(7)	120.8(4)	O(3)-C(75)-C(74)	106.9(4)

3 crystallizes in the monoclinic space group $P\,2_1/c$. It has a cyclic $Cr_3(\mu\text{-}N_2)_3$ core, with the THF on Cr2 bonded trans to those on Cr1 and Cr3. The geometry around each chromium is square pyramidal, with the THF molecules occupying the apical position for Cr2 and Cr3. For Cr1, THF occupies a basal site while one of the bridging nitrogen ligands is located in the apical position. The Cr-N distances to the coordinated N_2 molecules range from 2.081(3) to 2.235(4) Å. The corresponding N-N bond distances are 1.158(4), 1.168(4) and 1.158(4) Å. The N-N distance of free dinitrogen is 1.0975(2) Å.[13] The distances here imply a mild degree of reduction of the N_2 molecules. The N-Cr-N angles about chromium within the $Cr_3(\mu\text{-}N_2)$ triangle are 87.89(13), 83.42(13), 83.88(14)°. The effective magnetic moment for **3** at room temperature was measured to be 6.5(1) μ_B. For a system of three non-interacting chromium(I) high spin d^5 ions (assuming the N_2 ligands are not reduced), the expected magnetic moment is 10.2 μ_B. A possible interpretation of the lower moment of **3** is that the bridging N_2 ligands mediate antiferromagnetic coupling between the chromiums. The IR spectrum taken in the solid state showed two distinct stretches at 2124 and 2244 cm^{-1}, which are in the range of N≡N triple bond stretching frequencies.[14] The number of stretches in **3** under idealized C_{3v} symmetry is expected to be two.

A search of the CSD [15] showed three examples of $M_3(\mu\text{-}N_2)_3$ complex with a structure similar to **3**. The structure of $[(PMe_3)_3ReCl]_3(\mu\text{-}N_2)_3$ was deposited in the CSD database.[16] Holland et. al. reported the other two examples of low-valent trinuclear iron dinitrogen complexes supported by nacnac ligand. These complexes were synthesized by CsC_8 and RbC_8 reductions of iron halide precursor $[LFe(\mu\text{-}Cl)]_2$ (L = 2,4-bis(2,6- dimethylphenylimino)-3-methylpent-3-yl).[17] Therefore,

$Cs_2[L^{Me}Fe(\mu-N_2)]_3$ and $Rb_2[L^{Me}Fe(\mu-N_2)]_3$ are accompanied by alkali metal cations. These structures are depicted in Scheme 1.7.
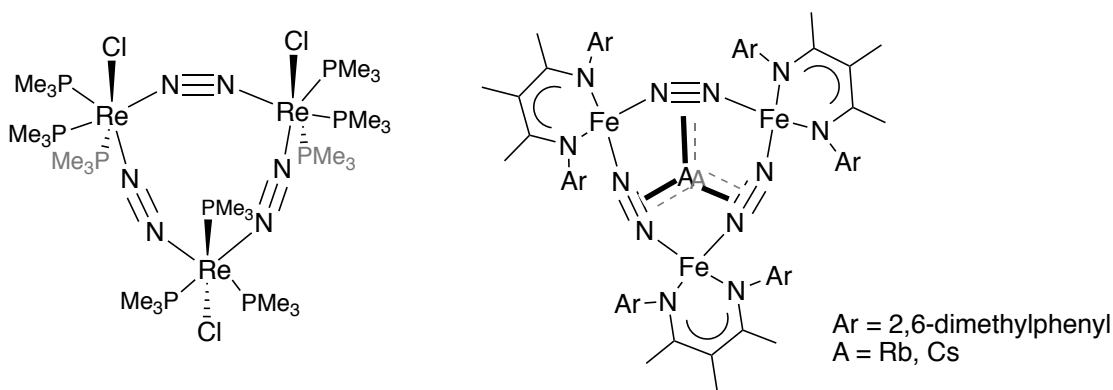
Scheme 1.7 Trinuclear dinitrogen complexes in the literature

The yield of **3** was measured to be only 20% (an average of three determinations), which led to the pursuit of other products in the Et_2O soluble fraction. Cooling the Et_2O solution to -30°C overnight gave a crystalline precipitate, which was collected and structurally characterized. $(L^{Me}Cr)_4(\mu-N_2)_4$ (**4**) was the product and its structure is shown in Figure 1.2, while the corresponding distances and angles are listed in Table 1.2. **4** is a tetranuclear chromium complex bridged by four N_2 ligands, coordinated in an end-on manner, i.e. $\mu-\kappa^1, \kappa^1-N_2$.

4 crystallizes in the monoclinic space group $C\,2/c$ and features a two-fold axis in the middle of the molecule. The geometry around each chromium is square planar, with sum of the bond angles about the chromiums being 361.8° and 363.9°. The Cr-N distances to the coordinated N_2 molecules (2.062(3)-2.092(3) Å) and the N-N distances (1.171(4) and 1.176(4) Å) are comparable to those observed in **3**. The

infrared spectrum showed one distinct stretching frequency of 2063 cm^{-1}, which was tentatively assigned as the N_2 ligands. The distances between the non-bonded Cr1···Cr1A and Cr2···Cr2A are 6.194(1) and 5.400(1) Å, respectively. They are longer than the distances between the chromium atoms of Cr-μ-κ^1,κ^1-N_2-Cr, specifically Cr1···Cr2 5.234(1) and Cr2···Cr1A 5.215(1) Å.

Figure 1.3 shows a side view of the core of the molecule. Four chromiums form an approximate tetrahedron and are connected by end-on bridging dinitrogen ligands. **4** is the second dinitrogen compound collected from this reaction, and it is also the first example of tetranuclear end-on bridged dinitrogen complex for any transition metals.
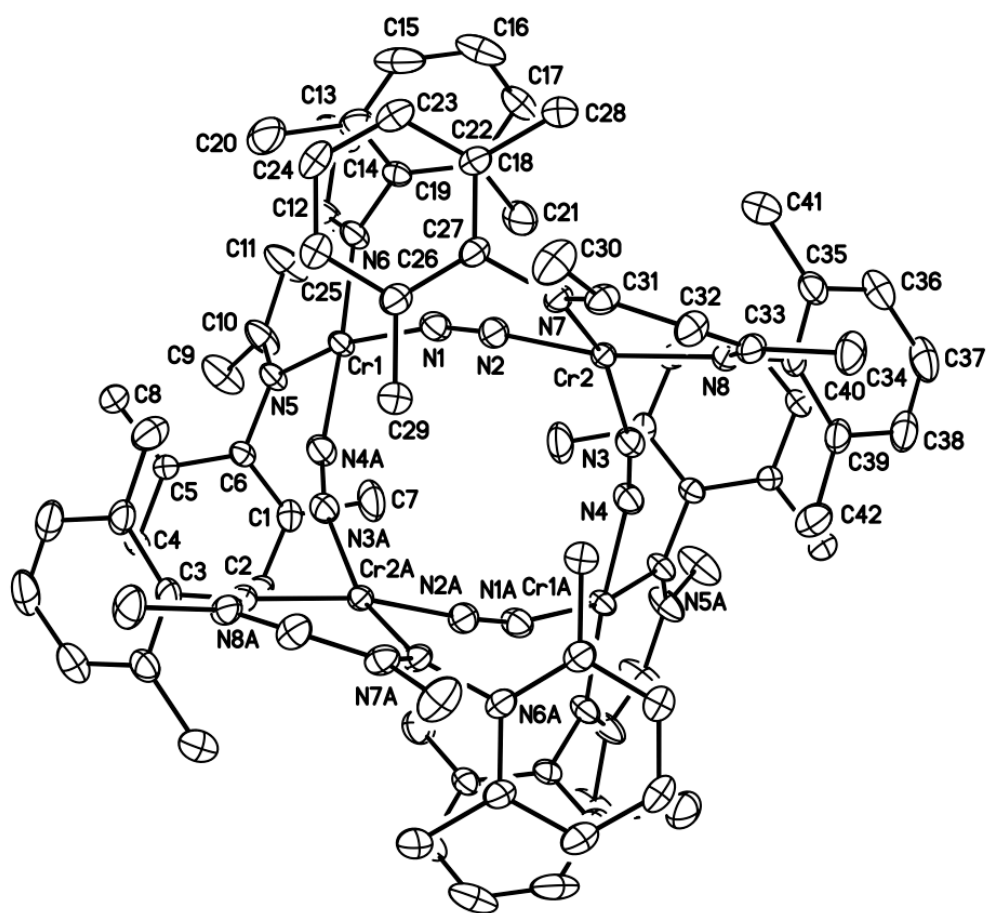
Figure 1.2   Molecular structure of $(L^{Me}Cr)_4(\mu\text{-}N_2)_4$ (**4**). Ellipsoids are drawn at the 30% probability level. Hydrogen atoms have been omitted for clarity.
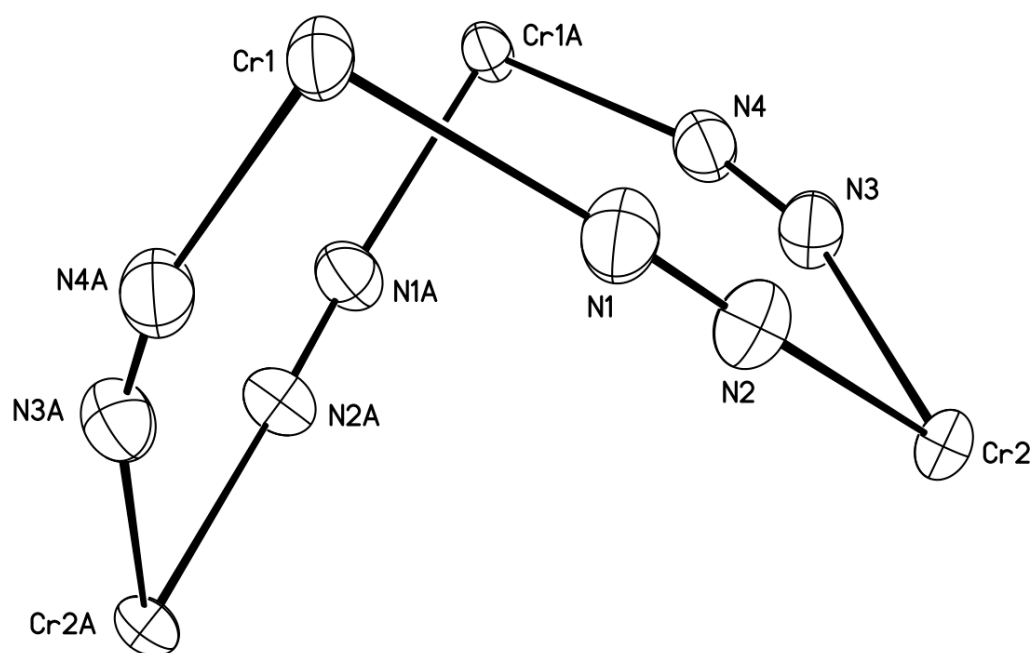
Figure 1.3   Molecular structure of the core of $(L^{Me}Cr)_4(\mu\text{-}N_2)_4$ (**4**). Ellipsoids are drawn at the 30% probability level. All ligand atoms have been omitted for clarity.

Table 1.2   Interatomic distances (Å) and angles (º) for $(L^{Me}Cr)_4(\mu\text{-}N_2)_4$ (**4**)

	Distances (Å)		
Cr(1)-N(5)	2.036(3)	C(12)-C(13)	1.532(5)
Cr(1)-N(6)	2.044(3)	C(14)-C(15)	1.377(6)
Cr(1)-N(1)	2.062(3)	C(14)-C(19)	1.402(5)
Cr(1)-N(4)A	2.092(3)	C(14)-C(20)	1.507(5)
Cr(2)-N(8)	2.037(2)	C(15)-C(16)	1.345(6)
Cr(2)-N(7)	2.047(3)	C(16)-C(17)	1.366(6)
Cr(2)-N(2)	2.064(3)	C(17)-C(18)	1.386(5)
Cr(2)-N(3)	2.085(3)	C(18)-C(19)	1.388(4)
N(1)-N(2)	1.171(4)	C(18)-C(21)	1.492(5)
N(3)-N(4)	1.176(4)	C(22)-C(27)	1.390(4)
N(4)-Cr(1)A	2.092(3)	C(22)-C(23)	1.393(5)
N(5)-C(10)	1.329(4)	C(22)-C(28)	1.500(5)
N(5)-C(6)	1.437(4)	C(23)-C(24)	1.386(5)
N(6)-C(12)	1.329(4)	C(24)-C(25)	1.378(5)
N(6)-C(19)	1.441(4)	C(25)-C(26)	1.405(5)
N(7)-C(31)	1.338(4)	C(26)-C(27)	1.395(4)
N(7)-C(27)	1.456(4)	C(26)-C(29)	1.502(5)
N(8)-C(33)	1.333(4)	C(30)-C(31)	1.515(5)
N(8)-C(40)	1.446(4)	C(31)-C(32)	1.391(4)
C(1)-C(2)	1.379(5)	C(32)-C(33)	1.392(5)
C(1)-C(6)	1.399(4)	C(33)-C(34)	1.518(4)
C(1)-C(7)	1.510(5)	C(35)-C(36)	1.381(5)
C(2)-C(3)	1.357(5)	C(35)-C(40)	1.386(5)
C(3)-C(4)	1.378(5)	C(35)-C(41)	1.525(5)
C(4)-C(5)	1.384(4)	C(36)-C(37)	1.368(6)
C(5)-C(6)	1.390(4)	C(37)-C(38)	1.368(6)
C(5)-C(8)	1.513(4)	C(38)-C(39)	1.396(5)
C(9)-C(10)	1.524(5)	C(39)-C(40)	1.412(5)
C(10)-C(11)	1.394(5)	C(39)-C(42)	1.506(5)
C(11)-C(12)	1.387(5)		

Angles (°)

N(5)-Cr(1)-N(6)	90.06(10)	N(6)-C(12)-C(13)	119.4(3)
N(5)-Cr(1)-N(1)	165.58(12)	C(11)-C(12)-C(13)	115.9(3)
N(6)-Cr(1)-N(1)	93.45(11)	C(15)-C(14)-C(19)	118.5(4)
N(5)-Cr(1)-N(4)A	94.70(10)	C(15)-C(14)-C(20)	121.4(4)
N(6)-Cr(1)-N(4)A	171.88(12)	C(19)-C(14)-C(20)	120.1(4)
N(1)-Cr(1)-N(4)A	83.56(11)	C(16)-C(15)-C(14)	121.8(4)
N(8)-Cr(2)-N(7)	90.37(10)	C(15)-C(16)-C(17)	119.9(4)
N(8)-Cr(2)-N(2)	167.60(11)	C(16)-C(17)-C(18)	121.1(4)
N(7)-Cr(2)-N(2)	92.75(10)	C(17)-C(18)-C(19)	118.6(3)
N(8)-Cr(2)-N(3)	93.40(10)	C(17)-C(18)-C(21)	120.2(3)
N(7)-Cr(2)-N(3)	161.74(11)	C(19)-C(18)-C(21)	121.2(3)
N(2)-Cr(2)-N(3)	87.37(11)	C(18)-C(19)-C(14)	120.0(3)
N(2)-N(1)-Cr(1)	166.6(3)	C(18)-C(19)-N(6)	120.0(3)
N(1)-N(2)-Cr(2)	173.8(3)	C(14)-C(19)-N(6)	120.0(3)
N(4)-N(3)-Cr(2)	163.7(2)	C(27)-C(22)-C(23)	118.0(3)
N(3)-N(4)-Cr(1)A	166.7(2)	C(27)-C(22)-C(28)	121.2(3)
C(10)-N(5)-C(6)	116.5(3)	C(23)-C(22)-C(28)	120.8(3)
C(10)-N(5)-Cr(1)	127.0(2)	C(24)-C(23)-C(22)	121.6(3)
C(6)-N(5)-Cr(1)	116.15(19)	C(25)-C(24)-C(23)	119.3(3)
C(12)-N(6)-C(19)	116.7(3)	C(24)-C(25)-C(26)	121.2(3)
C(12)-N(6)-Cr(1)	125.9(2)	C(27)-C(26)-C(25)	117.9(3)
C(19)-N(6)-Cr(1)	117.4(2)	C(27)-C(26)-C(29)	121.9(3)
C(31)-N(7)-C(27)	114.6(3)	C(25)-C(26)-C(29)	120.1(3)
C(31)-N(7)-Cr(2)	123.8(2)	C(22)-C(27)-C(26)	122.0(3)
C(27)-N(7)-Cr(2)	121.59(19)	C(22)-C(27)-N(7)	118.3(3)
C(33)-N(8)-C(40)	116.4(3)	C(26)-C(27)-N(7)	119.7(3)
C(33)-N(8)-Cr(2)	125.4(2)	N(7)-C(31)-C(32)	124.4(3)
C(40)-N(8)-Cr(2)	117.99(19)	N(7)-C(31)-C(30)	119.1(3)
C(2)-C(1)-C(6)	118.4(3)	C(32)-C(31)-C(30)	116.4(3)
C(2)-C(1)-C(7)	122.0(3)	C(31)-C(32)-C(33)	128.3(3)
C(6)-C(1)-C(7)	119.6(3)	N(8)-C(33)-C(32)	123.3(3)
C(3)-C(2)-C(1)	121.8(3)	N(8)-C(33)-C(34)	120.4(3)
C(2)-C(3)-C(4)	119.7(3)	C(32)-C(33)-C(34)	116.1(3)
C(3)-C(4)-C(5)	120.6(3)	C(36)-C(35)-C(40)	119.3(4)
C(4)-C(5)-C(6)	119.1(3)	C(36)-C(35)-C(41)	120.5(4)
C(4)-C(5)-C(8)	120.8(3)	C(40)-C(35)-C(41)	120.2(3)

C(6)-C(5)-C(8)	120.1(3)	C(37)-C(36)-C(35)	121.1(4)
C(5)-C(6)-C(1)	120.3(3)	C(36)-C(37)-C(38)	119.6(4)
C(5)-C(6)-N(5)	119.7(3)	C(37)-C(38)-C(39)	121.9(4)
C(1)-C(6)-N(5)	120.0(3)	C(38)-C(39)-C(40)	117.3(4)
N(5)-C(10)-C(11)	123.3(3)	C(38)-C(39)-C(42)	120.7(3)
N(5)-C(10)-C(9)	119.9(3)	C(40)-C(39)-C(42)	122.0(3)
C(11)-C(10)-C(9)	116.8(3)	C(35)-C(40)-C(39)	120.5(3)
C(12)-C(11)-C(10)	128.4(3)	C(35)-C(40)-N(8)	118.9(3)
N(6)-C(12)-C(11)	124.7(3)	C(39)-C(40)-N(8)	120.6(3)

Another product was crystallized from the same Et_2O extract with **4**, which was then structurally characterized as $(L^{Me}Cr)_2(\mu\text{-}N)(\mu\text{-}H)$ (**5**) (Figure 1.4). **4** and **5** have the same color (orange) and the co-occurrence of both complexes in the Et_2O extract may be attributed to their similar solubility. They are both soluble in THF, Et_2O, pentane, and toluene. The crystal structures of **4** and **5** were obtained by randomly selecting specimens from a mixture of crystals with visually the same shape and color. Accordingly, it was difficult to separate **4** and **5** apart by fractional crystallization technique. Their combined yield was calculated to be 22% (an average of three determinations).

5 crystallizes in the monoclinic space group *C* 2/*c*. The two chromium atoms are bridged by a nitride and a hydride ligand. The bridging hydride was located on the difference map and its position refined. The LIFDI mass spectrum supported the formulation of **5** (m/z = 729.3627 $[C_{42}H_{51}N_5Cr_2^+]$; calcd. m/z = 729.2957). The Cr1-N1 distance is 1.751(3) Å, which is comparable to bis(μ-nitrido) $[\{(iPr_2N)_2Cr(\mu\text{-}N)\}_2]$ reported by C. Cummins, with 1.743(3) Å and 1.730(3) Å.[18] These distances fall into the range between single bonds (e.g. $Cr\text{-}N_{avg}$ 2.068 Å in $(L^{iPr}Cr)_2(\mu\text{-}NH_2)_2$) and double bonds (e.g. $Cr\text{-}N_{avg}$ 1.661 Å in $L^{iPr}Cr(NAd)_2$).[19] The Cr···Cr separation is 2.6716(13) Å. The chromium(III) oxidation state finds expression in its preferred tetrahedral coordination geometry.

Figure 1.4   Molecular structure of $(L^{Me}Cr)_2(\mu\text{-N})(\mu\text{-H})$ (**5**). Ellipsoids are drawn at the 30% probability level. Hydrogen atoms, except the bridging hydride, and an Et_2O molecule have been omitted for clarity.

Table 1.3   Interatomic distances (Å) and angles (º) for (L^{Me}Cr)$_2$(μ-N)(μ-H) (**5**)

Distances (Å)

Cr(1)-N(1)	1.751(3)	C(4)-C(5)	1.389(5)
Cr(1)-N(2)	1.987(3)	C(5)-C(6)	1.409(5)
Cr(1)-N(3)	1.991(3)	C(5)-C(8)	1.506(5)
Cr(1)-Cr(1)A	2.6716(13)	C(9)-C(10)	1.518(5)
Cr(1)-H(1)	1.82(3)	C(10)-C(11)	1.396(5)
N(1)-Cr(1)A	1.751(3)	C(11)-C(12)	1.401(5)
N(2)-C(10)	1.335(4)	C(12)-C(13)	1.495(4)
N(2)-C(6)	1.451(4)	C(14)-C(15)	1.398(5)
N(3)-C(12)	1.341(4)	C(14)-C(19)	1.401(5)
N(3)-C(19)	1.450(4)	C(14)-C(20)	1.503(5)
C(1)-C(6)	1.397(5)	C(15)-C(16)	1.378(5)
C(1)-C(2)	1.399(5)	C(16)-C(17)	1.370(5)
C(1)-C(7)	1.504(5)	C(17)-C(18)	1.397(5)
C(2)-C(3)	1.371(5)	C(18)-C(19)	1.393(5)
C(3)-C(4)	1.379(5)	C(18)-C(21)	1.513(5)

Angles (°)

N(1)-Cr(1)-N(2)	128.36(8)	C(4)-C(5)-C(8)	120.9(3)
N(1)-Cr(1)-N(3)	118.19(12)	C(6)-C(5)-C(8)	121.3(3)
N(2)-Cr(1)-N(3)	91.58(11)	C(1)-C(6)-C(5)	121.3(3)
N(1)-Cr(1)-Cr(1)A	40.29(10)	C(1)-C(6)-N(2)	119.6(3)
N(2)-Cr(1)-Cr(1)A	122.35(8)	C(5)-C(6)-N(2)	119.0(3)
N(3)-Cr(1)-Cr(1)A	146.02(8)	N(2)-C(10)-C(11)	122.8(3)
N(1)-Cr(1)-H(1)	83.1(10)	N(2)-C(10)-C(9)	120.1(3)
N(2)-Cr(1)-H(1)	99.8(6)	C(11)-C(10)-C(9)	117.1(3)
N(3)-Cr(1)-H(1)	141.0(6)	C(10)-C(11)-C(12)	128.6(3)
Cr(1)A-Cr(1)-H(1)	42.8(9)	N(3)-C(12)-C(11)	122.7(3)
Cr(1)A-N(1)-Cr(1)	99.4(2)	N(3)-C(12)-C(13)	119.6(3)
C(10)-N(2)-C(6)	118.5(3)	C(11)-C(12)-C(13)	117.7(3)
C(10)-N(2)-Cr(1)	126.6(2)	C(15)-C(14)-C(19)	118.4(3)
C(6)-N(2)-Cr(1)	114.8(2)	C(15)-C(14)-C(20)	120.9(3)
C(12)-N(3)-C(19)	117.3(3)	C(19)-C(14)-C(20)	120.7(3)
C(12)-N(3)-Cr(1)	126.4(2)	C(16)-C(15)-C(14)	120.9(4)

C(19)-N(3)-Cr(1)	116.20(19)	C(17)-C(16)-C(15)	119.9(4)
C(6)-C(1)-C(2)	118.1(3)	C(16)-C(17)-C(18)	121.4(4)
C(6)-C(1)-C(7)	121.1(3)	C(19)-C(18)-C(17)	118.2(3)
C(2)-C(1)-C(7)	120.7(3)	C(19)-C(18)-C(21)	121.2(3)
C(3)-C(2)-C(1)	121.3(4)	C(17)-C(18)-C(21)	120.6(3)
C(2)-C(3)-C(4)	119.9(3)	C(18)-C(19)-C(14)	121.1(3)
C(3)-C(4)-C(5)	121.5(3)	C(18)-C(19)-N(3)	119.5(3)
C(4)-C(5)-C(6)	117.9(3)	C(14)-C(19)-N(3)	119.4(3)

After the isolation of complexes **3-5**, cooling the Et$_2$O solution for longer time (2 days at -30°C) led to precipitation of additional crystals, which were then structurally determined to be (L^{Me}Cr)$_3$(μ-N$_2$)$_3$(μ-N)CrL^{Me} (**6**). The molecular structure is shown in Figure 1.5, while the corresponding interatomic distances and angles are listed in Table 1.4. **6** is a tetranuclear complex. It is similar to complex **3**, but without the THF molecules; and contains an additional chromium fragment connected by a bridging nitrido ligand. **6** was isolated as an orange-red solid in 18% yield (an average of three determinations).

6 crystallizes in the triclinic space group $P\,\overline{1}$. Structural analysis shows that the bridging nitrido ligand suffers positional disorder. Thus, N15 was refined in two positions and modeled satisfactorily with a population ratio of 0.905 to 1. Repeating the X-ray diffraction experiment on another independently synthesized and crystallized sample consistently gave the same result, where the nitride ligand was positionally disordered over two positions.

The four-coordinate Cr2 and Cr3 in **6** exhibit slightly distorted square planar geometry, while Cr1 appears to be a five-coordinate ion but adopts an almost perfectly octahedral coordination sphere completed with both positions of the disordered nitride ligand. The geometry around Cr4 is best described as T-shaped, with angles of 174.1(2)° (N15-Cr4-N13), 91.8(2)° (N15-Cr4-N14), and 89.8(1)° (N14-Cr4-N13). This strongly suggests a second bridging ligand, possibly a hydride, which can not be resolved by crystallography due to the disordered nitrogen atom. LIFDI mass spectrometry was attempted but failed to provide molecular weight information.

The dinitrogen N-N distances in **6** are 1.161(4), 1.186(3) and 1.160(3) Å, which are comparable to those in **3** and **4**. The IR spectrum showed dinitrogen

23

stretching frequencies at 2139 and 2210 cm^{-1}. The distances of Cr1 to the coordinated N_2 molecules (Cr1-N1 2.116(3) and Cr1-N6 2.101(3) Å) are slightly longer than those of Cr2 and Cr3 to the coordinated N_2 molecules (spanning 2.036(3)-2.077(3) Å). Moreover, the distance between chromium and nitride, namely Cr1-N15 1.929(5) Å, is longer than that in **5** (Cr-$N_{nitride}$ 1.751(3) Å). The sterically crowded Cr1 environment might be responsible for this phenomenon. At $\mu_{eff} = 6.1(1)$ μ_B (293K), the magnetic moment of **6** indicates antiferromagnetic coupling between chromium ions.
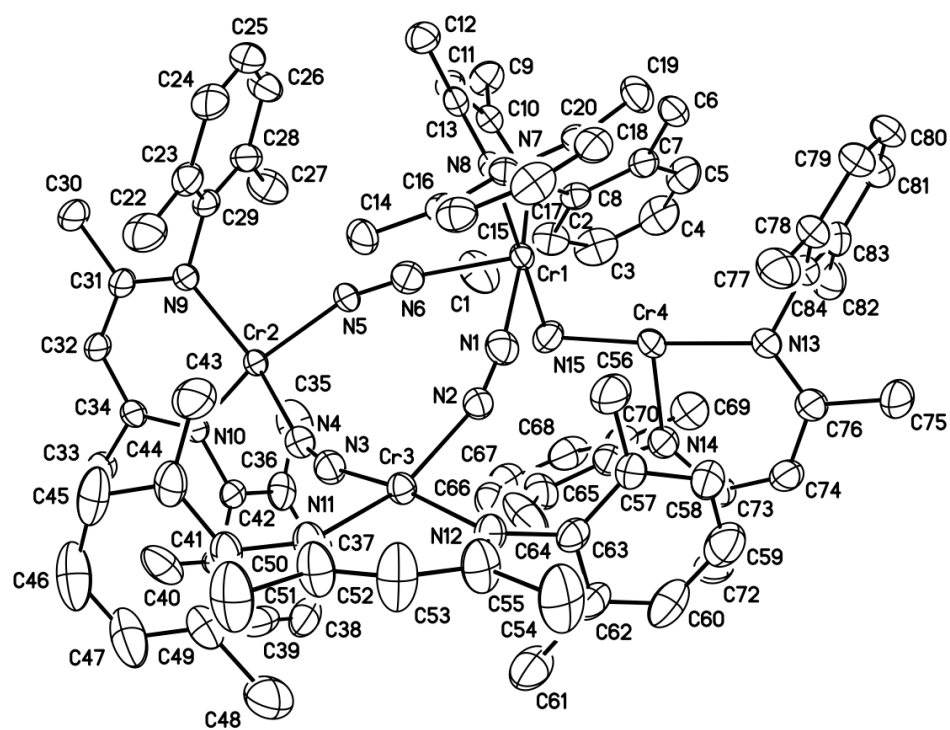
Figure 1.5   Molecular structure of $(L^{Me}Cr)_3(\mu\text{-}N_2)_3(\mu\text{-}N)CrL^{Me}$ (**6**). Ellipsoids are drawn at the 30% probability level. Hydrogen atoms have been omitted for clarity.

Table 1.4   Interatomic distances (Å) and angles (°) for (L^{Me}Cr)$_3$(μ-N$_2$)$_3$(μ-N)CrL^{Me}
(**6**)

Distances (Å)			
Cr(1)-N(15)	1.929(5)	C(23)-C(29)	1.379(4)
Cr(1)-N(7)	2.031(3)	C(23)-C(24)	1.415(5)
Cr(1)-N(8)	2.061(2)	C(24)-C(25)	1.360(5)
Cr(1)-N(6)	2.101(3)	C(25)-C(26)	1.350(5)
Cr(1)-N(1)	2.116(3)	C(26)-C(28)	1.377(5)
Cr(1)-Cr(4)	2.8195(9)	C(27)-C(28)	1.484(5)
Cr(2)-N(10)	2.021(2)	C(28)-C(29)	1.408(5)
Cr(2)-N(9)	2.026(2)	C(30)-C(31)	1.520(4)
Cr(2)-N(5)	2.036(3)	C(31)-C(32)	1.390(4)
Cr(2)-N(4)	2.077(3)	C(32)-C(34)	1.401(4)
Cr(3)-N(12)	2.019(3)	C(33)-C(34)	1.500(4)
Cr(3)-N(11)	2.028(3)	C(35)-C(36)	1.486(6)
Cr(3)-N(2)	2.050(3)	C(36)-C(42)	1.393(4)
Cr(3)-N(3)	2.076(3)	C(36)-C(37)	1.429(5)
Cr(4)-N(16)	1.911(5)	C(37)-C(38)	1.388(6)
Cr(4)-N(15)	1.942(6)	C(38)-C(39)	1.330(6)
Cr(4)-N(14)	2.041(3)	C(39)-C(41)	1.375(5)
Cr(4)-N(13)	2.043(3)	C(40)-C(41)	1.485(5)
N(1)-N(2)	1.161(4)	C(41)-C(42)	1.417(5)
N(3)-N(4)	1.186(3)	C(43)-C(44)	1.491(5)
N(5)-N(6)	1.160(3)	C(44)-C(50)	1.385(4)
N(7)-C(10)	1.336(3)	C(44)-C(45)	1.397(5)
N(7)-C(8)	1.437(3)	C(45)-C(46)	1.397(6)
N(8)-C(13)	1.328(4)	C(46)-C(47)	1.356(6)
N(8)-C(21)	1.444(4)	C(47)-C(49)	1.378(6)
N(9)-C(31)	1.325(4)	C(48)-C(49)	1.513(6)
N(9)-C(29)	1.446(4)	C(49)-C(50)	1.396(5)
N(10)-C(34)	1.340(4)	C(51)-C(52)	1.520(5)
N(10)-C(42)	1.428(3)	C(52)-C(53)	1.388(5)
N(11)-C(52)	1.344(4)	C(53)-C(55)	1.405(5)
N(11)-C(50)	1.439(4)	C(54)-C(55)	1.531(5)
N(12)-C(55)	1.314(4)	C(56)-C(57)	1.501(5)
N(12)-C(63)	1.434(4)	C(57)-C(58)	1.389(5)

N(13)-C(76)	1.333(4)	C(57)-C(63)	1.398(5)
N(13)-C(84)	1.433(4)	C(58)-C(59)	1.362(5)
N(14)-C(73)	1.329(4)	C(59)-C(60)	1.348(6)
N(14)-C(71)	1.438(4)	C(60)-C(62)	1.392(5)
C(1)-C(2)	1.503(5)	C(61)-C(62)	1.491(5)
C(2)-C(8)	1.395(4)	C(62)-C(63)	1.391(4)
C(2)-C(3)	1.404(5)	C(64)-C(65)	1.493(6)
C(3)-C(4)	1.367(6)	C(65)-C(66)	1.406(5)
C(4)-C(5)	1.350(5)	C(65)-C(71)	1.408(5)
C(5)-C(7)	1.396(4)	C(66)-C(67)	1.359(6)
C(6)-C(7)	1.517(4)	C(67)-C(68)	1.375(6)
C(7)-C(8)	1.398(4)	C(68)-C(70)	1.407(5)
C(9)-C(10)	1.514(4)	C(69)-C(70)	1.514(5)
C(10)-C(11)	1.397(4)	C(70)-C(71)	1.388(5)
C(11)-C(13)	1.398(4)	C(72)-C(73)	1.523(5)
C(12)-C(13)	1.521(4)	C(73)-C(74)	1.404(5)
C(14)-C(15)	1.502(4)	C(74)-C(76)	1.405(5)
C(15)-C(16)	1.393(4)	C(75)-C(76)	1.504(5)
C(15)-C(21)	1.401(4)	C(77)-C(78)	1.500(5)
C(16)-C(17)	1.369(5)	C(78)-C(79)	1.387(5)
C(17)-C(18)	1.376(5)	C(78)-C(84)	1.409(5)
C(18)-C(20)	1.390(4)	C(79)-C(80)	1.377(6)
C(19)-C(20)	1.510(4)	C(80)-C(81)	1.360(5)
C(20)-C(21)	1.392(4)	C(81)-C(83)	1.391(5)
C(22)-C(23)	1.484(5)	C(82)-C(83)	1.501(5)
		C(83)-C(84)	1.391(5)

Angles (°)

N(15)-Cr(1)-N(7)	90.69(18)	C(18)-C(20)-C(19)	120.2(3)
N(16)-Cr(1)-N(7)	94.52(17)	C(21)-C(20)-C(19)	121.6(3)
N(15)-Cr(1)-N(8)	179.36(19)	C(20)-C(21)-C(15)	121.7(3)
N(16)-Cr(1)-N(8)	95.04(15)	C(20)-C(21)-N(8)	118.8(3)
N(7)-Cr(1)-N(8)	89.63(9)	C(15)-C(21)-N(8)	119.6(3)
N(15)-Cr(1)-N(6)	87.77(18)	C(29)-C(23)-C(24)	117.8(4)
N(16)-Cr(1)-N(6)	171.09(17)	C(29)-C(23)-C(22)	121.1(3)
N(7)-Cr(1)-N(6)	91.37(11)	C(24)-C(23)-C(22)	121.1(3)

N(8)-Cr(1)-N(6)	91.66(10)	C(25)-C(24)-C(23)	119.8(3)
N(15)-Cr(1)-N(1)	84.93(19)	C(26)-C(25)-C(24)	121.7(4)
N(16)-Cr(1)-N(1)	91.47(17)	C(25)-C(26)-C(28)	121.0(4)
N(7)-Cr(1)-N(1)	172.28(10)	C(26)-C(28)-C(29)	118.0(3)
N(8)-Cr(1)-N(1)	94.69(10)	C(26)-C(28)-C(27)	121.5(3)
N(6)-Cr(1)-N(1)	82.13(11)	C(29)-C(28)-C(27)	120.5(3)
N(15)-Cr(1)-Cr(4)	43.44(17)	C(23)-C(29)-C(28)	121.5(3)
N(16)-Cr(1)-Cr(4)	42.58(14)	C(23)-C(29)-N(9)	120.0(3)
N(7)-Cr(1)-Cr(4)	98.87(7)	C(28)-C(29)-N(9)	118.5(3)
N(8)-Cr(1)-Cr(4)	137.03(7)	N(9)-C(31)-C(32)	124.3(3)
N(6)-Cr(1)-Cr(4)	129.77(7)	N(9)-C(31)-C(30)	119.1(3)
N(1)-Cr(1)-Cr(4)	82.30(8)	C(32)-C(31)-C(30)	116.6(3)
N(10)-Cr(2)-N(9)	90.19(9)	C(31)-C(32)-C(34)	128.4(3)
N(10)-Cr(2)-N(5)	154.68(10)	N(10)-C(34)-C(32)	122.2(3)
N(9)-Cr(2)-N(5)	95.98(10)	N(10)-C(34)-C(33)	120.1(3)
N(10)-Cr(2)-N(4)	100.95(10)	C(32)-C(34)-C(33)	117.7(3)
N(9)-Cr(2)-N(4)	149.84(10)	C(42)-C(36)-C(37)	118.1(4)
N(5)-Cr(2)-N(4)	85.85(10)	C(42)-C(36)-C(35)	120.9(3)
N(12)-Cr(3)-N(11)	89.86(11)	C(37)-C(36)-C(35)	121.0(3)
N(12)-Cr(3)-N(2)	93.63(11)	C(38)-C(37)-C(36)	117.5(4)
N(11)-Cr(3)-N(2)	160.94(10)	C(39)-C(38)-C(37)	123.6(4)
N(12)-Cr(3)-N(3)	165.42(10)	C(38)-C(39)-C(41)	121.4(4)
N(11)-Cr(3)-N(3)	95.23(11)	C(39)-C(41)-C(42)	117.5(4)
N(2)-Cr(3)-N(3)	86.00(11)	C(39)-C(41)-C(40)	121.1(4)
N(16)-Cr(4)-N(14)	172.21(18)	C(42)-C(41)-C(40)	121.3(3)
N(15)-Cr(4)-N(14)	91.76(18)	C(36)-C(42)-C(41)	121.9(3)
N(16)-Cr(4)-N(13)	92.60(17)	C(36)-C(42)-N(10)	118.8(3)
N(15)-Cr(4)-N(13)	174.08(19)	C(41)-C(42)-N(10)	119.2(3)
N(14)-Cr(4)-N(13)	89.77(11)	C(50)-C(44)-C(45)	118.9(4)
N(16)-Cr(4)-Cr(1)	44.11(16)	C(50)-C(44)-C(43)	120.9(3)
N(15)-Cr(4)-Cr(1)	43.07(15)	C(45)-C(44)-C(43)	120.2(4)
N(14)-Cr(4)-Cr(1)	132.84(8)	C(44)-C(45)-C(46)	118.2(4)
N(13)-Cr(4)-Cr(1)	136.68(7)	C(47)-C(46)-C(45)	123.1(4)
N(2)-N(1)-Cr(1)	166.3(3)	C(46)-C(47)-C(49)	118.7(5)
N(1)-N(2)-Cr(3)	163.4(2)	C(47)-C(49)-C(50)	119.9(4)
N(4)-N(3)-Cr(3)	166.2(3)	C(47)-C(49)-C(48)	119.4(4)
N(3)-N(4)-Cr(2)	158.0(2)	C(50)-C(49)-C(48)	120.7(4)

N(6)-N(5)-Cr(2)	162.8(2)	C(44)-C(50)-C(49)	121.1(3)
N(5)-N(6)-Cr(1)	171.7(3)	C(44)-C(50)-N(11)	120.7(3)
C(10)-N(7)-C(8)	116.5(2)	C(49)-C(50)-N(11)	118.3(3)
C(10)-N(7)-Cr(1)	122.66(19)	N(11)-C(52)-C(53)	124.0(3)
C(8)-N(7)-Cr(1)	120.76(18)	N(11)-C(52)-C(51)	119.8(3)
C(13)-N(8)-C(21)	116.6(2)	C(53)-C(52)-C(51)	116.2(3)
C(13)-N(8)-Cr(1)	122.87(19)	C(52)-C(53)-C(55)	128.1(4)
C(21)-N(8)-Cr(1)	120.45(18)	N(12)-C(55)-C(53)	122.2(4)
C(31)-N(9)-C(29)	117.1(2)	N(12)-C(55)-C(54)	120.9(3)
C(31)-N(9)-Cr(2)	126.0(2)	C(53)-C(55)-C(54)	116.8(4)
C(29)-N(9)-Cr(2)	116.65(18)	C(58)-C(57)-C(63)	117.6(3)
C(34)-N(10)-C(42)	118.1(2)	C(58)-C(57)-C(56)	120.6(4)
C(34)-N(10)-Cr(2)	127.44(19)	C(63)-C(57)-C(56)	121.8(3)
C(42)-N(10)-Cr(2)	114.14(18)	C(59)-C(58)-C(57)	121.1(4)
C(52)-N(11)-C(50)	114.5(3)	C(60)-C(59)-C(58)	121.0(4)
C(52)-N(11)-Cr(3)	124.5(2)	C(59)-C(60)-C(62)	120.9(4)
C(50)-N(11)-Cr(3)	120.8(2)	C(63)-C(62)-C(60)	118.2(4)
C(55)-N(12)-C(63)	116.5(3)	C(63)-C(62)-C(61)	120.8(3)
C(55)-N(12)-Cr(3)	127.7(2)	C(60)-C(62)-C(61)	120.9(3)
C(63)-N(12)-Cr(3)	115.6(2)	C(62)-C(63)-C(57)	121.2(3)
C(76)-N(13)-C(84)	116.1(3)	C(62)-C(63)-N(12)	118.0(3)
C(76)-N(13)-Cr(4)	124.6(2)	C(57)-C(63)-N(12)	120.8(3)
C(84)-N(13)-Cr(4)	118.9(2)	C(66)-C(65)-C(71)	117.3(4)
C(73)-N(14)-C(71)	117.7(3)	C(66)-C(65)-C(64)	121.1(4)
C(73)-N(14)-Cr(4)	125.2(2)	C(71)-C(65)-C(64)	121.5(4)
C(71)-N(14)-Cr(4)	117.1(2)	C(67)-C(66)-C(65)	121.1(4)
Cr(1)-N(15)-Cr(4)	93.5(2)	C(66)-C(67)-C(68)	121.2(4)
Cr(4)-N(16)-Cr(1)	93.3(2)	C(67)-C(68)-C(70)	120.3(4)
C(8)-C(2)-C(3)	117.0(4)	C(71)-C(70)-C(68)	118.1(4)
C(8)-C(2)-C(1)	122.4(3)	C(71)-C(70)-C(69)	121.9(3)
C(3)-C(2)-C(1)	120.5(3)	C(68)-C(70)-C(69)	120.0(4)
C(4)-C(3)-C(2)	122.3(4)	C(70)-C(71)-C(65)	122.0(3)
C(5)-C(4)-C(3)	119.4(4)	C(70)-C(71)-N(14)	118.4(3)
C(4)-C(5)-C(7)	122.0(4)	C(65)-C(71)-N(14)	119.6(3)
C(5)-C(7)-C(8)	118.0(3)	N(14)-C(73)-C(74)	123.3(3)
C(5)-C(7)-C(6)	120.1(3)	N(14)-C(73)-C(72)	120.3(3)
C(8)-C(7)-C(6)	121.8(3)	C(74)-C(73)-C(72)	116.4(3)

C(2)-C(8)-C(7)	121.3(3)	C(73)-C(74)-C(76)	127.6(3)
C(2)-C(8)-N(7)	120.8(3)	N(13)-C(76)-C(74)	124.2(3)
C(7)-C(8)-N(7)	117.9(3)	N(13)-C(76)-C(75)	119.8(3)
N(7)-C(10)-C(11)	124.1(3)	C(74)-C(76)-C(75)	116.1(3)
N(7)-C(10)-C(9)	120.0(3)	C(79)-C(78)-C(84)	117.9(4)
C(11)-C(10)-C(9)	115.8(3)	C(79)-C(78)-C(77)	120.9(3)
C(10)-C(11)-C(13)	127.3(3)	C(84)-C(78)-C(77)	121.1(3)
N(8)-C(13)-C(11)	123.8(2)	C(80)-C(79)-C(78)	120.7(4)
N(8)-C(13)-C(12)	119.8(3)	C(81)-C(80)-C(79)	121.1(4)
C(11)-C(13)-C(12)	116.3(3)	C(80)-C(81)-C(83)	120.4(4)
C(16)-C(15)-C(21)	117.6(3)	C(84)-C(83)-C(81)	118.8(3)
C(16)-C(15)-C(14)	120.1(3)	C(84)-C(83)-C(82)	120.2(3)
C(21)-C(15)-C(14)	122.2(3)	C(81)-C(83)-C(82)	121.1(4)
C(17)-C(16)-C(15)	121.4(3)	C(83)-C(84)-C(78)	121.1(3)
C(16)-C(17)-C(18)	120.1(3)	C(83)-C(84)-N(13)	118.5(3)
C(17)-C(18)-C(20)	121.0(3)	C(78)-C(84)-N(13)	120.4(3)
C(18)-C(20)-C(21)	118.1(3)		

The nitrogen complexes described above raised the question of the origin of bridging N_2 moieties. A reaction under vacuum (10^{-4} Torr) was then performed.[20] The products were found to be the same as those formed under a nitrogen atmosphere, with marginal differences in complex yields (15% of **3**, 22% of **4**+**5**, 16% of **6**). It is thus suggested that trimethylsilyl-diazomethane served as the nitrogen source for **3-6**.

The original expectation of this reaction was to prepare alkyl hydride **1** by alkylidene insertion from diazoalkane. Examination of the crude products by ^{1}H NMR spectroscopy failed to locate the resonances belonging to **1**. Although **1** was not formed in this reaction, the fate of the trimethylsilylmethylene fragment is of interest.

To work on the rest of the residue, the remaining Et_2O fraction was evaporated to dryness and pentane was used for further crystallization. Green crystals were grown from a chilled pentane solution overnight; these were then structurally characterized to be $(L^{Me}Cr)_2(\mu\text{-NSiMe}_3)(\mu\text{-H})$ (**7**) (13% yield, an average of three determinations). The structure of **7** is depicted in Figure 1.6 and the interatomic distances and angles are listed in Table 1.5. **7** crystallizes in the triclinic space group $P\bar{1}$. It consists of two chromium atoms bridged by a $NSiMe_3$ moiety and a hydride ligand; the latter was located on the difference map and its position refined. The geometry around the bridging nitrogen atom is approximately trigonal planar, i. e. N5 lies in the plane defined by Cr1-Cr2-Si1 (the sum of the bond angles is 359.3°). The molar mass for **7** was located by LIFDI spectrometry, with m/z: 802.3353 [M$^+$] (calcd. m/z: 802.3431). These data suggest the assignment of a dianionic $NSiMe_3$ moiety.

It is thus indicated that **7** is a mixed-valent compound, as is supported by the following structural descriptions. Cr1 has square planar geometry, while Cr2 adopts tetrahedral coordination. These specific geometries are preferred by four-coordinate

chromium(II) and chromium(III), respectively. This also correlates to the difference in bond distances between the chromium atoms and their adjacent ligands. The bond distances of Cr1 to the bridging atoms (Cr1-H1 1.88(2) and Cr1-N5 1.989(2) Å) are longer than those of Cr2 to the bridging atoms (Cr2-H1 1.65(2) and Cr2-N5 1.821(2) Å). The mixed-valent nature of the compound also influences the different bond distances between the chromiums and their coordinated nacnac ligands. The higher oxidation state Cr2 has slightly shorter bond distances to nacnac (Cr2-N3 2.005(2) and Cr2-N4 2.015(2) Å). In contrast, the lower oxidation state Cr1 has longer bond distances of to nacnac (Cr1-N1 2.054(2) and Cr1-N2 2.048(2) Å). The magnetic moment for the independent, i.e. magnetically non-interacting, Cr(III)-Cr(II) ($S = \frac{3}{2}$, $S = \frac{4}{2}$) is expected to be 6.2 μ_B. A room temperature magnetic moment was measured to be $\mu_{eff} = 6.3(1)$ μ_B, close to non-interacting Cr(III)-Cr(II) ions. It is, however, quite unusual for the two chromiums mediated by ligands like $NSiMe_3{}^{2-}$ to be magnetically independent.
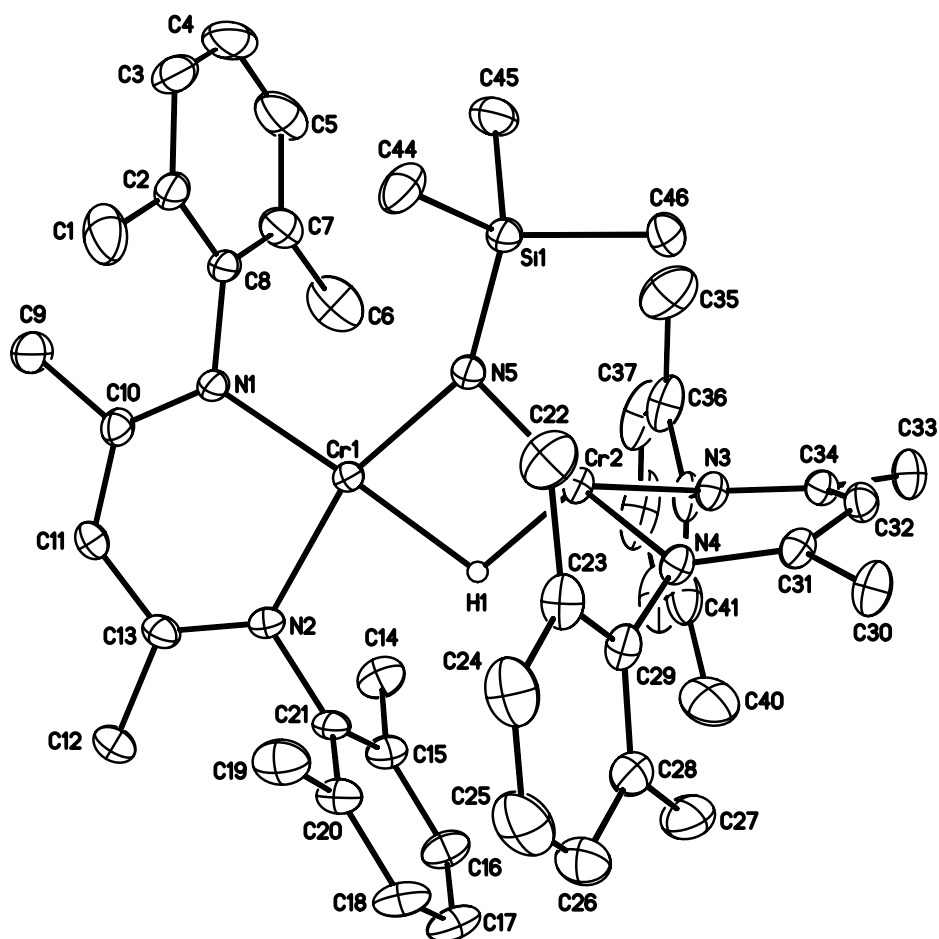
Figure 1.6   Molecular structure of (L^{Me}Cr)$_2$(μ-NSiMe$_3$)(μ-H) (**7**). Ellipsoids are drawn at the 30% probability level. Hydrogen atoms, except the bridging hydride, have been omitted for clarity.

Table 1.5   Interatomic distances (Å) and angles (°) for (L^{Me}Cr)$_2$(μ-NSiMe$_3$)(μ-H) (**7**)

<div align="center">Distances (Å)</div>

Cr(1)-N(5)	1.989(2)	C(11)-C(13)	1.392(4)
Cr(1)-N(2)	2.048(2)	C(12)-C(13)	1.506(3)
Cr(1)-N(1)	2.0537(19)	C(14)-C(15)	1.501(4)
Cr(1)-Cr(2)	2.7746(6)	C(15)-C(16)	1.388(4)
Cr(1)-H(1)	1.88(2)	C(15)-C(21)	1.403(4)
Cr(2)-N(5)	1.821(2)	C(16)-C(17)	1.368(4)
Cr(2)-N(3)	2.005(2)	C(17)-C(18)	1.380(4)
Cr(2)-N(4)	2.015(2)	C(18)-C(20)	1.391(4)
Cr(2)-H(1)	1.65(2)	C(19)-C(20)	1.503(4)
Si(1)-N(5)	1.737(2)	C(20)-C(21)	1.401(4)
Si(1)-C(45)	1.860(3)	C(22)-C(23)	1.502(4)
Si(1)-C(44)	1.868(3)	C(23)-C(24)	1.393(4)
Si(1)-C(46)	1.890(3)	C(23)-C(29)	1.396(4)
N(1)-C(10)	1.330(3)	C(24)-C(25)	1.369(5)
N(1)-C(8)	1.440(3)	C(25)-C(26)	1.365(5)
N(2)-C(13)	1.332(3)	C(26)-C(28)	1.391(4)
N(2)-C(21)	1.437(3)	C(27)-C(28)	1.503(4)
N(3)-C(34)	1.337(3)	C(28)-C(29)	1.399(4)
N(3)-C(42)	1.446(3)	C(30)-C(31)	1.505(4)
N(4)-C(31)	1.342(3)	C(31)-C(32)	1.393(4)
N(4)-C(29)	1.446(3)	C(32)-C(34)	1.397(4)
C(1)-C(2)	1.498(5)	C(33)-C(34)	1.506(3)
C(2)-C(8)	1.399(4)	C(35)-C(36)	1.498(5)
C(2)-C(3)	1.401(5)	C(36)-C(42)	1.397(4)
C(3)-C(4)	1.372(6)	C(36)-C(37)	1.399(4)
C(4)-C(5)	1.362(6)	C(37)-C(38)	1.367(6)
C(5)-C(7)	1.399(4)	C(38)-C(39)	1.366(6)
C(6)-C(7)	1.493(5)	C(39)-C(41)	1.398(5)
C(7)-C(8)	1.389(4)	C(40)-C(41)	1.489(5)
C(9)-C(10)	1.517(4)	C(41)-C(42)	1.404(4)
C(10)-C(11)	1.396(4)		

N(5)-Cr(1)-N(2)	159.54(8)	C(2)-C(8)-N(1)	118.8(3)
N(5)-Cr(1)-N(1)	110.44(8)	N(1)-C(10)-C(11)	124.0(2)
N(2)-Cr(1)-N(1)	89.79(8)	N(1)-C(10)-C(9)	120.8(2)
N(5)-Cr(1)-Cr(2)	40.94(6)	C(11)-C(10)-C(9)	115.2(2)
N(2)-Cr(1)-Cr(2)	119.62(6)	C(13)-C(11)-C(10)	128.6(2)
N(1)-Cr(1)-Cr(2)	149.71(6)	N(2)-C(13)-C(11)	123.5(2)
N(5)-Cr(1)-H(1)	76.2(7)	N(2)-C(13)-C(12)	119.8(2)
N(2)-Cr(1)-H(1)	84.6(7)	C(11)-C(13)-C(12)	116.7(2)
N(1)-Cr(1)-H(1)	166.8(7)	C(16)-C(15)-C(21)	118.3(3)
Cr(2)-Cr(1)-H(1)	35.2(7)	C(16)-C(15)-C(14)	121.5(3)
N(5)-Cr(2)-N(3)	125.78(9)	C(21)-C(15)-C(14)	120.3(2)
N(5)-Cr(2)-N(4)	132.29(9)	C(17)-C(16)-C(15)	121.4(3)
N(3)-Cr(2)-N(4)	90.21(8)	C(16)-C(17)-C(18)	120.0(3)
N(5)-Cr(2)-Cr(1)	45.69(6)	C(17)-C(18)-C(20)	121.1(3)
N(3)-Cr(2)-Cr(1)	128.61(6)	C(18)-C(20)-C(21)	118.1(3)
N(4)-Cr(2)-Cr(1)	135.12(6)	C(18)-C(20)-C(19)	121.2(3)
N(5)-Cr(2)-H(1)	87.0(8)	C(21)-C(20)-C(19)	120.7(2)
N(3)-Cr(2)-H(1)	109.8(8)	C(20)-C(21)-C(15)	121.1(2)
N(4)-Cr(2)-H(1)	111.2(8)	C(20)-C(21)-N(2)	119.8(2)
Cr(1)-Cr(2)-H(1)	41.3(8)	C(15)-C(21)-N(2)	119.1(2)
N(5)-Si(1)-C(45)	114.75(13)	C(24)-C(23)-C(29)	118.4(3)
N(5)-Si(1)-C(44)	111.69(13)	C(24)-C(23)-C(22)	120.1(3)
C(45)-Si(1)-C(44)	105.52(15)	C(29)-C(23)-C(22)	121.5(3)
N(5)-Si(1)-C(46)	109.69(11)	C(25)-C(24)-C(23)	121.3(3)
C(45)-Si(1)-C(46)	105.41(14)	C(26)-C(25)-C(24)	120.1(3)
C(44)-Si(1)-C(46)	109.47(13)	C(25)-C(26)-C(28)	121.0(3)
C(10)-N(1)-C(8)	114.8(2)	C(26)-C(28)-C(29)	118.7(3)
C(10)-N(1)-Cr(1)	126.30(17)	C(26)-C(28)-C(27)	119.9(3)
C(8)-N(1)-Cr(1)	118.77(15)	C(29)-C(28)-C(27)	121.3(3)
C(13)-N(2)-C(21)	116.1(2)	C(23)-C(29)-C(28)	120.5(3)
C(13)-N(2)-Cr(1)	126.81(16)	C(23)-C(29)-N(4)	121.2(2)
C(21)-N(2)-Cr(1)	117.07(15)	C(28)-C(29)-N(4)	118.3(2)
C(34)-N(3)-C(42)	118.6(2)	N(4)-C(31)-C(32)	122.9(2)
C(34)-N(3)-Cr(2)	123.44(17)	N(4)-C(31)-C(30)	120.0(2)
C(42)-N(3)-Cr(2)	117.99(15)	C(32)-C(31)-C(30)	117.0(2)
C(31)-N(4)-C(29)	115.9(2)	C(31)-C(32)-C(34)	127.9(2)

C(31)-N(4)-Cr(2)	122.32(17)	N(3)-C(34)-C(32)	122.7(2)
C(29)-N(4)-Cr(2)	121.74(15)	N(3)-C(34)-C(33)	119.8(2)
Si(1)-N(5)-Cr(2)	117.68(11)	C(32)-C(34)-C(33)	117.5(2)
Si(1)-N(5)-Cr(1)	148.27(12)	C(42)-C(36)-C(37)	118.2(3)
Cr(2)-N(5)-Cr(1)	93.37(9)	C(42)-C(36)-C(35)	121.2(3)
C(8)-C(2)-C(3)	117.5(3)	C(37)-C(36)-C(35)	120.6(3)
C(8)-C(2)-C(1)	121.3(3)	C(38)-C(37)-C(36)	120.9(4)
C(3)-C(2)-C(1)	121.1(3)	C(39)-C(38)-C(37)	120.6(4)
C(4)-C(3)-C(2)	121.1(4)	C(38)-C(39)-C(41)	121.3(4)
C(5)-C(4)-C(3)	120.4(3)	C(39)-C(41)-C(42)	117.8(4)
C(4)-C(5)-C(7)	121.1(4)	C(39)-C(41)-C(40)	120.9(3)
C(8)-C(7)-C(5)	118.0(3)	C(42)-C(41)-C(40)	121.3(3)
C(8)-C(7)-C(6)	121.1(3)	C(36)-C(42)-C(41)	121.2(3)
C(5)-C(7)-C(6)	120.8(3)	C(36)-C(42)-N(3)	120.1(3)
C(7)-C(8)-C(2)	121.8(3)	C(41)-C(42)-N(3)	118.6(3)
C(7)-C(8)-N(1)	119.4(2)		

The cumulative yield of the above products was calculated to be 73% (an average of three determinations). After isolating **3-7**, a brown product was occasionally isolated from the remaining residue after storing pentane solution at -30°C for more than 2 days in 9% yield (see the Experimental). The molecular structure of this product $(L^{Me}Cr)_2(\mu-NCH_2)(\mu-NH)$ (**8**) was determined. It is depicted in Figure 1.7, with the corresponding distances and angles listed in Table 1.6.

8 crystallizes in the monoclinic space group $P\,2_1/n$. It consists of two chromium fragments bridged by one monoanionic (NCH_2^-) and one dianionic (NH^{2-}) ligand. This assignment can be reasoned by the structural information. The N5 atom lies in the plane defined by Cr1-Cr2-C43. Together with the N5-C43 distance of 1.276(4) Å (this bond length corresponds to a N=C double bond [21]), this corresponds to the bridging NCH_2^- moiety. The bridging NH^{2-} ligand is validated by the bond distances of N6 to the chromium atoms. This distance (Cr-N_{avg} 1.8(3) Å) lies in between the N^{3-} moiety in **5** (Cr-N_{avg} 1.751(3) Å) and the other bridging NCH_2^- ligand (Cr-N_{avg} 2.0(1) Å).

8 is considered as another mixed-valent compound $(Cr^{II}-Cr^{III})$ found in this reaction. The corresponding coordination geometry of chromiums are square planar Cr1 and tetrahedral Cr2. The bond distances of bridging ligands to Cr1 (Cr1-N5 2.066(2) and Cr1-N6 2.060(2) Å) are longer than those to Cr2 (Cr2-N5 1.920(2) and Cr2-N6 1.598(2) Å). The mixed-valent **8** also shows different bond distances between nacnac ligands and chromiums. Cr1 to its coordinated nacnac has slightly longer bond distances (Cr1-N1 2.036(2) and Cr1-N2 2.048(2) Å). While the higher oxidation state Cr2 to nacnac shows slightly shorter bond distances (Cr2-N3 1.989(2) and Cr2-N4 1.981(2) Å).
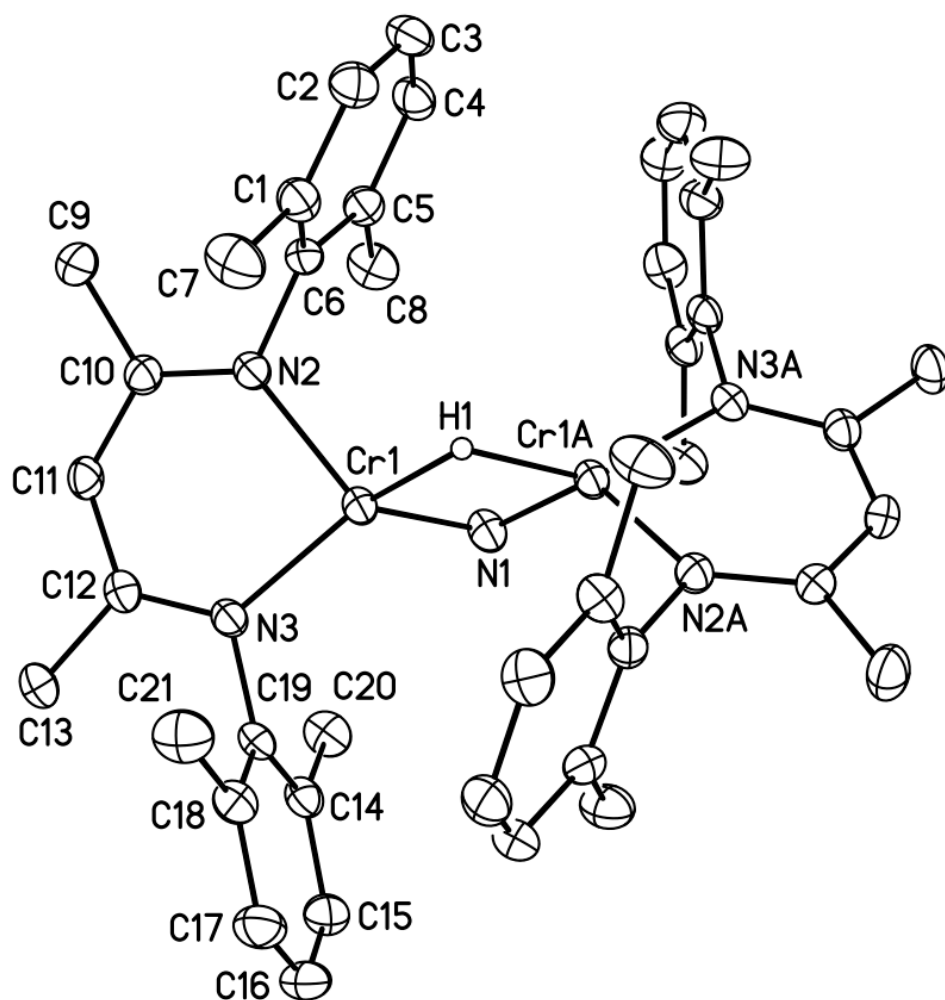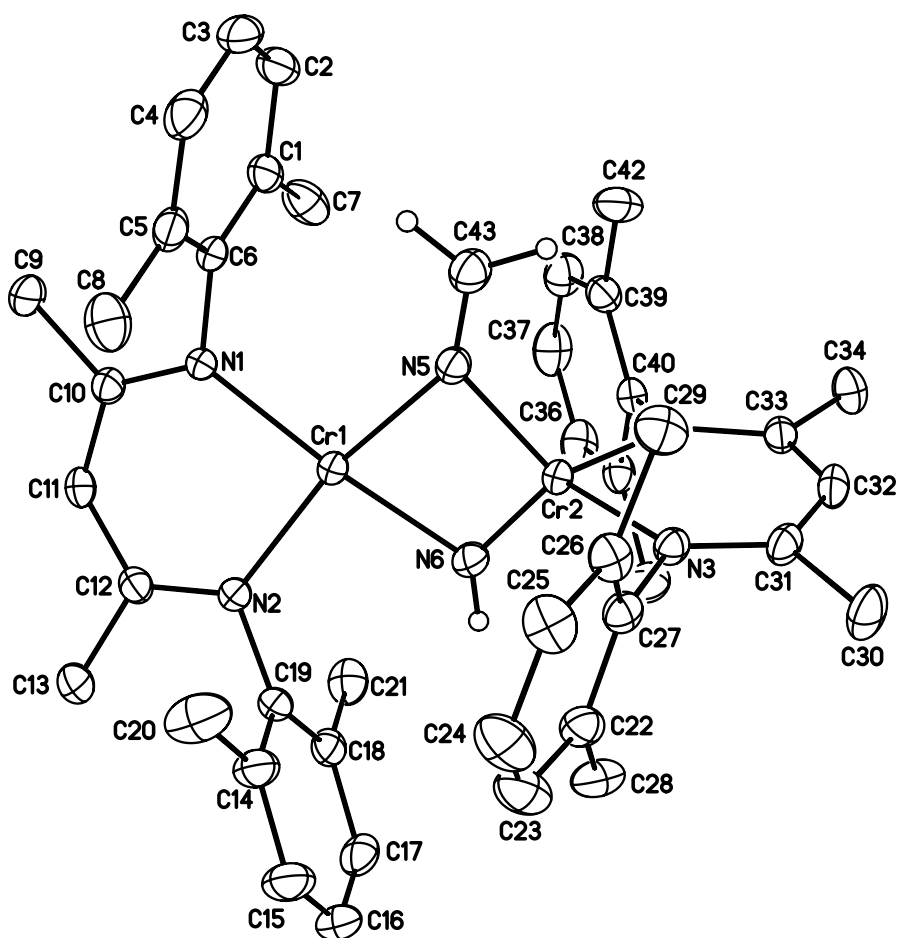
Figure 1.7   Molecular structure of $(L^{Me}Cr)_2(\mu\text{-}NCH_2)(\mu\text{-}NH)$ (**8**). Ellipsoids are drawn at the 30% probability level. Hydrogen atoms, except those in the core, and a pentane molecule have been omitted for clarity.

Table 1.6   Interatomic distances (Å) and angles (º) for (L^{Me}Cr)$_2$(µ-NCH$_2$)(µ-NH) (**8**)

Distances (Å)

Cr(1)-N(1)	2.036(2)	C(14)-C(15)	1.394(4)
Cr(1)-N(2)	2.048(2)	C(14)-C(19)	1.397(4)
Cr(1)-N(6)	2.060(2)	C(14)-C(20)	1.505(5)
Cr(1)-N(5)	2.066(2)	C(15)-C(16)	1.366(5)
Cr(2)-N(6)	1.598(2)	C(16)-C(17)	1.375(5)
Cr(2)-N(5)	1.920(2)	C(17)-C(18)	1.401(4)
Cr(2)-N(4)	1.981(2)	C(18)-C(19)	1.398(4)
Cr(2)-N(3)	1.989(2)	C(18)-C(21)	1.507(4)
N(1)-C(10)	1.335(3)	C(22)-C(23)	1.403(5)
N(1)-C(6)	1.434(3)	C(22)-C(27)	1.404(4)
N(2)-C(12)	1.324(3)	C(22)-C(28)	1.495(4)
N(2)-C(19)	1.438(3)	C(23)-C(24)	1.376(5)
N(3)-C(31)	1.327(3)	C(24)-C(25)	1.377(5)
N(3)-C(27)	1.439(3)	C(25)-C(26)	1.395(4)
N(4)-C(33)	1.337(3)	C(26)-C(27)	1.396(4)
N(4)-C(40)	1.444(3)	C(26)-C(29)	1.509(4)
N(5)-C(43)	1.276(4)	C(30)-C(31)	1.510(4)
C(1)-C(2)	1.384(4)	C(31)-C(32)	1.394(4)
C(1)-C(6)	1.401(4)	C(32)-C(33)	1.392(4)
C(1)-C(7)	1.511(4)	C(33)-C(34)	1.512(4)
C(2)-C(3)	1.364(5)	C(35)-C(36)	1.383(4)
C(3)-C(4)	1.373(5)	C(35)-C(40)	1.402(4)
C(4)-C(5)	1.398(4)	C(35)-C(41)	1.502(4)
C(5)-C(6)	1.393(4)	C(36)-C(37)	1.370(5)
C(5)-C(8)	1.503(4)	C(37)-C(38)	1.378(5)
C(9)-C(10)	1.516(4)	C(38)-C(39)	1.392(4)
C(10)-C(11)	1.389(4)	C(39)-C(40)	1.391(4)
C(11)-C(12)	1.404(4)	C(39)-C(42)	1.502(4)
C(12)-C(13)	1.514(4)		

Angles (º)

N(1)-Cr(1)-N(2)	89.69(9)	N(2)-C(12)-C(13)	120.3(3)
N(1)-Cr(1)-N(6)	165.57(9)	C(11)-C(12)-C(13)	115.6(2)

N(2)-Cr(1)-N(6)	91.00(9)	C(15)-C(14)-C(19)	118.7(3)
N(1)-Cr(1)-N(5)	101.39(9)	C(15)-C(14)-C(20)	120.3(3)
N(2)-Cr(1)-N(5)	166.35(9)	C(19)-C(14)-C(20)	121.0(3)
N(6)-Cr(1)-N(5)	80.26(9)	C(16)-C(15)-C(14)	120.9(3)
N(6)-Cr(2)-N(5)	97.80(11)	C(15)-C(16)-C(17)	120.5(3)
N(6)-Cr(2)-N(4)	115.86(11)	C(16)-C(17)-C(18)	120.7(3)
N(5)-Cr(2)-N(4)	117.13(9)	C(19)-C(18)-C(17)	118.3(3)
N(6)-Cr(2)-N(3)	115.70(11)	C(19)-C(18)-C(21)	120.8(3)
N(5)-Cr(2)-N(3)	120.15(9)	C(17)-C(18)-C(21)	120.9(3)
N(4)-Cr(2)-N(3)	91.78(9)	C(14)-C(19)-C(18)	120.8(3)
C(10)-N(1)-C(6)	116.7(2)	C(14)-C(19)-N(2)	119.0(2)
C(10)-N(1)-Cr(1)	126.27(18)	C(18)-C(19)-N(2)	120.1(3)
C(6)-N(1)-Cr(1)	117.01(16)	C(23)-C(22)-C(27)	117.6(3)
C(12)-N(2)-C(19)	115.5(2)	C(23)-C(22)-C(28)	120.4(3)
C(12)-N(2)-Cr(1)	126.30(18)	C(27)-C(22)-C(28)	122.0(3)
C(19)-N(2)-Cr(1)	118.10(16)	C(24)-C(23)-C(22)	121.0(3)
C(31)-N(3)-C(27)	119.4(2)	C(23)-C(24)-C(25)	120.5(3)
C(31)-N(3)-Cr(2)	126.47(19)	C(24)-C(25)-C(26)	120.9(3)
C(27)-N(3)-Cr(2)	114.01(17)	C(25)-C(26)-C(27)	118.2(3)
C(33)-N(4)-C(40)	118.6(2)	C(25)-C(26)-C(29)	120.3(3)
C(33)-N(4)-Cr(2)	126.73(18)	C(27)-C(26)-C(29)	121.5(3)
C(40)-N(4)-Cr(2)	114.09(16)	C(26)-C(27)-C(22)	121.8(3)
C(43)-N(5)-Cr(2)	129.8(2)	C(26)-C(27)-N(3)	118.9(3)
C(43)-N(5)-Cr(1)	143.9(2)	C(22)-C(27)-N(3)	119.3(3)
Cr(2)-N(5)-Cr(1)	86.31(9)	N(3)-C(31)-C(32)	123.4(2)
C(2)-C(1)-C(6)	117.9(3)	N(3)-C(31)-C(30)	119.6(3)
C(2)-C(1)-C(7)	121.3(3)	C(32)-C(31)-C(30)	117.0(3)
C(6)-C(1)-C(7)	120.7(3)	C(33)-C(32)-C(31)	128.3(3)
C(3)-C(2)-C(1)	121.5(3)	N(4)-C(33)-C(32)	122.9(3)
C(2)-C(3)-C(4)	120.4(3)	N(4)-C(33)-C(34)	119.2(2)
C(3)-C(4)-C(5)	120.6(3)	C(32)-C(33)-C(34)	117.9(2)
C(6)-C(5)-C(4)	118.1(3)	C(36)-C(35)-C(40)	117.9(3)
C(6)-C(5)-C(8)	120.9(3)	C(36)-C(35)-C(41)	121.3(3)
C(4)-C(5)-C(8)	121.0(3)	C(40)-C(35)-C(41)	120.8(3)
C(5)-C(6)-C(1)	121.4(3)	C(37)-C(36)-C(35)	121.8(3)
C(5)-C(6)-N(1)	118.9(2)	C(36)-C(37)-C(38)	119.5(3)
C(1)-C(6)-N(1)	119.7(3)	C(37)-C(38)-C(39)	121.2(3)

Cr(2)-N(6)-Cr(1)	95.62(11)	C(40)-C(39)-C(38)	118.2(3)
N(1)-C(10)-C(11)	123.8(3)	C(40)-C(39)-C(42)	121.8(3)
N(1)-C(10)-C(9)	119.7(2)	C(38)-C(39)-C(42)	120.1(3)
C(11)-C(10)-C(9)	116.5(2)	C(39)-C(40)-C(35)	121.4(3)
C(10)-C(11)-C(12)	127.8(3)	C(39)-C(40)-N(4)	120.9(2)
N(2)-C(12)-C(11)	124.1(2)	C(35)-C(40)-N(4)	117.6(2)

It is unclear how a reaction of $(L^{Me}Cr)_2(\mu\text{-}H)_2$ (**2**) with trimethylsilyl-diazomethane would result in a mixture of products **3-8**. In an attempt to provide clues about the mechanism, the reaction was repeated with more sterically protected nacnac ligand, i.e. L^{iPr} = 2,4-pentane-N,N'-bis(2,6-diisopropylphenyl)ketiminate. Treatment of $(L^{iPr}Cr)_2(\mu\text{-}H)_2$ [12] with 1.0 equiv. of trimethylsilyl-diazomethane in THF, with stirring for 12 hours at room temperature under a nitrogen atmosphere, led to only one isolable product in 40%. Figure 1.8 shows the solid-state structure of this product, $(L^{iPr}Cr)_2(\mu\text{-}N)(\mu\text{-}N(H)NC(H)SiMe_3)$ (**9**). The interatomic bond distances and angles are listed in Table 1.7.

9 crystallizes in the monoclinic space group $P\,2_1/n$. Binuclear **9** consists of two chromiums bridged by a nitride and a $N(H)NC(H)SiMe_3$ moiety. The bridging nitride N^{3-} was assigned instead of the NH^{2-} due to the short bond distances of Cr1-N5 (1.696(4) Å) and Cr2-N5 (1.837(4) Å). Comparing these numbers with the Cr-N distance of 1.751(3) Å of (μ-nitrido) **5**, the bridging Cr-N$_{nitride}$ bonds in **9** are considered to be a double and single bond, respectively. On the other side, the bridging $N(H)NC(H)SiMe_3$ moiety was indicated by single bond character of N6-N7 (1.360(5) Å) and a double bond to the N7-C59 bond (1.317(5) Å). The trigonal planar geometry around N7 is shown by the sum of the bond angles being 359.8°. The distance for Cr1-N6 (1.967(4) Å) is short when compared with Cr2-N7 (2.127(4) Å), indicating a dative bond for the latter. The Lewis structure representation is shown in Scheme 1.8. As a conclusion, the oxidation state assignments for **9** is best described as Cr(IV)-Cr(II). Due to the steric interactions between ligands, the preferred square planar coordination of Cr(II) is not expressed.
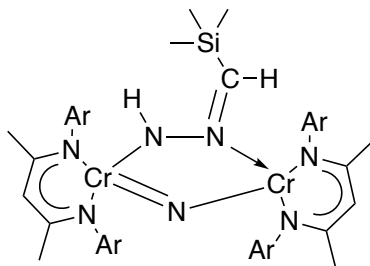
Scheme 1.8 The Lewis structure of **9**

The LIFDI mass spectrum showed the molecular ion of m/z: 1067.6648 [M^+], and it showed excellent agreement with the calculated isotope patterns of $C_{62}H_{93}N_7Cr_2Si$ (calcd. m/z: 1067.6077 [M^+]). The magnetic moment of **9** was measured to be 6.1(1) μ_B (293K), which is greater than magnetically non-interacting Cr(IV)-Cr(II) ($S = \frac{2}{2}$, $S = \frac{4}{2}$) moment of 5.6 μ_B, suggesting ferromagnetic coupling between the chromium centers.
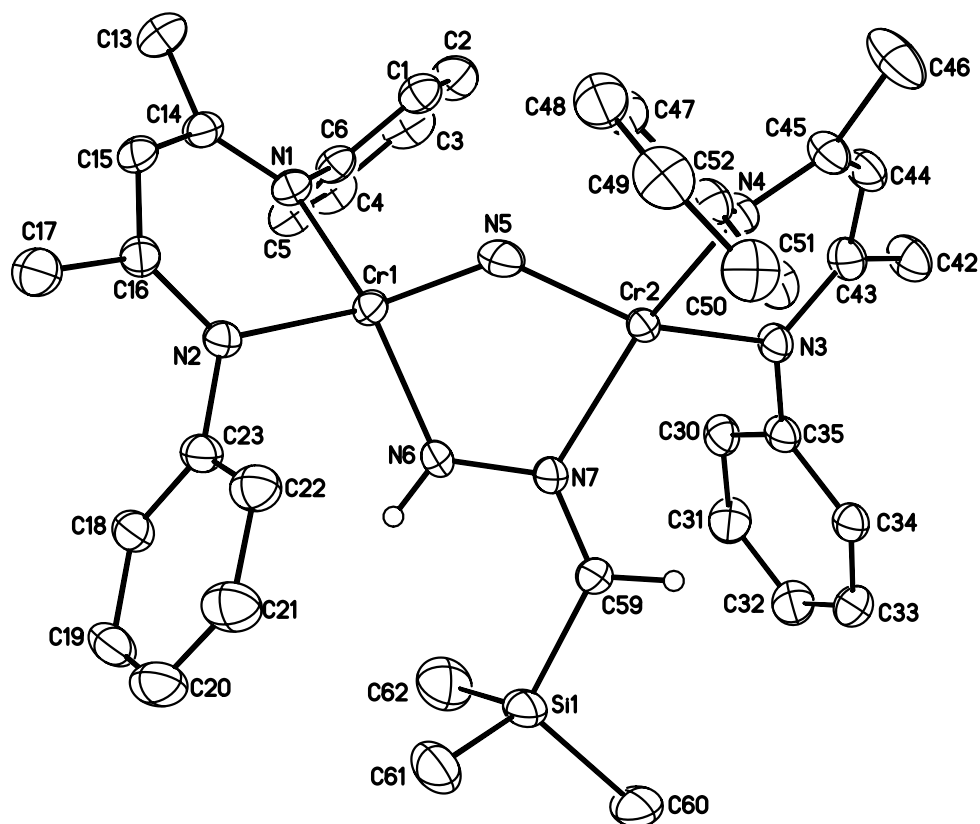
Figure 1.8   Molecular structure of $(L^{iPr}Cr)_2(\mu\text{-}N)(\mu\text{-}N(H)NC(H)SiMe_3)$ (**9**).
Ellipsoids are drawn at the 30% probability level. Hydrogen atoms,
except those located in the core, a pentane molecule, and isopropyl
groups have been omitted for clarity.

Table 1.7   Interatomic distances (Å) and angles (°) for (L^{iPr}Cr)$_2$(μ-N)(μ-
N(H)NC(H)SiMe$_3$) (**9**)

	Distances (Å)		
Cr(1)-N(5)	1.696(4)	Cr(2)-N(7)	2.127(4)
Cr(1)-N(6)	1.967(4)	Si(1)-C(60)	1.850(6)
Cr(1)-N(1)	2.007(3)	Si(1)-C(59)	1.856(5)
Cr(1)-N(2)	2.033(3)	Si(1)-C(61)	1.862(6)
N(1)-C(14)	1.322(5)	Si(1)-C(62)	1.862(7)
N(1)-C(6)	1.439(5)	N(3)-C(43)	1.354(6)
N(2)-C(16)	1.341(5)	N(3)-C(35)	1.440(5)
N(2)-C(23)	1.436(5)	N(4)-C(45)	1.323(6)
C(1)-C(2)	1.389(6)	N(4)-C(52)	1.449(5)
C(1)-C(6)	1.393(6)	N(6)-N(7)	1.360(5)
C(1)-C(7)	1.511(6)	N(7)-C(59)	1.317(5)
C(2)-C(3)	1.371(7)	C(30)-C(35)	1.399(6)
C(3)-C(4)	1.352(7)	C(30)-C(31)	1.399(7)
C(4)-C(5)	1.390(6)	C(30)-C(36)	1.495(7)
C(5)-C(6)	1.406(6)	C(31)-C(32)	1.371(8)
C(5)-C(10)	1.507(6)	C(32)-C(33)	1.375(7)
C(7)-C(9)	1.532(6)	C(33)-C(34)	1.381(6)
C(7)-C(8)	1.541(6)	C(34)-C(35)	1.403(6)
C(10)-C(11)	1.505(8)	C(34)-C(39)	1.533(7)
C(10)-C(12)	1.512(8)	C(36)-C(38)	1.519(7)
C(13)-C(14)	1.508(5)	C(36)-C(37)	1.522(7)
C(14)-C(15)	1.386(5)	C(39)-C(40)	1.512(8)
C(15)-C(16)	1.393(5)	C(39)-C(41)	1.512(8)
C(16)-C(17)	1.501(5)	C(42)-C(43)	1.507(6)
C(18)-C(19)	1.403(6)	C(43)-C(44)	1.380(7)
C(18)-C(23)	1.405(6)	C(44)-C(45)	1.386(7)
C(18)-C(24)	1.508(6)	C(45)-C(46)	1.515(7)
C(19)-C(20)	1.364(7)	C(47)-C(48)	1.392(7)
C(20)-C(21)	1.370(7)	C(47)-C(52)	1.408(7)
C(21)-C(22)	1.387(6)	C(47)-C(53)	1.502(7)
C(22)-C(23)	1.398(6)	C(48)-C(49)	1.362(8)
C(22)-C(27)	1.502(6)	C(49)-C(50)	1.359(8)
C(24)-C(25)	1.507(7)	C(50)-C(51)	1.419(7)

C(24)-C(26)	1.517(7)	C(51)-C(52)	1.407(7)
C(27)-C(29)	1.513(8)	C(51)-C(56)	1.506(7)
C(27)-C(28)	1.530(8)	C(53)-C(55)	1.521(9)
Cr(2)-N(5)	1.837(4)	C(53)-C(54)	1.541(8)
Cr(2)-N(4)	2.026(4)	C(56)-C(58)	1.493(9)
Cr(2)-N(3)	2.060(3)	C(56)-C(57)	1.503(9)

Angles (°)

N(5)-Cr(1)-N(6)	87.40(18)	C(60)-Si(1)-C(59)	106.5(3)
N(5)-Cr(1)-N(1)	108.11(17)	C(60)-Si(1)-C(61)	110.0(3)
N(6)-Cr(1)-N(1)	146.51(16)	C(59)-Si(1)-C(61)	109.7(3)
N(5)-Cr(1)-N(2)	132.97(19)	C(60)-Si(1)-C(62)	108.1(3)
N(6)-Cr(1)-N(2)	101.37(14)	C(59)-Si(1)-C(62)	110.3(3)
N(1)-Cr(1)-N(2)	89.62(13)	C(61)-Si(1)-C(62)	112.1(3)
C(14)-N(1)-C(6)	118.5(3)	C(43)-N(3)-C(35)	117.1(4)
C(14)-N(1)-Cr(1)	124.9(3)	C(43)-N(3)-Cr(2)	120.1(3)
C(6)-N(1)-Cr(1)	116.7(2)	C(35)-N(3)-Cr(2)	122.1(3)
C(16)-N(2)-C(23)	116.8(3)	C(45)-N(4)-C(52)	117.8(4)
C(16)-N(2)-Cr(1)	123.0(2)	C(45)-N(4)-Cr(2)	124.6(3)
C(23)-N(2)-Cr(1)	120.0(2)	C(52)-N(4)-Cr(2)	117.5(3)
C(2)-C(1)-C(6)	117.3(4)	Cr(1)-N(5)-Cr(2)	133.3(2)
C(2)-C(1)-C(7)	119.2(4)	N(7)-N(6)-Cr(1)	121.6(3)
C(6)-C(1)-C(7)	123.5(4)	C(59)-N(7)-N(6)	121.3(4)
C(3)-C(2)-C(1)	121.5(5)	C(59)-N(7)-Cr(2)	125.3(3)
C(4)-C(3)-C(2)	120.5(4)	N(6)-N(7)-Cr(2)	113.2(3)
C(3)-C(4)-C(5)	121.3(5)	C(35)-C(30)-C(31)	118.6(5)
C(4)-C(5)-C(6)	117.6(4)	C(35)-C(30)-C(36)	123.0(4)
C(4)-C(5)-C(10)	119.7(4)	C(31)-C(30)-C(36)	118.3(5)
C(6)-C(5)-C(10)	122.7(4)	C(32)-C(31)-C(30)	120.8(5)
C(1)-C(6)-C(5)	121.8(4)	C(31)-C(32)-C(33)	120.0(5)
C(1)-C(6)-N(1)	119.9(4)	C(32)-C(33)-C(34)	121.3(5)
C(5)-C(6)-N(1)	118.3(4)	C(33)-C(34)-C(35)	118.8(5)
C(1)-C(7)-C(9)	111.2(4)	C(33)-C(34)-C(39)	119.8(4)
C(1)-C(7)-C(8)	111.9(4)	C(35)-C(34)-C(39)	121.3(4)
C(9)-C(7)-C(8)	110.0(4)	C(30)-C(35)-C(34)	120.4(4)
C(11)-C(10)-C(5)	110.5(5)	C(30)-C(35)-N(3)	120.7(4)

C(11)-C(10)-C(12)	109.6(6)	C(34)-C(35)-N(3)	118.9(4)
C(5)-C(10)-C(12)	113.3(5)	C(30)-C(36)-C(38)	113.5(5)
N(1)-C(14)-C(15)	123.5(3)	C(30)-C(36)-C(37)	113.5(5)
N(1)-C(14)-C(13)	120.5(4)	C(38)-C(36)-C(37)	107.9(5)
C(15)-C(14)-C(13)	116.0(4)	C(40)-C(39)-C(41)	109.5(5)
C(14)-C(15)-C(16)	127.8(4)	C(40)-C(39)-C(34)	113.4(5)
N(2)-C(16)-C(15)	123.0(4)	C(41)-C(39)-C(34)	112.9(5)
N(2)-C(16)-C(17)	121.7(4)	N(3)-C(43)-C(44)	123.5(4)
C(15)-C(16)-C(17)	115.3(4)	N(3)-C(43)-C(42)	119.3(4)
C(19)-C(18)-C(23)	117.5(4)	C(44)-C(43)-C(42)	117.3(4)
C(19)-C(18)-C(24)	119.5(4)	C(43)-C(44)-C(45)	129.6(4)
C(23)-C(18)-C(24)	123.1(4)	N(4)-C(45)-C(44)	122.3(4)
C(20)-C(19)-C(18)	121.4(4)	N(4)-C(45)-C(46)	120.9(4)
C(19)-C(20)-C(21)	120.0(4)	C(44)-C(45)-C(46)	116.8(4)
C(20)-C(21)-C(22)	121.6(5)	C(48)-C(47)-C(52)	117.3(5)
C(21)-C(22)-C(23)	118.0(4)	C(48)-C(47)-C(53)	119.9(5)
C(21)-C(22)-C(27)	119.3(4)	C(52)-C(47)-C(53)	122.8(4)
C(23)-C(22)-C(27)	122.7(4)	C(49)-C(48)-C(47)	121.9(5)
C(22)-C(23)-C(18)	121.4(4)	C(50)-C(49)-C(48)	120.7(5)
C(22)-C(23)-N(2)	120.2(4)	C(49)-C(50)-C(51)	121.3(5)
C(18)-C(23)-N(2)	118.4(4)	C(52)-C(51)-C(50)	116.7(5)
C(25)-C(24)-C(18)	112.6(5)	C(52)-C(51)-C(56)	123.4(4)
C(25)-C(24)-C(26)	109.4(4)	C(50)-C(51)-C(56)	119.9(5)
C(18)-C(24)-C(26)	112.7(4)	C(47)-C(52)-C(51)	122.0(4)
C(22)-C(27)-C(29)	113.4(5)	C(47)-C(52)-N(4)	121.0(4)
C(22)-C(27)-C(28)	110.9(4)	C(51)-C(52)-N(4)	117.0(4)
C(29)-C(27)-C(28)	110.2(5)	C(47)-C(53)-C(55)	112.9(5)
N(5)-Cr(2)-N(4)	101.43(17)	C(47)-C(53)-C(54)	112.6(5)
N(5)-Cr(2)-N(3)	140.19(19)	C(55)-C(53)-C(54)	108.6(5)
N(4)-Cr(2)-N(3)	90.32(14)	C(58)-C(56)-C(57)	109.8(7)
N(5)-Cr(2)-N(7)	84.01(15)	C(58)-C(56)-C(51)	111.3(5)
N(4)-Cr(2)-N(7)	154.39(15)	C(57)-C(56)-C(51)	114.0(5)
N(3)-Cr(2)-N(7)	101.49(14)	N(7)-C(59)-Si(1)	129.5(4)

Based on the structure of **9**, a re-examination of the mixture of products from the reaction with L^{Me} was conducted. **9'**, in the form of $(L^{Me}Cr)_2(\mu\text{-N})(\mu\text{-N}(H)NC(H)SiMe_3)$ (m/z: 843.3405 [M$^+$], calcd. m/z: 843.3571), was evidenced by LIFDI mass spectrum of crude product, shown in Figure 1.9. The structure of **9'** could not be obtained, but **9'** could be an intermediate in the reaction. A proposed mechanism of the reaction of $(L^{Me}Cr)_2(\mu\text{-H})_2$ (**2**) with trimethylsilyl-diazomethane is depicted in **Appendix A**.
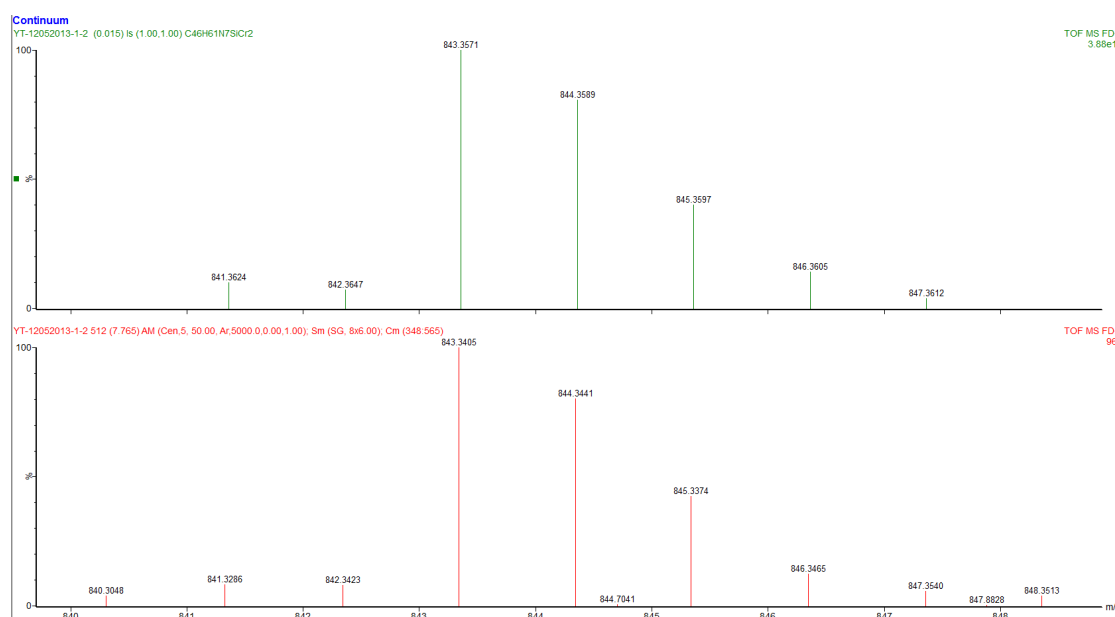
Figure 1.9   LIFDI mass spectrum of crude products showed the mass for **9'**, $(L^{Me}Cr)_2(\mu\text{-N})(\mu\text{-N}(H)NC(H)SiMe_3)$, and its predicted isotope pattern (top)

In conclusion, this chapter narrates the isolation of products from the reaction of $(L^{Me}Cr)_2(\mu\text{-H})_2$ (**2**) with 1.0 equiv. of trimethylsilyl-diazomethane, and discusses their characterizations, particularly focusing on the structural determinations. The

absence of the formation of alkyl hydride complex from the alkylidene insertion reaction was unexpected. Therefore, the synthesis of the chromium alkyl hydride requires additional investigation, and it will be further discussed in **Chapter 2**.

1.3 Experimental

1.3.1 General Considerations

All manipulations were carried out with standard Schlenk, vacuum line, and glovebox techniques. Pentane, diethyl ether and toluene were degassed and dried by passing through activated alumina. Tetrahydrofuran was distilled from purple Na benzophenone/ketyl solutions. THF-d_8 and C_6D_6 were predried with sodium and stored under vacuum over Na/K alloy. $CrCl_2$ (anhydrous) was purchased from Strem Chemical Co. Lithium triethylborohydride was purchased as a 1M solution in THF from Sigma-Aldrich. (Trimethylsilyl)diazomethane was purchased as a 2M solution in hexane from Acros Organics.

^{1}H NMR spectra were taken on a Bruker AVIII-400 spectrometer and were referenced to the residual protons of the solvent (C_6D_6, 7.15 ppm, THF-d_8 = 3.58 and 1.73 ppm). FT-IR spectra were obtained using a Nicolet Magna-IR 560 spectrometer with a resolution of 4 cm^{-1}. X-ray crystallographic studies were conducted at the University of Delaware X-ray Crystallography Laboratory. Elemental analyses were obtained from Robertson Microlit, Ledgewood, NJ. Mass spectra were obtained by the University of Delaware Mass Spectrometry Facility. Room temperature magnetic susceptibility measurements were carried out using a Johnson Matthey magnetic susceptibility balance. Measurement were corrected for diamagnetism using Pascal constants and converted into effective magnetic moments.[22]

1.3.2 Alternative preparation of (L^{Me}Cr)$_2$(μ-H)$_2$ (2)

Besides the reported synthesis of **2** by β-elimination from the product of the reaction of L^{Me}CrCl$_2$(THF)$_2$ with EtMgBr (2 equiv.),[3] another approach was used here, as discussed in the following.

[L^{Me}Cr(THF)]$_2$(*μ*-Cl)$_2$ [23] (1.00 g, 1.08 mmol) was dissolved in 50 mL THF giving a green solution. 2.1 equivalents of lithium triethylborohydride (1M in THF) (2.26 mL) was added dropwise with stirring over 1 minutes. The solution was stirred for 4 hours during which time the color changed to brown. The THF was removed in vacuo and the residue was extracted with toluene and the extract filtered through celite. The resulting solution was concentrated to 15 mL and cooled to -30°C overnight to yield red crystals of **2** (0.46 g, 60% yield). ^{1}H NMR (400 MHz, C$_6$D$_6$): 19.2 (br), 6.55 (br), 6.08 (br), 3.02 (br) ppm.

1.3.3 Preparation of complexes 3-8

The reacting ingredients used in the synthesis of these six complexes are exactly the same. (L^{Me}Cr)$_2$(μ-H)$_2$ (**2**) (1.00 g, 1.40 mmol) was dissolved in 60 mL pre-chilled (-30°C) THF giving a red solution. 1.0 equiv. of trimethylsilyl-diazomethane in hexanes (0.70 mL) was added dropwise with stirring over 3 minutes. The solution was then stirred for 12 hours during which time the color changed to emerald green. The complexes **3-8** are then separated by fractional crystallization (see below).

1.3.4 Isolation of [L^{Me}Cr(THF)]$_3$(μ-N$_2$)$_3$ (3)

After the reaction solution was stirred at room temperature for 12 hours, the THF was removed in vacuo. The residue was extracted with Et$_2$O and the extract was filtered through a glass filter funnel. The Et$_2$O insoluble orange powder collected on the filter was redissolved in THF and further filtered through celite, which was then

concentrated to 10 mL and cooled to -30℃ to yield red crystals of **3** (0.256 g, 20%

yield). ^{1}H NMR (400 MHz, C_6D_6): 69 (br), 9.4 (br), 7.94 (br), 6.06 (br), -4.7 (br),

-7.05 (br) ppm. IR (KBr): 3066 (w), 2971 (s), 2918 (m), 2860 (w), 2244 (w), 2124

(w), 1523 (s), 1454 (m), 1435 (s), 1389 (m), 1263 (m), 1243 (w), 1185 (m), 1095 (w),

1069 (w), 1024 (m), 984 (w), 964 (w), 918 (w), 886 (w), 850 (w), 764 (m) cm^{-1}. μ_{eff}

(293K) = 6.5(1) μ_B. Mp: 288°C. Mass Spectrum m/z: 1157.4965 [M$^+$- 3 C_4H_8O].

Calcd. m/z: 1156.4476 [M$^+$- 3 C_4H_8O]. Anal. calcd. for $C_{75}H_{99}N_{12}Cr_3O_3$: C, 65.62; H,

7.27; N, 12.24. Found: C, 66.90; H, 6.67; N, 10.50.

1.3.5   Isolation of (L^{Me}Cr)$_4$(μ-N$_2$)$_4$ (4) and (L^{Me}Cr)$_2$(μ-N)(μ-H) (5)

After the Et$_2$O insoluble product **3** had been filtered off, the Et$_2$O solution was

then concentrated to 15 mL and cooled to -30°C overnight to yield orange crystals,

which were a mixture of **4** and **5** (0.247 g, 23% yield, based on **4**). Crystals of **5** were

occasionally found to be more than **4** in the mixture, by checking the unit cells of

crystals with a match of mass analysis. As a result, two sets of resonances can be

distinguished. Therefore, separate ^{1}H NMR data are presented. ^{1}H NMR (400 MHz,

C_6D_6) for **4**: 8.68 (br), 6.80 (br), 6.19 (br), 2.10 (br) ppm. ^{1}H NMR (400 MHz, C_6D_6)

for **5**: 27.9 (br), 17.4 (br), 12.5 (br), -14.4 (br) ppm. Combined IR (KBr): 3058 (w),

3018 (w), 2958 (m), 2918 (m), 2840 (w), 2063 (m) (tentatively assigned as the N$_2$

stretch of **4**), 1529 (s), 1459 (m), 1438 (s), 1369 (s), 1263 (m), 1242 (w), 1185 (m),

1095 (w), 1022 (w), 964 (w), 853 (w), 762 (m) cm^{-1}. Mp: 217°C. Mass Spectrum m/z:

1540.5460 [M$^+$] (**4**), 729.3627 [M$^+$] (**5**). Calcd. m/z: 1540.5953 [M$^+$] (**4**), 729.2957

[M$^+$] (**5**).

1.3.6 Isolation of $(L^{Me}Cr)_3(\mu-N_2)_3(\mu-N)CrL^{Me}$ (6)

After the isolation of complexes **3-5**, the Et_2O solution was further cooled to -30℃ for two more days to yield red-orange crystals of **6** (0.181 g, 17% yield). ^1H NMR (400 MHz, THF-d_8): 67 (br), 39.4 (br), 10.0 (br), 8.54 (br), 7.89 (br), 5.77 (br), 5.04 (br), 3.64 (br), 2.68 (br), -16.8 (br), -20.9 (br) ppm. IR (KBr): 3015 (w), 2961 (m), 2921 (m), 2848 (w), 2210 (w), 2139 (w), 1525 (s), 1466 (w), 1439 (m), 1377 (s), 1262 (w), 1237 (w), 1184 (m), 1096 (w), 1023 (w), 963 (w), 853 (w), 764 (m) cm^{-1}. μ_{eff} (293K) = 6.1(1) μ_B. Mp: 226°C.

1.3.7 Isolation of $(L^{Me}Cr)_2(\mu-NSiMe_3)(\mu-H)$ (7)

From the remaining solution, Et_2O was removed in vacuo. The residue was extracted with pentane and the extract filtered through celite. The resulting solution was concentrated to 10 mL and cooled to -30℃ overnight to yield green crystals of **7** (0.168 g, 15% yield). ^1H NMR (400 MHz, C_6D_6): 13.1 (br), 10.4 (br), -6.3 (br), -9.1 (br) ppm. IR (KBr): 3066 (w), 2957 (w), 2924 (m), 2848 (w), 1530 (s), 1443 (m), 1388 (s), 1262 (w), 1233 (w), 1186 (m), 1095 (w), 1020 (w), 976 (w), 900 (w), 846 (w), 763 (m) cm^{-1}. μ_{eff} (293K) = 6.3(1) μ_B. Mp: 232°C. Mass Spectrum m/z: 802.3353 [M$^+$]. Calcd. m/z: 802.3431 [M$^+$]. Anal. calcd. for $C_{45}H_{60}N_5Cr_2Si_1$: C, 67.3; H, 7.53; N, 8.72. Found: C, 66.31; H, 7.75; N, 8.54.

1.3.8 Isolation of $(L^{Me}Cr)_2(\mu-NCH_2)(\mu-NH)$ (8)

After the isolation of **7** from pentane solution, the pentane solution was further cooled at -30℃ for more than 2 days. A brown solid was occasionally precipitated and collected. It was redissolved in pentane and further chilled at -30°C overnight to yield brown crystals of **8** (0.095 g, 9% yield). ^1H NMR (400 MHz, C_6D_6): 72.2 (br), 9.0 (br), 3.60 (br), 1.42 (br), 1.25 (br), 0.34 (br) ppm. IR (KBr): 3610 (w), 3011 (w), 2957

(m), 2921 (m), 2852 (w), 1528 (s), 1443 (s), 1390 (s), 1263 (w), 1186 (m), 1095 (m), 1021 (m), 851 (m), 764 (s) cm^{-1}. μ_{eff} (293K) = 4.4(1) μ_B. Mp: 230°C. Mass Spectrum m/z: 757.3699 [M$^+$]. Calcd. m/z: 757.3144 [M$^+$].

1.3.9 Preparation of (L^{iPr}Cr)$_2$(μ-N)(μ-N(H)NC(H)SiMe$_3$) (9)

(L^{iPr}Cr)$_2$(μ-H)$_2$ [12] (1.00 g, 1.06 mmol) was dissolved in 60 mL THF giving a violet solution. 1.0 equivalents of trimethylsilyl-diazomethane (0.53 mL), 2M in hexanes, was added dropwise with stirring over 3 minutes. The solution was stirred for 12 hours during which time the color changed to emerald green. The THF was removed in vacuo and the residue was extracted with diethyl ether and filtered over celite. The resulting solution was concentrated to 15 mL and cooled to -30°C overnight to yield red-brown crystals of **9** (0.448 g, 40% yield). ^{1}H NMR (400 MHz, C$_6$D$_6$): 113.0 (br), 103.0 (br), 18.2 (br), 15.6 (br), 12.4 (br), 10.90 (br), 10.19 (br), 9.09 (br), 6.72 (br), 3.43 (br), 2.33 (br), -0.46 (br), -5.3 (br), -8.0 (br), -17.2 (br) ppm. IR (KBr): 3581 (m), 3057 (w), 2962 (s), 2926 (w), 2868 (m), 2066 (m), 1526 (s), 1462 (w), 1436 (w), 1385 (s), 1361 (w), 1318 (m), 1254 (w), 1176 (w), 1102 (w), 1024 (w), 968 (w), 935 (w), 850 (m), 795 (w), 760 (w) cm^{-1}. μ_{eff} (293K) = 6.1(1) μ_B. Mp: 235°C. Mass Spectrum m/z: 1067.6648 [M$^+$]. Calcd. m/z: 1067.6077 [M$^+$]. Anal. calcd. for C$_{62}$H$_{93}$N$_7$Cr$_2$Si$_1$: C, 69.69; H, 8.77; N, 9.18. Found: C, 68.12; H, 8.88; N, 8.24.

Table 1.8	3 kla0574	4 kla0505	5 kla0554
Formula	$C_{83}H_{115}Cr_3N_{12}O_5$	$C_{84}H_{100}Cr_4N_{16}$	$C_{89}H_{112}Cr_4N_{15}$
Formula wt., g/mol	1516.86	1541.79	1599.93
Temp, K	200(2)	200(2)	200(2)
Wavelength, Å	0.71073	0.71073	0.71073
Crystal size, mm	0.246 x 0.264 x 0.355	0.222 x 0.255 x 0.303	0.185 x 0.261 x 0.504
Color	red	orange	orange
Crystal system	monoclinic	monoclinic	triclinic
Space group	$P\,2_1/c$	$C\,2/c$	$P\,\bar{1}$
a, Å	15.446(2)	26.373(2)	15.392(4)
b, Å	18.250(3)	12.0970(10)	17.075(5)
c, Å	29.782(5)	27.564(2)	18.110(5)
α, deg	90	90	102.301(5)
β, deg	99.621(3)	110.2530(17)	93.785(5)
γ, deg	90	90	107.056(5)
Volume, Å^3	8277.0(2)	8250.2(12)	4404.0(2)
Z	4	4	2
D(calcd), g/cm^3	1.217	1.241	1.207
Abs. coefficient, mm^{-1}	0.443	0.565	0.532
Tmax/Tmin	0.7456/0.6795	0.7456/0.6921	0.7456/0.6556
Data/restraints/params	19193/363/928	9470/143/481	20211/1695/994
GOF on F^2	1.019	1.027	1.036
Final R indices, I>2σ(I)	R1 = 0.0679, wR^2 = 0.1658	R1 = 0.0551, wR^2 = 0.1341	R1 = 0.0627, wR^2 = 0.1310
R indices (all data)	R1 = 0.1569, wR^2 = 0.2101	R1 = 0.0982, wR^2 = 0.1568	R1 = 0.1545, wR^2 = 0.1626

Table 1.9	6	7	8
	kla0542	kla0546	kla0513
Formula	$C_{46}H_{61}Cr_2N_5O$	$C_{45}H_{60}Cr_2N_5Si$	$C_{91}H_{118}Cr_4N_{12}$
Formula wt., g/mol	803.99	803.07	1587.97
Temp, K	200(2)	200(2)	200(2)
Wavelength, Å	0.71073	0.71073	0.71073
Crystal size, mm	0.103 x 0.118 x 0.406	0.352 x 0.421 x 0.459	0.170 x 0.290 x 0.367
Color	orange	green	brown
Crystal system	monoclinic	triclinic	monoclinic
Space group	$C\,2/c$	$P\,\bar{1}$	$P\,2_1/n$
a, Å	22.055(7)	11.0915(10)	10.8781(3)
b, Å	8.444(3)	11.6587(11)	30.6170(9)
c, Å	23.985(8)	19.1428(18)	13.0108(4)
α, deg	90	81.080(4)	90
β, deg	95.113(7)	83.485(3)	93.2010(8)
γ, deg	90	64.660(3)	90
Volume, $Å^3$	4449.0(3)	2207.1(4)	4326.5(2)
Z	4	2	2
D(calcd), g/cm^3	1.200	1.208	1.219
Abs. coefficient, mm^{-1}	0.527	0.555	0.54
T_{max}/T_{min}	0.7456/0.6563	0.7456/0.7068	0.7456/0.6828
Data/restraints/params	5098/24/269	10406/0/497	9915/54/510
GOF on F^2	1.004	1.036	1.014
Final R indices, I>2σ(I)	R1 = 0.0564, wR^2 = 0.1246	R1 = 0.0478, wR^2 = 0.1013	R1 = 0.0512, wR^2 = 0.1215
R indices (all data)	R1 = 0.1271, wR^2 = 0.1570	R1 = 0.0780, wR^2 = 0.1182	R1 = 0.0862, wR^2 = 0.1396

Table 1.10	9
	kla0529
Formula	$C_{67}H_{105}Cr_2N_7Si$
Formula wt., g/mol	1140.66
Temp, K	200(2)
Wavelength, Å	1.54178
Crystal size, mm	0.080 x 0.168 x 0.244
Color	red-orange
Crystal system	monoclinic
Space group	$P\,2_1/n$
a, Å	20.6905(12)
b, Å	15.6741(9)
c, Å	22.0784(12)
α, deg	90
β, deg	109.368(4)
γ, deg	90
Volume, Å^3	6754.9(7)
Z	4
D(calcd), g/cm^3	1.122
Abs. coefficient, mm^{-1}	3.131
T_{max}/T_{min}	0.7456/0.6684
Data/restraints/params	15429/1293/786
GOF on F^2	1.085
Final R indices, I>2σ(I)	R1 = 0.0746, wR^2 = 0.1664
R indices (all data)	R1 = 0.1471, wR^2 = 0.1990

REFERENCES

1. Bourget-Merle, L.; Lappert, M.; Severn, J., *Chem. Rev.* **2002,** *102* (9), 3031.

2. Webster, R., *Dalton Trans.* **2017,** *46* (14), 4483.

3. MacAdams, L. A.; Buffone, G. P.; Incarvito, C. D.; Golen, J. A.; Rheingold, A. L.; Theopold, K. H., *Chem. Commun.* **2003,** (10), 1164.

4. Halpern, J., *Acc. Chem. Res.* **1982,** *15* (8), 238.

5. Janowicz, A.; Bergman, R., *J. Am. Chem. Soc.* **1983,** *105* (12), 3929.

6. Bergman, R., *Science* **1984,** *223* (4639), 902.

7. Herrmann, W., *Angew. Chem. Int. Ed.* **1975,** *14* (5), 355.

8. Herrmann, W.; Biersack, H., *Chem. Ber.* **1977,** *110* (3), 896.

9. Herrmann, W., *Angew. Chem. Int. Ed.* **1978,** *17* (11), 800.

10. Carlucci, L.; Ciani, G.; vonGudenberg, D.; DAlfonso, G., *J. Organomet. Chem.* **1997,** *534* (1-2), 233.

11. Mindiola, D.; Hillhouse, G., *J. Am. Chem. Soc.* **2002,** *124* (34), 9976.

12. MacAdams, L. A. University of Delaware Ph.D. thesis, 2002.

13. Sutton, L. E., *Tables of interatomic distances and configurations in molecules and ions*. 1958.

14. Chatt, J.; Dilworth, J.; Richards, R., *Chem. Rev.* **1978,** *78* (6), 589.

15. The Cambridge Structural Database is a resource for small molecules and metal-organic crystal structures, containing over 900,000 entries from X-ray and neutron diffraction analyses.

16. Liu, X. Y.; Schmalle, H. W.; Berke, H., CCDC deposit number 296929.

17. Grubel, K.; Brennessel, W.; Mercado, B.; Holland, P., *J. Am. Chem. Soc.* **2014,** *136* (48), 16807.

18. Odom, A.; Cummins, C., *Organometallics* **1996,** *15* (3), 898.

19. Monillas, W. H. University of Delaware Ph.D. thesis, 2009.

20. The preparation was by adding measured **2** in a glass ampoule in a glove-box. The ampoule was then evacuated and to this vessel 1.0 equivalent of trimethylsilyl-diazomethane and THF mixture was vacuum-transferred. The solution was allowed to warm to room temperature, yielding a green-brown solution.

21. Allen, F.; Kennard, O.; Watson, D.; Brammer, L.; Orpen, A.; Taylor, R., *J. Chem. Soc. Perkin Trans. 2* **1987,** (12), S1.

22. Bain, G.; Berry, J., *J. Chem. Educ.* **2008,** *85* (4), 532.

23. Charbonneau, F.; Oguadinma, P.; Schaper, F., *Inorg. Chem. Acta.* **2010,** *363* (8), 1779.

Chapter 2

BINUCLEAR ALKYL HYDRIDES OF CHROMIUM AND THEIR REACTION WITH HYDROCARBONS

2.1   Introductions

This chapter is the continuation of the study on curiously stable alkyl hydride complex $(L^{Me}Cr)_2(\mu\text{-}CH_2SiMe_3)(\mu\text{-}H)$ (**1**).[1] Stable alkyl hydride complexes of first row transition metals like **1** are rare, decomposing by reductive elimination of alkane. For example, nickel methyl hydride and nickel phenyl hydride complexes supported by bis(tricyclohexylphosphine) ligand were formed by alkylating halide precursor, as depicted in Scheme 2.1. These two complexes were spectroscopically characterized. They were found to be room temperature stable but were sensitive to light, which led to the loss of methane and benzene, respectively.[2]
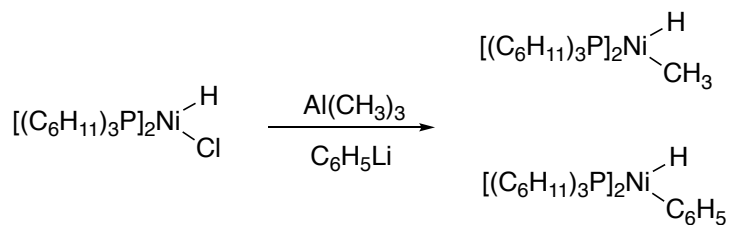
Scheme 2.1   Nickel alkyl/aryl hydride complexes

A CSD search only showed a small number of structures bearing first row transition metals with alkyl and hydride ligands. Scheme 2.2 shows the formation of

bis-alkyl bridging hydride from the exchange of bridging alkoxide group by reacting with phenylsilane. It was proposed that steric protection by the bis(trimethylsilyl)methyl groups leads to the stability of this complex.[3]
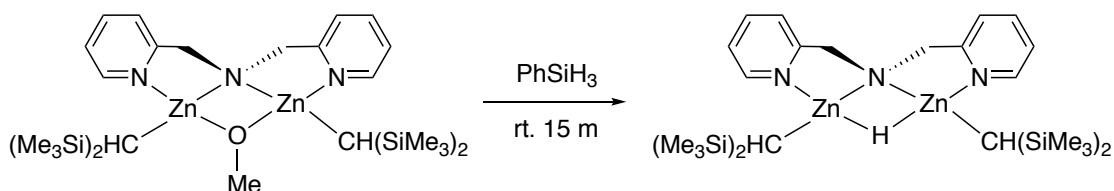
Scheme 2.2 Formation of bis(alkylzinc) bridging hydride complex

Maron and Okuda et. al. reported an ethyl hydride structure in the absence of chelating ligand. [(IMes)ZnEtH]$_2$ was found to be room temperature stable over a week with the support from N-heterocyclic carbene IMes [1,3-bis(2,4,6-trimethylphenyl)imidazol-2-ylidene]. The alkyl hydrido zinc complex was formed by comproportionation of [(IMes)ZnH$_2$]$_2$ and [(IMes)ZnEt]$_2$ (Scheme 2.3).[4]

Mes = 2,4,6-trimethylphenyl
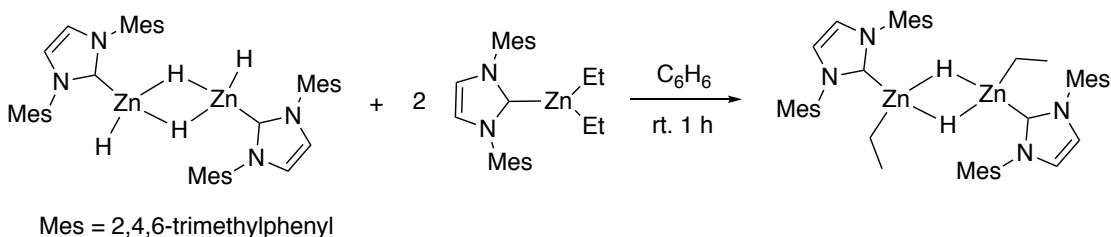
Scheme 2.3 Bis(ethylzinc) bridging hydride complex supported by NHC ligand

The same group has also reported on a scandium ethyl hydride complex. The complex showing in Scheme 2.4 is a dimer with two scandium centers bridged by one

hydride and one amido N-atom of the macrocycle ligand, with one terminal ethyl group bonded to a scandium atom. It was described that this complex slowly decomposed into intractable mixtures with concomitant formation of ethane.[5]
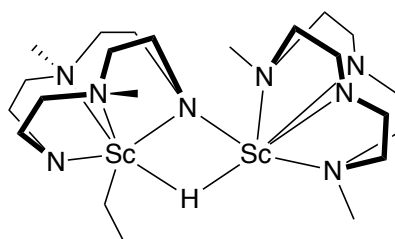
Scheme 2.4 Alkyl hydride complex supported by macrocycle ligands

Hagadorn et. al. reported a binuclear titanium complex bridged by a methyl and a hydride. It was supported by a binucleating bis(amidinate) ligand. This paramagnetic alkyl hydride was synthesized by hydrogenation of a titanium methyl complex, as shown in Scheme 2.5.[6] The reaction was performed at 65°C, presumably the titanium methyl hydride is thermally stable at least up to this temperature.
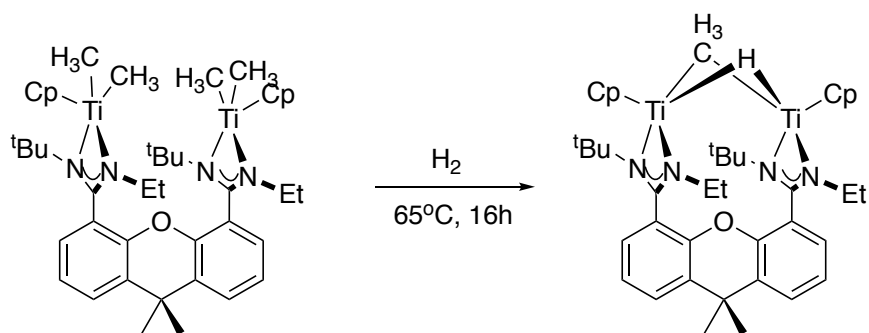
Scheme 2.5 Synthesis of titanium methyl hydride by hydrogenolysis

Our group has also previously reported a thermally stable aryl hydride of chromium, namely $(L^{iPr}Cr)_2(\mu\text{-}C_6H_5)(\mu\text{-}H)$.[7] This complex was formed by hydrogenolysis of chromium phenyl monomer, which is depicted in Scheme 2.6. The reductive elimination of phenyl hydride was not observed upon heating. Its isomeric complex, $(L^{iPr}Cr)_2(\mu_2\text{-}\eta^6{:}\eta^6\text{-}C_6H_6)$, was independently prepared by chemical reduction of chromium halide in the presence of benzene. Both $(L^{iPr}Cr)_2(\mu\text{-}C_6H_5)(\mu\text{-}H)$ and $(L^{iPr}Cr)_2(\mu_2\text{-}\eta^6{:}\eta^6\text{-}C_6H_6)$ were well characterized. The two isomers are related by a C-H bond formation and cleavage, respectively. However, the interconversion was not observed either thermally or photolytically. It was suggested that possible metal-metal bonding in $(L^{iPr}Cr)_2(\mu\text{-}C_6H_5)(\mu\text{-}H)$ may prevent orbital overlap or spin blocking due to the different spin states of the two isomers.
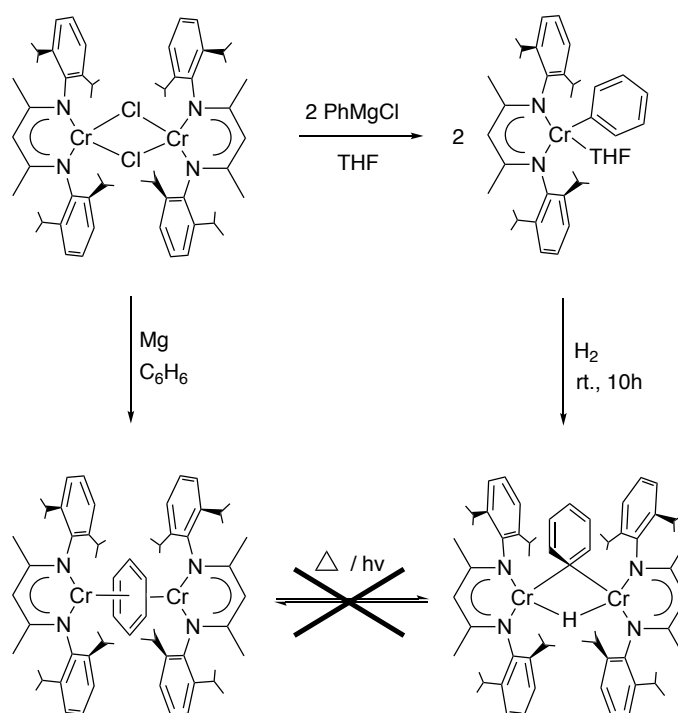
Scheme 2.6 Synthesis of chromium phenyl hydride and its isomeric complex

Oxidative addition of alkanes has shown to generate transition metal alkyl hydrides.[8, 9] Reductive elimination of an alkane from an alkyl hydride complex is the microscopic reverse of oxidative addition of an alkane C-H bond. Although **1** was not formed by the direct oxidative addition of an alkane, the isolable **1** is considered to undergo the reductive elimination of an alkane. However, **1** was found to be stable after heating at 100°C for several days.[1] In order to better understand **1**, synthesizing binuclear chromium alkyl hydride analogs is the goal. Alkylidene insertion attempt has been discussed in **Chapter 1** and the results suggest that the formation of alkyl hydride complexes cannot be accomplished by alkylidene/carbene insertion.

The reported preparation of **1** involves hydrogenolysis of $L^{Me}Cr^{III}(CH_2SiMe_3)_2$.[1] A reasonable mechanism of formation of **1** was shown in Leonard MacAdams' dissertation [10] in Scheme 2.7. In principle, **1** might be accessible via hydrogenolysis of a chromium(II) alkyl. A possible reaction pathway is pictured in Scheme 2.8.
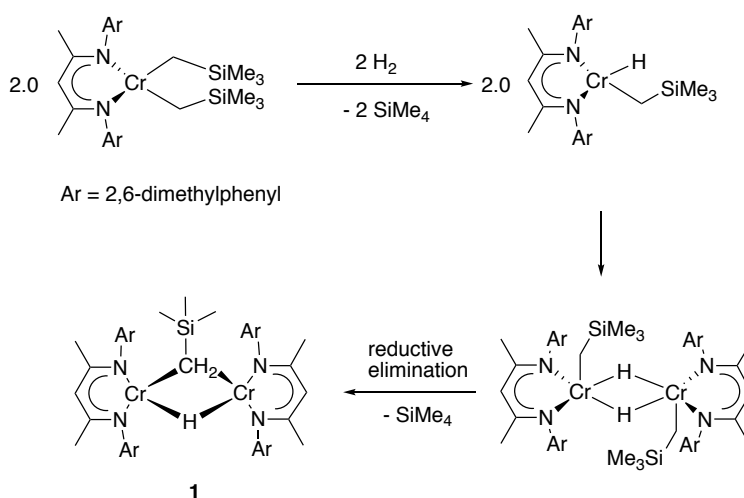
Scheme 2.7 Mechanism of the formation of **1** from reaction of $L^{Me}Cr^{III}(CH_2SiMe_3)_2$ with H_2
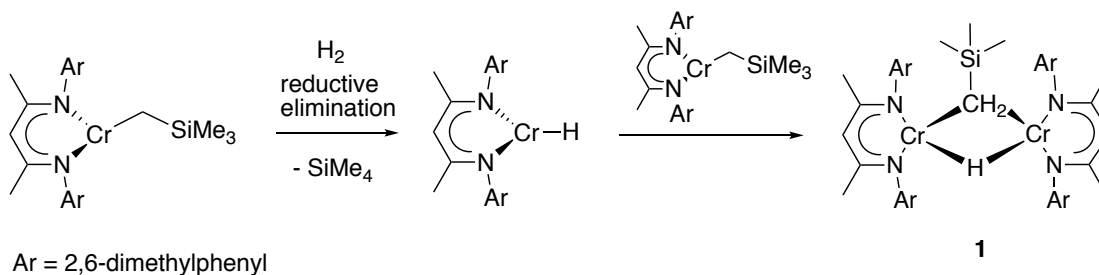
Scheme 2.8 Proposed mechanism for the formation of **1** from reaction of $L^{Me}Cr^{II}(CH_2SiMe_3)$ with H_2

This chapter addresses the synthesis of chromium(II) alkyl complexes, and their hydrogenolysis reactions leading to binuclear chromium alkyl hydride analogs. Further explorations of reactivity were also investigated.

2.2 Results and Discussion

2.2.1 Synthesis of chromium(II) alkyls and their thermal decomposition products

Reactions of $[L^{Me}Cr(THF)]_2(\mu\text{-}Cl)_2$ [11] with Grignard reagents (Me_3SiCH_2MgCl, Me_3CCH_2MgCl) were conducted. These reactions yielded chromium(II) alkyls in the form of $L^{Me}CrR(THF)$ (**10**, R = CH_2SiMe_3 and **11**, R = CH_2CMe_3), as shown in Scheme 2.9. Reaction of $[L^{Me}Cr(THF)]_2(\mu\text{-}Cl)_2$ [11] with Grignard reagent $C_6H_5CH_2MgCl$ did not lead to analogous complex $L^{Me}CrBn(THF)$. However, reduction of chromium(III) dibenzyl complex $L^{Me}CrBn_2$ [10] with H_2 yielded monomeric $L^{Me}Cr(\eta^2\text{-}CH_2C_6H_5)$ (**12**) (Scheme 2.10). The benzyl ligand exhibits η^2-coordination to chromium so that the coordination environment of chromium is relatively sterically saturated. These monomeric chromium(II) alkyl complexes were fully characterized and their molecular structures are shown in Figures 2.1-2.3.
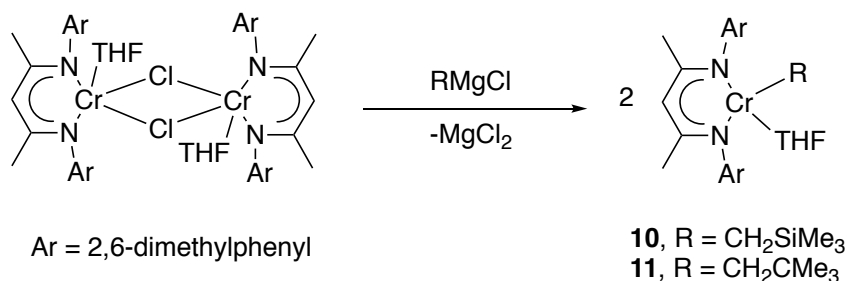
Scheme 2.9 Synthesis of **10** and **11**
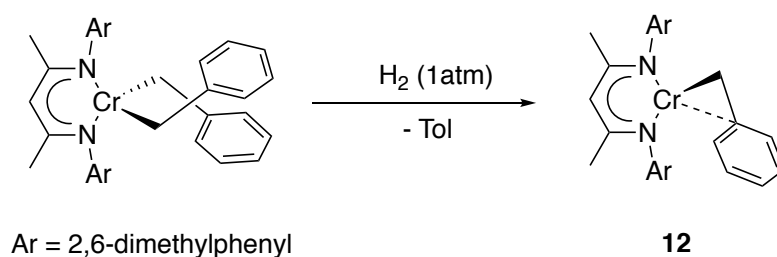
Scheme 2.10 Synthesis of **12**

Monomeric chromium(II) alkyl complexes **10-12** share some common features. ^{1}H NMR spectra showed similar isotropically shifted resonances, with particularly marked resemblance between **10** and **11**. The room temperature magnetic moments (4.5(1) μ_B for **10**, 4.4(1) μ_B for **11**, and 4.4(1) μ_B for **12**), all lower than theoretical value for an isolated high spin d^4 system (4.9μ_B). Susceptibilities have all been corrected for diamagnetism, as a result, unknown systematic errors or potential inorganic impurities (salts) were considered to cause this phenomenon. Structurally, the coordination geometry of the chromium centers in **10-12** is best described as distorted square planar. The sum of the angles around chromium center are 367.15° for **10**, 369.66° for **11**, and 360.42° for **12**. The dihedral angles between the two planes defined by N1-Cr1-N2 and C22-Cr1-O1 are 30.2° for **10** and 36.7° for **11**. The

dihedral angle between the two planes defined by N1-Cr1-N2 and C22-Cr1-C23 is 16.8° for **12**. The two hydrogen atoms of the methylene group bonded to the chromium center were located on a difference map. The η^2-coordination in **12** is indicated by a short distance between chromium and the arene ipso carbon, i.e., Cr1-C23 = 2.246(3) Å, as compared to the single bond distance of 2.147(4) Å for Cr1-C22.
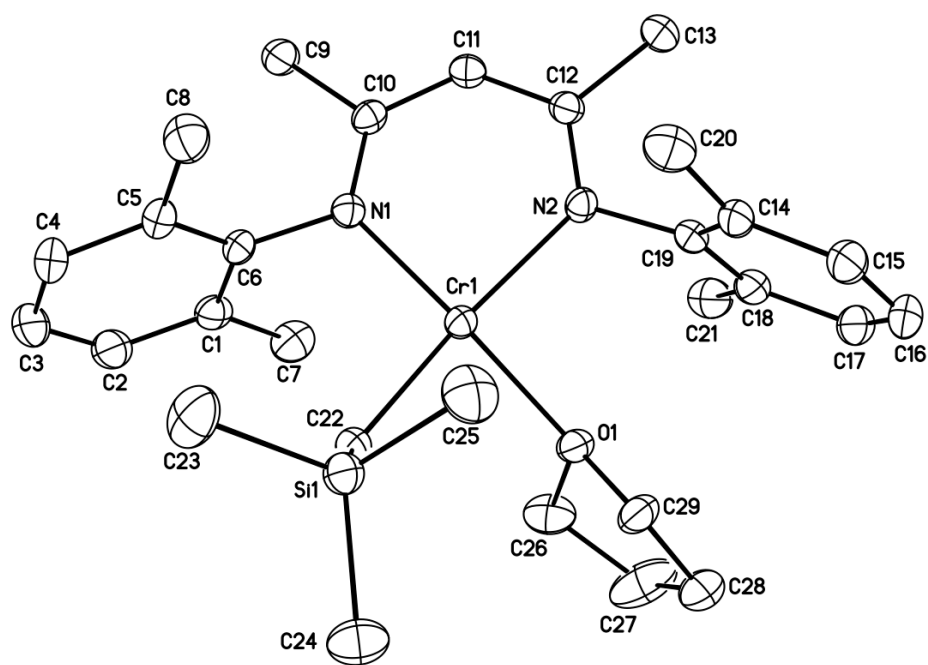
Figure 2.1   Molecular structure of L^{Me}Cr(CH$_2$SiMe$_3$)(THF) (**10**). Ellipsoids are drawn at the 30% probability level. Hydrogen atoms have been omitted for clarity.

Table 2.1   Interatomic distances (Å) and angles (º) for $L^{Me}Cr(CH_2SiMe_3)(THF)$ (**10**)

Distances (Å)

Cr(1)-N(1)	2.048(5)	C(4)-C(5)	1.397(9)
Cr(1)-N(2)	2.097(5)	C(5)-C(6)	1.391(9)
Cr(1)-O(1)	2.119(4)	C(5)-C(8)	1.500(9)
Cr(1)-C(22)	2.146(6)	C(9)-C(10)	1.526(8)
Si(1)-C(22)	1.843(7)	C(10)-C(11)	1.384(8)
Si(1)-C(25)	1.882(7)	C(11)-C(12)	1.401(8)
Si(1)-C(24)	1.889(7)	C(12)-C(13)	1.515(8)
Si(1)-C(23)	1.880(7)	C(14)-C(19)	1.391(9)
O(1)-C(29)	1.441(7)	C(14)-C(15)	1.394(9)
O(1)-C(26)	1.454(8)	C(14)-C(20)	1.505(9)
N(1)-C(10)	1.342(7)	C(15)-C(16)	1.364(11)
N(1)-C(6)	1.437(7)	C(16)-C(17)	1.390(12)
N(2)-C(12)	1.325(7)	C(17)-C(18)	1.392(9)
N(2)-C(19)	1.444(7)	C(18)-C(19)	1.403(9)
C(1)-C(6)	1.408(9)	C(18)-C(21)	1.503(10)
C(1)-C(2)	1.397(9)	C(26)-C(27)	1.504(10)
C(1)-C(7)	1.497(9)	C(27)-C(28)	1.502(12)
C(2)-C(3)	1.365(11)	C(28)-C(29)	1.507(9)
C(3)-C(4)	1.400(11)		

Angles (°)

N(1)-Cr(1)-N(2)	89.04(19)	C(6)-C(5)-C(8)	120.4(6)
N(1)-Cr(1)-O(1)	155.08(19)	C(1)-C(6)-C(5)	120.7(6)
N(2)-Cr(1)-O(1)	90.22(17)	C(1)-C(6)-N(1)	118.6(6)
N(1)-Cr(1)-C(22)	99.6(2)	C(5)-C(6)-N(1)	120.7(6)
N(2)-Cr(1)-C(22)	162.4(2)	N(1)-C(10)-C(11)	124.9(5)
O(1)-Cr(1)-C(22)	88.3(2)	N(1)-C(10)-C(9)	119.0(5)
C(22)-Si(1)-C(25)	113.3(3)	C(11)-C(10)-C(9)	116.1(5)
C(22)-Si(1)-C(24)	113.6(3)	C(10)-C(11)-C(12)	129.0(5)
C(25)-Si(1)-C(24)	104.4(4)	N(2)-C(12)-C(11)	122.8(6)
C(22)-Si(1)-C(23)	112.4(3)	N(2)-C(12)-C(13)	120.7(6)
C(25)-Si(1)-C(23)	105.4(4)	C(11)-C(12)-C(13)	116.5(5)
C(24)-Si(1)-C(23)	107.1(4)	C(19)-C(14)-C(15)	118.9(7)

C(29)-O(1)-C(26)	105.4(5)	C(19)-C(14)-C(20)	121.4(6)
C(29)-O(1)-Cr(1)	126.7(4)	C(15)-C(14)-C(20)	119.7(7)
C(26)-O(1)-Cr(1)	117.6(4)	C(16)-C(15)-C(14)	121.1(8)
C(10)-N(1)-C(6)	117.0(5)	C(15)-C(16)-C(17)	119.7(8)
C(10)-N(1)-Cr(1)	126.1(4)	C(18)-C(17)-C(16)	121.1(8)
C(6)-N(1)-Cr(1)	116.1(4)	C(17)-C(18)-C(19)	118.2(7)
C(12)-N(2)-C(19)	118.0(5)	C(17)-C(18)-C(21)	120.2(7)
C(12)-N(2)-Cr(1)	127.2(4)	C(19)-C(18)-C(21)	121.7(6)
C(19)-N(2)-Cr(1)	114.6(4)	C(14)-C(19)-C(18)	120.8(6)
C(6)-C(1)-C(2)	118.2(6)	C(14)-C(19)-N(2)	119.9(6)
C(6)-C(1)-C(7)	120.7(6)	C(18)-C(19)-N(2)	119.3(6)
C(2)-C(1)-C(7)	121.1(6)	Si(1)-C(22)-Cr(1)	120.1(3)
C(3)-C(2)-C(1)	121.7(7)	O(1)-C(26)-C(27)	105.0(7)
C(2)-C(3)-C(4)	120.0(7)	C(26)-C(27)-C(28)	105.3(7)
C(5)-C(4)-C(3)	119.8(7)	C(27)-C(28)-C(29)	105.5(6)
C(4)-C(5)-C(6)	119.6(6)	O(1)-C(29)-C(28)	105.8(6)
C(4)-C(5)-C(8)	120.0(6)		
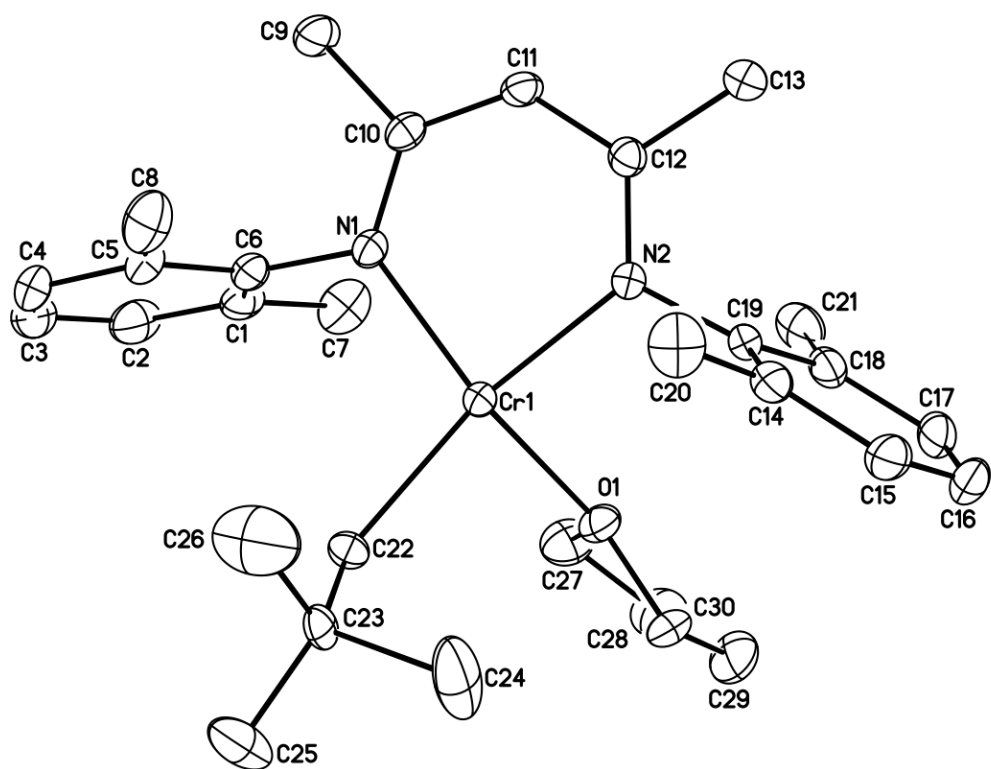
Figure 2.2   Molecular structure of L^{Me}Cr(CH$_2$CMe$_3$)(THF) (**11**). Ellipsoids are drawn at the 30% probability level. Hydrogen atoms have been omitted for clarity.

Table 2.2   Interatomic distances (Å) and angles (º) for L^{Me}Cr(CH$_2$CMe$_3$)(THF) (**11**)

Distances (Å)

Cr(1)-N(1)	2.059(2)	C(10)-C(11)	1.386(4)
Cr(1)-N(2)	2.098(2)	C(11)-C(12)	1.404(4)
Cr(1)-O(1)	2.147(2)	C(12)-C(13)	1.514(4)
Cr(1)-C(22)	2.175(5)	C(14)-C(19)	1.394(4)
O(1)-C(30)	1.446(4)	C(14)-C(15)	1.397(4)
O(1)-C(27)	1.452(4)	C(14)-C(20)	1.511(5)
N(1)-C(10)	1.343(4)	C(15)-C(16)	1.368(6)
N(1)-C(6)	1.442(4)	C(16)-C(17)	1.382(6)
N(2)-C(12)	1.326(3)	C(17)-C(18)	1.401(5)
N(2)-C(19)	1.437(3)	C(18)-C(19)	1.399(4)
C(1)-C(2)	1.398(5)	C(18)-C(21)	1.506(5)
C(1)-C(6)	1.407(4)	C(22)-C(23)	1.529(16)
C(1)-C(7)	1.494(5)	C(23)-C(25)	1.474(16)
C(2)-C(3)	1.368(6)	C(23)-C(26)	1.529(18)
C(3)-C(4)	1.381(6)	C(23)-C(24)	1.631(12)
C(4)-C(5)	1.408(5)	C(27)-C(28)	1.516(6)
C(5)-C(6)	1.393(4)	C(28)-C(29)	1.507(7)
C(5)-C(8)	1.496(5)	C(29)-C(30)	1.507(6)
C(9)-C(10)	1.525(4)		

Angles (°)

N(1)-Cr(1)-N(2)	88.91(8)	C(11)-C(10)-C(9)	115.8(3)
N(1)-Cr(1)-O(1)	148.40(9)	C(10)-C(11)-C(12)	129.0(3)
N(2)-Cr(1)-O(1)	90.63(8)	N(2)-C(12)-C(11)	123.1(2)
N(1)-Cr(1)-C(22)	103.05(16)	N(2)-C(12)-C(13)	120.7(2)
N(2)-Cr(1)-C(22)	160.55(16)	C(11)-C(12)-C(13)	116.3(2)
O(1)-Cr(1)-C(22)	87.07(15)	C(19)-C(14)-C(15)	118.9(3)
C(30)-O(1)-C(27)	106.6(3)	C(19)-C(14)-C(20)	121.1(3)
C(30)-O(1)-Cr(1)	133.5(2)	C(15)-C(14)-C(20)	119.9(3)
C(27)-O(1)-Cr(1)	113.4(2)	C(16)-C(15)-C(14)	120.7(3)
C(10)-N(1)-C(6)	115.9(2)	C(15)-C(16)-C(17)	120.3(3)
C(10)-N(1)-Cr(1)	126.44(19)	C(16)-C(17)-C(18)	120.9(3)
C(6)-N(1)-Cr(1)	116.78(17)	C(19)-C(18)-C(17)	118.2(3)

C(12)-N(2)-C(19)	117.6(2)	C(19)-C(18)-C(21)	121.4(3)
C(12)-N(2)-Cr(1)	127.30(17)	C(17)-C(18)-C(21)	120.4(3)
C(19)-N(2)-Cr(1)	114.92(16)	C(14)-C(19)-C(18)	120.9(3)
C(2)-C(1)-C(6)	118.5(3)	C(14)-C(19)-N(2)	119.0(3)
C(2)-C(1)-C(7)	120.5(3)	C(18)-C(19)-N(2)	120.0(3)
C(6)-C(1)-C(7)	121.0(3)	C(23)-C(22)-Cr(1)	120.2(5)
C(3)-C(2)-C(1)	121.1(4)	C(25)-C(23)-C(22)	116.1(8)
C(2)-C(3)-C(4)	120.1(3)	C(25)-C(23)-C(26)	108.5(10)
C(3)-C(4)-C(5)	121.2(4)	C(22)-C(23)-C(26)	110.9(11)
C(6)-C(5)-C(4)	117.9(3)	C(25)-C(23)-C(24)	106.4(11)
C(6)-C(5)-C(8)	121.7(3)	C(22)-C(23)-C(24)	111.1(10)
C(4)-C(5)-C(8)	120.4(3)	C(26)-C(23)-C(24)	102.9(10)
C(5)-C(6)-C(1)	121.3(3)	O(1)-C(27)-C(28)	106.3(3)
C(5)-C(6)-N(1)	120.9(3)	C(29)-C(28)-C(27)	104.8(4)
C(1)-C(6)-N(1)	117.9(3)	C(30)-C(29)-C(28)	105.9(3)
N(1)-C(10)-C(11)	124.7(2)	O(1)-C(30)-C(29)	104.0(3)
N(1)-C(10)-C(9)	119.5(3)		
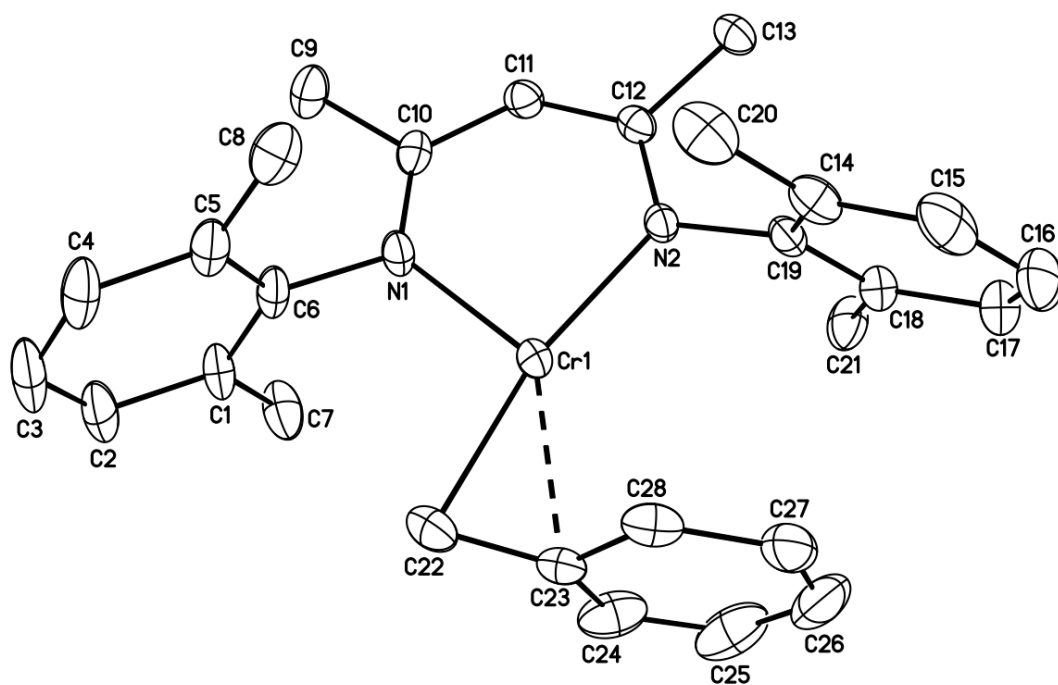
Figure 2.3   Molecular structure of $L^{Me}Cr(\eta^2\text{-}CH_2C_6H_5)$ (**12**). Ellipsoids are drawn at the 30% probability level. Hydrogen atoms have been omitted for clarity.

Table 2.3   Interatomic distances (Å) and angles (°) for $L^{Me}Cr(\eta^2\text{-}CH_2C_6H_5)$ (**12**)

Distances (Å)

Cr(1)-N(1)	2.007(2)	C(11)-C(12)	1.402(5)
Cr(1)-N(2)	2.039(2)	C(12)-C(13)	1.513(4)
Cr(1)-C(22)	2.147(4)	C(14)-C(15)	1.394(5)
Cr(1)-C(23)	2.246(3)	C(14)-C(19)	1.406(5)
N(1)-C(10)	1.331(4)	C(14)-C(20)	1.513(5)
N(1)-C(6)	1.450(4)	C(15)-C(16)	1.381(6)
N(2)-C(12)	1.332(4)	C(16)-C(17)	1.366(6)
N(2)-C(19)	1.451(4)	C(17)-C(18)	1.385(5)
C(1)-C(2)	1.396(5)	C(18)-C(19)	1.393(5)
C(1)-C(6)	1.400(6)	C(18)-C(21)	1.497(5)
C(1)-C(7)	1.496(6)	C(22)-C(23)	1.419(5)
C(2)-C(3)	1.362(6)	C(23)-C(28)	1.403(6)
C(3)-C(4)	1.373(6)	C(23)-C(24)	1.408(6)
C(4)-C(5)	1.410(5)	C(24)-C(25)	1.342(7)
C(5)-C(6)	1.395(6)	C(25)-C(26)	1.368(9)
C(5)-C(8)	1.497(6)	C(26)-C(27)	1.344(8)
C(9)-C(10)	1.517(4)	C(27)-C(28)	1.426(5)
C(10)-C(11)	1.397(4)		

Angles (°)

N(1)-Cr(1)-N(2)	91.99(10)	N(2)-C(12)-C(11)	123.6(3)
N(1)-Cr(1)-C(22)	100.53(13)	N(2)-C(12)-C(13)	119.5(3)
N(2)-Cr(1)-C(22)	167.48(13)	C(11)-C(12)-C(13)	116.9(3)
N(1)-Cr(1)-C(23)	135.98(13)	C(15)-C(14)-C(19)	118.1(4)
N(2)-Cr(1)-C(23)	130.30(12)	C(15)-C(14)-C(20)	121.5(4)
C(22)-Cr(1)-C(23)	37.60(13)	C(19)-C(14)-C(20)	120.4(3)
C(10)-N(1)-C(6)	118.5(2)	C(16)-C(15)-C(14)	121.1(4)
C(10)-N(1)-Cr(1)	125.5(2)	C(17)-C(16)-C(15)	119.5(4)
C(6)-N(1)-Cr(1)	115.87(19)	C(16)-C(17)-C(18)	122.0(4)
C(12)-N(2)-C(19)	118.1(2)	C(17)-C(18)-C(19)	118.3(4)
C(12)-N(2)-Cr(1)	124.7(2)	C(17)-C(18)-C(21)	120.5(4)
C(19)-N(2)-Cr(1)	117.07(19)	C(19)-C(18)-C(21)	121.2(3)
C(2)-C(1)-C(6)	117.2(4)	C(18)-C(19)-C(14)	121.0(3)

C(2)-C(1)-C(7)	120.9(4)	C(18)-C(19)-N(2)	121.1(3)
C(6)-C(1)-C(7)	121.8(3)	C(14)-C(19)-N(2)	117.8(3)
C(3)-C(2)-C(1)	121.7(4)	C(23)-C(22)-Cr(1)	74.99(19)
C(2)-C(3)-C(4)	120.3(4)	C(28)-C(23)-C(24)	115.5(4)
C(3)-C(4)-C(5)	121.1(4)	C(28)-C(23)-C(22)	119.7(4)
C(6)-C(5)-C(4)	117.0(4)	C(24)-C(23)-C(22)	123.2(4)
C(6)-C(5)-C(8)	121.7(3)	C(28)-C(23)-Cr(1)	82.4(2)
C(4)-C(5)-C(8)	121.2(4)	C(24)-C(23)-Cr(1)	109.2(3)
C(5)-C(6)-C(1)	122.5(3)	C(22)-C(23)-Cr(1)	67.4(2)
C(5)-C(6)-N(1)	117.8(4)	C(25)-C(24)-C(23)	122.6(4)
C(1)-C(6)-N(1)	119.6(4)	C(24)-C(25)-C(26)	120.8(5)
N(1)-C(10)-C(11)	123.9(3)	C(27)-C(26)-C(25)	120.8(5)
N(1)-C(10)-C(9)	119.9(3)	C(26)-C(27)-C(28)	119.2(5)
C(11)-C(10)-C(9)	116.3(3)	C(23)-C(28)-C(27)	120.8(5)
C(10)-C(11)-C(12)	128.7(3)		

In an attempt to test the relative stability of these chromium(II) alkyls, **10-12** were heated to elevated temperatures. **12** turned out to be very stable; for instance, heating a C_6D_6 solution of **12** to 120°C for several days did not produce any signs of decomposition by ^{1}H NMR spectroscopy. **10** and **11** gradually decomposed (100°C 4 hours for **10** and room temperature 4 hours for **11**)[12] in nonaromatic solvent (cyclohexane was used in this case). The decomposition products were characterized by X-ray diffraction; they are the binuclear complexes **13** and **14** respectively. The crystal structures of **13** and **14** are shown in Figures 2.4 and 2.5, respectively. **13** and **14** both consist of two chromiums bridged by an alkyl and a methylene which arose from intramolecular C-H bond activation of one methyl group of a ligand aryl substituent. When the decompositions of **10** and **11** in CyH-d_{12} were monitored by ^{1}H NMR spectroscopy, the organic products were observed as tetramethylsilane (0.02 ppm) and neopentane (0.94 ppm), respectively. **13** and **14** share broadly similar physical properties, such as color, melting point, and chemical shifts in their ^{1}H NMR spectra.

For both **13** and **14**, the geometry around each chromium atom is best described as distorted square planar. The sum of the bond angles about the chromium centers are 365.16° (Cr1) and 374.95° (Cr2) for **13**; 365.20° (Cr1) and 369.87° (Cr2) for **14**. The distortion may be attributed to the activated ligand methylene group incorporated within the core. It is also noted that the core is puckered, i. e., the two planes (Cr1-C43-Cr2 and Cr1-C21-Cr2) span a dihedral angle of 124° in **13** and 121° in **14**. A binuclear chromium bridging methyl complex supported by L[iPr] ligand, i. e. [L[iPr]Cr(μ-Me)]$_2$,[10] also adopts a puckered geometry of the Cr_2Me_2 core. The angle between the two planes defined by the two chromium atoms and both bridging methyl

groups is 147°. The metric parameters are essentially similar for **13** and **14**, with the exception of those distances and angles pertaining to the bridging alkyl group.

To further test the stability of **13** and **14**, more extreme conditions (100°C for 2 days in cyclohexane) were applied. It turned out the remaining alkyl bridge can be released, with a second intramolecular C-H bond activation of the other nacnac ligand arm. The resulting molecular structure was determined. **15** is the product and its structure is depicted in Figure 2.6. In **15**, the two chromium centers are only bridged by one methylene group, with C21 as the bridge. The other activated ligand methylene group spans the core and having C42 atom connected to Cr1, results in a 4-coordinate Cr1 and a 3-coordinate Cr2. C42 is non-bonded to Cr2 with a distance of 3.456(7) Å. The geometry of Cr1 is square planar, with the sum of bond angles about Cr1 being 359.34°. The geometry around Cr2 is best described as T-shaped, with angles of 162.36° (C21-Cr2-N3), 105.87° (C21-Cr2-N4), and 90.14° (N3-Cr2-N4). The dihedral angle between the two planes defined by N4 Cr2 N3 and N4 Cr2 C21 is 7.5°. The Cr-Cr distances for **13**, **14**, and **15** are 2.4942(4) Å, 2.4504(6) Å, and 2.4987(11) Å, respectively. The possibility of significant metal-metal bonding cannot be dismissed.[13] The room temperature magnetic moments for **13**, **14**, and **15** were determined (1.8μ_B for **13**, 1.8μ_B for **14** and 2.0μ_B for **15**). The magnetic moment of a complex with two independent Cr(II) high spin d^4 system is expected to be 6.8 μ_B; the lower values for **13**, **14**, and **15** suggest strong antiferromagnetic coupling between the metal centers. It is worth noting that the decomposition of **10** and **11** is by two successive reductive elimination of alkanes rather than reductive coupling of alkyl/alkyl.
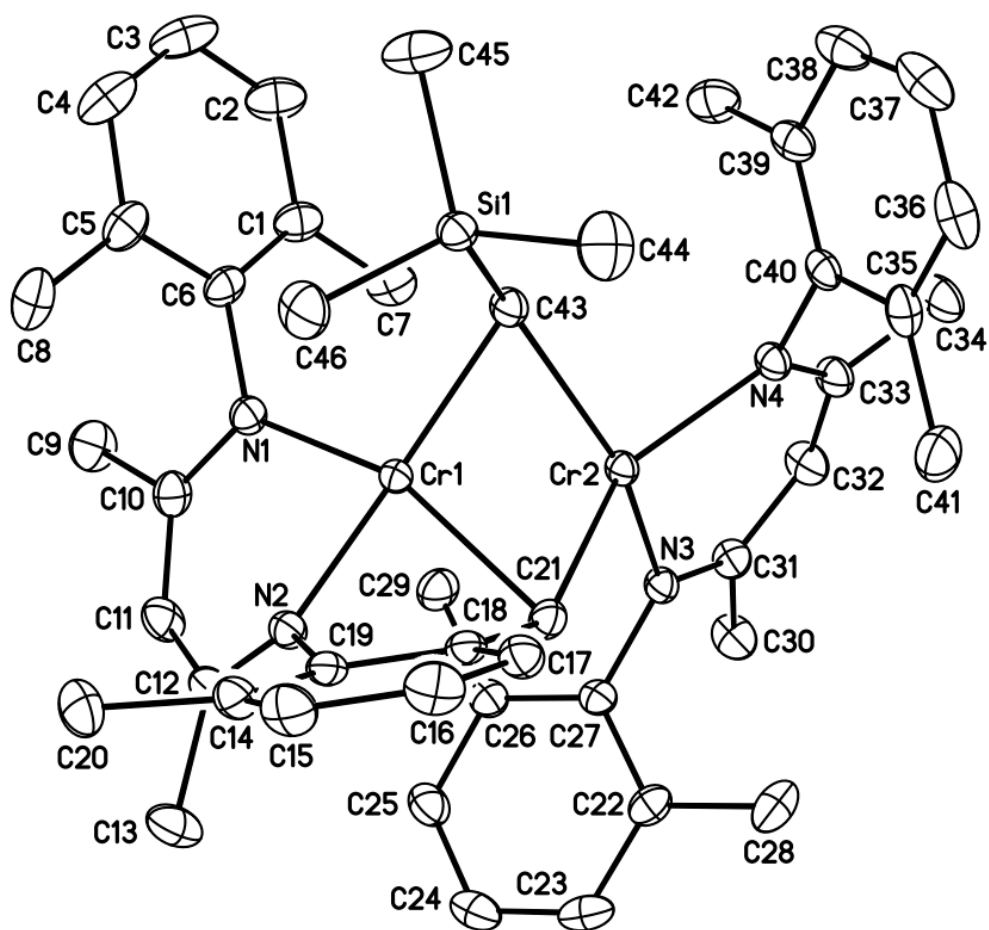
Figure 2.4   Molecular structure of $L^{Me}Cr(\mu\text{-}CH_2SiMe_3)CrNArC(CH_3)CHC(CH_3)N\text{-}$
Me-$C_6H_3(\mu\text{-}CH_2)$ (**13**). Ar = 2,6-dimethylphenyl. Ellipsoids are drawn at
the 30% probability level. Hydrogen atoms have been omitted for clarity.

Table 2.4 Interatomic distances (Å) and angles (º) for $L^{Me}Cr(\mu$-CH$_2$SiMe$_3$)CrNArC(CH$_3$)CHC(CH$_3$)N-Me-C$_6$H$_3(\mu$-CH$_2$) (**13**). Ar = 2,6-dimethylphenyl.

Distances (Å)			
Cr(1)-N(2)	1.9955(16)	C(11)-C(12)	1.396(3)
Cr(1)-N(1)	2.0591(16)	C(12)-C(13)	1.510(3)
Cr(1)-C(43)	2.142(2)	C(14)-C(15)	1.392(3)
Cr(1)-C(21)	2.273(2)	C(14)-C(19)	1.399(3)
Cr(1)-Cr(2)	2.4942(4)	C(14)-C(20)	1.510(3)
Cr(2)-N(3)	2.0518(16)	C(15)-C(16)	1.378(3)
Cr(2)-N(4)	2.0741(16)	C(16)-C(17)	1.384(3)
Cr(2)-C(21)	2.238(2)	C(17)-C(18)	1.390(3)
Cr(2)-C(43)	2.287(2)	C(18)-C(19)	1.413(3)
Si(1)-C(44)	1.860(2)	C(18)-C(21)	1.504(3)
Si(1)-C(45)	1.861(2)	C(22)-C(23)	1.394(3)
Si(1)-C(43)	1.867(2)	C(22)-C(27)	1.401(3)
Si(1)-C(46)	1.872(2)	C(22)-C(28)	1.501(3)
N(1)-C(10)	1.343(3)	C(23)-C(24)	1.376(3)
N(1)-C(6)	1.437(3)	C(24)-C(25)	1.373(3)
N(2)-C(12)	1.317(3)	C(25)-C(26)	1.394(3)
N(2)-C(19)	1.417(2)	C(26)-C(27)	1.393(3)
N(3)-C(31)	1.338(2)	C(26)-C(29)	1.502(3)
N(3)-C(27)	1.447(2)	C(30)-C(31)	1.517(3)
N(4)-C(33)	1.337(2)	C(31)-C(32)	1.395(3)
N(4)-C(40)	1.442(2)	C(32)-C(33)	1.394(3)
C(1)-C(2)	1.397(3)	C(33)-C(34)	1.514(3)
C(1)-C(6)	1.403(3)	C(35)-C(40)	1.398(3)
C(1)-C(7)	1.498(3)	C(35)-C(36)	1.398(3)
C(2)-C(3)	1.373(4)	C(35)-C(41)	1.504(3)
C(3)-C(4)	1.376(4)	C(36)-C(37)	1.374(4)
C(4)-C(5)	1.390(3)	C(37)-C(38)	1.367(4)
C(5)-C(6)	1.405(3)	C(38)-C(39)	1.392(3)
C(5)-C(8)	1.506(3)	C(39)-C(40)	1.402(3)
C(9)-C(10)	1.513(3)	C(39)-C(42)	1.496(3)
C(10)-C(11)	1.397(3)		

N(2)-Cr(1)-N(1)	86.77(6)	C(12)-C(11)-C(10)	126.67(19)
N(2)-Cr(1)-C(43)	158.02(7)	N(2)-C(12)-C(11)	119.96(18)
N(1)-Cr(1)-C(43)	104.34(8)	N(2)-C(12)-C(13)	121.25(19)
N(2)-Cr(1)-C(21)	78.10(7)	C(11)-C(12)-C(13)	118.75(19)
N(1)-Cr(1)-C(21)	156.78(8)	C(15)-C(14)-C(19)	117.83(19)
C(43)-Cr(1)-C(21)	95.95(8)	C(15)-C(14)-C(20)	119.7(2)
N(2)-Cr(1)-Cr(2)	128.67(5)	C(19)-C(14)-C(20)	122.3(2)
N(1)-Cr(1)-Cr(2)	127.34(5)	C(16)-C(15)-C(14)	121.8(2)
C(43)-Cr(1)-Cr(2)	58.53(6)	C(15)-C(16)-C(17)	120.1(2)
C(21)-Cr(1)-Cr(2)	55.75(5)	C(16)-C(17)-C(18)	120.4(2)
N(3)-Cr(2)-N(4)	89.82(6)	C(17)-C(18)-C(19)	118.79(18)
N(3)-Cr(2)-C(21)	95.97(7)	C(17)-C(18)-C(21)	122.91(18)
N(4)-Cr(2)-C(21)	144.86(7)	C(19)-C(18)-C(21)	118.30(17)
N(3)-Cr(2)-C(43)	155.02(7)	C(14)-C(19)-C(18)	121.07(18)
N(4)-Cr(2)-C(43)	96.20(7)	C(14)-C(19)-N(2)	124.44(18)
C(21)-Cr(2)-C(43)	92.96(7)	C(18)-C(19)-N(2)	113.04(16)
N(3)-Cr(2)-Cr(1)	114.40(5)	C(18)-C(21)-Cr(2)	144.61(14)
N(4)-Cr(2)-Cr(1)	147.90(5)	C(18)-C(21)-Cr(1)	88.23(11)
C(21)-Cr(2)-Cr(1)	57.11(5)	Cr(2)-C(21)-Cr(1)	67.14(6)
C(43)-Cr(2)-Cr(1)	53.03(5)	C(23)-C(22)-C(27)	118.4(2)
C(44)-Si(1)-C(45)	111.17(13)	C(23)-C(22)-C(28)	120.7(2)
C(44)-Si(1)-C(43)	107.45(11)	C(27)-C(22)-C(28)	120.9(2)
C(45)-Si(1)-C(43)	107.55(11)	C(24)-C(23)-C(22)	121.0(2)
C(44)-Si(1)-C(46)	106.20(12)	C(25)-C(24)-C(23)	120.1(2)
C(45)-Si(1)-C(46)	107.87(13)	C(24)-C(25)-C(26)	120.8(2)
C(43)-Si(1)-C(46)	116.64(10)	C(27)-C(26)-C(25)	118.8(2)
C(10)-N(1)-C(6)	117.20(17)	C(27)-C(26)-C(29)	121.45(18)
C(10)-N(1)-Cr(1)	121.98(13)	C(25)-C(26)-C(29)	119.7(2)
C(6)-N(1)-Cr(1)	120.79(13)	C(26)-C(27)-C(22)	120.84(18)
C(12)-N(2)-C(19)	129.33(17)	C(26)-C(27)-N(3)	119.90(17)
C(12)-N(2)-Cr(1)	127.70(14)	C(22)-C(27)-N(3)	119.26(18)
C(19)-N(2)-Cr(1)	102.83(11)	N(3)-C(31)-C(32)	124.36(18)
C(31)-N(3)-C(27)	115.27(16)	N(3)-C(31)-C(30)	119.98(18)
C(31)-N(3)-Cr(2)	125.14(13)	C(32)-C(31)-C(30)	115.62(18)
C(27)-N(3)-Cr(2)	119.28(12)	C(33)-C(32)-C(31)	128.68(19)
C(33)-N(4)-C(40)	116.69(16)	N(4)-C(33)-C(32)	123.51(18)

C(33)-N(4)-Cr(2)	125.86(13)	N(4)-C(33)-C(34)	120.44(18)
C(40)-N(4)-Cr(2)	117.02(11)	C(32)-C(33)-C(34)	116.03(18)
C(2)-C(1)-C(6)	118.1(2)	C(40)-C(35)-C(36)	118.6(2)
C(2)-C(1)-C(7)	120.6(2)	C(40)-C(35)-C(41)	121.3(2)
C(6)-C(1)-C(7)	121.26(19)	C(36)-C(35)-C(41)	120.1(2)
C(3)-C(2)-C(1)	121.2(3)	C(37)-C(36)-C(35)	121.1(2)
C(2)-C(3)-C(4)	120.3(2)	C(38)-C(37)-C(36)	119.9(2)
C(3)-C(4)-C(5)	120.9(2)	C(37)-C(38)-C(39)	121.3(2)
C(4)-C(5)-C(6)	118.6(2)	C(38)-C(39)-C(40)	118.7(2)
C(4)-C(5)-C(8)	119.8(2)	C(38)-C(39)-C(42)	119.6(2)
C(6)-C(5)-C(8)	121.5(2)	C(40)-C(39)-C(42)	121.62(19)
C(1)-C(6)-C(5)	120.9(2)	C(35)-C(40)-C(39)	120.36(19)
C(1)-C(6)-N(1)	119.98(18)	C(35)-C(40)-N(4)	118.88(18)
C(5)-C(6)-N(1)	119.08(19)	C(39)-C(40)-N(4)	120.73(18)
N(1)-C(10)-C(11)	124.68(19)	Si(1)-C(43)-Cr(1)	105.31(9)
N(1)-C(10)-C(9)	118.71(19)	Si(1)-C(43)-Cr(2)	142.31(12)
C(11)-C(10)-C(9)	116.61(19)	Cr(1)-C(43)-Cr(2)	68.44(6)
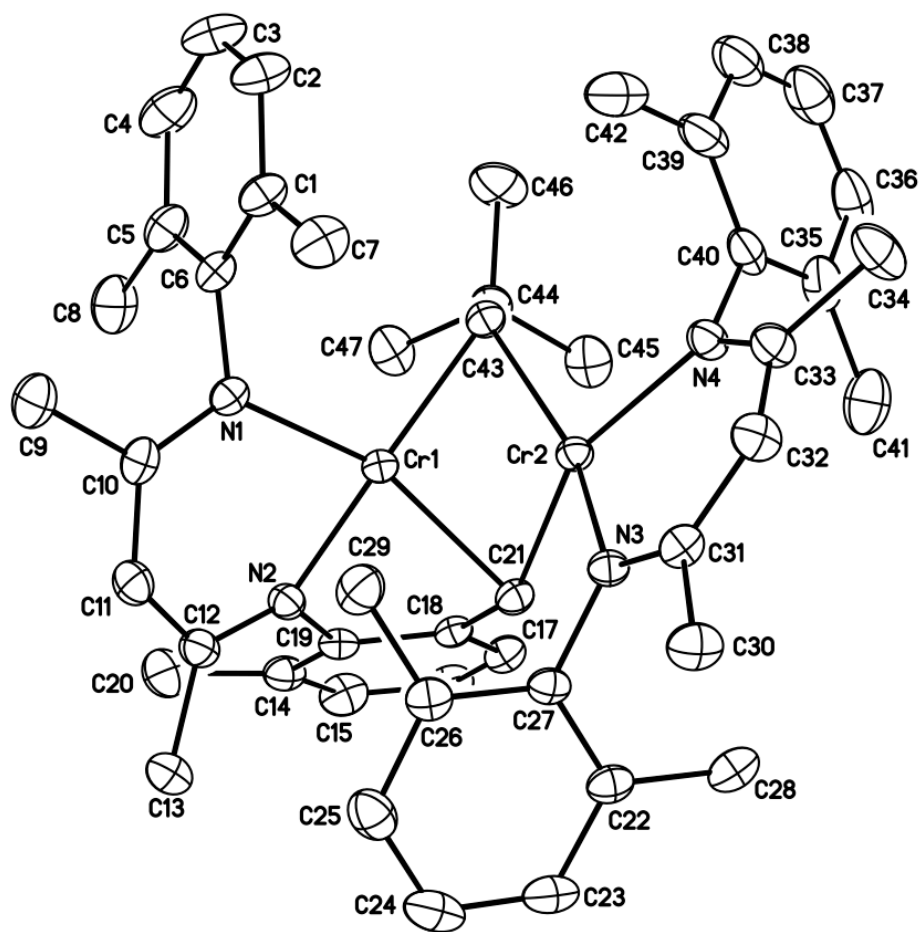
Figure 2.5   Molecular structure of $L^{Me}Cr(\mu-CH_2CMe_3)CrNArC(CH_3)CHC(CH_3)N-Me-C_6H_3(\mu-CH_2)$ (**14**). Ar = 2,6-dimethylphenyl. Ellipsoids are drawn at the 30% probability level. Hydrogen atoms and another molecule (of two) have been omitted for clarity.

Table 2.5   Interatomic distances (Å) and angles (º) for $L^{Me}Cr(\mu$-
CH$_2$CMe$_3$)CrNArC(CH$_3$)CHC(CH$_3$)N-Me-C$_6$H$_3$(μ-CH$_2$) (**14**). Ar = 2,6-
dimethylphenyl.

		Distances (Å)	
Cr(1)-N(2)	2.002(2)	C(14)-C(20)	1.513(4)
Cr(1)-N(1)	2.068(2)	C(15)-C(16)	1.369(4)
Cr(1)-C(43)	2.183(3)	C(16)-C(17)	1.392(4)
Cr(1)-C(21)	2.261(3)	C(17)-C(18)	1.388(3)
Cr(1)-Cr(2)	2.4504(6)	C(18)-C(19)	1.416(3)
Cr(2)-N(3)	2.080(2)	C(18)-C(21)	1.507(3)
Cr(2)-N(4)	2.092(2)	C(22)-C(23)	1.388(4)
Cr(2)-C(21)	2.273(3)	C(22)-C(27)	1.399(3)
Cr(2)-C(43)	2.336(3)	C(22)-C(28)	1.503(4)
N(1)-C(10)	1.340(3)	C(23)-C(24)	1.373(4)
N(1)-C(6)	1.442(3)	C(24)-C(25)	1.379(4)
N(2)-C(12)	1.329(3)	C(25)-C(26)	1.387(4)
N(2)-C(19)	1.423(3)	C(26)-C(27)	1.394(4)
N(3)-C(31)	1.338(3)	C(26)-C(29)	1.499(4)
N(3)-C(27)	1.444(3)	C(30)-C(31)	1.512(3)
N(4)-C(33)	1.336(3)	C(31)-C(32)	1.398(4)
N(4)-C(40)	1.441(3)	C(32)-C(33)	1.391(4)
C(1)-C(2)	1.386(4)	C(33)-C(34)	1.521(4)
C(1)-C(6)	1.398(4)	C(35)-C(40)	1.390(4)
C(1)-C(7)	1.501(4)	C(35)-C(36)	1.420(4)
C(2)-C(3)	1.373(5)	C(35)-C(41)	1.494(5)
C(3)-C(4)	1.370(5)	C(36)-C(37)	1.378(5)
C(4)-C(5)	1.396(4)	C(37)-C(38)	1.353(5)
C(5)-C(6)	1.399(4)	C(38)-C(39)	1.372(4)
C(5)-C(8)	1.506(4)	C(39)-C(40)	1.418(4)
C(9)-C(10)	1.517(4)	C(39)-C(42)	1.499(5)
C(10)-C(11)	1.394(4)	C(43)-C(44)	1.560(4)
C(11)-C(12)	1.393(4)	C(44)-C(45)	1.514(4)
C(12)-C(13)	1.512(4)	C(44)-C(46)	1.538(4)
C(14)-C(15)	1.394(4)	C(44)-C(47)	1.539(4)
C(14)-C(19)	1.398(3)		

N(2)-Cr(1)-N(1)	86.28(8)	C(19)-C(14)-C(20)	122.7(3)
N(2)-Cr(1)-C(43)	157.39(10)	C(16)-C(15)-C(14)	121.7(3)
N(1)-Cr(1)-C(43)	103.62(9)	C(15)-C(16)-C(17)	120.1(3)
N(2)-Cr(1)-C(21)	78.69(9)	C(18)-C(17)-C(16)	120.6(3)
N(1)-Cr(1)-C(21)	157.24(9)	C(17)-C(18)-C(19)	118.4(2)
C(43)-Cr(1)-C(21)	96.61(10)	C(17)-C(18)-C(21)	123.0(2)
N(2)-Cr(1)-Cr(2)	129.75(6)	C(19)-C(18)-C(21)	118.6(2)
N(1)-Cr(1)-Cr(2)	125.25(6)	C(14)-C(19)-C(18)	121.1(2)
C(43)-Cr(1)-Cr(2)	60.22(7)	C(14)-C(19)-N(2)	124.6(2)
C(21)-Cr(1)-Cr(2)	57.53(7)	C(18)-C(19)-N(2)	113.2(2)
N(3)-Cr(2)-N(4)	88.22(8)	C(18)-C(21)-Cr(1)	91.52(15)
N(3)-Cr(2)-C(21)	93.76(8)	C(18)-C(21)-Cr(2)	150.12(18)
N(4)-Cr(2)-C(21)	152.06(9)	Cr(1)-C(21)-Cr(2)	65.44(7)
N(3)-Cr(2)-C(43)	159.34(9)	C(23)-C(22)-C(27)	118.1(3)
N(4)-Cr(2)-C(43)	95.79(9)	C(23)-C(22)-C(28)	120.6(2)
C(21)-Cr(2)-C(43)	92.10(9)	C(27)-C(22)-C(28)	121.3(2)
N(3)-Cr(2)-Cr(1)	114.02(6)	C(24)-C(23)-C(22)	121.2(3)
N(4)-Cr(2)-Cr(1)	145.33(6)	C(23)-C(24)-C(25)	119.9(3)
C(21)-Cr(2)-Cr(1)	57.04(7)	C(24)-C(25)-C(26)	121.0(3)
C(43)-Cr(2)-Cr(1)	54.21(7)	C(25)-C(26)-C(27)	118.3(3)
C(10)-N(1)-C(6)	118.7(2)	C(25)-C(26)-C(29)	120.7(3)
C(10)-N(1)-Cr(1)	123.32(17)	C(27)-C(26)-C(29)	121.0(2)
C(6)-N(1)-Cr(1)	117.94(16)	C(26)-C(27)-C(22)	121.4(2)
C(12)-N(2)-C(19)	127.0(2)	C(26)-C(27)-N(3)	119.4(2)
C(12)-N(2)-Cr(1)	127.22(17)	C(22)-C(27)-N(3)	119.2(2)
C(19)-N(2)-Cr(1)	105.38(15)	N(3)-C(31)-C(32)	124.2(2)
C(31)-N(3)-C(27)	114.3(2)	N(3)-C(31)-C(30)	120.3(2)
C(31)-N(3)-Cr(2)	127.01(17)	C(32)-C(31)-C(30)	115.5(2)
C(27)-N(3)-Cr(2)	118.67(15)	C(33)-C(32)-C(31)	128.3(2)
C(33)-N(4)-C(40)	114.3(2)	N(4)-C(33)-C(32)	124.0(2)
C(33)-N(4)-Cr(2)	127.12(18)	N(4)-C(33)-C(34)	120.3(2)
C(40)-N(4)-Cr(2)	118.30(16)	C(32)-C(33)-C(34)	115.7(2)
C(2)-C(1)-C(6)	118.4(3)	C(40)-C(35)-C(36)	117.8(3)
C(2)-C(1)-C(7)	120.4(3)	C(40)-C(35)-C(41)	120.7(3)
C(6)-C(1)-C(7)	121.1(2)	C(36)-C(35)-C(41)	121.5(3)
C(3)-C(2)-C(1)	121.7(3)	C(37)-C(36)-C(35)	119.6(4)

C(4)-C(3)-C(2)	119.5(3)	C(38)-C(37)-C(36)	121.8(3)
C(3)-C(4)-C(5)	121.3(3)	C(37)-C(38)-C(39)	121.2(4)
C(4)-C(5)-C(6)	118.4(3)	C(38)-C(39)-C(40)	118.4(3)
C(4)-C(5)-C(8)	120.7(3)	C(38)-C(39)-C(42)	119.8(3)
C(6)-C(5)-C(8)	120.9(3)	C(40)-C(39)-C(42)	121.8(3)
C(1)-C(6)-C(5)	120.6(3)	C(35)-C(40)-C(39)	121.3(3)
C(1)-C(6)-N(1)	120.2(2)	C(35)-C(40)-N(4)	119.0(3)
C(5)-C(6)-N(1)	119.0(2)	C(39)-C(40)-N(4)	119.7(3)
N(1)-C(10)-C(11)	124.0(2)	C(44)-C(43)-Cr(1)	110.03(17)
N(1)-C(10)-C(9)	119.9(2)	C(44)-C(43)-Cr(2)	131.15(19)
C(11)-C(10)-C(9)	116.1(2)	Cr(1)-C(43)-Cr(2)	65.57(7)
C(12)-C(11)-C(10)	126.9(2)	C(45)-C(44)-C(46)	109.1(3)
N(2)-C(12)-C(11)	120.4(2)	C(45)-C(44)-C(47)	108.9(3)
N(2)-C(12)-C(13)	121.3(2)	C(46)-C(44)-C(47)	107.8(2)
C(11)-C(12)-C(13)	118.1(2)	C(45)-C(44)-C(43)	110.8(2)
C(15)-C(14)-C(19)	118.0(3)	C(46)-C(44)-C(43)	108.9(2)
C(15)-C(14)-C(20)	119.2(3)	C(47)-C(44)-C(43)	111.2(2)
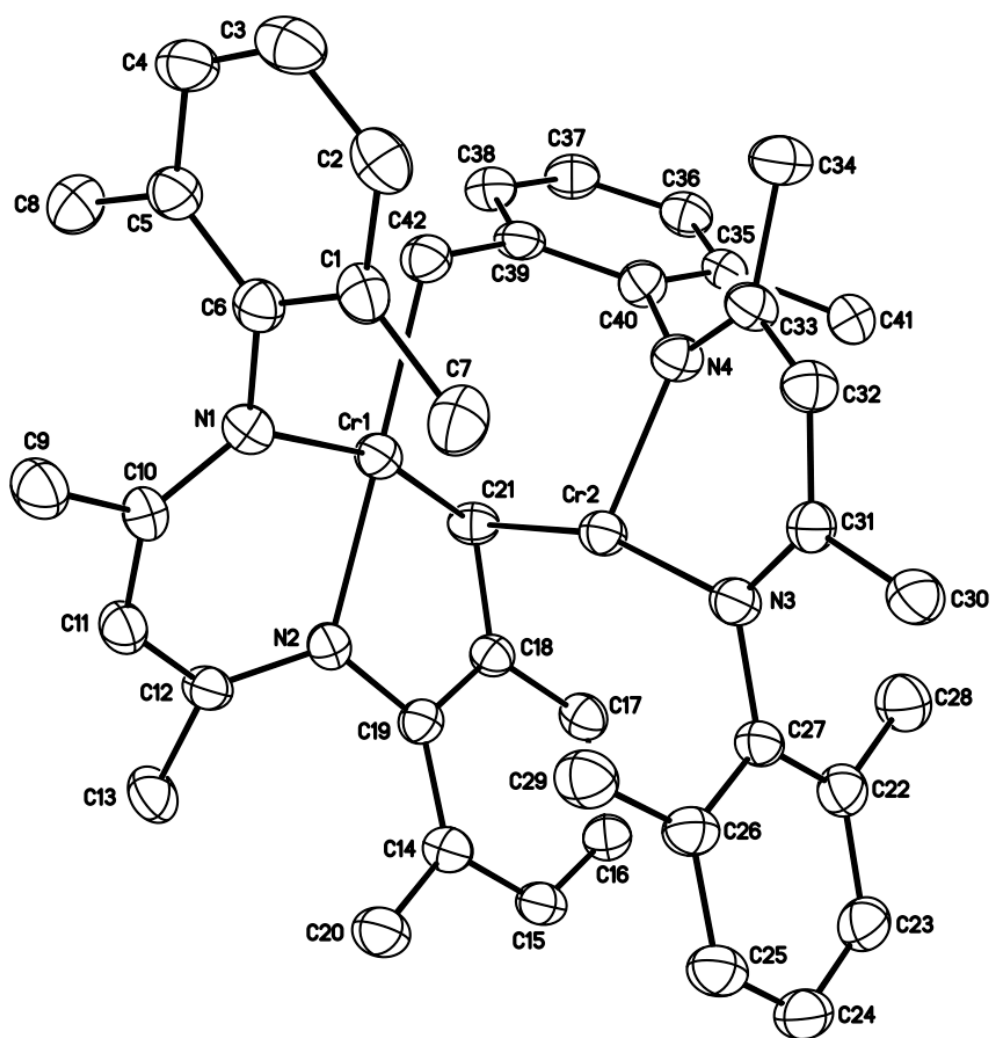
Figure 2.6   Molecular structure of [ArNC(CH$_3$)CHC(CH$_3$)N-Me-C$_6$H$_3$]Cr(μ_2-CH$_2$)Cr[NArC(CH$_3$)CHC(CH$_3$)N-Me-C$_6$H$_3$](μ_1-CH$_2$) (**15**). Ar = 2,6-dimethylphenyl. Ellipsoids are drawn at the 30% probability level. Hydrogen atoms have been omitted for clarity.

Table 2.6   Interatomic distances (Å) and angles (°) for [ArNC(CH₃)CHC(CH₃)N-Me-C₆H₃]Cr(μ₂-CH₂)Cr[NArC(CH₃)CHC(CH₃)N-Me-C₆H₃](μ₁-CH₂) (**15**). Ar = 2,6-dimethylphenyl.

Distances (Å)			
Cr(1)-N(2)	2.056(4)	C(14)-C(15)	1.385(7)
Cr(1)-N(1)	2.065(4)	C(14)-C(19)	1.408(7)
Cr(1)-C(42)	2.145(5)	C(14)-C(20)	1.513(7)
Cr(1)-C(21)	2.255(5)	C(15)-C(16)	1.379(7)
Cr(1)-Cr(2)	2.4987(11)	C(16)-C(17)	1.384(7)
Cr(2)-N(4)	1.998(4)	C(17)-C(18)	1.404(7)
Cr(2)-N(3)	2.005(4)	C(18)-C(19)	1.421(6)
Cr(2)-C(21)	2.152(5)	C(18)-C(21)	1.473(7)
N(1)-C(10)	1.332(6)	C(22)-C(27)	1.384(7)
N(1)-C(6)	1.435(6)	C(22)-C(23)	1.399(7)
N(2)-C(12)	1.353(6)	C(22)-C(28)	1.500(8)
N(2)-C(19)	1.420(6)	C(23)-C(24)	1.382(8)
N(3)-C(31)	1.347(6)	C(24)-C(25)	1.362(8)
N(3)-C(27)	1.454(6)	C(25)-C(26)	1.396(7)
N(4)-C(33)	1.328(6)	C(26)-C(27)	1.403(7)
N(4)-C(40)	1.434(6)	C(26)-C(29)	1.506(8)
C(1)-C(2)	1.388(7)	C(30)-C(31)	1.507(7)
C(1)-C(6)	1.391(7)	C(31)-C(32)	1.381(7)
C(1)-C(7)	1.513(8)	C(32)-C(33)	1.413(7)
C(2)-C(3)	1.379(9)	C(33)-C(34)	1.500(7)
C(3)-C(4)	1.375(9)	C(35)-C(36)	1.386(7)
C(4)-C(5)	1.386(7)	C(35)-C(40)	1.392(7)
C(5)-C(6)	1.398(7)	C(35)-C(41)	1.505(7)
C(5)-C(8)	1.503(8)	C(36)-C(37)	1.387(8)
C(9)-C(10)	1.513(7)	C(37)-C(38)	1.380(7)
C(10)-C(11)	1.404(7)	C(38)-C(39)	1.388(7)
C(11)-C(12)	1.380(7)	C(39)-C(40)	1.413(7)
C(12)-C(13)	1.516(7)	C(39)-C(42)	1.491(7)

Angles (°)			
N(2)-Cr(1)-N(1)	89.50(16)	C(15)-C(14)-C(19)	118.2(5)
N(2)-Cr(1)-C(42)	172.05(19)	C(15)-C(14)-C(20)	118.2(5)

N(1)-Cr(1)-C(42)	96.03(18)	C(19)-C(14)-C(20)	123.5(5)
N(2)-Cr(1)-C(21)	76.87(17)	C(16)-C(15)-C(14)	122.6(5)
N(1)-Cr(1)-C(21)	164.92(17)	C(15)-C(16)-C(17)	119.4(5)
C(42)-Cr(1)-C(21)	96.94(19)	C(16)-C(17)-C(18)	120.8(5)
N(2)-Cr(1)-Cr(2)	85.46(11)	C(17)-C(18)-C(19)	118.5(4)
N(1)-Cr(1)-Cr(2)	132.68(12)	C(17)-C(18)-C(21)	123.4(4)
C(42)-Cr(1)-Cr(2)	94.90(15)	C(19)-C(18)-C(21)	117.5(4)
C(21)-Cr(1)-Cr(2)	53.54(13)	C(14)-C(19)-N(2)	125.2(4)
N(4)-Cr(2)-N(3)	90.14(16)	C(14)-C(19)-C(18)	120.4(4)
N(4)-Cr(2)-C(21)	105.87(17)	N(2)-C(19)-C(18)	114.2(4)
N(3)-Cr(2)-C(21)	162.36(18)	C(18)-C(21)-Cr(2)	77.2(3)
N(4)-Cr(2)-Cr(1)	93.28(13)	C(18)-C(21)-Cr(1)	106.0(3)
N(3)-Cr(2)-Cr(1)	130.41(13)	Cr(2)-C(21)-Cr(1)	69.04(15)
C(21)-Cr(2)-Cr(1)	57.42(14)	C(27)-C(22)-C(23)	118.1(5)
C(10)-N(1)-C(6)	118.4(4)	C(27)-C(22)-C(28)	121.5(5)
C(10)-N(1)-Cr(1)	123.3(3)	C(23)-C(22)-C(28)	120.4(5)
C(6)-N(1)-Cr(1)	118.2(3)	C(24)-C(23)-C(22)	120.9(5)
C(12)-N(2)-C(19)	122.7(4)	C(25)-C(24)-C(23)	120.0(5)
C(12)-N(2)-Cr(1)	121.5(3)	C(24)-C(25)-C(26)	121.4(5)
C(19)-N(2)-Cr(1)	114.6(3)	C(25)-C(26)-C(27)	117.8(5)
C(31)-N(3)-C(27)	117.3(4)	C(25)-C(26)-C(29)	120.4(5)
C(31)-N(3)-Cr(2)	125.7(3)	C(27)-C(26)-C(29)	121.8(4)
C(27)-N(3)-Cr(2)	117.0(3)	C(22)-C(27)-C(26)	121.7(4)
C(33)-N(4)-C(40)	120.3(4)	C(22)-C(27)-N(3)	119.5(4)
C(33)-N(4)-Cr(2)	126.5(3)	C(26)-C(27)-N(3)	118.8(4)
C(40)-N(4)-Cr(2)	113.2(3)	N(3)-C(31)-C(32)	122.8(5)
C(2)-C(1)-C(6)	119.1(5)	N(3)-C(31)-C(30)	119.7(4)
C(2)-C(1)-C(7)	120.2(5)	C(32)-C(31)-C(30)	117.3(5)
C(6)-C(1)-C(7)	120.7(5)	C(31)-C(32)-C(33)	128.2(5)
C(3)-C(2)-C(1)	120.5(6)	N(4)-C(33)-C(32)	121.9(4)
C(4)-C(3)-C(2)	120.2(5)	N(4)-C(33)-C(34)	120.3(5)
C(3)-C(4)-C(5)	120.7(5)	C(32)-C(33)-C(34)	117.8(5)
C(4)-C(5)-C(6)	118.8(5)	C(36)-C(35)-C(40)	118.7(5)
C(4)-C(5)-C(8)	119.5(5)	C(36)-C(35)-C(41)	120.0(5)
C(6)-C(5)-C(8)	121.6(5)	C(40)-C(35)-C(41)	121.3(5)
C(1)-C(6)-C(5)	120.6(5)	C(35)-C(36)-C(37)	120.4(5)
C(1)-C(6)-N(1)	119.3(5)	C(38)-C(37)-C(36)	119.7(5)

C(5)-C(6)-N(1)	120.0(5)	C(37)-C(38)-C(39)	122.4(5)
N(1)-C(10)-C(11)	123.8(5)	C(38)-C(39)-C(40)	116.4(5)
N(1)-C(10)-C(9)	120.4(5)	C(38)-C(39)-C(42)	123.5(5)
C(11)-C(10)-C(9)	115.8(4)	C(40)-C(39)-C(42)	120.0(5)
C(12)-C(11)-C(10)	129.4(5)	C(35)-C(40)-C(39)	122.2(4)
N(2)-C(12)-C(11)	121.7(4)	C(35)-C(40)-N(4)	119.6(4)
N(2)-C(12)-C(13)	121.3(4)	C(39)-C(40)-N(4)	117.9(4)
C(11)-C(12)-C(13)	117.0(4)	C(39)-C(42)-Cr(1)	114.1(3)

2.2.2   Synthesis of chromium alkyl hydrides and their characterizations

Reactions of **10-12** in pentane with excess hydrogen gas were carried out. These reactions yielded the desired complexes in the form of $(L^{Me}Cr)_2(\mu\text{-}R)(\mu\text{-}H)$ (**1**, R = CH_2SiMe_3, **16**, R = CH_2CMe_3 and **17**, R = $CH_2C_6H_5$). Products were isolated in moderate to high yields (51% for **1**, 68% for **16** and 54% for **17**). The pentane insoluble orange powders were precipitated. This byproduct was identified as $(L^{Me}Cr)_2(\mu\text{-}H)_2$ (**2**).[1] **2** could be removed by filtration of the pentane solution. The mechanism for the formation of the alkyl hydrides presumably involves reductive elimination of an alkane ($Si(CH_3)_4$ for **1**, $C(CH_3)_4$ for **16** and C_7H_8 for **17**), resulting in a chromium hydride, which is further trapped by another chromium alkyl (see Scheme 2.8). The crystal structures of **16** and **17** are shown in Figures 2.7 and 2.8; **1** has been reported earlier.[1] The characterizations of the alkyl hydride complexes are described in the following.

Complexes **1**, **16**, and **17** are binuclear chromium complexes in which each chromium is coordinated by one nacnac ligand; in each case, the two chromium atoms are joined by a bridging hydride and the carbon of a bridging alkyl group. Except for compound **16**, the hydrides were located and their positions refined. The bridging hydride in **16** was not located on a difference map; however, intact mass by LIFDI mass spectrometry of **16** is consistent with the whole molecule being $C_{47}H_{62}N_4Cr_2$. H1 was then placed in an idealized position, based on similar structure **1** and refined. The coordination geometry about each chromium atom is best described as distorted square planar and the dihedral angles between the two nacnac planes vary, with 43.9° for **1**, 52.5° for **16** and 48.9° for **17**. The steric interactions force the cores into a butterfly configuration, similar to what had been observed for **1**. The Cr-Cr distances of **16** and **17** are close to that in **1**, with 2.6026(9) Å for **1**, 2.5134(14) Å for **16**, and 2.5906(13) Å

for **17**. As had been described for **1**, these Cr-Cr distances are indicative of possible metal-metal bonding.

Beyond the geometrical similarities, the ^{1}H NMR spectra of **1**, **16**, and **17** also exhibited a similar pattern, with several isotropically shifted and broadened resonances, as expected of paramagnetic compounds. The room temperature magnetic moments were determined; the values are close to those of a class of Cr^{II} dimers ($2.5\mu_B$ for **1**, $2.3\mu_B$ for **16** and $2.4\mu_B$ for **17**). The low magnetic moments of all were presumably caused by antiferromagnetic coupling of the Cr^{II} ions mediated by the bridging ligands, or metal-metal bonding, or both.

Considering the successful synthesis of alkyl hydrides by hydrogenolysis of chromium(II) alkyls, it was reasonable to ask whether hydrogenation of the intramolecular C-H activation products **13** and **14** might produce the corresponding alkyl hydrides. However, $(L^{Me}Cr)_2(\mu-H)_2$ (**2**) was the major inorganic product for both reactions, with the elimination of $Si(CH_3)_4$ and $C(CH_3)_4$, identified by ^{1}H NMR spectroscopy. The possible intermediates $(L^{Me}Cr)_2(\mu-R)(\mu-H)$ (R = CH_2SiMe_3 for **13**, R = CH_2CMe_3 for **14**) were not detected by monitoring ^{1}H NMR spectra. Therefore, the other possible intermediate $L^{Me}Cr(\mu-H)CrNArC(CH_3)CHC(CH_3)N-Me-C_6H_3(\mu-CH_2)$, Ar = 2,6-dimethylphenyl, was then predicted, shown in Scheme 2.11. This intermediate was proposed by eliminating $(L^{Me}Cr)_2(\mu-R)(\mu-H)$. With no clue of what this intermediate might look like in terms of the chemical shifts in the ^{1}H NMR spectrum, hydrogenation of **15** was tested. $(L^{Me}Cr)_2(\mu-H)_2$ (**2**) turned out to be the only major product in this reaction, so the existence of the postulated intermediate in these reactions cannot be verified at this point.
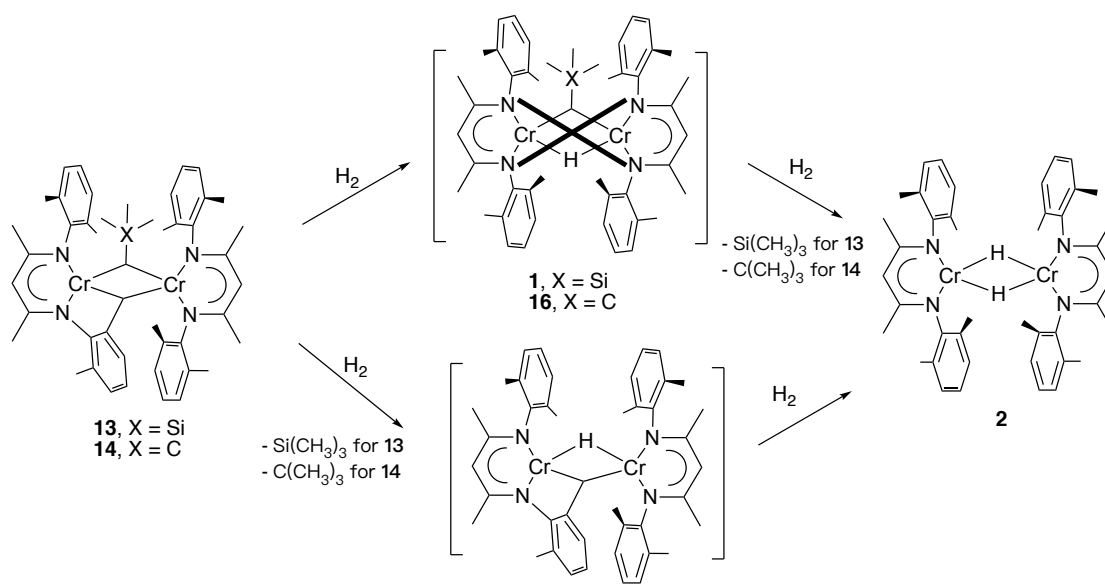
Scheme 2.11   Hydrogenation of **13** and **14** together with predicted intermediates
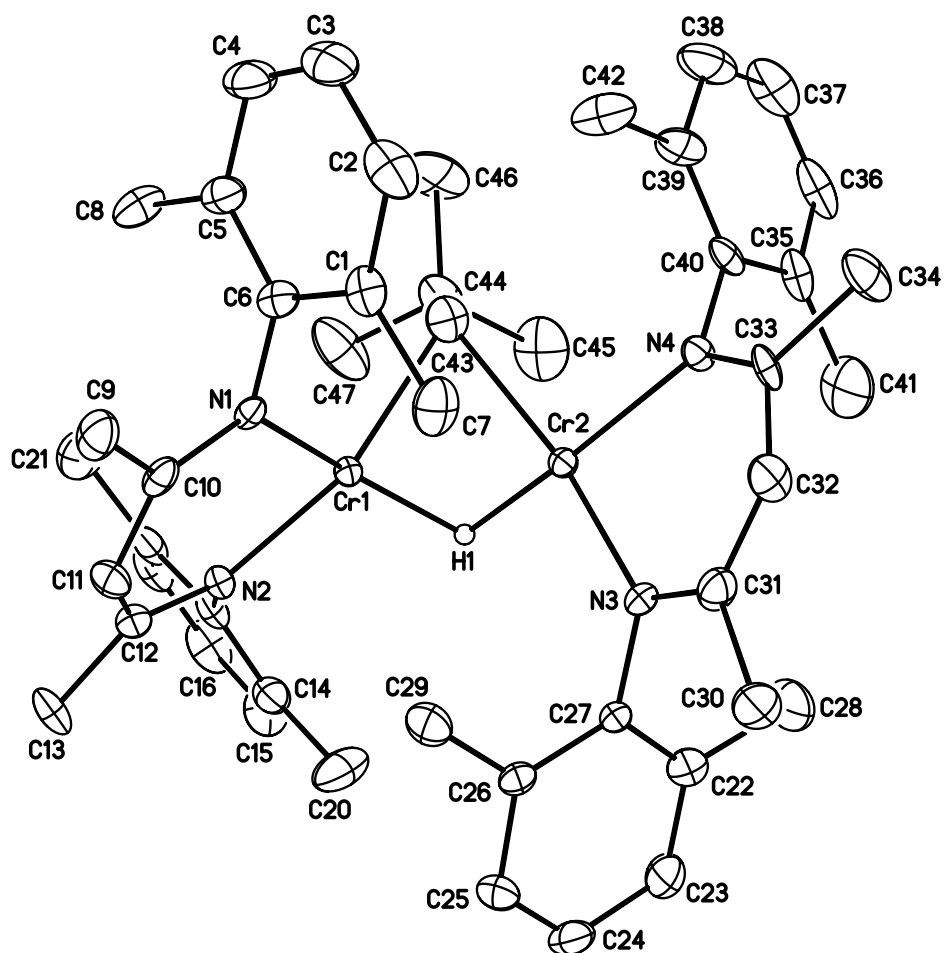
Figure 2.7   Molecular structure of $(L^{Me}Cr)_2(\mu\text{-}CH_2CMe_3)(\mu\text{-}H)$ (**16**). Ellipsoids are drawn at the 20% probability level. Hydrogen atoms, except the bridging hydride, have been omitted for clarity.

Table 2.7   Interatomic distances (Å) and angles (°) for $(L^{Me}Cr)_2(\mu\text{-}CH_2CMe_3)(\mu\text{-}H)$ (**16**)

	Distances (Å)		
Cr(1)-N(2)	2.055(5)	C(14)-C(20)	1.499(10)
Cr(1)-N(1)	2.057(5)	C(15)-C(16)	1.359(11)
Cr(1)-C(43)	2.213(8)	C(16)-C(17)	1.357(11)
Cr(1)-Cr(2)	2.5134(14)	C(17)-C(18)	1.399(11)
Cr(1)-H(1)	1.715(19)	C(18)-C(19)	1.403(9)
Cr(2)-N(3)	2.037(5)	C(18)-C(21)	1.508(11)
Cr(2)-N(4)	2.079(5)	C(22)-C(23)	1.375(11)
Cr(2)-C(43)	2.306(8)	C(22)-C(27)	1.403(10)
Cr(2)-H(1)	1.714(19)	C(22)-C(28)	1.527(11)
N(1)-C(10)	1.333(8)	C(23)-C(24)	1.379(11)
N(1)-C(6)	1.426(8)	C(24)-C(25)	1.383(11)
N(2)-C(12)	1.332(8)	C(25)-C(26)	1.395(10)
N(2)-C(19)	1.437(8)	C(26)-C(27)	1.391(9)
N(4)-C(33)	1.297(7)	C(26)-C(29)	1.491(10)
N(4)-C(40)	1.447(8)	C(30)-C(31)	1.531(9)
N(3)-C(31)	1.335(8)	C(31)-C(32)	1.391(9)
N(3)-C(27)	1.439(8)	C(32)-C(33)	1.425(9)
C(1)-C(6)	1.402(9)	C(33)-C(34)	1.515(9)
C(1)-C(2)	1.401(10)	C(35)-C(40)	1.388(9)
C(1)-C(7)	1.503(10)	C(35)-C(36)	1.400(11)
C(2)-C(3)	1.385(12)	C(35)-C(41)	1.495(12)
C(3)-C(4)	1.357(11)	C(36)-C(37)	1.351(12)
C(4)-C(5)	1.390(10)	C(37)-C(38)	1.351(13)
C(5)-C(6)	1.401(9)	C(38)-C(39)	1.406(11)
C(5)-C(8)	1.517(10)	C(39)-C(40)	1.387(10)
C(9)-C(10)	1.524(9)	C(39)-C(42)	1.529(11)
C(10)-C(11)	1.395(9)	C(43)-C(44)	1.533(11)
C(11)-C(12)	1.397(9)	C(44)-C(47)	1.533(11)
C(12)-C(13)	1.523(9)	C(44)-C(46)	1.552(11)
C(14)-C(15)	1.392(10)	C(44)-C(45)	1.569(12)
C(14)-C(19)	1.412(10)		

Angles (°)

N(2)-Cr(1)-N(1)	89.1(2)	C(15)-C(14)-C(19)	119.8(7)
N(2)-Cr(1)-C(43)	149.4(3)	C(15)-C(14)-C(20)	120.7(7)
N(1)-Cr(1)-C(43)	101.6(2)	C(19)-C(14)-C(20)	119.5(7)
N(2)-Cr(1)-Cr(2)	141.78(15)	C(16)-C(15)-C(14)	120.3(8)
N(1)-Cr(1)-Cr(2)	114.63(14)	C(17)-C(16)-C(15)	120.8(8)
C(43)-Cr(1)-Cr(2)	58.0(2)	C(16)-C(17)-C(18)	121.5(8)
N(2)-Cr(1)-H(1)	103.3(9)	C(17)-C(18)-C(19)	118.6(7)
N(1)-Cr(1)-H(1)	151.6(14)	C(17)-C(18)-C(21)	121.5(7)
C(43)-Cr(1)-H(1)	80.7(15)	C(19)-C(18)-C(21)	119.9(7)
Cr(2)-Cr(1)-H(1)	42.9(6)	C(18)-C(19)-C(14)	119.0(7)
N(3)-Cr(2)-N(4)	89.1(2)	C(18)-C(19)-N(2)	119.5(6)
N(3)-Cr(2)-C(43)	166.3(3)	C(14)-C(19)-N(2)	121.5(6)
N(4)-Cr(2)-C(43)	95.5(2)	C(23)-C(22)-C(27)	118.8(7)
N(3)-Cr(2)-Cr(1)	115.32(15)	C(23)-C(22)-C(28)	119.5(8)
N(4)-Cr(2)-Cr(1)	141.25(15)	C(27)-C(22)-C(28)	121.6(7)
C(43)-Cr(2)-Cr(1)	54.5(2)	C(24)-C(23)-C(22)	121.6(8)
N(3)-Cr(2)-H(1)	100.3(17)	C(23)-C(24)-C(25)	119.5(8)
N(4)-Cr(2)-H(1)	165.4(17)	C(24)-C(25)-C(26)	120.3(7)
C(43)-Cr(2)-H(1)	78.0(15)	C(27)-C(26)-C(25)	119.4(7)
Cr(1)-Cr(2)-H(1)	42.9(6)	C(27)-C(26)-C(29)	121.5(6)
Cr(1)-H(1)-Cr(2)	94(1)	C(25)-C(26)-C(29)	119.1(7)
C(10)-N(1)-C(6)	115.5(5)	C(26)-C(27)-C(22)	120.2(6)
C(10)-N(1)-Cr(1)	123.9(4)	C(26)-C(27)-N(3)	120.7(6)
C(6)-N(1)-Cr(1)	120.4(4)	C(22)-C(27)-N(3)	119.1(6)
C(12)-N(2)-C(19)	116.1(5)	N(3)-C(31)-C(32)	124.0(6)
C(12)-N(2)-Cr(1)	126.5(4)	N(3)-C(31)-C(30)	119.9(6)
C(19)-N(2)-Cr(1)	116.9(4)	C(32)-C(31)-C(30)	116.1(6)
C(33)-N(4)-C(40)	115.4(5)	C(31)-C(32)-C(33)	127.6(6)
C(33)-N(4)-Cr(2)	124.5(4)	N(4)-C(33)-C(32)	123.2(6)
C(40)-N(4)-Cr(2)	120.0(4)	N(4)-C(33)-C(34)	122.6(6)
C(31)-N(3)-C(27)	115.4(5)	C(32)-C(33)-C(34)	113.8(5)
C(31)-N(3)-Cr(2)	123.9(4)	C(40)-C(35)-C(36)	119.0(8)
C(27)-N(3)-Cr(2)	120.6(4)	C(40)-C(35)-C(41)	120.2(7)
C(6)-C(1)-C(2)	117.7(7)	C(36)-C(35)-C(41)	120.8(8)
C(6)-C(1)-C(7)	122.0(6)	C(37)-C(36)-C(35)	121.0(8)
C(2)-C(1)-C(7)	120.3(7)	C(38)-C(37)-C(36)	119.8(8)

C(3)-C(2)-C(1)	121.3(8)	C(37)-C(38)-C(39)	122.1(9)
C(4)-C(3)-C(2)	120.1(8)	C(40)-C(39)-C(38)	117.7(8)
C(3)-C(4)-C(5)	121.0(8)	C(40)-C(39)-C(42)	122.1(6)
C(4)-C(5)-C(6)	119.1(7)	C(38)-C(39)-C(42)	120.1(8)
C(4)-C(5)-C(8)	120.4(7)	C(35)-C(40)-C(39)	120.4(6)
C(6)-C(5)-C(8)	120.5(6)	C(35)-C(40)-N(4)	118.8(6)
C(5)-C(6)-C(1)	120.7(6)	C(39)-C(40)-N(4)	120.8(6)
C(5)-C(6)-N(1)	119.1(6)	C(44)-C(43)-Cr(1)	113.0(5)
C(1)-C(6)-N(1)	120.2(6)	C(44)-C(43)-Cr(2)	120.8(5)
N(1)-C(10)-C(11)	124.8(6)	Cr(1)-C(43)-Cr(2)	67.6(2)
N(1)-C(10)-C(9)	120.3(6)	C(47)-C(44)-C(43)	110.9(7)
C(11)-C(10)-C(9)	114.8(6)	C(47)-C(44)-C(46)	107.2(8)
C(10)-C(11)-C(12)	128.1(6)	C(43)-C(44)-C(46)	109.5(7)
N(2)-C(12)-C(11)	122.4(6)	C(47)-C(44)-C(45)	108.7(8)
N(2)-C(12)-C(13)	120.1(6)	C(43)-C(44)-C(45)	109.8(7)
C(11)-C(12)-C(13)	117.5(6)	C(46)-C(44)-C(45)	110.7(8)

Figure 2.8   Molecular structure of (L^Me Cr)$_2$(μ-CH$_2$C$_6$H$_5$)(μ-H) (**17**). Ellipsoids are drawn at the 20% probability level. Hydrogen atoms, except the bridging hydride, and a diethyl ether molecule have been omitted for clarity.

Table 2.8   Interatomic distances (Å) and angles (°) for $(L^{Me}Cr)_2(\mu\text{-}CH_2C_6H_5)(\mu\text{-}H)$ (**17**)

Distances (Å)			
Cr(1)-N(1)	2.014(5)	C(15)-C(16)	1.375(12)
Cr(1)-N(2)	2.062(5)	C(16)-C(17)	1.360(12)
Cr(1)-C(43)	2.303(7)	C(17)-C(18)	1.408(11)
Cr(1)-Cr(2)	2.5906(13)	C(18)-C(19)	1.390(10)
Cr(1)-H(1)	1.78(7)	C(18)-C(21)	1.502(10)
Cr(2)-N(4)	2.042(5)	C(22)-C(23)	1.383(10)
Cr(2)-N(3)	2.052(5)	C(22)-C(27)	1.415(10)
Cr(2)-C(43)	2.181(7)	C(22)-C(28)	1.523(10)
Cr(2)-H(1)	1.73(7)	C(23)-C(24)	1.372(11)
N(1)-C(10)	1.345(8)	C(24)-C(25)	1.395(12)
N(1)-C(6)	1.452(9)	C(25)-C(26)	1.402(9)
N(2)-C(12)	1.323(8)	C(26)-C(27)	1.404(9)
N(2)-C(19)	1.436(9)	C(26)-C(29)	1.507(10)
N(3)-C(31)	1.348(8)	C(30)-C(31)	1.500(9)
N(3)-C(27)	1.438(8)	C(31)-C(32)	1.385(10)
N(4)-C(33)	1.329(8)	C(32)-C(33)	1.393(10)
N(4)-C(40)	1.439(8)	C(33)-C(34)	1.547(8)
C(1)-C(2)	1.396(10)	C(35)-C(36)	1.396(10)
C(1)-C(6)	1.400(10)	C(35)-C(40)	1.398(10)
C(1)-C(7)	1.508(10)	C(35)-C(41)	1.527(10)
C(2)-C(3)	1.390(11)	C(36)-C(37)	1.378(11)
C(3)-C(4)	1.377(11)	C(37)-C(38)	1.393(11)
C(4)-C(5)	1.404(10)	C(38)-C(39)	1.380(10)
C(5)-C(6)	1.391(10)	C(39)-C(40)	1.390(10)
C(5)-C(8)	1.499(10)	C(39)-C(42)	1.515(10)
C(9)-C(10)	1.507(10)	C(43)-C(44)	1.499(9)
C(10)-C(11)	1.401(10)	C(44)-C(45)	1.393(9)
C(11)-C(12)	1.413(10)	C(44)-C(49)	1.405(10)
C(12)-C(13)	1.523(8)	C(45)-C(46)	1.399(10)
C(14)-C(19)	1.413(10)	C(46)-C(47)	1.382(11)
C(14)-C(15)	1.419(11)	C(47)-C(48)	1.392(11)
C(14)-C(20)	1.500(11)	C(48)-C(49)	1.405(11)

N(1)-Cr(1)-N(2)	89.7(2)	C(19)-C(14)-C(20)	121.1(7)
N(1)-Cr(1)-C(43)	173.0(2)	C(15)-C(14)-C(20)	119.9(7)
N(2)-Cr(1)-C(43)	94.8(2)	C(16)-C(15)-C(14)	120.1(8)
N(1)-Cr(1)-Cr(2)	121.48(15)	C(17)-C(16)-C(15)	120.3(8)
N(2)-Cr(1)-Cr(2)	143.76(18)	C(16)-C(17)-C(18)	121.9(8)
C(43)-Cr(1)-Cr(2)	52.53(15)	C(19)-C(18)-C(17)	118.6(7)
N(1)-Cr(1)-H(1)	92(2)	C(19)-C(18)-C(21)	122.5(7)
N(2)-Cr(1)-H(1)	167(2)	C(17)-C(18)-C(21)	118.9(7)
C(43)-Cr(1)-H(1)	84(2)	C(18)-C(19)-C(14)	120.2(7)
Cr(2)-Cr(1)-H(1)	42(2)	C(18)-C(19)-N(2)	122.1(6)
N(4)-Cr(2)-N(3)	90.4(2)	C(14)-C(19)-N(2)	117.7(6)
N(4)-Cr(2)-C(43)	148.5(2)	C(23)-C(22)-C(27)	119.5(7)
N(3)-Cr(2)-C(43)	98.0(2)	C(23)-C(22)-C(28)	120.8(7)
N(4)-Cr(2)-Cr(1)	138.34(17)	C(27)-C(22)-C(28)	119.7(6)
N(3)-Cr(2)-Cr(1)	124.27(17)	C(24)-C(23)-C(22)	121.9(8)
C(43)-Cr(2)-Cr(1)	56.95(18)	C(23)-C(24)-C(25)	118.8(7)
N(4)-Cr(2)-H(1)	96(2)	C(24)-C(25)-C(26)	121.5(7)
N(3)-Cr(2)-H(1)	155(2)	C(25)-C(26)-C(27)	118.6(7)
C(43)-Cr(2)-H(1)	89(2)	C(25)-C(26)-C(29)	118.5(6)
Cr(1)-Cr(2)-H(1)	43(2)	C(27)-C(26)-C(29)	122.9(6)
Cr(1)-H(1)-Cr(2)	95(4)	C(26)-C(27)-C(22)	119.6(6)
C(10)-N(1)-C(6)	115.0(6)	C(26)-C(27)-N(3)	122.3(6)
C(10)-N(1)-Cr(1)	126.0(5)	C(22)-C(27)-N(3)	118.1(6)
C(6)-N(1)-Cr(1)	119.1(4)	N(3)-C(31)-C(32)	122.3(6)
C(12)-N(2)-C(19)	117.1(5)	N(3)-C(31)-C(30)	120.2(6)
C(12)-N(2)-Cr(1)	123.6(5)	C(32)-C(31)-C(30)	117.4(6)
C(19)-N(2)-Cr(1)	119.2(4)	C(31)-C(32)-C(33)	128.3(6)
C(31)-N(3)-C(27)	116.7(5)	N(4)-C(33)-C(32)	125.0(6)
C(31)-N(3)-Cr(2)	124.2(5)	N(4)-C(33)-C(34)	118.5(6)
C(27)-N(3)-Cr(2)	118.4(4)	C(32)-C(33)-C(34)	116.5(6)
C(33)-N(4)-C(40)	117.8(5)	C(36)-C(35)-C(40)	119.7(7)
C(33)-N(4)-Cr(2)	121.7(5)	C(36)-C(35)-C(41)	119.8(7)
C(40)-N(4)-Cr(2)	120.0(4)	C(40)-C(35)-C(41)	120.5(7)
C(2)-C(1)-C(6)	118.4(7)	C(37)-C(36)-C(35)	120.7(7)
C(2)-C(1)-C(7)	119.7(7)	C(36)-C(37)-C(38)	119.2(7)

C(6)-C(1)-C(7)	121.8(6)	C(39)-C(38)-C(37)	120.9(8)
C(3)-C(2)-C(1)	120.7(8)	C(38)-C(39)-C(40)	120.1(7)
C(4)-C(3)-C(2)	119.4(8)	C(38)-C(39)-C(42)	119.1(7)
C(3)-C(4)-C(5)	122.1(8)	C(40)-C(39)-C(42)	120.8(6)
C(6)-C(5)-C(4)	117.1(7)	C(39)-C(40)-C(35)	119.5(6)
C(6)-C(5)-C(8)	122.8(6)	C(39)-C(40)-N(4)	120.5(6)
C(4)-C(5)-C(8)	120.1(7)	C(35)-C(40)-N(4)	119.9(6)
C(5)-C(6)-C(1)	122.2(7)	C(44)-C(43)-Cr(2)	91.1(4)
C(5)-C(6)-N(1)	119.8(6)	C(44)-C(43)-Cr(1)	128.8(5)
C(1)-C(6)-N(1)	117.9(6)	Cr(2)-C(43)-Cr(1)	70.5(2)
N(1)-C(10)-C(11)	123.0(7)	C(45)-C(44)-C(49)	117.4(6)
N(1)-C(10)-C(9)	121.6(6)	C(45)-C(44)-C(43)	122.3(6)
C(11)-C(10)-C(9)	115.5(6)	C(49)-C(44)-C(43)	120.2(6)
C(10)-C(11)-C(12)	126.7(6)	C(44)-C(45)-C(46)	121.6(7)
N(2)-C(12)-C(11)	125.1(6)	C(47)-C(46)-C(45)	120.7(7)
N(2)-C(12)-C(13)	119.5(6)	C(46)-C(47)-C(48)	118.9(7)
C(11)-C(12)-C(13)	115.4(6)	C(47)-C(48)-C(49)	120.5(7)
C(19)-C(14)-C(15)	118.9(7)	C(48)-C(49)-C(44)	120.9(7)

2.2.3 Thermal stability of chromium alkyl hydrides

With the three chromium alkyl hydrides in hand, the influence of different substituents on complex stability was then explored. Thermal reactions of **1**, **16**, and **17** in neat benzene-d_6 at 80°C led to decomposition, as evidenced by ^{1}H NMR spectroscopy. The reactants were consumed via a first order process with observed rate constants of 2.40 ($\pm$ 0.05) x10^{-6} s^{-1} (R^2= 0.992) for **1**, 2.62 ($\pm$ 0.06) x10^{-5} s^{-1} (R^2= 0.994) for **16**, and 8.69 ($\pm$ 0.30) x10^{-5} s^{-1} (R^2= 0.992) for **17**. Kinetic measurements are detailed in **Appendix B**.

Decomposition of **17** exhibits the fastest rate constant, and the decomposition products have been identified by LIFDI and ^{1}H NMR spectroscopies, to be a mixture of $(L^{Me}Cr)_2(\mu\text{-H})_2$ (**2**) and Cr(II) benzyl precursor $L^{Me}Cr(\eta^2\text{-CH}_2C_6H_5)$ (**12**). The formation ratio of these two products is roughly 1:2 by ^{1}H NMR spectrum. Toluene as an organic product was not detected.

The decomposition of **16** is slower than that of **17**, and the products were recognized to be $(L^{Me}Cr)_2(\mu\text{-H})_2$ (**2**) and $(L^{Me}Cr)_2(\mu\text{-C}_6D_5)(\mu\text{-H})$ (**18-d$_5$**). The latter compound will be further discussed in **Section 2.2.5**. The generation of **18-d$_5$** presumably involved a C-D bond activation. The incorporation of deuterated phenyl group was supported by the infrared spectrum taken of the crude products, with ν = 2268 cm^{-1} as a distinct C-D bond stretching frequency.

Thermal decomposition of **1** in benzene-d_6 proceeded with the slowest rate among all. Considering the high resemblance between **1** and **16** (bridging -CH$_2$SiMe$_3$ and -CH$_2$CMe$_3$ ligand), the reason for the discrepancy between their decomposition rates is unclear. The resulting products were, however, found to be analogous to those found in **16**. The organic product generated from **1** was analyzed by GC/MS spectroscopy on the volatile portion transferred, shown in Figure 2.9. Fragments 73

$[CH_2DSiMe_3 - CH_2D]^+$, 74 $[CH_2DSiMe_3 - CH_3]^+$, and parent ion 89 $[CH_2DSiMe_3^+]$ were observed.
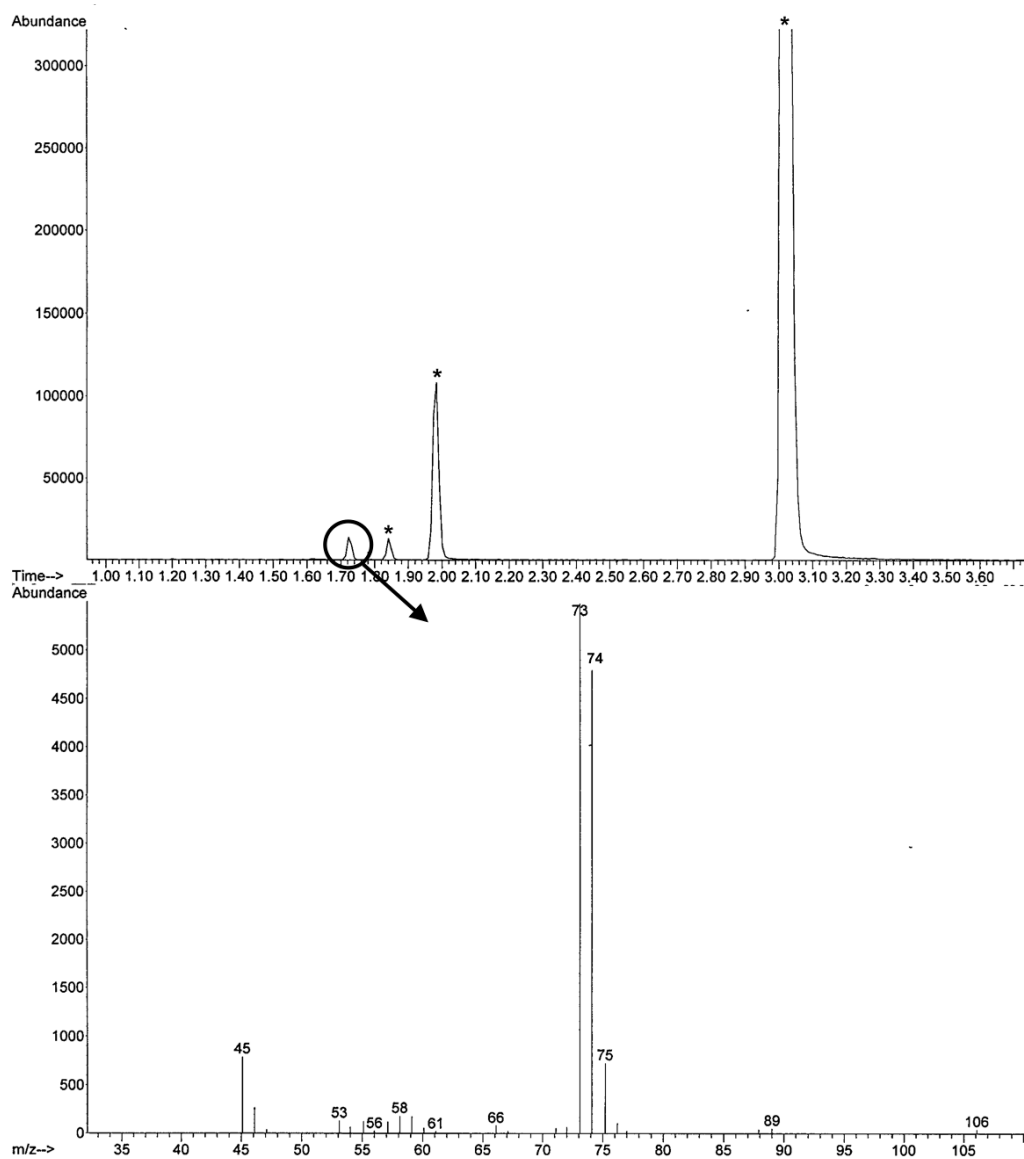
Figure 2.9   GCMS of sample showing peaks at 73 $[SiMe_3^+]$, 74 $[CH_2DSiMe_2^+]$ which are fragments of 89 $[CH_2DSiMe_3^+]$. Asterisk signs (*) represent solvent signals.

2.2.4 C-H bond activation reaction exploration

As mentioned, **1** and **16** underwent C-D bond activation upon heating in C_6D_6 solution. In order to probe the mechanism, the reactivity of **16** was explored. In addition to benzene activation, thermal reactions of **16** in other organic substrates, i. e. tetramethylsilane and toluene resulted in similar consequences. Scheme 2.12 summarizes the C-H bond activations discovered during the course of this study, which resulted in the interconversion of various chromium alkyl/aryl hydrides. The activation reactions (**16** + RH, R = CH_2SiMe_3, C_6H_5, C_6H_4Me) described below were accompanied by the formation of **2** as inorganic byproduct and the elimination of neopentane. In addition, the possible formation of $(L^{Me}Cr)_2(\mu-CH_2CMe_3)_2$, $(L^{Me}Cr)_2(\mu-CH_2CMe_3)(\mu-R)$, or $(L^{Me}Cr)_2(\mu-R)_2$ were all excluded by mass spectrometry analysis of crude samples.
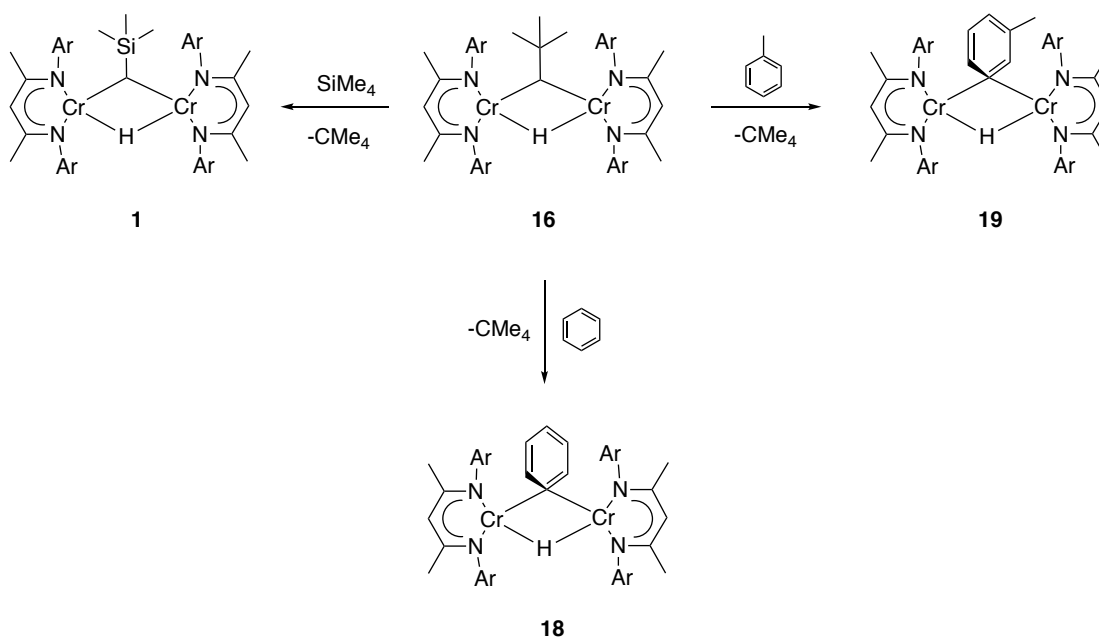
Scheme 2.12 C-H bond activation reactions of **16** with hydrocarbon substrates. Ar = 2,6-dimethylphenyl.

Thermolysis of **16** in tetramethylsilane at 50°C for 5 days resulted in the formation of **1**. Neopentane organic product was revealed by GC/MS analysis, with fragment 57 $[(CH_3)_4C - CH_3]^+$ observed, as shown in Figure 2.10. The relative amounts of **1** and **2** generated were in roughly 1:1 ratio by ^1H NMR spectroscopy.
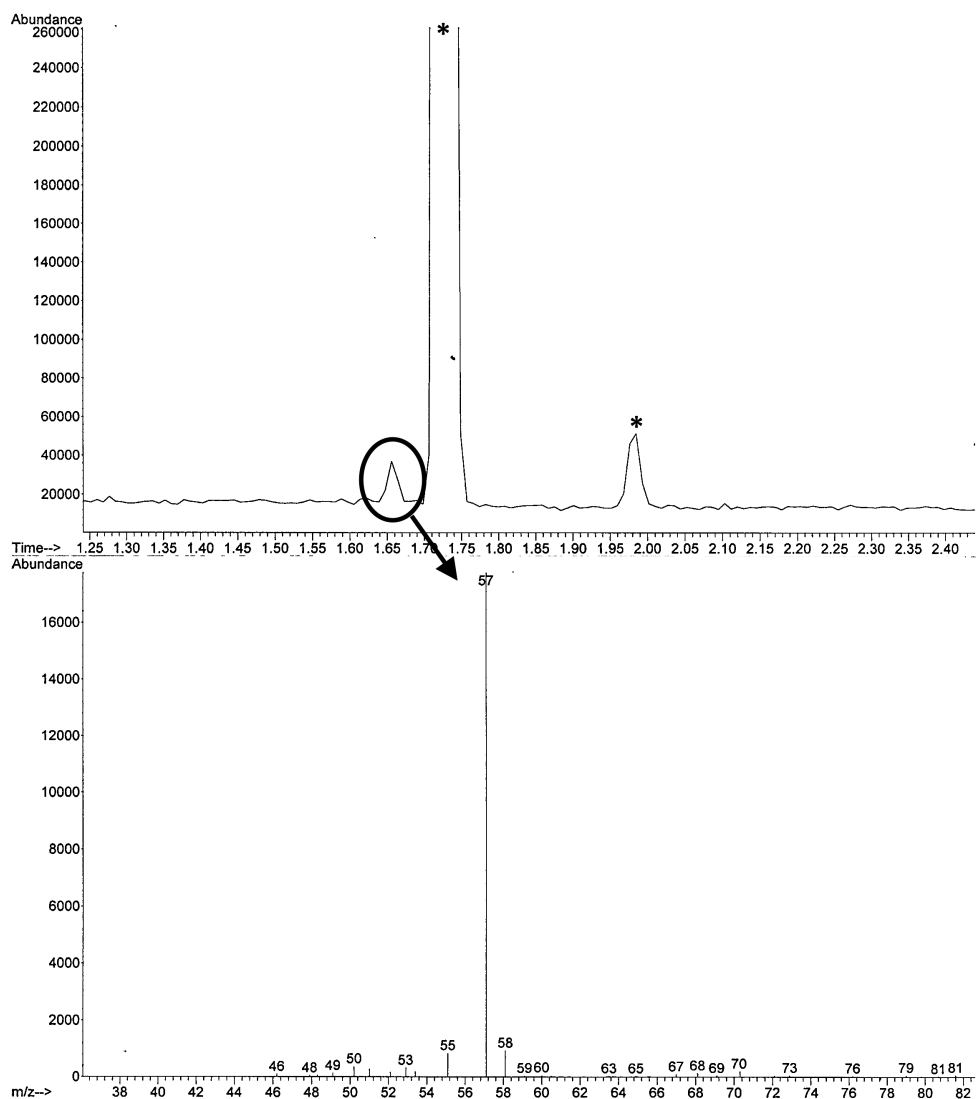
Figure 2.10   GCMS of sample showing peak at 57 $[C(CH_3)_3^+]$, which is fragment of 72 neopentane $C(CH_3)_4$. Asterisk signs (*) represent solvent signals.

104

Thermolysis of **16** in toluene resulted in the formation of $(L^{Me}Cr)_2(\mu\text{-m-}$ $CH_3C_6H_4)(\mu\text{-H})$ (**19**), which was characterized by X-ray crystallography. In this particular case, the known chromium benzyl hydride **17** was not observed. Despite the absence of **17**, the possibility of the formation of other isomers needed to be considered. To confirm this, an independent analysis was carried out and described in the following. After heating a toluene solution of **16** in an ampoule (~10 mg in 5 mL) at 80°C under vacuum for 16 hours, the ampoule was brought back into the glovebox where the toluene was removed in vacuo. Cyclohexane (1 mL) was used to dissolve the residue and the extract was filtered through celite (byproduct **2** is not very soluble in CyH and thus could be removed). ^2H NMR spectroscopic analysis of the volatile products of the reaction of filtered C_6H_{12} solution with DCl (1M in diethyl ether) was performed. It was reasonable to expect that the functionalized deuterated toluene was generated from the above reaction. Figure 2.11 shows the ^2H NMR spectrum, and the result was consistent with the formation of $(CH_3)C_6H_4D$. The major resonance at 7.12 ppm relates to the meta substituted d_1-Toluene (see below). Moreover, in Figure 2.11, a smaller peak at 7.03 ppm suggests the isomers of d_1-Toluene. A strong suggestion is para substituted d_1-Toluene. The ortho substituted d_1-Toluene is less preferred because complex like $(L^{Me}Cr)_2(\mu\text{-o-}CH_3C_6H_4)(\mu\text{-H})$ would be sterically crowded for the coordination sphere. Due to lower resolution by the limitation of ^2H NMR spectroscopy, proton-deuterium couplings were not observed.

Structure **19** was obtained by recrystallization from a pentane solution, and the structural data was of good quality. Modeling a partially occupied para-methyl of the bridging tolyl ligand did not converge, indicated that $(L^{Me}Cr)_2(\mu\text{-p-}CH_3C_6H_4)(\mu\text{-H})$

did not co-crystallize with **19**. It was thus suggested that **19** was selectively

crystallized under such conditions.
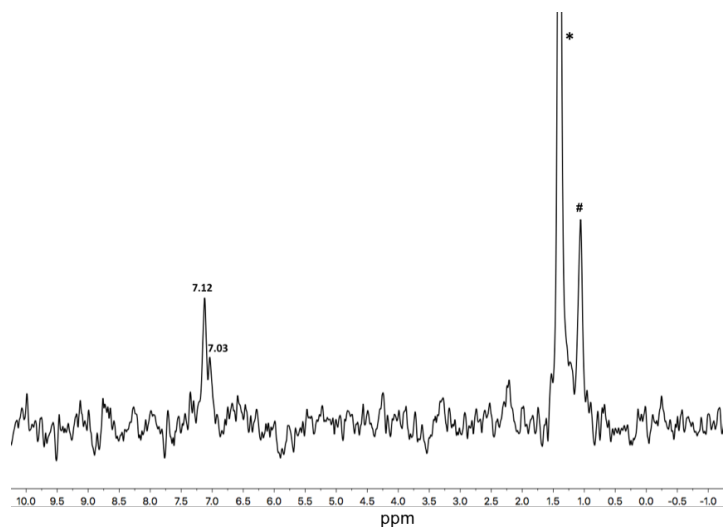
Figure 2.11 ^{2}H NMR spectrum of volatile products. Asterisk (*) represents C_6H_{12} and
pound (#) represents DCl. Horizontal axis presents chemical shift with
units in ppm.

An independent synthesis of **19** was carried out (see the **2.2.5**). Treatment of

C_6H_{12} solution of **19** with equivalent amount of DCl (1M in diethyl ether) was

conducted. ^{2}H NMR spectroscopic analysis of the volatile was consistent with a

characteristic peak at 7.12 ppm. This reaction is depicted in Scheme 2.13.
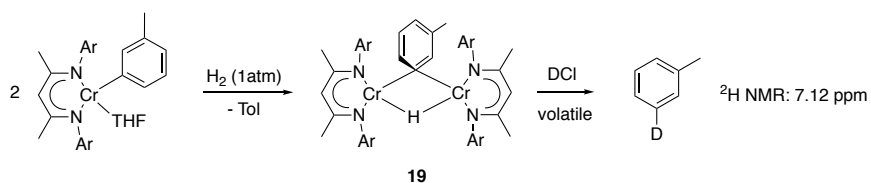
Scheme 2.13   Reference for meta substituted d$_1$-Toluene

2.2.5 Synthesis of chromium aryl hydride

The newly formed aryl hydride complexes **18** and **19** can be independently synthesized by hydrogenation of chromium(II) aryls. Reactions of $L^{Me}Cr(C_6H_5)(THF)$ (**20**) and $L^{Me}Cr(m\text{-}CH_3C_6H_4)(THF)$ (**21**) in pentane with excess hydrogen gas yielded complexes **18** and **19**, respectively (Scheme 2.14). The molecular structures of **18** and **19**, as determined by X-ray diffraction, are shown in Figures 2.12 and 2.13.

Ar = 2,6-dimethylphenyl

18, R = C_6H_5
19, R = m-$CH_3C_6H_4$
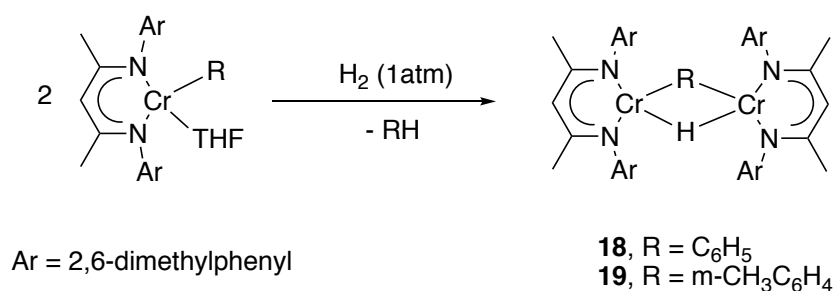
Scheme 2.14   Synthesis of chromium aryl hydrides **18** and **19**

18 and **19** are binuclear complexes which are individually held together by a bridging hydride (located in the X-ray difference maps) and a bridging aryl ligand (phenyl for **18** and meta-tolyl for **19**). The formation of **18** is reminiscent of a previously reported compound with L^{iPr} ligand, namely $(L^{iPr}Cr)_2(\mu\text{-}C_6H_5)(\mu\text{-}H)$. The Cr-Cr separation of 2.6277(10) Å was described to have some degree of metal-metal bonding.[7] The Cr-Cr separations (of 2.7282(5) Å for **18** and 2.720(1) Å for **19**) are comparable to each other. These distances are slightly longer than that in $(L^{iPr}Cr)_2(\mu\text{-}C_6H_5)(\mu\text{-}H)$, and also longer than those in alkyl hydrides **1**, **16**, and **17**.

The magnetic moment of a complex with two independent Cr(II) high spin d^4 system is expected to be 6.8 μ_B. At $\mu_{eff} = 2.7$ μ_B (293K) for both **18** and **19**, the

moments indicate strong antiferromagnetic coupling between the two Cr^{II} ions, but metal-metal bonding cannot be dismissed. The ^1H NMR spectra of **18** and **19** exhibited similar resonances pattern. The LIFDI mass spectra showed the molecular ions (m/z = 792.3384 [M$^+$] for **18** and m/z 806.3613 [M$^+$] for **19**) as the base peaks with excellent agreement with calculated isotope patterns.

18 was found to be thermally stable at 80°C for two weeks, which was monitored by ^1H NMR spectroscopy in C_6D_6. The formation of **18-d$_5$** by C-D bond activation was ruled out by mass spectrometry analysis of the products.

$L^{Me}Cr(C_6H_5)(THF)$ (**20**) was fully characterized and its molecular structure is depicted in Figure 2.14. $L^{Me}Cr(m\text{-}CH_3C_6H_4)(THF)$ (**21**) was only characterized by ^1H NMR spectrum and is reported in the synthesis of **19** in the experimental section.
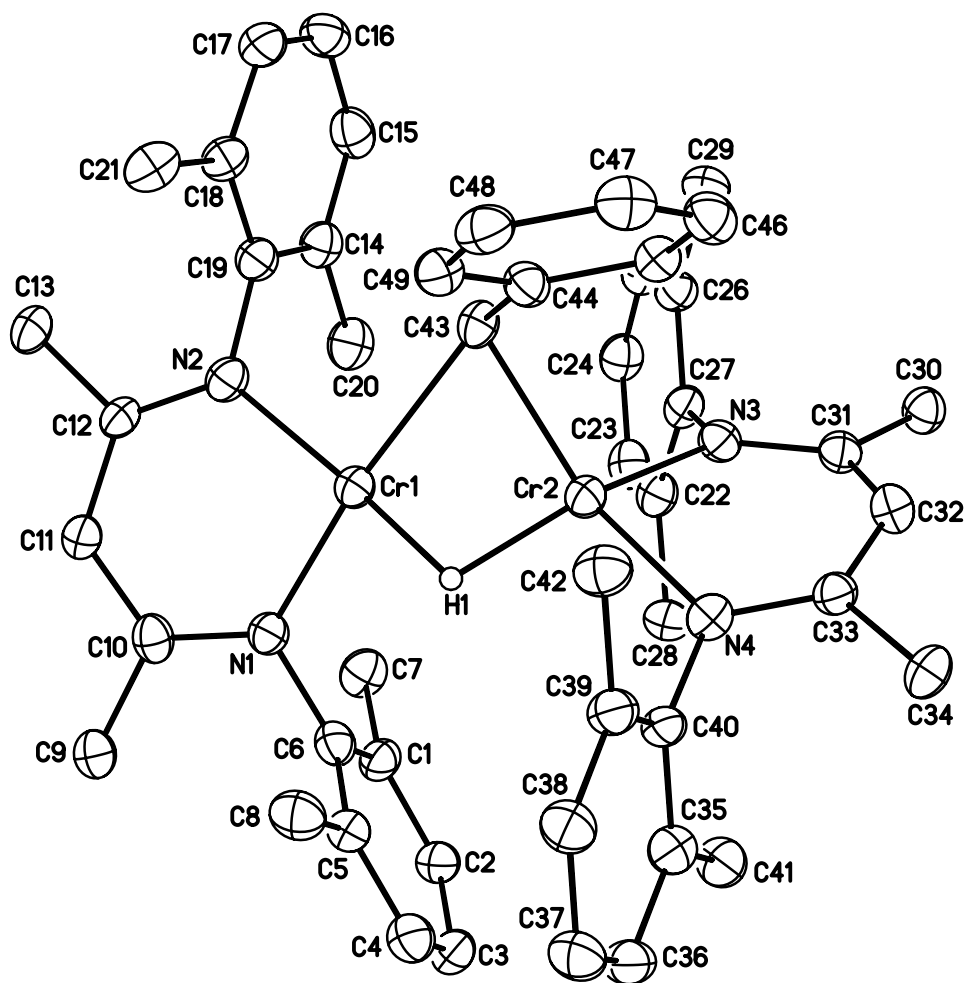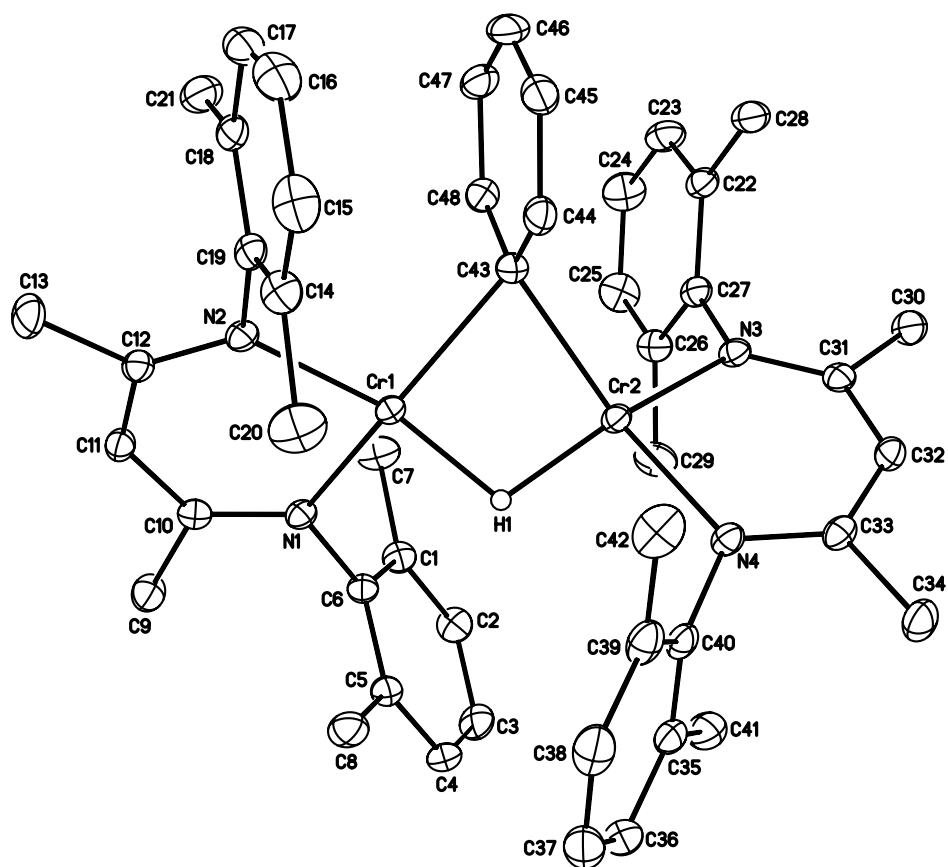
Figure 2.12 Molecular structure of $(L^{Me}Cr)_2(\mu\text{-}C_6H_5)(\mu\text{-}H)$ (**18**). Ellipsoids are drawn at the 30% probability level. Hydrogen atoms, except the bridging hydride, have been omitted for clarity.

Table 2.9   Interatomic distances (Å) and angles (º) for (L^Me Cr)$_2$(μ-C$_6$H$_5$)(μ-H) (**18**)

Distances (Å)			
Cr(1)-N(2)	2.035(4)	C(15)-C(16)	1.368(9)
Cr(1)-N(1)	2.062(3)	C(16)-C(17)	1.393(9)
Cr(1)-C(43)	2.220(4)	C(17)-C(18)	1.389(7)
Cr(1)-Cr(2)	2.7201(9)	C(18)-C(19)	1.395(7)
Cr(1)-H(1)	1.71(2)	C(18)-C(21)	1.512(7)
Cr(2)-N(3)	2.033(3)	C(22)-C(23)	1.388(6)
Cr(2)-N(4)	2.075(3)	C(22)-C(27)	1.404(6)
Cr(2)-C(43)	2.238(4)	C(22)-C(28)	1.503(6)
Cr(2)-H(1)	1.73(2)	C(23)-C(24)	1.381(6)
N(1)-C(10)	1.332(5)	C(24)-C(25)	1.381(6)
N(1)-C(6)	1.437(5)	C(25)-C(26)	1.386(6)
N(2)-C(12)	1.340(5)	C(26)-C(27)	1.399(5)
N(2)-C(19)	1.434(6)	C(26)-C(29)	1.508(6)
N(3)-C(31)	1.335(5)	C(30)-C(31)	1.510(6)
N(3)-C(27)	1.431(5)	C(31)-C(32)	1.387(5)
N(4)-C(33)	1.327(5)	C(32)-C(33)	1.399(6)
N(4)-C(40)	1.437(5)	C(33)-C(34)	1.523(5)
C(1)-C(6)	1.397(6)	C(35)-C(36)	1.389(7)
C(1)-C(2)	1.396(6)	C(35)-C(40)	1.401(6)
C(1)-C(7)	1.497(6)	C(35)-C(41)	1.502(7)
C(2)-C(3)	1.380(7)	C(36)-C(37)	1.367(8)
C(3)-C(4)	1.374(7)	C(37)-C(38)	1.382(8)
C(4)-C(5)	1.396(6)	C(38)-C(39)	1.392(7)
C(5)-C(6)	1.405(6)	C(39)-C(40)	1.403(6)
C(5)-C(8)	1.497(6)	C(39)-C(42)	1.498(7)
C(9)-C(10)	1.512(6)	C(43)-C(44)	1.397(6)
C(10)-C(11)	1.398(6)	C(43)-C(48)	1.410(6)
C(11)-C(12)	1.385(6)	C(44)-C(45)	1.405(6)
C(12)-C(13)	1.520(6)	C(45)-C(46)	1.366(7)
C(14)-C(15)	1.374(8)	C(45)-C(49)	1.481(7)
C(14)-C(19)	1.418(7)	C(46)-C(47)	1.385(7)
C(14)-C(20)	1.486(8)	C(47)-C(48)	1.403(6)

Angles (°)			
N(2)-Cr(1)-N(1)	89.59(14)	C(19)-C(14)-C(20)	120.6(5)
N(2)-Cr(1)-C(43)	150.17(16)	C(16)-C(15)-C(14)	122.1(6)
N(1)-Cr(1)-C(43)	100.99(14)	C(15)-C(16)-C(17)	120.2(6)
N(2)-Cr(1)-Cr(2)	128.99(11)	C(16)-C(17)-C(18)	120.3(6)
N(1)-Cr(1)-Cr(2)	139.69(10)	C(17)-C(18)-C(19)	118.6(5)
C(43)-Cr(1)-Cr(2)	52.69(11)	C(17)-C(18)-C(21)	120.8(5)
N(1)-Cr(1)-H(1)	93.6(8)	C(19)-C(18)-C(21)	120.7(4)
N(2)-Cr(1)-H(1)	151.7(8)	C(18)-C(19)-C(14)	121.4(5)
C(43)-Cr(1)-H(1)	88.3(8)	C(18)-C(19)-N(2)	118.8(4)
Cr(2)-Cr(1)-H(1)	37.7(8)	C(14)-C(19)-N(2)	119.8(5)
N(3)-Cr(2)-N(4)	90.11(13)	C(23)-C(22)-C(27)	118.6(4)
N(3)-Cr(2)-C(43)	152.95(15)	C(23)-C(22)-C(28)	121.2(4)
N(4)-Cr(2)-C(43)	100.64(14)	C(27)-C(22)-C(28)	120.2(4)
N(3)-Cr(2)-Cr(1)	121.41(9)	C(24)-C(23)-C(22)	121.3(4)
N(4)-Cr(2)-Cr(1)	148.45(10)	C(25)-C(24)-C(23)	119.5(4)
C(43)-Cr(2)-Cr(1)	52.09(11)	C(24)-C(25)-C(26)	121.2(4)
N(4)-Cr(2)-H(1)	93.4(8)	C(25)-C(26)-C(27)	118.9(4)
N(3)-Cr(2)-H(1)	155.7(8)	C(25)-C(26)-C(29)	120.7(4)
C(43)-Cr(2)-H(1)	88.4(8)	C(27)-C(26)-C(29)	120.3(4)
Cr(1)-Cr(2)-H(1)	37.3(8)	C(26)-C(27)-C(22)	120.5(4)
Cr(1)-H(1)-Cr(2)	105(1)	C(26)-C(27)-N(3)	119.6(4)
C(10)-N(1)-C(6)	117.7(3)	C(22)-C(27)-N(3)	119.9(3)
C(10)-N(1)-Cr(1)	125.9(3)	N(3)-C(31)-C(32)	123.8(4)
C(6)-N(1)-Cr(1)	115.5(3)	N(3)-C(31)-C(30)	119.6(4)
C(12)-N(2)-C(19)	117.5(4)	C(32)-C(31)-C(30)	116.6(4)
C(12)-N(2)-Cr(1)	126.0(3)	C(31)-C(32)-C(33)	128.6(4)
C(19)-N(2)-Cr(1)	116.4(3)	N(4)-C(33)-C(32)	124.1(4)
C(31)-N(3)-C(27)	117.1(3)	N(4)-C(33)-C(34)	120.4(4)
C(31)-N(3)-Cr(2)	126.9(3)	C(32)-C(33)-C(34)	115.4(4)
C(27)-N(3)-Cr(2)	115.9(3)	C(36)-C(35)-C(40)	118.8(5)
C(33)-N(4)-C(40)	116.9(3)	C(36)-C(35)-C(41)	119.5(5)
C(33)-N(4)-Cr(2)	125.5(3)	C(40)-C(35)-C(41)	121.7(4)
C(40)-N(4)-Cr(2)	116.8(3)	C(37)-C(36)-C(35)	120.9(5)
C(6)-C(1)-C(2)	118.5(4)	C(36)-C(37)-C(38)	120.3(5)
C(6)-C(1)-C(7)	121.4(4)	C(39)-C(38)-C(37)	121.0(5)
C(2)-C(1)-C(7)	120.1(4)	C(38)-C(39)-C(40)	118.1(5)

C(3)-C(2)-C(1)	120.5(5)	C(38)-C(39)-C(42)	121.5(5)
C(4)-C(3)-C(2)	120.4(4)	C(40)-C(39)-C(42)	120.4(4)
C(3)-C(4)-C(5)	121.4(4)	C(35)-C(40)-C(39)	120.9(4)
C(4)-C(5)-C(6)	117.6(4)	C(35)-C(40)-N(4)	121.0(4)
C(4)-C(5)-C(8)	121.2(4)	C(39)-C(40)-N(4)	118.1(4)
C(6)-C(5)-C(8)	121.2(4)	C(44)-C(43)-C(48)	114.9(4)
C(1)-C(6)-C(5)	121.6(4)	C(44)-C(43)-Cr(1)	109.3(3)
C(1)-C(6)-N(1)	117.7(4)	C(48)-C(43)-Cr(1)	124.5(3)
C(5)-C(6)-N(1)	120.7(4)	C(44)-C(43)-Cr(2)	121.7(3)
N(1)-C(10)-C(11)	123.7(4)	C(48)-C(43)-Cr(2)	106.2(3)
N(1)-C(10)-C(9)	120.1(4)	Cr(1)-C(43)-Cr(2)	75.22(13)
C(11)-C(10)-C(9)	116.2(4)	C(43)-C(44)-C(45)	124.0(5)
C(12)-C(11)-C(10)	128.3(4)	C(46)-C(45)-C(44)	118.2(5)
N(2)-C(12)-C(11)	123.7(4)	C(46)-C(45)-C(49)	119.5(5)
N(2)-C(12)-C(13)	120.2(4)	C(44)-C(45)-C(49)	122.3(5)
C(11)-C(12)-C(13)	116.0(4)	C(45)-C(46)-C(47)	121.5(4)
C(15)-C(14)-C(19)	117.5(6)	C(46)-C(47)-C(48)	119.0(5)
C(15)-C(14)-C(20)	121.9(5)	C(47)-C(48)-C(43)	122.5(5)

Figure 2.13   Molecular structure of $(L^{Me}Cr)_2(\mu$-m-CH$_3$C$_6$H$_4)(\mu$-H) (**19**). Ellipsoids are drawn at the 30% probability level. Hydrogen atoms, except the bridging hydride, have been omitted for clarity.

Table 2.10   Interatomic distances (Å) and angles (°) for $(L^{Me}Cr)_2(\mu\text{-}m\text{-}CH_3C_6H_4)(\mu\text{-}H)$ (**19**)

		Distances (Å)	
Cr(1)-N(2)	2.035(4)	C(15)-C(16)	1.368(9)
Cr(1)-N(1)	2.062(3)	C(16)-C(17)	1.393(9)
Cr(1)-C(43)	2.220(4)	C(17)-C(18)	1.389(7)
Cr(1)-Cr(2)	2.7201(9)	C(18)-C(19)	1.395(7)
Cr(1)-H(1)	1.69(6)	C(18)-C(21)	1.512(7)
Cr(2)-N(3)	2.033(3)	C(22)-C(23)	1.388(6)
Cr(2)-N(4)	2.075(3)	C(22)-C(27)	1.404(6)
Cr(2)-C(43)	2.238(4)	C(22)-C(28)	1.503(6)
Cr(2)-H(1)	1.73(6)	C(23)-C(24)	1.381(6)
N(1)-C(10)	1.332(5)	C(24)-C(25)	1.381(6)
N(1)-C(6)	1.437(5)	C(25)-C(26)	1.386(6)
N(2)-C(12)	1.340(5)	C(26)-C(27)	1.399(5)
N(2)-C(19)	1.434(6)	C(26)-C(29)	1.508(6)
N(3)-C(31)	1.335(5)	C(30)-C(31)	1.510(6)
N(3)-C(27)	1.431(5)	C(31)-C(32)	1.387(5)
N(4)-C(33)	1.327(5)	C(32)-C(33)	1.399(6)
N(4)-C(40)	1.437(5)	C(33)-C(34)	1.523(5)
C(1)-C(6)	1.397(6)	C(35)-C(36)	1.389(7)
C(1)-C(2)	1.396(6)	C(35)-C(40)	1.401(6)
C(1)-C(7)	1.497(6)	C(35)-C(41)	1.502(7)
C(2)-C(3)	1.380(7)	C(36)-C(37)	1.367(8)
C(3)-C(4)	1.374(7)	C(37)-C(38)	1.382(8)
C(4)-C(5)	1.396(6)	C(38)-C(39)	1.392(7)
C(5)-C(6)	1.405(6)	C(39)-C(40)	1.403(6)
C(5)-C(8)	1.497(6)	C(39)-C(42)	1.498(7)
C(9)-C(10)	1.512(6)	C(43)-C(44)	1.397(6)
C(10)-C(11)	1.398(6)	C(43)-C(48)	1.410(6)
C(11)-C(12)	1.385(6)	C(44)-C(45)	1.405(6)
C(12)-C(13)	1.520(6)	C(45)-C(46)	1.366(7)
C(14)-C(15)	1.374(8)	C(45)-C(49)	1.481(7)
C(14)-C(19)	1.418(7)	C(46)-C(47)	1.385(7)
C(14)-C(20)	1.486(8)	C(47)-C(48)	1.403(6)

N(2)-Cr(1)-N(1)	89.59(14)	C(19)-C(14)-C(20)	120.6(5)
N(2)-Cr(1)-C(43)	150.17(16)	C(16)-C(15)-C(14)	122.1(6)
N(1)-Cr(1)-C(43)	100.99(14)	C(15)-C(16)-C(17)	120.2(6)
N(2)-Cr(1)-Cr(2)	128.99(11)	C(16)-C(17)-C(18)	120.3(6)
N(1)-Cr(1)-Cr(2)	139.69(10)	C(17)-C(18)-C(19)	118.6(5)
C(43)-Cr(1)-Cr(2)	52.69(11)	C(17)-C(18)-C(21)	120.8(5)
N(2)-Cr(1)-H(1)	92(2)	C(19)-C(18)-C(21)	120.7(4)
N(1)-Cr(1)-H(1)	155(2)	C(18)-C(19)-C(14)	121.4(5)
C(43)-Cr(1)-H(1)	89(2)	C(18)-C(19)-N(2)	118.8(4)
Cr(2)-Cr(1)-H(1)	38(2)	C(14)-C(19)-N(2)	119.8(5)
N(3)-Cr(2)-N(4)	90.11(13)	C(23)-C(22)-C(27)	118.6(4)
N(3)-Cr(2)-C(43)	152.95(15)	C(23)-C(22)-C(28)	121.2(4)
N(4)-Cr(2)-C(43)	100.64(14)	C(27)-C(22)-C(28)	120.2(4)
N(3)-Cr(2)-Cr(1)	121.41(9)	C(24)-C(23)-C(22)	121.3(4)
N(4)-Cr(2)-Cr(1)	148.45(10)	C(25)-C(24)-C(23)	119.5(4)
C(43)-Cr(2)-Cr(1)	52.09(11)	C(24)-C(25)-C(26)	121.2(4)
N(3)-Cr(2)-H(1)	95(2)	C(25)-C(26)-C(27)	118.9(4)
N(4)-Cr(2)-H(1)	150.6(19)	C(25)-C(26)-C(29)	120.7(4)
C(43)-Cr(2)-H(1)	88(2)	C(27)-C(26)-C(29)	120.3(4)
Cr(1)-Cr(2)-H(1)	37(2)	C(26)-C(27)-C(22)	120.5(4)
Cr(1)-H(1)-Cr(2)	105(3)	C(26)-C(27)-N(3)	119.6(4)
C(10)-N(1)-C(6)	117.7(3)	C(22)-C(27)-N(3)	119.9(3)
C(10)-N(1)-Cr(1)	125.9(3)	N(3)-C(31)-C(32)	123.8(4)
C(6)-N(1)-Cr(1)	115.5(3)	N(3)-C(31)-C(30)	119.6(4)
C(12)-N(2)-C(19)	117.5(4)	C(32)-C(31)-C(30)	116.6(4)
C(12)-N(2)-Cr(1)	126.0(3)	C(31)-C(32)-C(33)	128.6(4)
C(19)-N(2)-Cr(1)	116.4(3)	N(4)-C(33)-C(32)	124.1(4)
C(31)-N(3)-C(27)	117.1(3)	N(4)-C(33)-C(34)	120.4(4)
C(31)-N(3)-Cr(2)	126.9(3)	C(32)-C(33)-C(34)	115.4(4)
C(27)-N(3)-Cr(2)	115.9(3)	C(36)-C(35)-C(40)	118.8(5)
C(33)-N(4)-C(40)	116.9(3)	C(36)-C(35)-C(41)	119.5(5)
C(33)-N(4)-Cr(2)	125.5(3)	C(40)-C(35)-C(41)	121.7(4)
C(40)-N(4)-Cr(2)	116.8(3)	C(37)-C(36)-C(35)	120.9(5)
C(6)-C(1)-C(2)	118.5(4)	C(36)-C(37)-C(38)	120.3(5)
C(6)-C(1)-C(7)	121.4(4)	C(39)-C(38)-C(37)	121.0(5)

C(2)-C(1)-C(7)	120.1(4)	C(38)-C(39)-C(40)	118.1(5)
C(3)-C(2)-C(1)	120.5(5)	C(38)-C(39)-C(42)	121.5(5)
C(4)-C(3)-C(2)	120.4(4)	C(40)-C(39)-C(42)	120.4(4)
C(3)-C(4)-C(5)	121.4(4)	C(35)-C(40)-C(39)	120.9(4)
C(4)-C(5)-C(6)	117.6(4)	C(35)-C(40)-N(4)	121.0(4)
C(4)-C(5)-C(8)	121.2(4)	C(39)-C(40)-N(4)	118.1(4)
C(6)-C(5)-C(8)	121.2(4)	C(44)-C(43)-C(48)	114.9(4)
C(1)-C(6)-C(5)	121.6(4)	C(44)-C(43)-Cr(1)	109.3(3)
C(1)-C(6)-N(1)	117.7(4)	C(48)-C(43)-Cr(1)	124.5(3)
C(5)-C(6)-N(1)	120.7(4)	C(44)-C(43)-Cr(2)	121.7(3)
N(1)-C(10)-C(11)	123.7(4)	C(48)-C(43)-Cr(2)	106.2(3)
N(1)-C(10)-C(9)	120.1(4)	Cr(1)-C(43)-Cr(2)	75.22(13)
C(11)-C(10)-C(9)	116.2(4)	C(43)-C(44)-C(45)	124.0(5)
C(12)-C(11)-C(10)	128.3(4)	C(46)-C(45)-C(44)	118.2(5)
N(2)-C(12)-C(11)	123.7(4)	C(46)-C(45)-C(49)	119.5(5)
N(2)-C(12)-C(13)	120.2(4)	C(44)-C(45)-C(49)	122.3(5)
C(11)-C(12)-C(13)	116.0(4)	C(45)-C(46)-C(47)	121.5(4)
C(15)-C(14)-C(19)	117.5(6)	C(46)-C(47)-C(48)	119.0(5)
C(15)-C(14)-C(20)	121.9(5)	C(47)-C(48)-C(43)	122.5(5)

Figure 2.14   Molecular structure of $L^{Me}Cr(C_6H_5)(THF)$ (**20**). Ellipsoids are drawn at the 30% probability level. Hydrogen atoms have been omitted for clarity.

Table 2.11   Interatomic distances (Å) and angles (°) for $L^{Me}Cr(C_6H_5)(THF)$ (**20**)

Distances (Å)

Cr(1)-N(1)	2.037(2)	C(11)-C(12)	1.397(4)
Cr(1)-O(1)	2.082(2)	C(12)-C(13)	1.515(4)
Cr(1)-N(2)	2.101(3)	C(14)-C(15)	1.385(6)
Cr(1)-C(22)	2.114(3)	C(14)-C(19)	1.413(5)
O(1)-C(28)	1.440(4)	C(14)-C(20)	1.492(6)
O(1)-C(31)	1.439(4)	C(15)-C(16)	1.364(8)
N(1)-C(10)	1.328(4)	C(16)-C(17)	1.380(7)
N(1)-C(6)	1.444(3)	C(17)-C(18)	1.395(5)
N(2)-C(12)	1.332(4)	C(18)-C(19)	1.390(5)
N(2)-C(19)	1.436(4)	C(18)-C(21)	1.502(6)
C(1)-C(2)	1.387(4)	C(22)-C(27)	1.410(4)
C(1)-C(6)	1.403(4)	C(22)-C(23)	1.401(5)
C(1)-C(7)	1.493(5)	C(23)-C(24)	1.392(5)
C(2)-C(3)	1.374(5)	C(24)-C(25)	1.380(5)
C(3)-C(4)	1.379(5)	C(25)-C(26)	1.378(5)
C(4)-C(5)	1.393(4)	C(26)-C(27)	1.386(5)
C(5)-C(6)	1.400(4)	C(28)-C(29)	1.460(6)
C(5)-C(8)	1.511(5)	C(29)-C(30)	1.507(7)
C(9)-C(10)	1.506(4)	C(30)-C(31)	1.507(5)
C(10)-C(11)	1.414(4)		

Angles (°)

N(1)-Cr(1)-O(1)	174.06(9)	C(11)-C(10)-C(9)	116.2(3)
N(1)-Cr(1)-N(2)	88.99(10)	C(12)-C(11)-C(10)	128.0(3)
O(1)-Cr(1)-N(2)	89.81(9)	N(2)-C(12)-C(11)	124.0(3)
N(1)-Cr(1)-C(22)	95.69(11)	N(2)-C(12)-C(13)	119.8(3)
O(1)-Cr(1)-C(22)	86.01(10)	C(11)-C(12)-C(13)	116.2(3)
N(2)-Cr(1)-C(22)	173.26(11)	C(15)-C(14)-C(19)	118.1(4)
C(28)-O(1)-C(31)	108.2(3)	C(15)-C(14)-C(20)	120.9(4)
C(28)-O(1)-Cr(1)	117.2(2)	C(19)-C(14)-C(20)	120.9(3)
C(31)-O(1)-Cr(1)	125.6(2)	C(16)-C(15)-C(14)	121.7(4)
C(10)-N(1)-C(6)	118.0(2)	C(15)-C(16)-C(17)	120.1(4)
C(10)-N(1)-Cr(1)	127.28(19)	C(18)-C(17)-C(16)	120.6(5)

C(6)-N(1)-Cr(1)	114.60(18)	C(19)-C(18)-C(17)	118.9(4)
C(12)-N(2)-C(19)	118.0(2)	C(19)-C(18)-C(21)	120.4(3)
C(12)-N(2)-Cr(1)	125.1(2)	C(17)-C(18)-C(21)	120.8(4)
C(19)-N(2)-Cr(1)	116.89(19)	C(18)-C(19)-C(14)	120.6(3)
C(2)-C(1)-C(6)	118.2(3)	C(18)-C(19)-N(2)	119.5(3)
C(2)-C(1)-C(7)	120.9(3)	C(14)-C(19)-N(2)	119.7(3)
C(6)-C(1)-C(7)	120.8(3)	C(27)-C(22)-C(23)	113.8(3)
C(3)-C(2)-C(1)	121.8(3)	C(27)-C(22)-Cr(1)	125.0(2)
C(2)-C(3)-C(4)	119.7(3)	C(23)-C(22)-Cr(1)	121.1(2)
C(3)-C(4)-C(5)	120.7(3)	C(22)-C(23)-C(24)	123.7(3)
C(6)-C(5)-C(4)	118.9(3)	C(25)-C(24)-C(23)	119.7(3)
C(6)-C(5)-C(8)	120.2(3)	C(24)-C(25)-C(26)	119.1(3)
C(4)-C(5)-C(8)	120.9(3)	C(25)-C(26)-C(27)	120.2(3)
C(5)-C(6)-C(1)	120.6(3)	C(26)-C(27)-C(22)	123.3(3)
C(5)-C(6)-N(1)	118.5(3)	O(1)-C(28)-C(29)	107.5(4)
C(1)-C(6)-N(1)	120.7(3)	C(28)-C(29)-C(30)	106.1(4)
N(1)-C(10)-C(11)	123.3(3)	C(29)-C(30)-C(31)	102.5(3)
N(1)-C(10)-C(9)	120.3(3)	O(1)-C(31)-C(30)	104.0(3)

2.2.6 Mechanistic studies on C-H bond activation reaction

The outcomes of thermal reactions of benzene with **1** and **16** were closely related, while leaving **17** discordant. The formation of stable η^2-coordinated **12** from **17** was likely responsible for the absence of benzene activation product. Indeed, heating a benzene-d_6 solution of **12** up to 120°C for days did not lead to observable change in the ^{1}H NMR spectrum. The thermolysis of **17** is depicted in Scheme 2.15.

17, Ar = 2,6-dimethylphenyl   **12**   **2**
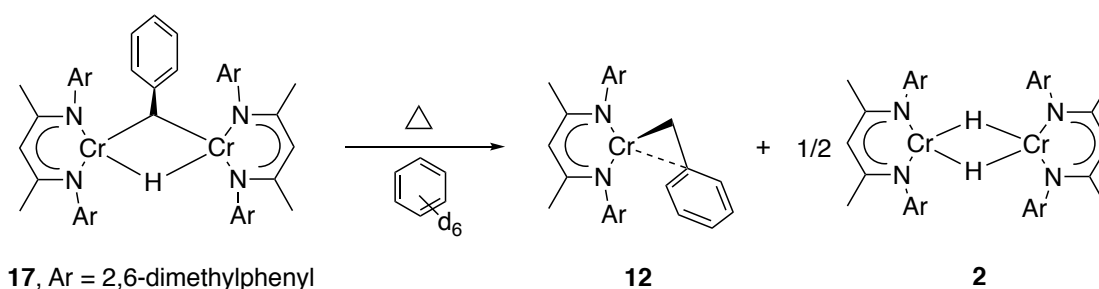
Scheme 2.15   The products for thermal reaction of **17**

It is believed that the lack of reactivity with benzene is due to the robust nature of **12**; in other words, the coordinatively saturated chromium center does not suffer C-H activation. Following this logic, the key to the activation is a coordinatively unsaturated chromium monomer. The following experiments were designed to test this hypothesis. Decomposing **10** and **11** separately in benzene upon heating (100°C) for 2.5 hours produced a new complex, $(L^{Me}Cr)_2(\mu_2\text{-}\eta^6\text{:}\eta^6\text{-}C_6H_5Ph)$ (**22**). Figure 2.15 shows this molecule; the two $L^{Me}Cr$ fragments are joined by a bridging biphenyl ligand, which keeps the two chromium centers at a distance of 3.564 Å. The solid state structure also reveals that only one of the phenyl rings is η^6-coordinated to both chromiums, while the other phenyl is not bound to any chromium. The C-C_{avg} of the

bridging phenyl fragment was determined to be 1.43(2) Å, which is slightly longer than the other phenyl C-C$_{avg}$, which was found to be 1.39(2) Å. The phenomenon of the observed elongated C-C bond distances of the bridged benzene was also found in our previously reported complex, (L^{iPr}Cr)$_2$(μ_2-η^6:η^6-C$_6$H$_6$),[7] where the C-C$_{avg}$ on the bridging benzene fragment was 1.441(7) Å. The proposed mechanism of this reaction is depicted in Scheme 2.16.

X = Si (**10**), C (**11**)
Ar = 2,6-dimethylphenyl
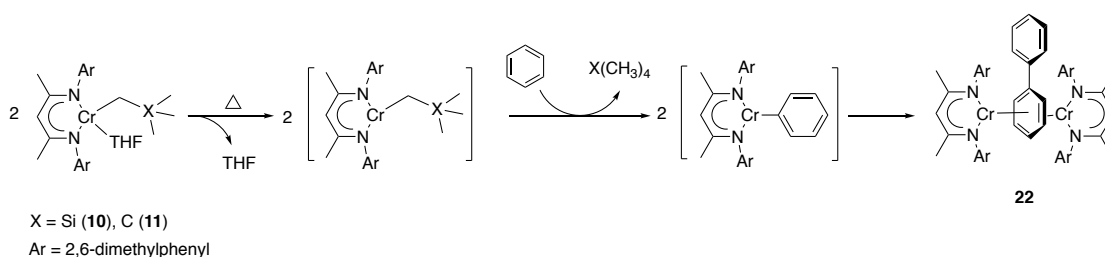
Scheme 2.16   Mechanism of the formation of **22** from **10** and **11**

The mechanism in Scheme 2.16 suggests the coordinatively unsaturated chromium phenyl would lead to **22**. To test this, L^{Me}Cr(C$_6$H$_5$)(THF) (**20**) was heated to 100°C in cyclohexane. After 2.5 hours, **22** was yielded as expected.
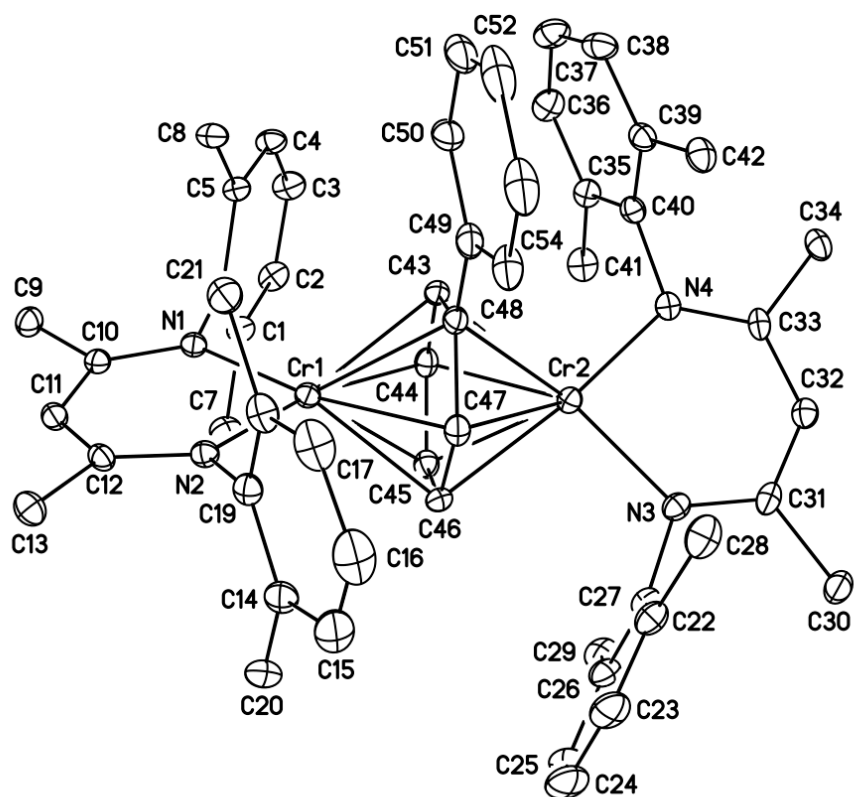
Figure 2.15 Molecular structure of $(L^{Me}Cr)_2(\mu_2\text{-}\eta^6\text{:}\eta^6\text{-}C_6H_5Ph)$ (**22**). Ellipsoids are drawn at the 30% probability level. Hydrogen atoms have been omitted for clarity.

Table 2.12   Interatomic distances (Å) and angles (º) for $(L^{Me}Cr)_2(\mu_2\text{-}\eta^6\text{:}\eta^6\text{-}C_6H_5Ph)$ (**22**)

	Distances (Å)		
Cr(1)-N(1)	2.036(4)	C(15)-C(16)	1.383(11)
Cr(1)-N(2)	2.039(4)	C(16)-C(17)	1.384(11)
Cr(1)-C(46)	2.240(4)	C(17)-C(18)	1.371(8)
Cr(1)-C(44)	2.272(4)	C(18)-C(19)	1.393(7)
Cr(1)-C(43)	2.273(4)	C(18)-C(21)	1.512(8)
Cr(1)-C(45)	2.278(4)	C(22)-C(23)	1.376(8)
Cr(1)-C(47)	2.305(5)	C(22)-C(27)	1.392(7)
Cr(1)-C(48)	2.356(5)	C(22)-C(28)	1.504(8)
Cr(2)-N(3)	2.032(4)	C(23)-C(24)	1.380(10)
Cr(2)-N(4)	2.034(4)	C(24)-C(25)	1.380(10)
Cr(2)-C(44)	2.254(4)	C(25)-C(26)	1.391(8)
Cr(2)-C(47)	2.264(5)	C(26)-C(27)	1.394(7)
Cr(2)-C(45)	2.275(5)	C(26)-C(29)	1.506(8)
Cr(2)-C(46)	2.283(5)	C(30)-C(31)	1.516(7)
Cr(2)-C(43)	2.309(4)	C(31)-C(32)	1.394(7)
Cr(2)-C(48)	2.340(4)	C(32)-C(33)	1.393(7)
N(1)-C(10)	1.335(5)	C(33)-C(34)	1.524(7)
N(1)-C(6)	1.444(5)	C(35)-C(40)	1.381(6)
N(2)-C(12)	1.334(6)	C(35)-C(36)	1.395(7)
N(2)-C(19)	1.429(5)	C(35)-C(41)	1.508(7)
N(3)-C(31)	1.345(6)	C(36)-C(37)	1.366(9)
N(3)-C(27)	1.446(6)	C(37)-C(38)	1.380(9)
N(4)-C(33)	1.329(5)	C(38)-C(39)	1.387(7)
N(4)-C(40)	1.441(5)	C(39)-C(40)	1.402(6)
C(1)-C(6)	1.385(6)	C(39)-C(42)	1.489(7)
C(1)-C(2)	1.391(6)	C(43)-C(44)	1.410(7)
C(1)-C(7)	1.506(7)	C(43)-C(48)	1.449(6)
C(2)-C(3)	1.377(7)	C(44)-C(45)	1.427(6)
C(3)-C(4)	1.359(7)	C(45)-C(46)	1.446(7)
C(4)-C(5)	1.383(6)	C(46)-C(47)	1.422(7)
C(5)-C(6)	1.401(6)	C(47)-C(48)	1.451(6)
C(5)-C(8)	1.504(6)	C(48)-C(49)	1.476(7)
C(9)-C(10)	1.504(6)	C(49)-C(50)	1.397(8)

C(10)-C(11)	1.394(6)	C(49)-C(54)	1.400(8)
C(11)-C(12)	1.385(6)	C(50)-C(51)	1.397(9)
C(12)-C(13)	1.512(6)	C(51)-C(52)	1.348(14)
C(14)-C(15)	1.388(8)	C(52)-C(53)	1.389(14)
C(14)-C(19)	1.402(7)	C(53)-C(54)	1.379(9)
C(14)-C(20)	1.510(8)		

Angles (°)

N(1)-Cr(1)-N(2)	89.63(14)	C(19)-C(14)-C(20)	122.0(5)
N(1)-Cr(1)-C(46)	146.90(17)	C(16)-C(15)-C(14)	121.9(7)
N(2)-Cr(1)-C(46)	104.07(16)	C(15)-C(16)-C(17)	119.5(7)
N(1)-Cr(1)-C(44)	97.48(15)	C(18)-C(17)-C(16)	120.6(7)
N(2)-Cr(1)-C(44)	169.24(15)	C(17)-C(18)-C(19)	119.4(6)
C(46)-Cr(1)-C(44)	65.73(16)	C(17)-C(18)-C(21)	120.6(6)
N(1)-Cr(1)-C(43)	106.05(15)	C(19)-C(18)-C(21)	120.0(5)
N(2)-Cr(1)-C(43)	148.39(17)	C(18)-C(19)-C(14)	121.4(5)
C(46)-Cr(1)-C(43)	77.69(16)	C(18)-C(19)-N(2)	118.8(4)
C(44)-Cr(1)-C(43)	36.15(16)	C(14)-C(19)-N(2)	119.7(5)
N(1)-Cr(1)-C(45)	113.08(17)	C(23)-C(22)-C(27)	119.7(6)
N(2)-Cr(1)-C(45)	132.88(16)	C(23)-C(22)-C(28)	119.6(6)
C(46)-Cr(1)-C(45)	37.32(17)	C(27)-C(22)-C(28)	120.8(5)
C(44)-Cr(1)-C(45)	36.55(16)	C(22)-C(23)-C(24)	119.9(7)
C(43)-Cr(1)-C(45)	66.07(16)	C(23)-C(24)-C(25)	120.4(7)
N(1)-Cr(1)-C(47)	170.43(16)	C(24)-C(25)-C(26)	120.9(7)
N(2)-Cr(1)-C(47)	97.74(16)	C(25)-C(26)-C(27)	118.0(6)
C(46)-Cr(1)-C(47)	36.43(17)	C(25)-C(26)-C(29)	121.0(6)
C(44)-Cr(1)-C(47)	76.14(16)	C(27)-C(26)-C(29)	121.0(5)
C(43)-Cr(1)-C(47)	64.58(16)	C(22)-C(27)-C(26)	121.1(5)
C(45)-Cr(1)-C(47)	65.94(17)	C(22)-C(27)-N(3)	118.7(5)
N(1)-Cr(1)-C(48)	134.57(15)	C(26)-C(27)-N(3)	120.0(5)
N(2)-Cr(1)-C(48)	114.59(16)	N(3)-C(31)-C(32)	123.5(4)
C(46)-Cr(1)-C(48)	66.43(16)	N(3)-C(31)-C(30)	118.8(5)
C(44)-Cr(1)-C(48)	65.54(17)	C(32)-C(31)-C(30)	117.6(5)
C(43)-Cr(1)-C(48)	36.42(16)	C(33)-C(32)-C(31)	128.5(5)
C(45)-Cr(1)-C(48)	78.90(16)	N(4)-C(33)-C(32)	123.6(5)
C(47)-Cr(1)-C(48)	36.26(15)	N(4)-C(33)-C(34)	119.2(4)

N(3)-Cr(2)-N(4)	89.99(16)	C(32)-C(33)-C(34)	117.2(4)
N(3)-Cr(2)-C(44)	143.92(17)	C(40)-C(35)-C(36)	117.7(5)
N(4)-Cr(2)-C(44)	106.33(16)	C(40)-C(35)-C(41)	122.0(5)
N(3)-Cr(2)-C(47)	106.99(16)	C(36)-C(35)-C(41)	120.2(5)
N(4)-Cr(2)-C(47)	145.77(17)	C(37)-C(36)-C(35)	121.1(6)
C(44)-Cr(2)-C(47)	77.31(16)	C(36)-C(37)-C(38)	120.3(6)
N(3)-Cr(2)-C(45)	110.79(16)	C(37)-C(38)-C(39)	120.9(6)
N(4)-Cr(2)-C(45)	135.11(17)	C(38)-C(39)-C(40)	117.4(5)
C(44)-Cr(2)-C(45)	36.71(16)	C(38)-C(39)-C(42)	121.2(5)
C(47)-Cr(2)-C(45)	66.66(17)	C(40)-C(39)-C(42)	121.3(5)
N(3)-Cr(2)-C(46)	96.41(16)	C(35)-C(40)-C(39)	122.4(4)
N(4)-Cr(2)-C(46)	171.56(16)	C(35)-C(40)-N(4)	119.3(4)
C(44)-Cr(2)-C(46)	65.32(16)	C(39)-C(40)-N(4)	118.1(4)
C(47)-Cr(2)-C(46)	36.45(17)	C(44)-C(43)-C(48)	122.5(4)
C(45)-Cr(2)-C(46)	36.99(17)	C(44)-C(43)-Cr(1)	71.9(3)
N(3)-Cr(2)-C(43)	171.56(16)	C(48)-C(43)-Cr(1)	74.9(3)
N(4)-Cr(2)-C(43)	97.83(15)	C(44)-C(43)-Cr(2)	69.9(2)
C(44)-Cr(2)-C(43)	35.97(17)	C(48)-C(43)-Cr(2)	73.0(2)
C(47)-Cr(2)-C(43)	64.66(16)	Cr(1)-C(43)-Cr(2)	102.15(16)
C(45)-Cr(2)-C(43)	65.54(16)	C(43)-C(44)-C(45)	122.0(4)
C(46)-Cr(2)-C(43)	76.13(15)	C(43)-C(44)-Cr(2)	74.1(3)
N(3)-Cr(2)-C(48)	136.94(17)	C(45)-C(44)-Cr(2)	72.4(3)
N(4)-Cr(2)-C(48)	112.51(16)	C(43)-C(44)-Cr(1)	72.0(3)
C(44)-Cr(2)-C(48)	66.08(17)	C(45)-C(44)-Cr(1)	72.0(3)
C(47)-Cr(2)-C(48)	36.70(16)	Cr(2)-C(44)-Cr(1)	103.91(18)
C(45)-Cr(2)-C(48)	79.30(16)	C(44)-C(45)-C(46)	116.9(4)
C(46)-Cr(2)-C(48)	66.05(16)	C(44)-C(45)-Cr(2)	70.8(3)
C(43)-Cr(2)-C(48)	36.31(16)	C(46)-C(45)-Cr(2)	71.8(3)
C(10)-N(1)-C(6)	117.9(4)	C(44)-C(45)-Cr(1)	71.5(2)
C(10)-N(1)-Cr(1)	126.9(3)	C(46)-C(45)-Cr(1)	69.9(2)
C(6)-N(1)-Cr(1)	115.2(3)	Cr(2)-C(45)-Cr(1)	103.02(19)
C(12)-N(2)-C(19)	117.4(4)	C(47)-C(46)-C(45)	120.8(4)
C(12)-N(2)-Cr(1)	127.2(3)	C(47)-C(46)-Cr(1)	74.2(3)
C(19)-N(2)-Cr(1)	115.1(3)	C(45)-C(46)-Cr(1)	72.8(2)
C(31)-N(3)-C(27)	118.5(4)	C(47)-C(46)-Cr(2)	71.0(3)
C(31)-N(3)-Cr(2)	126.8(3)	C(45)-C(46)-Cr(2)	71.2(3)
C(27)-N(3)-Cr(2)	114.7(3)	Cr(1)-C(46)-Cr(2)	103.99(17)

C(33)-N(4)-C(40)	117.2(4)	C(46)-C(47)-C(48)	122.5(4)
C(33)-N(4)-Cr(2)	127.4(3)	C(46)-C(47)-Cr(2)	72.5(3)
C(40)-N(4)-Cr(2)	115.4(3)	C(48)-C(47)-Cr(2)	74.5(3)
C(6)-C(1)-C(2)	118.4(4)	C(46)-C(47)-Cr(1)	69.3(3)
C(6)-C(1)-C(7)	120.8(4)	C(48)-C(47)-Cr(1)	73.8(3)
C(2)-C(1)-C(7)	120.8(4)	Cr(2)-C(47)-Cr(1)	102.56(18)
C(3)-C(2)-C(1)	120.9(5)	C(43)-C(48)-C(47)	115.0(4)
C(4)-C(3)-C(2)	119.8(5)	C(43)-C(48)-C(49)	122.7(4)
C(3)-C(4)-C(5)	121.8(5)	C(47)-C(48)-C(49)	122.3(5)
C(4)-C(5)-C(6)	118.0(4)	C(43)-C(48)-Cr(2)	70.7(2)
C(4)-C(5)-C(8)	120.9(4)	C(47)-C(48)-Cr(2)	68.8(2)
C(6)-C(5)-C(8)	121.1(4)	C(49)-C(48)-Cr(2)	131.4(3)
C(1)-C(6)-C(5)	121.1(4)	C(43)-C(48)-Cr(1)	68.7(2)
C(1)-C(6)-N(1)	120.2(4)	C(47)-C(48)-Cr(1)	70.0(3)
C(5)-C(6)-N(1)	118.6(4)	C(49)-C(48)-Cr(1)	129.8(3)
N(1)-C(10)-C(11)	123.6(4)	Cr(2)-C(48)-Cr(1)	98.77(17)
N(1)-C(10)-C(9)	119.6(4)	C(50)-C(49)-C(54)	116.9(6)
C(11)-C(10)-C(9)	116.8(4)	C(50)-C(49)-C(48)	121.4(6)
C(12)-C(11)-C(10)	128.6(4)	C(54)-C(49)-C(48)	121.7(5)
N(2)-C(12)-C(11)	123.4(4)	C(51)-C(50)-C(49)	120.7(8)
N(2)-C(12)-C(13)	119.1(4)	C(52)-C(51)-C(50)	121.5(9)
C(11)-C(12)-C(13)	117.5(4)	C(51)-C(52)-C(53)	118.9(7)
C(15)-C(14)-C(19)	117.2(6)	C(54)-C(53)-C(52)	120.6(9)
C(15)-C(14)-C(20)	120.8(6)	C(53)-C(54)-C(49)	121.4(8)

Additional information regarding the origin of the bridging hydride needed to be gathered in order to elucidate the mechanism of the C-H bond activation. Labeling experiments were then designed and carried out. Complexes **16** and its labeled analog, $(L^{Me}Cr)_2(\mu\text{-}CH_2CMe_3)(\mu\text{-}D)$ (**16-d₁**), were prepared. **16-d₁** was synthesized in a fashion analogous to **16**, except D_2 gas was used. **16** was treated with C_6D_6; whereas labeled **16-d₁** was reacted with C_6H_6. Both mixtures were heated at 80°C under vacuum. After 16 hours the solvents were removed in vacuo. The products were analyzed by LIFDI mass spectrometry. The comparisons between the composition of the products and the modeled isotope mass spectra are shown below.

Thermal reaction of **16** (m/z: 786.3787; calcd. m/z: 786.3713) in C_6D_6 led to **18-d₅** and $(L^{Me}Cr)_2(\mu\text{-}H)_2$ (**2**). The products and their idealized isotopic patterns are shown in Figures 2.16 and 2.17.
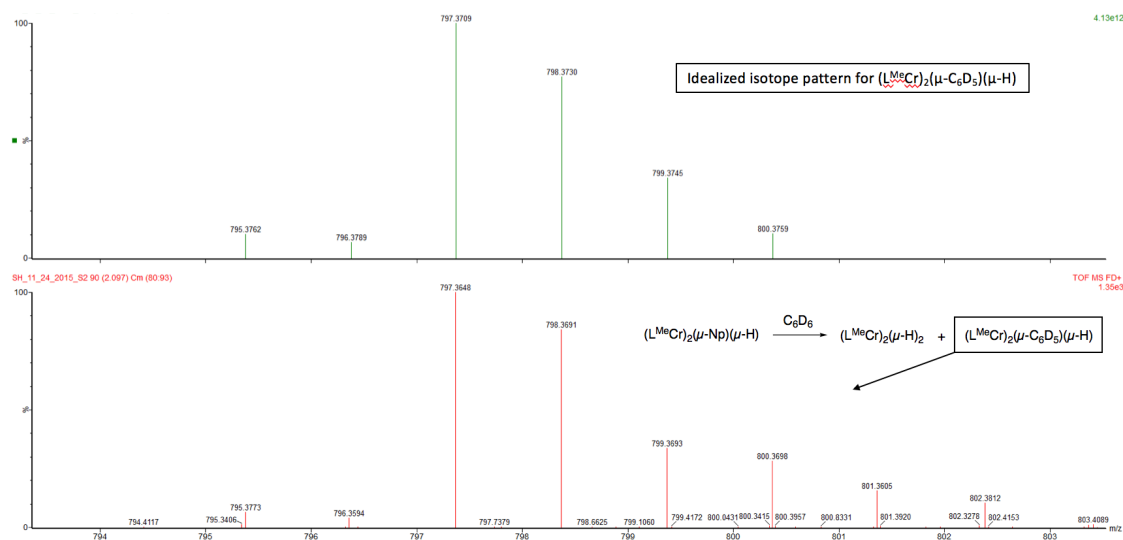
Figure 2.16   LIFDI mass spectrum of product **18-d₅** and its predicted pattern
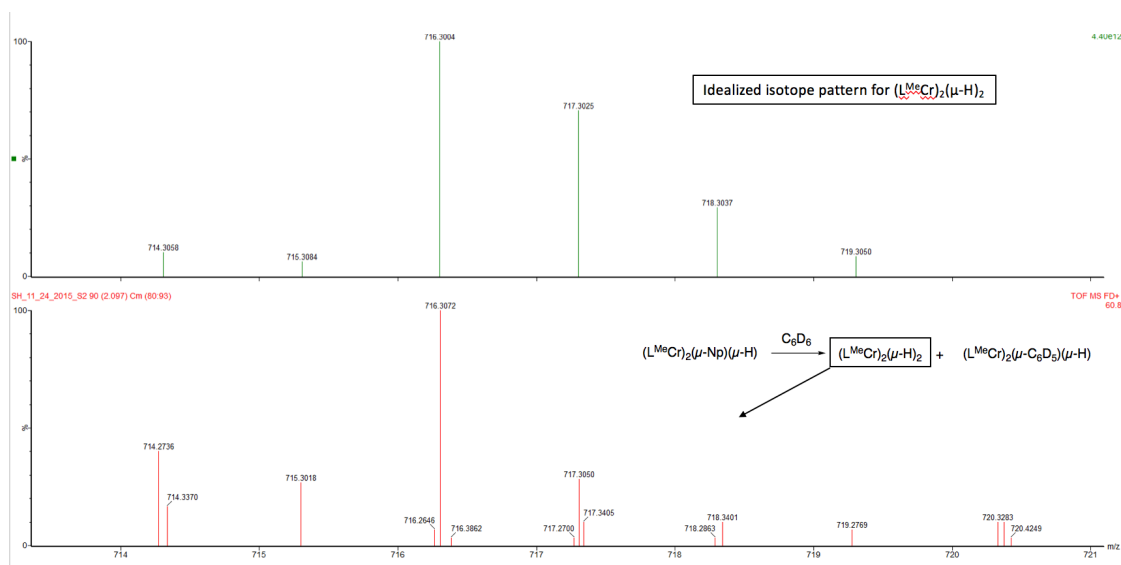
Figure 2.17   LIFDI mass spectrum of product $(L^{Me}Cr)_2(\mu-H)_2$ (**2**) and its predicted pattern

Thermal reaction of **16-d$_1$** (m/z: 787.3817; calcd. m/z: 787.3865) in C_6H_6 led to **18-d$_1$** and $(L^{Me}Cr)_2(\mu-D)_2$ (**2-d$_2$**). The products and their idealized isotopic patterns are shown in Figures 2.18 and 2.19.
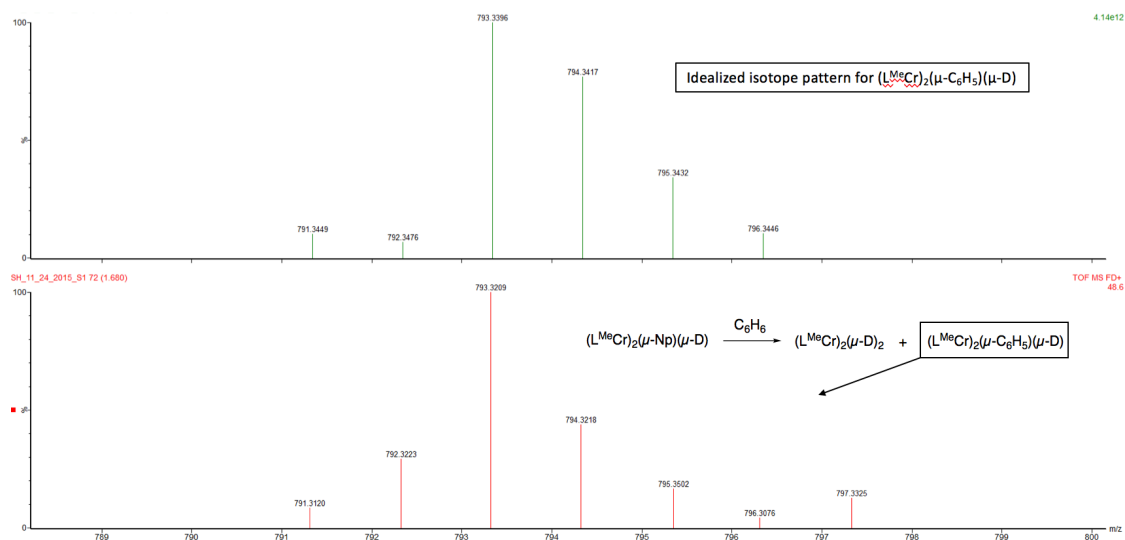
Figure 2.18 LIFDI mass spectrum of product **18-d₁** and its predicted pattern
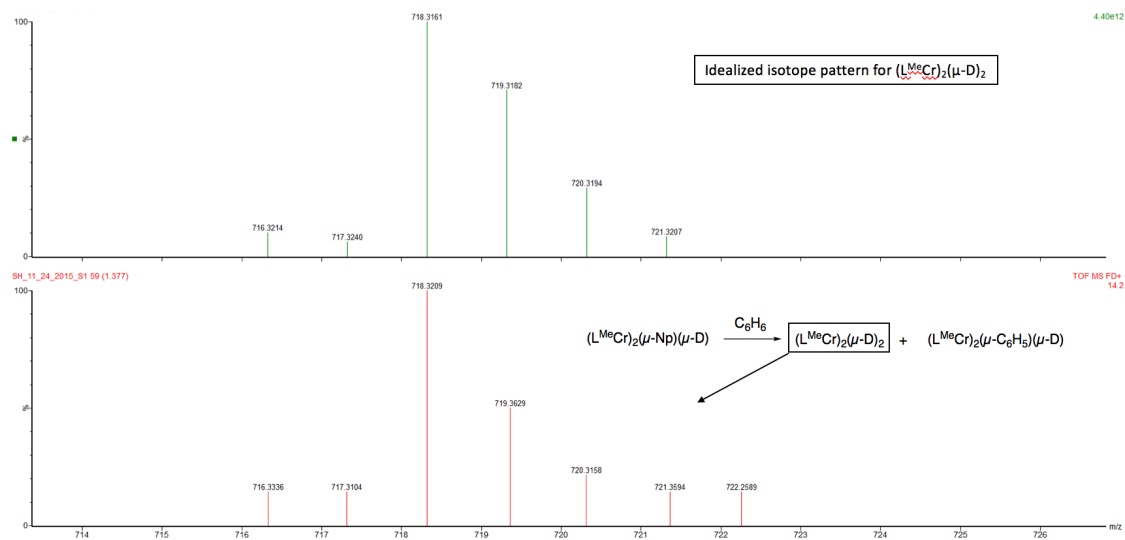
Figure 2.19 LIFDI mass spectrum of product $(L^{Me}Cr)_2(\mu\text{-}D)_2$ (**2-d₂**) and its predicted pattern

The reactions are depicted in Scheme 2.17. The results from labeling experiments were consistent with the interpretation that the bridging hydride or deuteride of the reactant was preserved in the product. The LIFDI mass spectrum shown in Figure 2.20 presents a comparison of these two experiments.
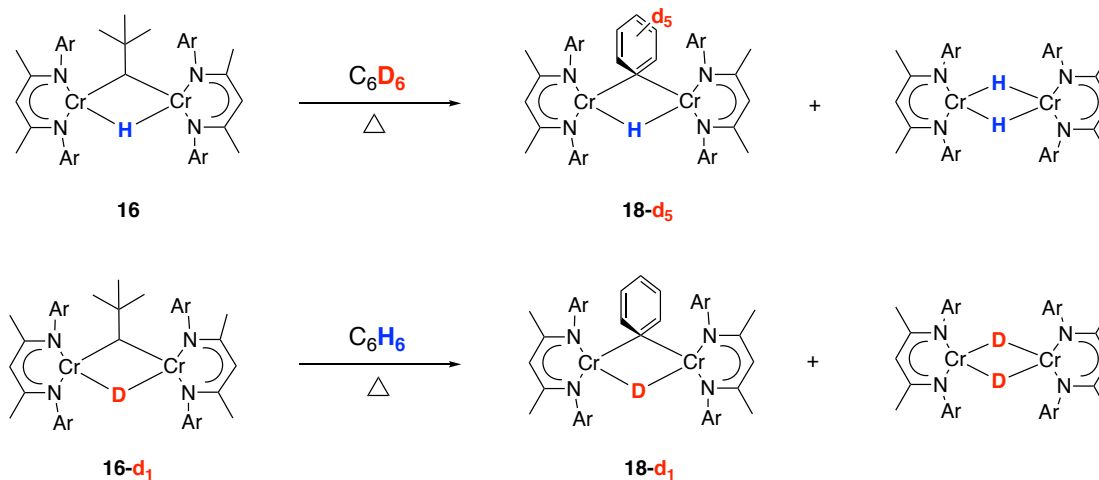
Scheme 2.17   The results of labeling experiments. Ar = 2,6-dimethylphenyl.
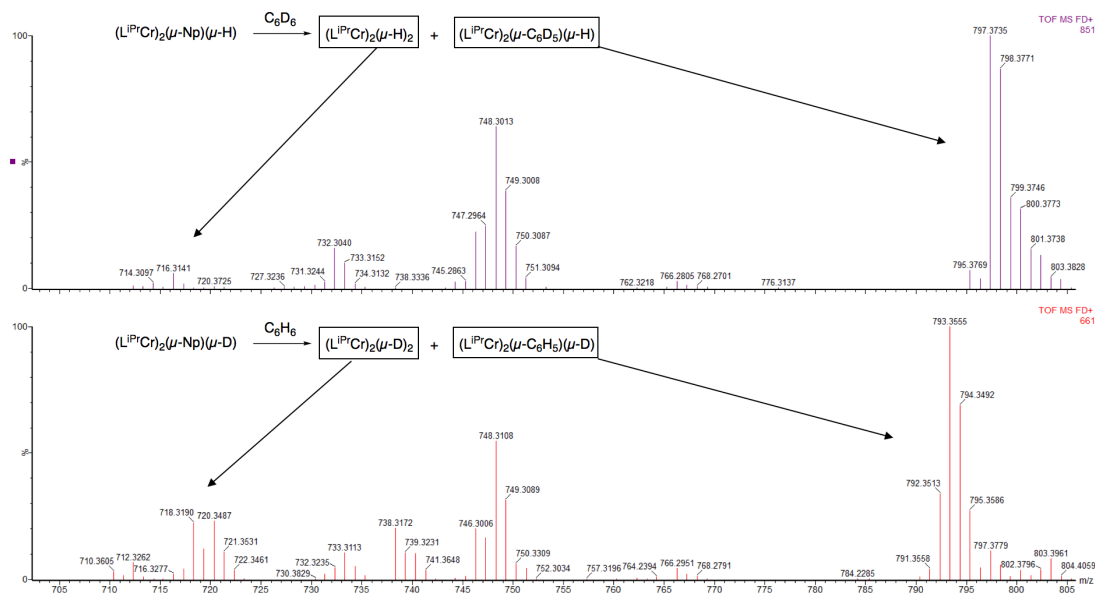
Figure 2.20   LIFDI mass spectra of labeling experiments, with products identified

Based on the aforementioned observations, the transformation of chromium alkyl hydrides can be rationalized by the mechanism shown in Scheme 2.18. First, binuclear **16** dissociates into monomeric fragments, chromium-neopentyl (**A**) and chromium-hydride (**B**). The observed $(L^{Me}Cr)_2(\mu\text{-H})_2$ (**2**) is reasonably derived from the dimerization of **B**. The reactive **A** undergoes both decomposition and a C-H activation reaction. **15** is the thermal decomposition product of **A**, which has been discussed in **Section 2.2.1**. C-H bond activation occurred via sigma-bond metathesis between **A** and organic substrates, which results in elimination of neopentane and the formation of a new chromium-alkyl (**C**). Finally, the reactive **C** dimerizes with **B** to give the alkyl/aryl hydride product.
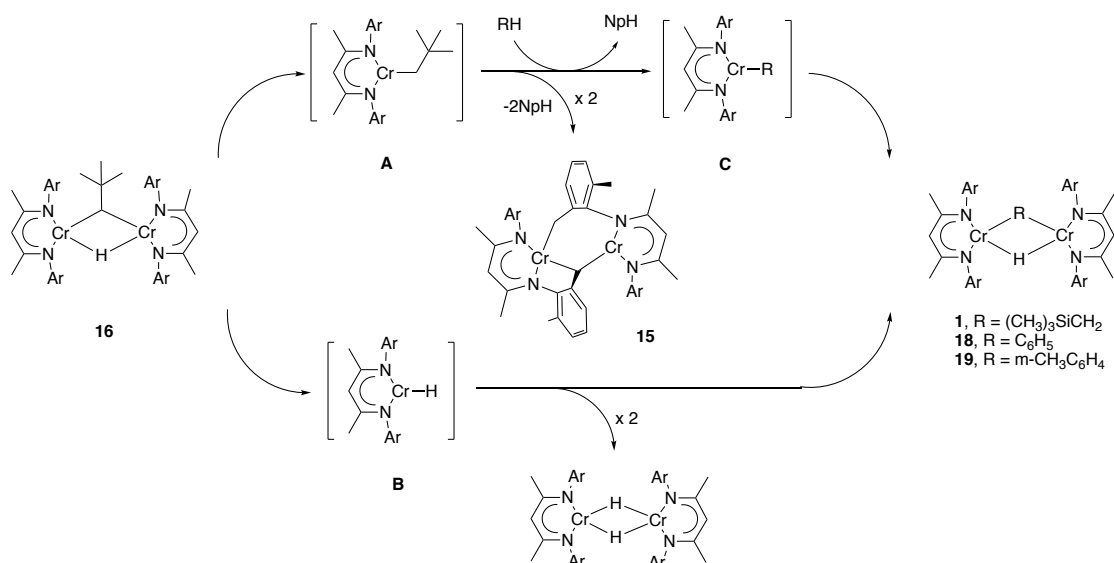
Scheme 2.18 Mechanism for activation reaction of **16** with hydrocarbon substrates. **A**, **B** and **C** are listed as intermediates. Ar = 2,6-dimethylphenyl.

2.3 Conclusions

The synthesis and structural characterization of several chromium(II) alkyls as well as their thermal stabilities have been established. The formation of chromium alkyl hydrides, specifically $(L^{Me}Cr)_2(\mu\text{-}CH_2SiMe_3)(\mu\text{-}H)$ (**1**), $(L^{Me}Cr)_2(\mu\text{-}CH_2CMe_3)(\mu\text{-}H)$ (**16**), and $(L^{Me}Cr)_2(\mu\text{-}CH_2C_6H_5)(\mu\text{-}H)$ (**17**), has been achieved by hydrogenolysis of the chromium(II) alkyl precursors. The reactivities of these alkyl hydride complexes have been evaluated and **16** was found to undergo C-H bond activation in the presence of a number of organic substrates, such as benzene, toluene and tetramethylsilane. These activations led to the transformation into $(L^{Me}Cr)_2(\mu\text{-}C_6H_5)(\mu\text{-}H)$ (**18**), $(L^{Me}Cr)_2(\mu\text{-}m\text{-}CH_3C_6H_4)(\mu\text{-}H)$ (**19**), and **1**, respectively. Mechanistic studies for these activation reactions, including the labeling experiments, were carried out. A proposed mechanism suggested that this transformation was accomplished by a

dissociation of a binuclear alkyl hydride complex, followed by C-H bond activation, which occurred via a σ-bond metathesis pathway.

2.4 Experimental

2.4.1 General Considerations

All manipulations were carried out with standard Schlenk, vacuum line, and glovebox techniques. Pentane, diethyl ether, toluene and tetrahydrofuran were degassed and dried by passing through activated alumina. THF-d_8 and C_6D_6 were predried with sodium and stored under vacuum over Na/K alloy. $CrCl_2$ (anhydrous) was purchased from Strem Chemical Co. Hydrogen gas was purchased from Keen Compressed Gas Co. and dried with an inline moisture trap. Grignard reagents and DCl (1M in diethyl ether) were purchased from Aldrich. Cyclohexane and benzene solvents were purchased from Fisher and predried with sodium and stored over Na/K alloy in drybox. $L^{Me}Cr(CH_2C_6H_5)_2$ was prepared according to the literature procedure.[10]

^{1}H NMR spectra were taken on a Bruker AVIII-400 spectrometer and were referenced to the residual protons of the solvent (C_6D_6, 7.15 ppm, THF-d_8 = 3.58 and 1.73 ppm). FT-IR spectra were obtained using a Nicolet Magna-IR 560 spectrometer with a resolution of 4 cm^{-1}. X-ray crystallographic studies were conducted at the University of Delaware X-ray Crystallography Laboratory. Elemental analyses were obtained from Robertson Microlit, Ledgewood, NJ. Mass spectra were obtained by the University of Delaware Mass Spectrometry Facility. Room temperature magnetic susceptibility measurements were carried out using a Johnson Matthey magnetic

susceptibility balance. Measurement were corrected for diamagnetism using Pascal constants and converted into effective magnetic moments.[14]

2.4.2   Preparation of $L^{Me}Cr(CH_2SiMe_3)(THF)$ (10)

$[L^{Me}Cr(THF)]_2(\mu\text{-}Cl)_2$ [11] (2.00 g, 2.16 mmol) was dissolved in 60 mL THF giving a green solution. 2 equivalents of Me_3SiCH_2MgCl (2.69 mL of 1.6 M THF solution) was added dropwise with stirring over 3 minutes. The solution was stirred for 4 hours during which time the color changed to violet. The THF was removed in vacuo and the residue was extracted with pentane and filtered through celite. The resulting solution was concentrated to 15 mL and cooled to -30°C overnight to yield violet crystals of **10** (1.18 g, 53% yield). ^{1}H NMR (400 MHz, C_6D_6): 119.8 (br), 22.3 (br), 8.90 (br), 6.68 (br), 3.41 (br), 1.81 (br) ppm. IR (KBr): 3070 (w), 2948 (s), 3015 (w), 2884 (w), 1531 (s), 1445 (m), 1386 (s), 1263 (m), 1241 (m), 1186 (s), 1095 (w), 1024 (m), 982 (w), 850 (s), 767 (s) cm^{-1}. μ_{eff} (293K) = 4.5(1) μ_B. Mp: 135°C. Mass Spectrum m/z (%): 444.2073 (100) $[M^+\text{-}C_4H_8O]$. Calcd. m/z: 444.2053 $[M^+\text{-}C_4H_8O]$. Anal. calcd. for $C_{29}H_{44}N_2CrOSi$: C, 67.40; H, 8.58; N, 5.42. Found: C, 66.59; H, 8.29; N, 5.51.

2.4.3   Preparation of $L^{Me}Cr(CH_2CMe_3)(THF)$ (11)

$[L^{Me}Cr(THF)]_2(\mu\text{-}Cl)_2$ [11] (2.00 g, 2.16 mmol) was dissolved in 200 mL pentane giving a green solution. 2 equivalents of Me_3CCH_2MgCl (4.30 mL of 1.0 M THF solution) was added dropwise with stirring over 1 minute. The solution was stirred for 10 minutes during which time the color changed to violet. The pentane solution was filtered over a pad of celite and was concentrated to 15 mL and cooled to -30°C overnight to yield violet crystals of **11** (1.21 g, 56% yield). ^{1}H NMR (400 MHz,

C_6D_6): 115.4 (br), 18.4 (br), 9.19 (br), 3.82 (br), -0.15 (br), -2.76 (br) ppm. IR (KBr): 2947 (s), 2922 (s), 2849 (m), 2806 (w), 1526 (s), 1448 (m), 1389 (s), 1263 (m), 1184 (s), 1094 (m), 1032 (m), 885 (w), 839 (w), 764 (s) cm^{-1}. μ_{eff} (293K) = 4.4(1) μ_B. Mp: 85°C. Mass Spectrum m/z (%): 428.2290 (56) [M$^+$-C$_4$H$_8$O]. Calcd. m/z: 428.2284 [M$^+$-C$_4$H$_8$O]. Anal. calcd. for $C_{30}H_{44}N_2CrO$: C, 71.97; H, 8.86; N, 5.60. Found: C, 70.37; H, 8.36; N, 5.59.

2.4.4   Preparation of $L^{Me}Cr(\eta^2$-CH$_2$C$_6$H$_5$) (12)

$L^{Me}Cr(CH_2C_6H_5)_2$ [10] (0.38 g, 0.71 mmol) was dissolved in 30 mL pentane (giving a dark red solution) and placed in a 250 mL ampoule. The ampoule was evacuated and filled with H$_2$ (1 atm), and the solution was allowed to stir for 8 hours at room temperature, during which time the solution color became brown. The hydrogen was removed in vacuo and the solution was filtered through a pad of celite. The solution was concentrated to 8 mL and cooled to -30°C to yield red brown crystals of **12** (0.12 mg, 38% yield). ^{1}H NMR (400 MHz, C$_6$D$_6$): 45.1 (br), 11.0 (br), 6.19 (br), -38.1 (br) ppm. IR (KBr): 3016 (w), 2963 (w), 2917 (m), 2848 (w), 1592 (m), 1523 (s), 1471(m), 1438 (m), 1386 (s), 1264 (m), 1183 (s), 1095 (m), 1026 (m), 988 (w), 849 (m), 762 (s), 700 (w), 525 (m) cm^{-1}. μ_{eff} (293K) = 4.4(1) μ_B. Mp. 96°C. Mass Spectrum m/z (%): 448.2052 (33) [M$^+$]. Calcd. m/z: 448.1971 [M$^+$]. Anal. calcd. for $C_{28}H_{32}N_2Cr$: C 74.97, H 7.19, N 6.25; found: C 68.00, H 6.76, N 6.21.

2.4.5   Preparation of $L^{Me}Cr(\mu$-CH$_2$SiMe$_3$)CrNArC(CH$_3$)CHC(CH$_3$)N-Me-C$_6$H$_3(\mu$-CH$_2$) (13). Ar = 2,6-dimethylphenyl.

$L^{Me}Cr(CH_2SiMe_3)(THF)$ (**10**) (0.500 g, 0.968 mmol) was dissolved in 50 mL cyclohexane (giving a purple-red solution) and placed in a 250 mL ampoule. The ampoule was evacuated and was heated to 100°C for 4 hours, during which time the

color changed to green. The solvent was then removed and the residue was extracted with 10 mL pentane and cooled to -30°C overnight to yield green crystals of **13** (0.190 g, 49% yield). ^{1}H NMR (400 MHz, C$_6$D$_6$): 8.33 (br), 7.82 (br), 7.36 (br), 6.96 (br), 6.81 (br), 5.80 (br), 4.96 (br), 3.46 (br), 2.23 (br) ppm. IR (KBr): 3011 (w), 2953 (s), 2922 (s), 2852 (w), 1529 (s), 1439 (m), 1375 (s), 1262 (m), 1241 (s), 1182 (s), 1095 (m), 1020 (m), 950 (w), 935 (w), 842 (s), 764 (s), 722 (w) cm^{-1}. μ_{eff} (293K) = 1.8(1) μ_B. Mp: 260°C. Mass Spectrum m/z (%): 800.3494 (100) [M$^+$]. Calcd. m/z: 800.3400 [M$^+$]. Anal. calcd. for C$_{46}$H$_{60}$N$_4$Cr$_2$Si: C, 68.97; H, 7.55; N, 6.99. Found: C, 67.01; H, 7.50; N, 6.72.

2.4.6   Preparation of L^{Me}Cr(μ-CH$_2$CMe$_3$)CrNArC(CH$_3$)CHC(CH$_3$)N-Me-C$_6$H$_3$(μ-CH$_2$) (14). Ar = 2,6-dimethylphenyl.

L^{Me}Cr(CH$_2$CMe$_3$)(THF) (**11**) (0.500 g, 0.998 mmol) was dissolved in 50mL pentane, giving a purple solution. The solution was stirred at room temperature for 4 hours, during which time the color changed to green. The pentane solution was concentrated to 10 mL and cooled to -30°C overnight to yield green crystals of **14** (0.183 g, 40% yield). ^{1}H NMR (400 MHz, C$_6$D$_6$): 7.48 (br), 7.01 (br), 6.83 (br), 6.39 (br), 6.07 (br), 5.83 (br), 5.53 (br), 5.12 (br), 3.81 (br), 3.34 (br), 2.22 (br) ppm. IR (KBr): 3019 (w), 2957 (s), 2923 (s), 2856 (w), 1530 (s), 1439 (m), 1377 (s), 1262 (m), 1243 (w), 1181 (s), 1095 (m), 1020 (m), 933 (w), 844 (w), 763 (s) cm^{-1}. μ_{eff} (293K) = 1.8(1) μ_B. Mp: 270°C. Mass Spectrum m/z (%): 784.3287 (30) [M$^+$]. Calcd. m/z: 784.3630 [M$^+$]. Anal. calcd. for C$_{47}$H$_{60}$N$_4$Cr$_2$: C, 71.91; H, 7.70; N, 7.14. Found: C, 67.38; H, 7.32; N, 6.73.

2.4.7 Preparation of [ArNC(CH₃)CHC(CH₃)N-Me-C₆H₃]Cr(μ₂-CH₂)Cr[NArC(CH₃)CHC(CH₃)N-Me-C₆H₃](μ₁-CH₂) (15). Ar = 2,6-dimethylphenyl.

L^{Me}Cr(CH₂SiMe₃)(THF) (**10**) (0.200 g, 0.387 mmol) was dissolved in 50 mL cyclohexane (giving a purple-red solution) and placed in a 250 mL ampoule. The ampoule was evacuated and was heated to 100°C for 2 days, during which time the color changed to brown. The cyclohexane was then removed and the residue was extracted with 10 mL pentane and cooled to -30°C overnight to yield reddish brown crystals of **15** (0.050 g, 36% yield). ^{1}H NMR (400 MHz, C₆D₆): 12.3 (br), 7.06 (br), 6.62 (br), 6.38 (br), 5.43 (br), 5.05 (br), 2.56 (br) ppm. IR (KBr): 3062 (w), 2969 (s), 2919 (s), 2840 (w), 1548 (s), 1525 (s), 1459 (s), 1378 (s), 1283 (w), 1261 (w), 1181 (s), 1095 (m), 1023 (s), 976 (w), 929 (w), 856 (m), 764 (s) cm^{-1}. μ$_{eff}$ (293K) = 2.0(1) μ$_B$. Mp: 190°C. Mass Spectrum m/z (%): 712.2748 (12) [M$^+$]. Calcd. m/z: 712.2691 [M$^+$].

2.4.8 Preparation of (L^{Me}Cr)₂(μ-CH₂CMe₃)(μ-H) (16)

L^{Me}Cr(CH₂CMe₃)(THF) (**11**) (0.500 g, 0.998 mmol) was dissolved in pentane and placed in an ampoule. The ampoule was evacuated and filled with H₂ (1 atm), and the solution was allowed to stir 40 minutes while cooled to -41°C, in an acetonitrile/dry ice bath, during which time the solution became brown and cloudy. The hydrogen was removed in vacuo, and the pentane solution was filtered through a pad of celite. The byproduct filtered off was identified by ^{1}H NMR spectroscopy as (L^{Me}Cr)₂(μ-H)₂ (**2**). The solution was concentrated and cooled to -30°C to yield yellow-orange crystals of **16** (0.267 g, 68% yield). ^{1}H NMR (400 MHz, C₆D₆): 11.0 (br), 6.41 (br), 3.98 (br), 2.15 (br) ppm. IR (KBr): 2951 (m), 2922 (m), 2860 (w), 1529 (s), 1470 (m), 1435 (m), 1375 (s), 1283 (w), 1260 (w), 1237 (w), 1186 (s), 1097 (m),

1019 (m), 972 (s), 855 (m), 762 (s), 669 (m) cm^{-1}. μ_{eff} (293K) = 2.3(1) μ_B. Mp. 143°C. Mass Spectrum m/z (%): 786.3713 (100) [M$^+$]. Calcd. m/z: 786.3787 [M$^+$]. Anal. calcd. for C$_{47}$H$_{62}$N$_4$Cr$_2$: C 71.73, H 7.94, N 7.12; found: C 64.05, H 7.08, N 6.77.

2.4.9 Preparation of (L^{Me}Cr)$_2$(μ-CH$_2$C$_6$H$_5$)(μ-H) (17)

L^{Me}Cr(η^2-CH$_2$C$_6$H$_5$) (12) (0.500 g, 0.926 mmol) was dissolved in pentane and placed in an ampoule. The ampoule was evacuated and filled with H$_2$ (0.9 atm), and the solution was allowed to stir at room temperature for 2 days, during which time the solution became brownish green. The hydrogen was removed in vacuo and the solution was filtered through a pad of celite. The byproduct filtered off was identified by ^{1}H NMR spectroscopy as (L^{Me}Cr)$_2$(μ-H)$_2$ (2). The solution was concentrated and cooled to -30°C to yield bright green crystals of 17 (0.201 g, 54% yield). ^{1}H NMR (400 MHz, C$_6$D$_6$): 13.7 (br), 7.09 (br), 6.27 (br), 2.20 (br) ppm. IR (KBr): 3020 (w), 2965 (m), 2919 (m), 2852 (w), 1524 (s), 1467 (m), 1437 (m), 1372 (s), 1286 (w), 1261 (w), 1240 (w), 1182 (s), 1097 (m), 1024 (m), 976 (m), 856 (m), 761 (s), 730 (w), 672 (s), 598 (w) cm^{-1}. μ_{eff} (293K) = 2.4(1) μ_B. Mp. >310°C. Mass Spectrum m/z (%): 806.3829 (100) [M$^+$]. Calcd. m/z: 806.3474 [M$^+$]. Anal. calcd. for C$_{49}$H$_{58}$N$_4$Cr$_2$: C 72.93, H 7.24, N 6.94; found: C 66.56, H 6.87, N 6.72.

2.4.10 Preparation of (L^{Me}Cr)$_2$(μ-C$_6$H$_5$)(μ-H) (18)

L^{Me}Cr(C$_6$H$_5$)(THF) (20) (see below) (0.50 g, 0.99 mmol) was dissolved in pentane and placed in an ampoule. The ampoule was evacuated and filled with H$_2$ (0.9 atm), and the solution was allowed to stir at room temperature for 2 hours, during which time the solution became cloudy. The hydrogen was removed in vacuo and the solution was filtered through a pad of celite. The byproduct filtered off was identified

by ^{1}H NMR spectroscopy as $(L^{Me}Cr)_2(\mu\text{-H})_2$ (**2**). The solution was concentrated and cooled to -30°C to yield green crystals of **18** (0.29 g, 73% yield). ^{1}H NMR (400 MHz, C_6D_6): 31.4 (br), 7.57 (br), 5.07 (br), 3.56 (br), -3.48 (br) ppm. IR (KBr): 3035 (w), 3011 (w), 2957 (m), 2919 (m), 2848 (w), 1526 (s), 1439 (m), 1376 (s), 1263 (m), 1242 (w), 1184 (s), 1094 (m), 1025 (m), 977 (m), 855 (w), 763 (s), 696 (w), 676 (m) cm^{-1}. μ_{eff} (293K) = 2.7(1) μ_B. Mp. 218°C. Mass Spectrum m/z (%): 792.3384 (100) [M$^+$]. Calcd. m/z: 792.3318 [M$^+$]. Anal. calcd. for $C_{48}H_{56}N_4Cr_2$: C 72.70, H 7.12, N 7.07; found: C 71.91, H 7.06, N 6.96.

2.4.11 Preparation of $(L^{Me}Cr)_2(\mu\text{-m-CH}_3C_6H_4)(\mu\text{-H})$ (19)

Step 1. $[L^{Me}Cr(THF)]_2(\mu\text{-Cl})_2$ [11] (1.00 g, 1.08 mmol) was dissolved in 40 mL THF giving a green solution. 2 equivalents of m-TolMgCl (2.15 mL of 1.0 M THF solution) was added dropwise with stirring over 2 minutes. The solution was stirred for 50 minutes during which time the color changed to red. The THF was removed in vacuo and the residue was extracted with cold diethyl ether and filtered through celite. The resulting solution was concentrated and cooled to -30°C overnight to yield orange crystals of $L^{Me}Cr(m\text{-CH}_3C_6H_4)(THF)$ (**21**) (0.75 g, 67%). ^{1}H NMR (400 MHz, C_6D_6): 124.8 (br), 100.8 (br), 45.7 (br), 10.1 (br), 5.18 (br), 3.39 (br), -1.05 (br), -7.1 (br), -25.5 (br), -63.5 (br) ppm.

Step 2. $L^{Me}Cr(m\text{-CH}_3C_6H_4)(THF)$ (**21**) (0.50 g, 0.96 mmol) was dissolved in pentane and placed in an ampoule. The ampoule was evacuated and filled with H_2 (0.9 atm), and the solution was allowed to stir 2.5 hours, during which time the solution became cloudy. The hydrogen was removed in vacuo and the solution was filtered through a pad of celite. The byproduct filtered off was identified by ^{1}H NMR spectroscopy as $(L^{Me}Cr)_2(\mu\text{-H})_2$ (**2**). The solution was concentrated and cooled to -

30°C to yield green crystals of **19** (0.14 g, 35% yield). ^{1}H NMR (400 MHz, C$_6$D$_6$):
31.1 (br), 12.2 (br), 7.55 (br), 5.06 (br), 3.65 (br), -2.76 (br) ppm. IR (KBr): 3019 (w),
2957 (w), 2919 (m), 2848 (m), 1525 (s), 1465 (m), 1437 (m), 1373 (s), 1286 (w), 1261
(w), 1240 (w), 1183 (s), 1094 (m), 1025 (m), 977 (m), 855 (w), 760 (s), 673 (m) cm^{-1}.
μ_{eff} (293K) = 2.7(1) μ_B. Mp. 200°C. Mass Spectrum m/z (%): 806.3613 (100) [M$^+$].
Calcd. m/z: 806.3474 [M$^+$]. Anal. calcd. for C$_{49}$H$_{58}$N$_4$Cr$_2$: C 72.93, H 7.24, N 6.94;
found: C 67.88, H 6.94, N 6.88.

2.4.12 Preparation of L^{Me}Cr(C$_6$H$_5$)(THF) (20)

[L^{Me}Cr(THF)]$_2$(μ-Cl)$_2$ [11] (2.00 g, 2.16 mmol) was dissolved in 60 mL THF
giving a green solution. 2 equivalents of PhMgCl (4.30 mL of 1.0 M THF solution)
was added dropwise with stirring over 3 minutes. The solution was stirred for 30
minutes during which time the color changed to red. The THF was removed in vacuo
and the residue was extracted with cold diethyl ether and filtered through celite. The
resulting solution was concentrated to 15 mL and cooled to -30°C overnight to yield
orange crystals of **20** (1.592 g, 73% yield). ^{1}H NMR (400 MHz, C$_6$D$_6$): 122.6 (br),
44.0 (br), 10.1 (br), 6.48 (br), 3.95 (br), 1.68 (br), -64.2 (br) ppm. IR (KBr): 3036 (m),
2962 (s), 2920 (s), 2848 (m), 1523 (s), 1442 (m), 1389 (s), 1376 (m), 1263 (m), 1182
(m), 1095 (w), 1027 (m), 977 (w), 939 (w), 854 (m), 768 (s), 724 (w), 706 (w) cm^{-1}.
μ_{eff} (293K) = 4.6(1) μ_B. Mp: 95°C. Mass Spectrum m/z (%): 434.1864 (15) [M$^+$-
C$_4$H$_8$O]. Calcd. m/z: 434.1814 [M$^+$-C$_4$H$_8$O]. Anal. calcd. for C$_{31}$H$_{38}$N$_2$CrO: C, 73.49;
H, 7.56; N, 5.53. Found: C, 71.36; H, 7.25; N, 5.73.

2.4.13 Preparation of $(L^{Me}Cr)_2(\mu_2-\eta^6:\eta^6-C_6H_5Ph)$ (22)

$L^{Me}Cr(C_6H_5)(THF)$ (**20**) (0.500 g, 0.99 mmol) was dissolved in 20 mL toluene giving a red solution. The solution was evacuated and stirred at 100°C for 2.5 hours, during which time the color changed to dark red. The toluene was removed in vacuo and the residue was extracted with diethyl ether and filtered through celite. The resulting solution was concentrated to 8mL and cooled to -30°C overnight to yield dark red crystals of **22** (0.172 g, 40% yield). ^{1}H NMR (400 MHz, C_6D_6): 102.1 (br), 26.2 (br), 12.6 (br), 2.94 (br), -4.9 (br), -12.7 (br), -54.3 (br) ppm. IR (KBr): 3020 (w), 2957 (m), 2917 (s), 2849 (w), 1592 (w), 1525 (s), 1441 (m), 1376 (s), 1261 (m), 1233 (w), 1184 (s), 1096 (m), 1023 (m), 976 (w), 852 (w), 762 (s), 738 (s), 700 (m), 669 (w) cm^{-1}. μ_{eff} (293K) = 5.9(1) μ_B. Mp: 176°C. Mass Spectrum m/z (%): 868.3878 (100) [M$^+$]. Calcd. m/z: 868.3631 [M$^+$].

Table 2.13	10	11	12
	kla0543	**kla0550**	**kla0713**
Formula	$C_{29}H_{44}CrN_2OSi$	$C_{30}H_{44}CrN_2O$	$C_{28}H_{32}CrN_2$
Formula wt., g/mol	516.75	500.67	448.55
Temp, K	200(2)	200(2)	200(2)
Wavelength, Å	0.71073	0.71073	0.71073
Crystal size, mm	0.094 x 0.228 x 0.287	0.390 x 0.544 x 0.647	0.176 x 0.348 x 0.600
Color	violet	purple-red	red
Crystal system	orthorhombic	orthorhombic	monoclinic
Space group	$P\,2_1\,2_1\,2_1$	$P\,2_1\,2_1\,2_1$	$P\,2_1$
a, Å	8.580(3)	8.4775(4)	11.5726(16)
b, Å	12.871(5)	12.8892(6)	9.4355(13)
c, Å	26.693(9)	26.1904(11)	11.7101(16)
α, deg	90	90	90
β, deg	90	90	108.337(2)
γ, deg	90	90	90
Volume, Å^3	2947.8(18)	2861.8(2)	1213.7(3)
Z	4	4	2
D(calcd), g/cm^3	1.164	1.162	1.227
Abs. coefficient, mm^{-1}	0.451	0.423	0.488
T_{max}/T_{min}	0.7456/0.6064	0.7456/0.6674	0.7456/0.6518
Data/restraints/params	6819/94/316	6646/48/335	5632/1/286
GOF on F^2	0.962	1.023	1.005
Final R indices, $I>2\sigma(I)$	R1 = 0.0591, wR^2 = 0.1216	R1 = 0.0387, wR^2 = 0.0919	R1 = 0.0397, wR^2 = 0.0841
R indices (all data)	R1 = 0.1312, wR^2 = 0.1575	R1 = 0.0497, wR^2 = 0.0976	R1 = 0.0550, wR^2 = 0.0922

Table 2.14	13 kla0825	14 kla0678	15 kla0923
Formula	$C_{46}H_{60}Cr_2N_4Si$	$C_{47}H_{60}Cr_2N_4$	$C_{42}H_{47}Cr_2N_4$
Formula wt., g/mol	801.07	784.99	711.83
Temp, K	200(2)	200(2)	200(2)
Wavelength, Å	0.71073	0.71073	1.54178
Crystal size, mm	0.254 x 0.369 x 0.375	0.222 x 0.354 x 0.593	0.167 x 0.176 x 0.230
Color	dark green-red	green	dark brown-red
Crystal system	monoclinic	triclinic	monoclinic
Space group	$P\,2_1/n$	$P\,\bar{1}$	$P\,2_1/n$
a, Å	12.5071(8)	14.8723(11)	10.7716(3)
b, Å	18.8857(12)	17.2898(13)	19.0247(5)
c, Å	18.6739(12)	19.2445(14)	19.1450(5)
α, deg	90	98.6380(10)	90
β, deg	97.8950(10)	95.997(2)	93.782(2)
γ, deg	90	101.2650(10)	90
Volume, $Å^3$	4369.1(5)	4752.2(6)	3914.77(18)
Z	4	4	4
D(calcd), g/cm^3	1.218	1.097	1.208
Abs. coefficient, mm^{-1}	0.56	0.49	4.812
T_{max}/T_{min}	0.7456/0.7119	0.8990/0.7600	0.7539/0.5023
Data/restraints/params	10149/0/504	22022/59/1015	7800 / 0 / 443
GOF on F^2	1.039	1.006	1.058
Final R indices, $I>2\sigma(I)$	R1 = 0.0427, wR^2 = 0.0885	R1 = 0.0488, wR^2 = 0.1055	R1 = 0.0931, wR^2 = 0.2409
R indices (all data)	R1 = 0.0624, wR^2 = 0.0961	R1 = 0.0969, wR^2 = 0.1253	R1 = 0.1300, wR^2 = 0.2821

Table 2.15	16 kla0697	17 kla0729	18 kla0515
Formula	$C_{47}H_{62}Cr_2N_4$	$C_{53}H_{68}Cr_2N_4O$	$C_{48}H_{56}Cr_2N_4$
Formula wt., g/mol	787.01	881.11	792.96
Temp, K	200(2)	200(2)	200(2)
Wavelength, Å	0.71073	1.54178	0.71073
Crystal size, mm	0.174 x 0.458 x 0.484	0.078 x 0.164 x 0.271	0.194 x 0.440 x 0.556
Color	yellow	green-brown	green
Crystal system	monoclinic	triclinic	monoclinic
Space group	$C\,2/c$	$P\,\bar{1}$	$P\,2_1/n$
a, Å	36.922(8)	11.2004(5)	10.5601(7)
b, Å	12.299(3)	11.8200(5)	22.7220(14)
c, Å	21.848(5)	18.4636(8)	17.6067(11)
α, deg	90	87.585(3)	90
β, deg	110.212(4)	86.817(3)	97.6600(10)
γ, deg	90	79.713(3)	90
Volume, Å^3	9310.(4) Å^3	2400.08(18)	4187.0(5)
Z	8	2	4
D(calcd), g/cm^3	1.123	1.219	1.258
Abs. coefficient, mm^{-1}	0.5	4.034	0.557
T_{max}/T_{min}	0.7450/0.6341	0.7531/0.5747	0.7456/0.6456
Data/restraints/params	10718/49/499	8503/0/562	9697/0/503
GOF on F^2	1.02	0.994	1.026
Final R indices, I>2σ(I)	R1 = 0.1150, wR^2 = 0.2190	R1 = 0.0930, wR^2 = 0.2539	R1 = 0.0436, wR^2 = 0.0936
R indices (all data)	R1 = 0.2209, wR^2 = 0.2671	R1 = 0.1354, wR^2 = 0.3064	R1 = 0.0714, wR^2 = 0.1052

Table 2.16	19	20	22
	kla0832	kla0485	kla0736
Formula	$C_{49}H_{58}Cr_2N_4$	$C_{31}H_{38}CrN_2O$	$C_{54}H_{60}Cr_2N_4$
Formula wt., g/mol	806.99	506.63	869.06
Temp, K	200(2)	200(2)	200(2)
Wavelength, Å	1.54178	0.71073	1.54178
Crystal size, mm	0.078 x 0.147 x 0.526	0.183 x 0.233 x 0.263	0.102 x 0.177 x 0.259
Color	green	orange	red
Crystal system	monoclinic	monoclinic	monoclinic
Space group	$P\,2_1/n$	$P\,2_1/c$	$C\,2/c$
a, Å	10.9325(3)	13.115(7)	34.5480(11)
b, Å	22.7754(5)	13.708(8)	14.2329(5)
c, Å	17.6190(4)	16.000(9)	24.0798(14)
α, deg	90	90	90
β, deg	97.8680(10)	109.218(11)	127.412(2)
γ, deg	90	90	90
Volume, Å^3	4345.69(18)	2716.(3)	9404.7(7)
Z	4	4	8
D(calcd), g/cm^3	1.233	1.239	1.228
Abs. coefficient, mm^{-1}	4.394	0.447	4.099
T_{max}/T_{min}	0.7538/0.4252	0.7452/0.5789	0.7538/0.6407
Data/restraints/params	8579/0/512	8221/0/322	9492/0/553
GOF on F^2	1.077	1.002	1.06
Final R indices, I>2σ(I)	R1 = 0.0702, wR^2 = 0.1864	R1 = 0.0711, wR^2 = 0.1682	R1 = 0.0782, wR^2 = 0.2074
R indices (all data)	R1 = 0.0996, wR^2 = 0.2051	R1 = 0.1296, wR^2 = 0.2054	R1 = 0.1174, wR^2 = 0.2537

REFERENCES

1.   MacAdams, L. A.; Buffone, G. P.; Incarvito, C. D.; Golen, J. A.; Rheingold, A. L.; Theopold, K. H., *Chem. Commun.* **2003,** (10), 1164.

2.   Jonas, K.; Wilke, G., *Angew. Chem. Int. Ed.* **1969,** *8* (7), 519.

3.   Krieck, S.; Gorls, H.; Westerhausen, M., *Organometallics* **2010,** *29* (24), 6790.

4.   Rit, A.; Spaniol, T.; Maron, L.; Okuda, J., *Organometallics* **2014,** *33* (8), 2039.

5.   Cui, P.; Spaniol, T.; Maron, L.; Okuda, J., *Chem. Comm.* **2014,** *50* (4), 424.

6.   Hagadorn, J.; McNevin, M., *Organometallics* **2003,** *22* (4), 609.

7.   Monillas, W.; Yap, G.; Theopold, K., *Angew. Chem. Int. Ed.* **2007,** *46* (35), 6692.

8.   Janowicz, A.; Bergman, R., *J. Am. Chem. Soc.* **1982,** *104* (1), 352.

9.   Bergman, R., *Science* **1984,** *223* (4639), 902.

10. MacAdams, L. A. University of Delaware Ph.D. thesis, 2002.

11. Charbonneau, F.; Oguadinma, P.; Schaper, F., *Inorg. Chem. Acta.* **2010,** *363* (8), 1779.

12. The room temperature unstable **11** was observed by obtaining **14** when the reaction was kept at room temperature over time. The preparation of the alkyl hydride was done at low temperature, see Experimental.

13. Cotton, F. A.; Murillo, C. A.; Walton, R. A., *Multiple bonds between metal atoms*. Third ed.; Springer Science and Business Media, Inc., New York: 2005; p 35.

14. Bain, G.; Berry, J., *J. Chem. Educ.* **2008,** *85* (4), 532.

Chapter 3

SYNTHESIS OF CHROMIUM NITRIDO COMPLEXES SUPPORTED BY β–DIKETIMINATE LIGANDS, AND THEIR RELATIONSHIPS TO ISOMERIC DINITROGEN COMPLEXES

3.1 Introduction

Chromium complexes supported by β-diketiminate ligands (*nacnac*) have shown the capability for small molecules activation. For example, $(L^{iPr}Cr)_2(\mu_2-\eta^2:\eta^2-N_2)$ (**23**) was synthesized and has shown to activate dioxygen to yield mononuclear $L^{iPr}Cr(O)_2$.[1] We were then interested in the mechanism of such transformation because it showed the ability of the complex to coordinate and split dioxygen into oxygen atoms. It was further suggested by mechanistic studies that an asymmetric bis(μ-oxo) complex, $(L^{iPr}Cr)_2(\mu-O)_2$, was an intermediate during this reaction.[2]

23, Ar = 2,6-diisopropylphenyl
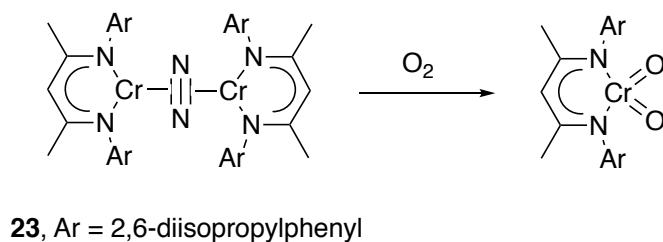
Scheme 3.1 Reaction of **23** with dioxygen to yield $L^{iPr}Cr(O)_2$

With the success with dioxygen activation by **23**, it would be interesting to further explore the chemistry in dinitrogen activation; in particular, the split of dinitrogen of **23** into nitrogen atoms, namely the nitrido isomer (Scheme 3.2).

N
M—|||—M ⇌ M⟨N⟩M
N   N
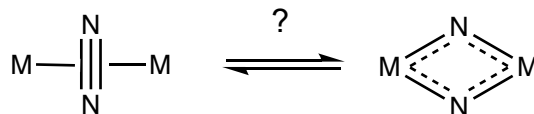
Scheme 3.2 Schematic isomeric dinitrogen complex and bis(μ-nitrido) complex

A literature search showed only a limited number of examples that reported the coexistence of both a dinitrogen complex and its isomeric bis(μ-nitrido) complex, with both compounds well characterized and interconverting.[3-11] This class of study is important because N≡N bond cleavage potentially promotes N-atom functionalization and even extends to catalytic nitrogen fixation.[12]

In 1995, Cummins et al. first established that the binuclear μ-N_2 complex [Mo(NRAr)$_3$]$_2$(μ-η^1:η^1-N_2) (R = C(CH$_3$)$_3$; Ar = 3,5-(Me$_2$)-C$_6$H$_3$) underwent thermally promoted N≡N bond cleavage to the nitrido molybdenum(VI) product N≡Mo(NRAr)$_3$ (Mo≡N 1.651(4) Å) (t$_{1/2}$ ≈ 35 min at 30°C) (Scheme 3.3).[3, 7] The success of the spontaneous thermal N≡N bond cleavage was attributed not only to both the σ- and π-donor properties of the anilide ligands, but also to the flexibility about the Mo−N$_{anilide}$ units. Computational studies suggested that a zig-zag transition state structure played an important role in reducing the kinetic barrier toward N−N bond cleavage under thermal conditions, which was achieved by the rotation of anilide ligands. This was the first example of the cleavage of N_2 mediated by a transition metal complex, and it initiated the research area of dinitrogen/nitrido chemistry and the subsequent nitrogen transformation.
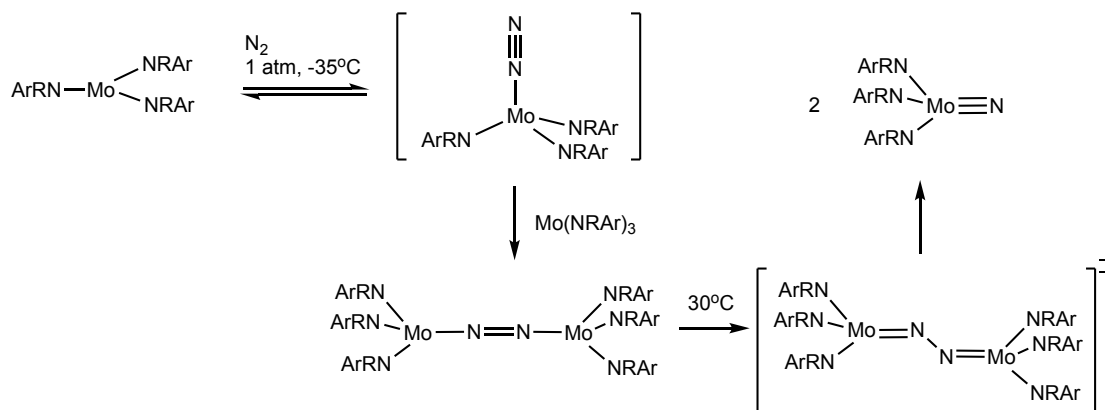
Scheme 3.3   Cleavage of N_2 by Mo(NRAr)$_3$, to yield N≡Mo(NRAr)$_3$

In 2001, Floriani et. al. compared their [Mo(Mes)$_3$] fragment (Mes = 2,4,6-Me$_3$C$_6$H$_2$) with Cummins', [Mo(NRAr)$_3$] (see above). Despite the thermal stability of [(Mes)$_3$Mo]$_2$(μ-N$_2$), the cleavage of its NN bond was achieved by exposure to UV light (λ = 365 nm).[4] Scheme 3.4 shows the mechanism. The photolysis of [(Mes)$_3$Mo]$_2$(μ-N$_2$) fragmented the NN bond, and the 2 equiv. of NMo(Mes)$_3$ generated were quickly trapped by [(Mes)$_3$Mo]$_2$(μ-N$_2$), forming (μ-N$_2$)[(Mes)$_3$MoNMo(Mes)$_3$]$_2$. The loss of N$_2$ from the suggested intermediate enabled the observed product, which was identified as a bridging mono-nitrido complex [(Mes)$_3$Mo]$_2$(μ-N).
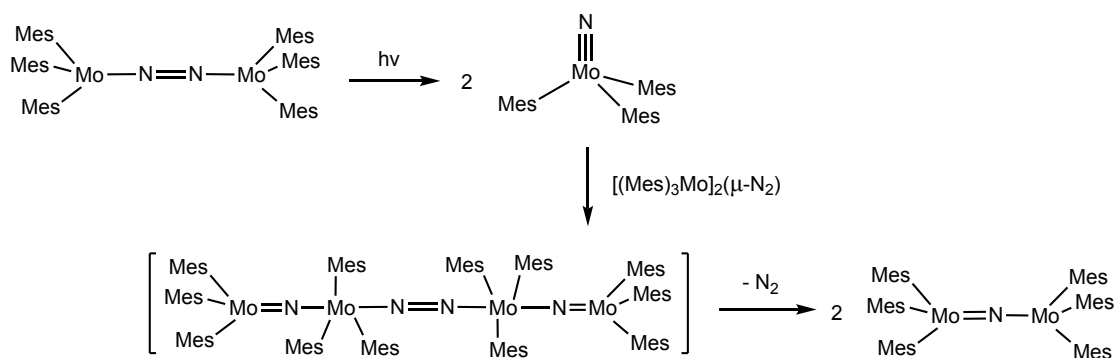
Scheme 3.4 Photolytic conversion of $[(Mes)_3Mo]_2(\mu-N_2)$ to $[(Mes)_3Mo]_2(\mu-N)$

Fryzuk et. al. reported in 2002 that a niobium dinitrogen complex, i. e., $([P_2N_2]Nb)_2(\mu-N_2)$ (where $[P_2N_2] = PhP(CH_2SiMe_2NSiMe_2CH_2)_2PPh$), thermally transformed into a bridging nitride species, with one nitrogen atom inserted into the macrocycle backbone to form $[P_2N_2]Nb(\mu-N)Nb[PN_3]$.[5] The insertion of N atom from the activated N_2 into a Si-C bond resulted in one of the $[P_2N_2]$ ligands undergoing considerable rearrangement (Scheme 3.5). The authors suggested that the overall transformation involved the attack of the phosphine donor on the putative niobium bis(μ-nitrido), leading to the oxidation of phosphine.
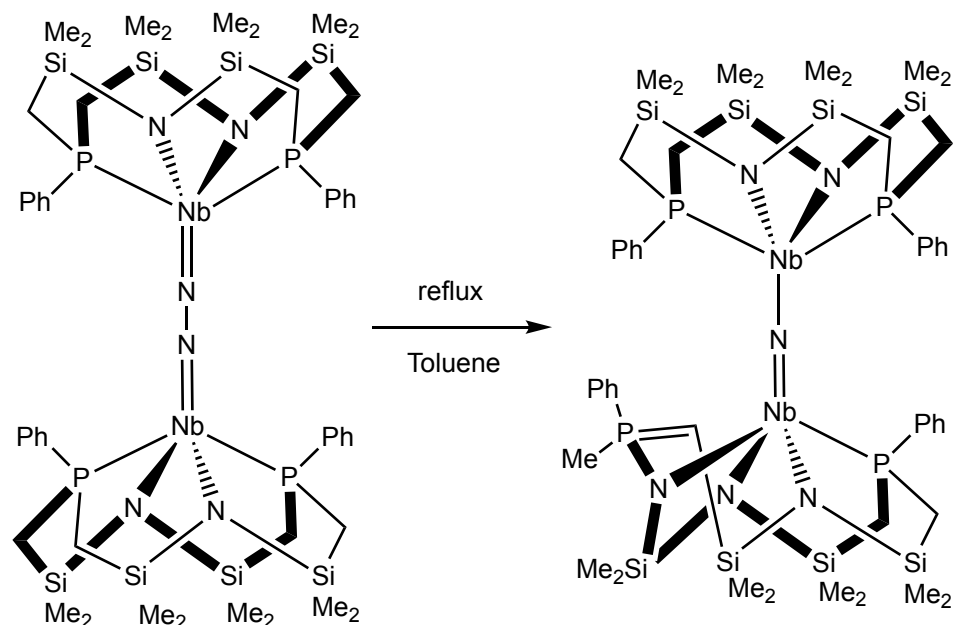
Scheme 3.5   Thermolysis of ([P$_2$N$_2$]Nb)$_2$(μ-N$_2$) to form bridging nitrido complex

In 2007, Sita et. al. reported that the end-on bridged [Ta]$_2$(μ-N$_2$) complex, [Ta] = (η^5-C$_5$Me$_5$)[N(^{i}Pr)C(Me)N(^{i}Pr)]Ta, transformed into the bis(μ-nitrido) isomer thermally, without the participation of the supporting ligand framework.[13] Later, they extended the reaction scope to Nb, Mo and W.[8, 10, 14] These transformations were either thermal or photolytic processes (Scheme 3.6). Additional computational and experimental results support that the transformation proceeded by an intramolecular isomerization process, rather than a fragmentation of the N$_2$ ligand and recombination of nitrides. The authors further proposed that the transformation involved an intramolecular μ-η^1:η^1-N$_2$ to μ-η^2:η^2-N$_2$ structural isomerization prior to the N≡N bond cleavage.[8] Kinetic investigations of the thermal conversion of [Ta]$_2$(μ-N$_2$) to [Ta]$_2$(μ-N)$_2$ was conducted by UV-vis spectroscopy. The experimentally-derived enthalpy of activation parameter was found to be 21.5 kcal/mol.
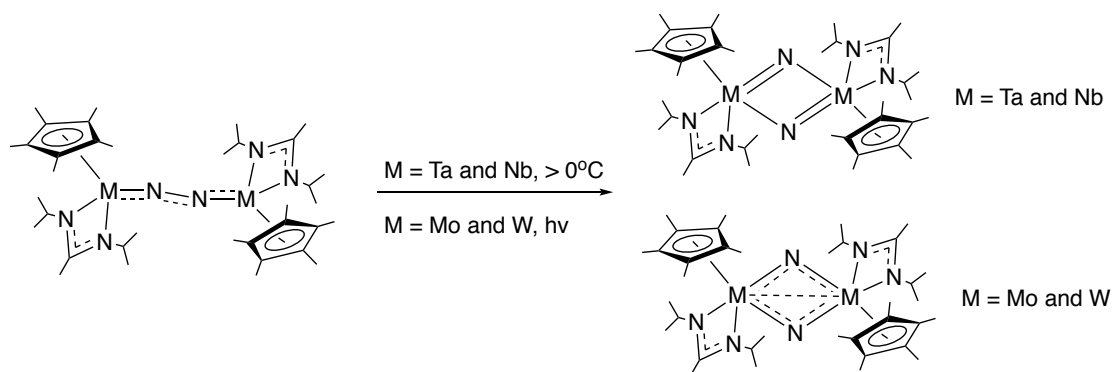
Scheme 3.6 Transformation of end-on bridged (μ-N$_2$) to the corresponding bis(μ-nitrido)

In 2014, Nishibayashi et. al. reported both the cleavage and formation of molecular dinitrogen in a single system.[9] They found that a neutral dinitrogen-bridged dimolybdenum complex underwent visible light irradiation at room temperature to give two equiv. of a molybdenum nitrodo complex. Conversely, the dicationic bridging dinitrogen complex was reformed when the nitrido complex was oxidized at room temperature with FcBAr$^F_4$ (ferrocenium tetrakis[3,5-bis(trifluoromethyl)phenylborate]) (Scheme 3.7).
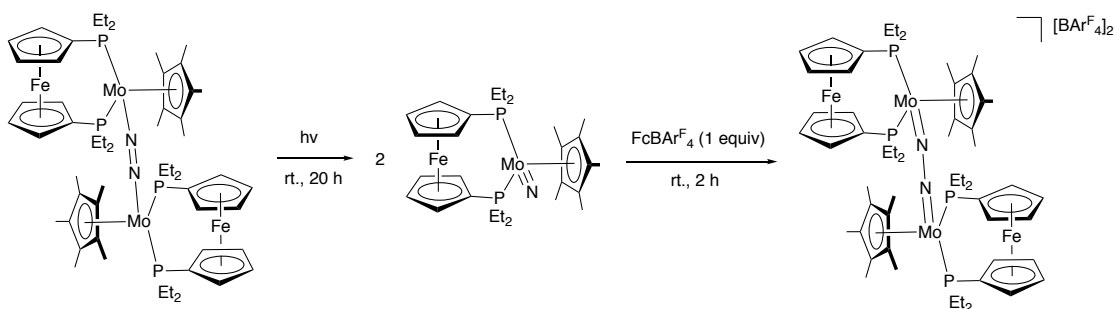
Scheme 3.7 Cleavage and formation of molecular dinitrogen in a single system

Examples of the microscopic reverse of N≡N bond cleavage, namely the coupling of nitride ligands to form dinitrogen complexes, have also been in the literature.[15-17] For example, Peters et. al. reported the tetrahedrally coordinated terminal iron nitride ($[Fe]^{IV}\equiv N$, $[Fe] = PhB(CH_2P^iPr_2)_3Fe$) transforming into bimolecular end-on bridged dinitrogen complex ($[Fe]^I-N_2-[Fe]^I$) (Scheme 3.8).[18] This was the first example of a 6-electron redox process mediated by two iron centers. $[Fe]^{IV}\equiv N$ was prepared by treating $[Fe]^{II}Cl$ with Li(dbabh) (dbabh = 2,3: 5,6-dibenzo-7-aza bicyclo[2.2.1]hepta-2,5-diene). The intermediate $[Fe]^{II}$(dbabh) was thermally unstable, producing equivalent amounts of anthracene and $[Fe]^{IV}\equiv N$, which was spectroscopically characterized. The geometric and electronic structure of $[Fe]^{IV}\equiv N$ was supported by DFT calculations. The $[Fe]^{IV}\equiv N$ underwent nitride coupling under argon atmosphere or vacuum at room temperature to result in $[Fe]^I-N_2-[Fe]^I$ ($t_{1/2} \approx$ 11 min at 22°C). The converse of this pathway, namely the cleavage of N_2 ligand to two $[Fe]^{IV}\equiv N$, proved not thermally accessible (60°C led to gradual degradation).
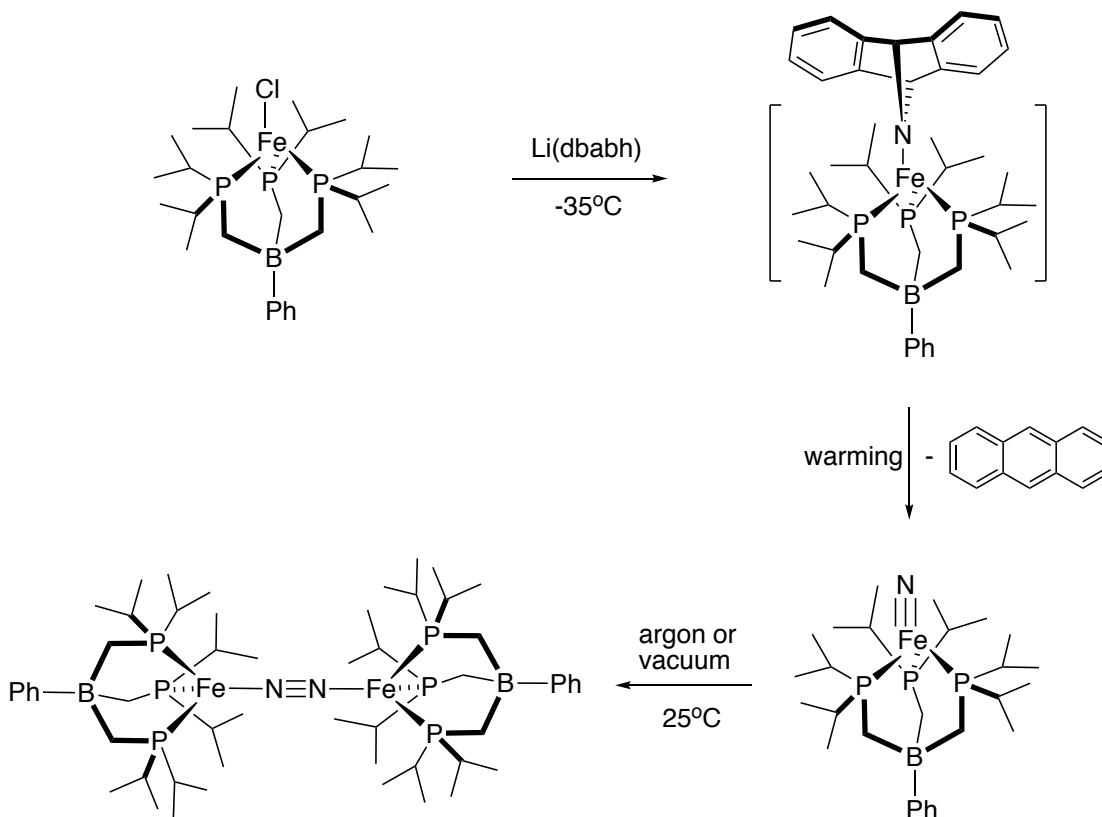
Scheme 3.8 Mononuclear terminal nitride coupling to binuclear dinitrogen complex

Mindiola et. al. have both terminal nitrido and end-on bridged dinitrogen complexes supported by a nacnac ligand and an aryloxide ligand; the complexes were independently synthesized.[19] However, they did not observe interconversion of these two complexes under thermal or photolytic conditions (Scheme 3.9). A DFT calculation showed the conversion from dinitrogen to its cleavage product faces a high barrier (83 kcal/mol, above the dinitrogen complex). The access of nitride from dinitrogen is both thermally and kinetically inhibited. The authors speculated that the more constrained geometry of the dinitrogen complex (due to the chelating ligand)

might prevent the formation of a zig-zag transition state, which has been proven to facilitate N_2 splitting.[7]

Ar = 2,6-diisopropylphenyl
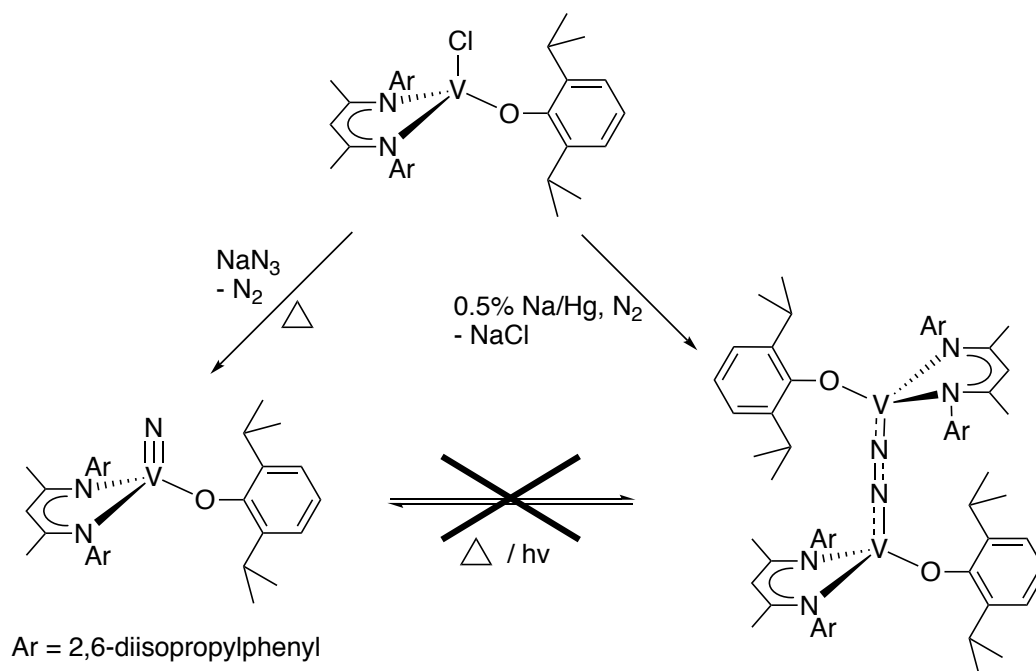
Scheme 3.9 The non-interconversion of isomeric nitrogen complexes

The chromium dinitrogen complex, $(L^{iPr}Cr)_2(\mu_2\text{-}\eta^2\text{:}\eta^2\text{-}N_2)$ (**23**), has been studied and reported by Wesley Monillas.[20] Yet the potential isomerization of **23** has not been observed. Encouraged by the aforementioned examples, this chapter focuses on the approaches of the isomeric complex of **23**. This chapter is organized into three parts. The first part describes the discovery of bis(μ-nitrido) complexes that were found in the mixture of products from irradiation of azide precursors. The second part summarizes the attempts to approach clean formation of chromium nitride focusing on L^{iPr} ligand type. The last part outlines the successful synthetic route to bis(μ-nitrido)

complex, along with its transformation into, and comparison with its dinitrogen complex isomer, $(L^{iPr}Cr)_2(\mu_2\text{-}\eta^2\text{:}\eta^2\text{-}N_2)$ (**23**).

3.2 Results and Discussion

3.2.1 Preliminary results of irradiation of Cr(II) azide supported by L^{iPr}

In the past, our group has treated $(L^{iPr}Cr)_2(\mu\text{-}I)_2$ with NaN_3 to obtain the bridging azido complex, $(L^{iPr}Cr)_2(\mu\text{-}N_3)_2$ (**24**).[20] **24** can also be obtained by reacting NaN_3 with chromium chloride precursor, as depicted in Scheme 3.10. Further transformations of **24** had not been previously explored, and some relevant results are detailed in the following.

Ar = 2,6-diisopropylphenyl   **24**
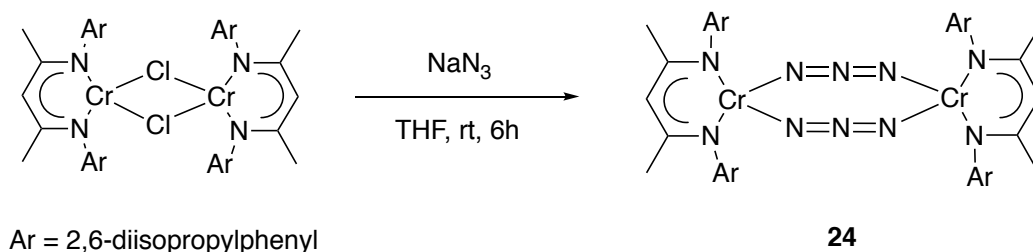
Scheme 3.10   Synthesis of $(L^{iPr}Cr)_2(\mu\text{-}N_3)_2$ (**24**)

Irradiation (254nm light) of **24** in a quartz NMR tube (with J. Young valve) in C_6D_6 under vacuum led to decomposition; after 24 hours, the major inorganic product was identified by ^1H NMR spectroscopy as the previously reported side-on bridged dinitrogen complex $(L^{iPr}Cr)_2(\mu_2\text{-}\eta^2\text{:}\eta^2\text{-}N_2)$ (**23**), which can also be synthesized by the reduction of $(L^{iPr}Cr)_2(\mu\text{-}I)_2$ with Mg in the presence of N_2.[1] Monitoring the photolysis of **24** by ^1H NMR spectroscopy showed changes of the reaction composition (Figure

3.1). An intermediate was observed during the photolytic process. Scaling up the reaction in a quartz ampoule, the intermediate was obtained from a THF solution of **24** irradiated for 12 hours. Upon removal of solvent and extraction with pentane, the solution was concentrated and cooled overnight to give orange crystals (roughly 5% yield) that were suitable for X-ray diffraction. This was shown to be the bis(µ-nitrido) complex $(L^{iPr}Cr)_2(\mu\text{-}N)_2$ (**25**) by X-ray diffraction. The photolysis reaction is shown in Scheme 3.11.
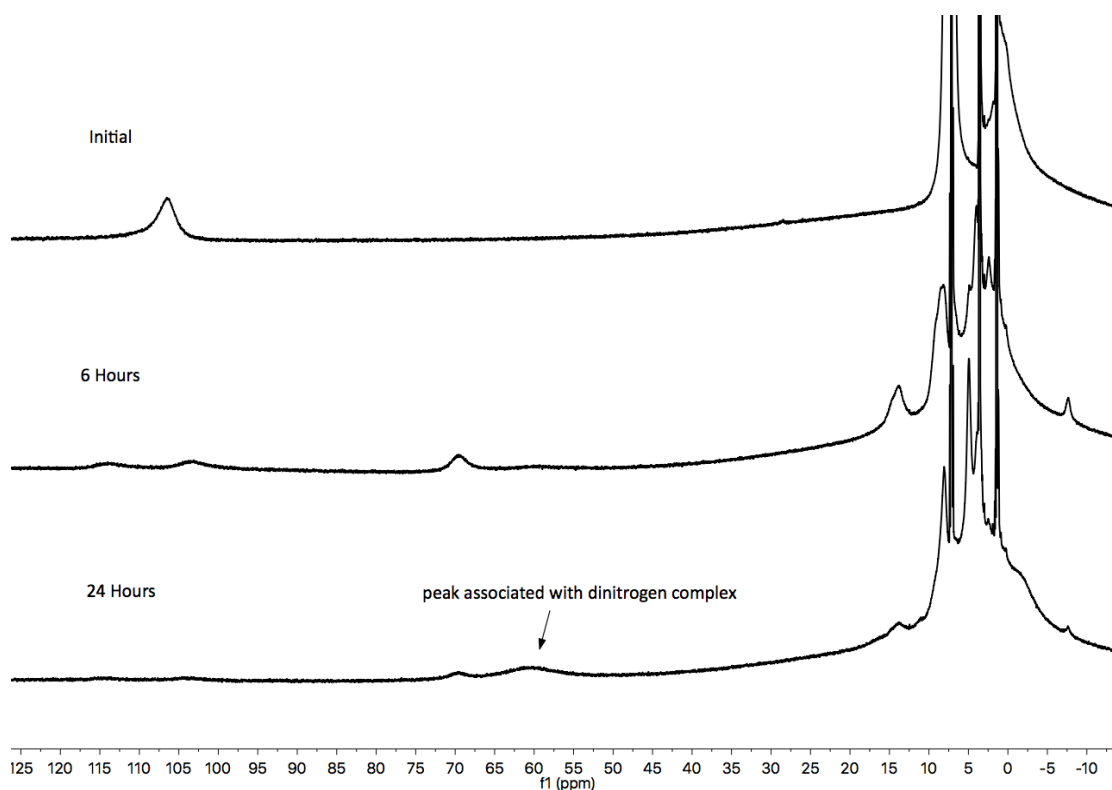
Figure 3.1　^{1}H NMR spectra during the photolysis of **24** in C_6D_6, with a resonance of the dinitrogen complex **23** identified

24, Ar = 2,6-diisopropylphenyl   **25**   **23**
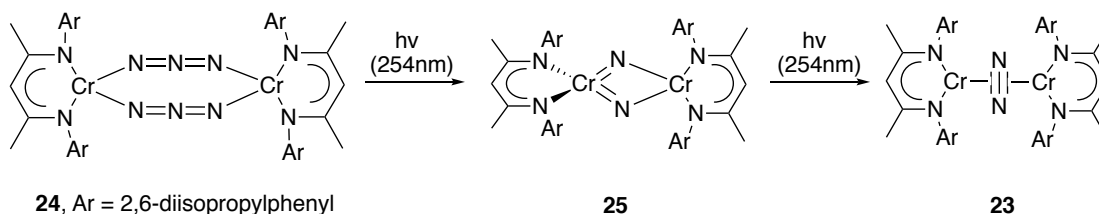
Scheme 3.11   Irradiation of **24**

Unfortunately, this structure **25** was of low quality, due to a lack of diffraction data at high angle. However, the molecular structure of **25** is depicted in Figure 3.1 to show connectivity. The core of **25** consists of two chromiums bridged by two nitrido ligands. The geometries around the two metal centers are tetrahedral Cr1 and square planar Cr2. The bond distances between Cr1 and the bridging nitrogen atoms − while not trustworthy in detail − (1.64(1) and 1.80(1) Å) are shorter than those between Cr2 and the bridging nitrides (2.00(1) and 2.09(1) Å). Due to the inability of isolating pure **25**, further characterization was limited at this point. However, a more detailed discussion regarding the synthesis and characterization of **25** will be shown later in this chapter (**Section 3.2.5**). Besides photolysis, thermal reaction of azide **24** was also tried. **24** was found to be unchanged upon heating at 100°C in C$_6$D$_6$ solution for 2 days under vacuum.

Although this photolytic reaction was a slow process (hours of reaction time were required), the relative rates of conversion of **24** to **25** and **25** to **23** limited the ability to isolate **25** from the mixture. **25** is difficult to cleanly separate from **23** or **24** by fractional crystallization. Column chromatography was also attempted, but decomposition was observed during the elution. In order to carry out more studies on the bis(μ-nitrido) complex, isolation of **25** is required.
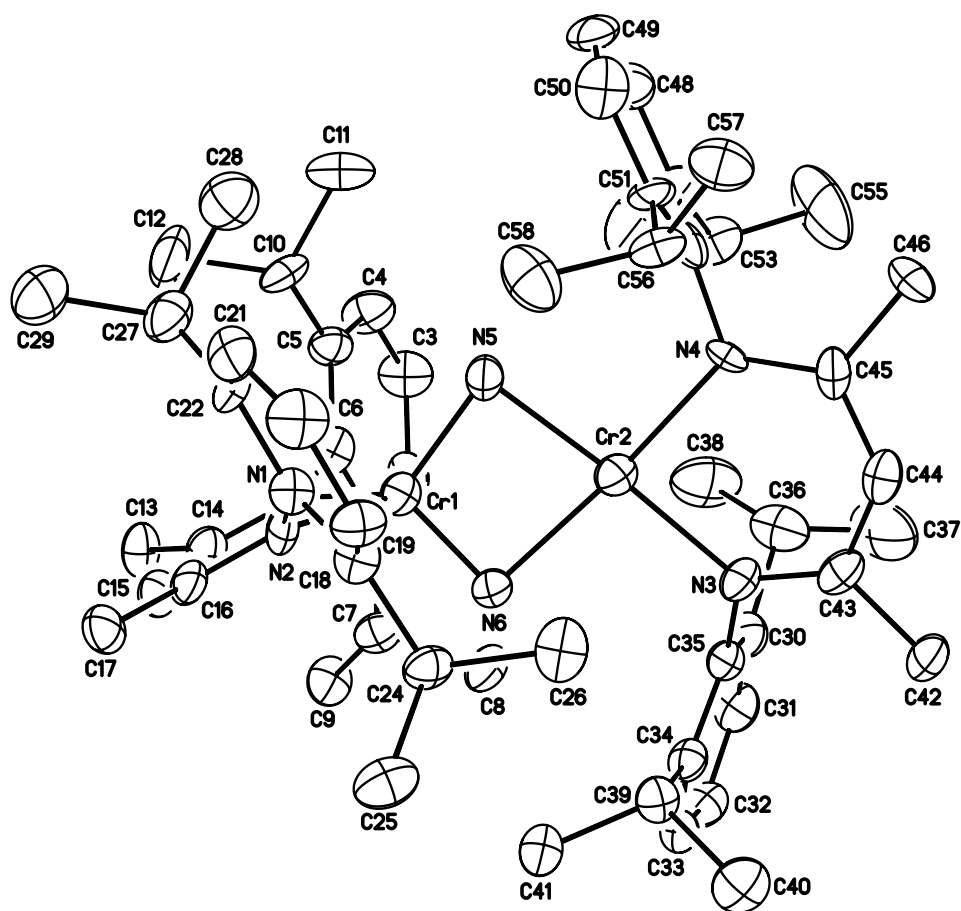
Figure 3.2   Molecular structure of $(L^{iPr}Cr)_2(\mu\text{-}N)_2$ (**25**). Ellipsoids are drawn at the 20% probability level. Hydrogen atoms have been omitted for clarity. Note low quality of this structure, and a better structure will be shown on p.242.

3.2.2 Synthesis and structures of additional Cr(II) azides

Sterically-tuned ligand systems may provide a way to isolate nitrido species by altering the rate of conversion from bis(μ-nitrido) to dinitrogen compound. As a result, chromium(II) azido complexes supported by β–diketiminate ligands with different substitution patterns have been explored, and their syntheses as well as characterizations will be discussed below.

Addition of NaN$_3$ to a THF solution of (LCr)$_2$(μ-Cl)$_2$ (L = L^{Me}, L^{Et}, *L^{iPr}, and *L^{Me}) (L^R = 2,4-pentane-N,N'-bis-2,6-R$_2$-phenyl-diketiminato; *L^R = 2,2,6,6-tetramethylheptane-3,5,N,N'-bis-2,6-R$_2$-phenyl-diketiminato), followed by removal of solvent and extraction with pentane or Et$_2$O allowed for the production of new azido complexes. The starting chloride compounds have been previously reported.[20, 21] The azido complexes possessing less bulky L^{Me} and L^{Et} ligands were synthesized and their structures were determined to be tetranulear complexes with four bridging azido ligands, i. e. μ$_{1,3}$-N$_3$, **26** and **27**, respectively (Scheme 3.12).

26, Ar = 2,6-dimethylphenyl
27, Ar = 2,6-diethylphenyl
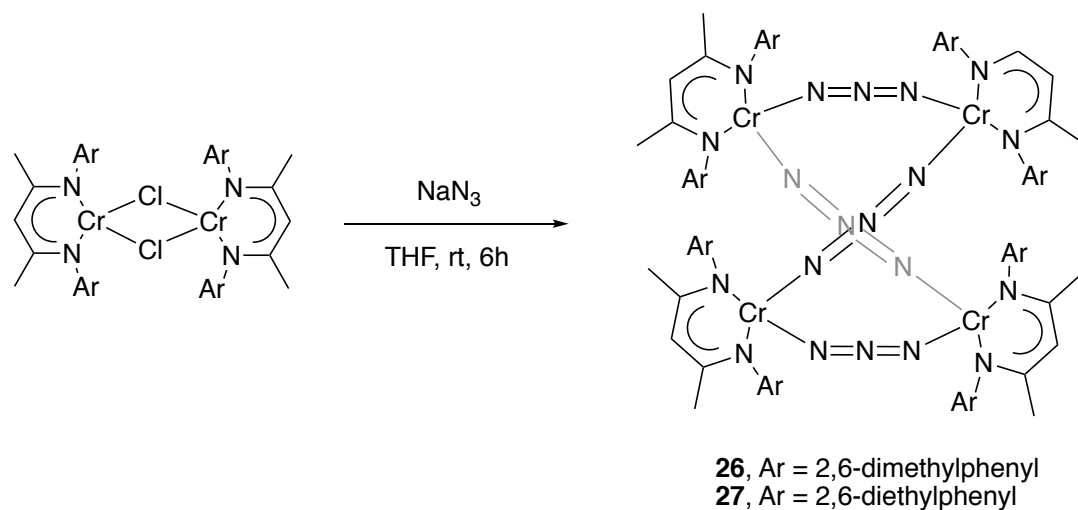
Scheme 3.12   Synthesis of (L^{Me}Cr)$_4$(μ-N$_3$)$_4$ (**26**) and (L^{Et}Cr)$_4$(μ-N$_3$)$_4$ (**27**)

26 and **27** have similar bond distances associated with their core, with Cr-N$_{avg}$ 2.035(9) Å and N-N$_{avg}$ 1.155(7) Å for **26**, Cr-N$_{avg}$ 2.018(16) Å and N-N$_{avg}$ 1.162(17) Å for **27**. The coordination of each chromium center can be best described as square planar, with the sum of the bond angles about each chromium being 360.07, 362.56, 361.17 and 361.38° for **26** and 360.1, 361.3, 360.2 and 362.9° for **27**. For both **26** and **27**, both the crystal structures show that the tetranuclear compound have two different sets of Cr···Cr distances. Specifically, the distances of Cr1-Cr4 5.688(1) (**26**), 5.828(1) (**27**) Å and Cr2-Cr3 5.420(1) (**26**), 5.798(2) (**27**) Å are longer than the distances of Cr1-Cr2 6.280(1) (**26**), 6.242(2) (**27**) Å and Cr3-Cr4 6.320(1) (**26**), 6.264(2) (**27**) Å. Therefore, the symmetry of **26** and **27** is best described as *D*2. The infrared spectra of **26** and **27** are also very similar, with azido stretching frequencies of 2190, 2141, 2110, 2058 cm^{-1} for **26** and 2194, 2149, 2109, 2056 cm^{-1} for **27**. With effective *D*2 symmetry, the number of azide stretches is expected to be four. Room temperature magnetic moment measurements were performed on both **26** and **27**; the results were 6.8μ$_B$ for **26** and 7.0μ$_B$ for **27**. The effective magnetic moment of a complex with four magnetically independent Cr(II) (S $= \frac{4}{2}$) is expected to be 9.8μ$_B$; the lower values of **26** and **27** therefore suggest antiferromagnetic coupling between metal centers. The reactivity of **26** and **27** will be discussed later.
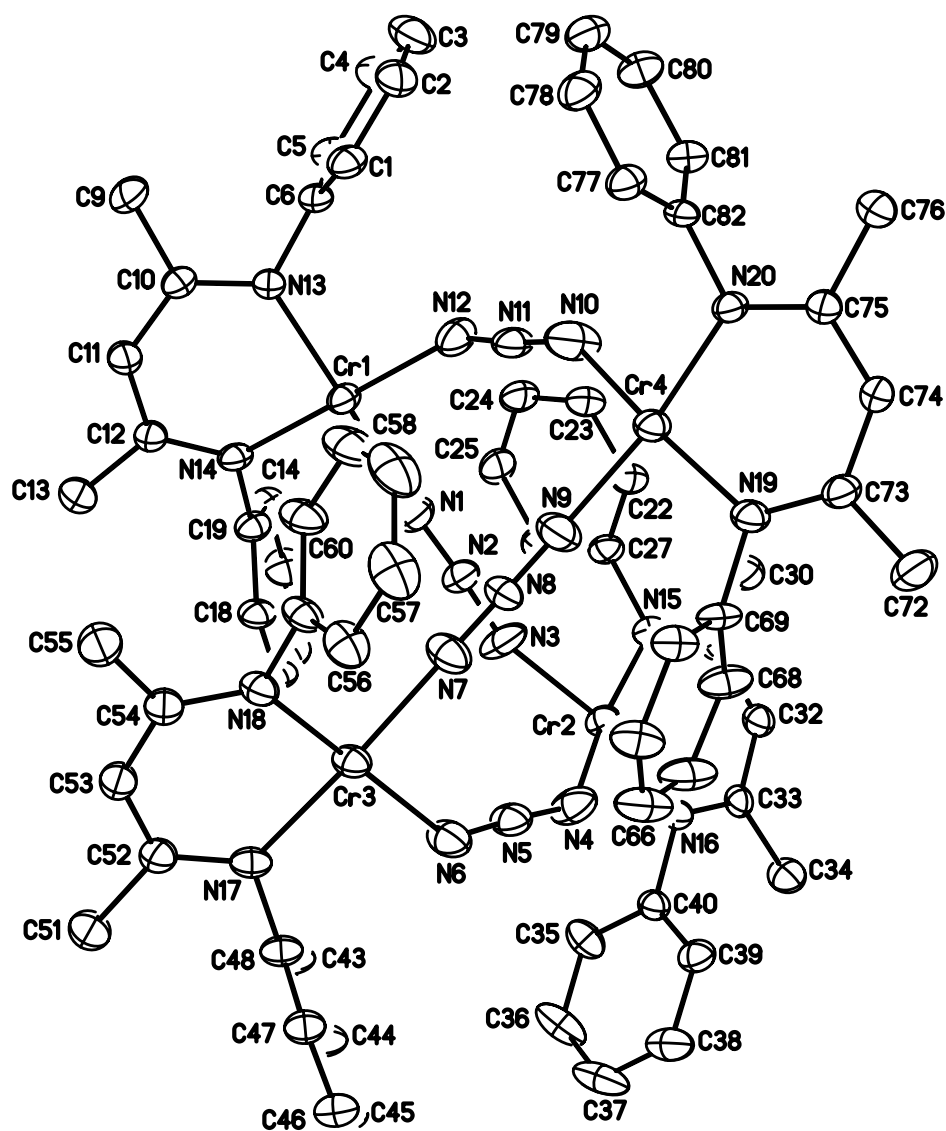
Figure 3.3   Molecular structure of $(L^{Me}Cr)_4(\mu\text{-}N_3)_4$ (**26**). Ellipsoids are drawn at the 30% probability level. Hydrogen atoms and methyl groups on aryls have been omitted for clarity.

Table 3.1   Interatomic distances (Å) and angles (°) for $(L^{Me}Cr)_4(\mu\text{-}N_3)_4$ (**26**)

Distances (Å)			
Cr(1)-N(1)	2.027(4)	C(22)-C(23)	1.374(7)
Cr(1)-N(14)	2.034(4)	C(22)-C(27)	1.394(7)
Cr(1)-N(13)	2.040(4)	C(22)-C(28)	1.512(8)
Cr(1)-N(12)	2.042(5)	C(23)-C(24)	1.379(9)
Cr(2)-N(3)	2.022(5)	C(24)-C(25)	1.374(9)
Cr(2)-N(15)	2.029(4)	C(25)-C(26)	1.393(8)
Cr(2)-N(16)	2.032(4)	C(26)-C(27)	1.403(7)
Cr(2)-N(4)	2.046(6)	C(26)-C(29)	1.493(8)
Cr(3)-N(18)	2.029(4)	C(30)-C(31)	1.508(8)
Cr(3)-N(7)	2.039(5)	C(31)-C(32)	1.390(7)
Cr(3)-N(17)	2.045(4)	C(32)-C(33)	1.397(7)
Cr(3)-N(6)	2.046(5)	C(33)-C(34)	1.510(7)
Cr(4)-N(20)	2.029(4)	C(35)-C(36)	1.377(9)
Cr(4)-N(9)	2.029(5)	C(35)-C(40)	1.388(7)
Cr(4)-N(10)	2.032(5)	C(35)-C(41)	1.501(9)
Cr(4)-N(19)	2.041(4)	C(36)-C(37)	1.365(10)
N(1)-N(2)	1.156(6)	C(37)-C(38)	1.382(10)
N(2)-N(3)	1.166(6)	C(38)-C(39)	1.385(8)
N(4)-N(5)	1.153(7)	C(39)-C(40)	1.387(7)
N(5)-N(6)	1.165(7)	C(39)-C(42)	1.504(8)
N(7)-N(8)	1.150(6)	C(43)-C(44)	1.379(7)
N(8)-N(9)	1.155(6)	C(43)-C(48)	1.393(7)
N(10)-N(11)	1.150(6)	C(43)-C(49)	1.513(8)
N(11)-N(12)	1.147(6)	C(44)-C(45)	1.370(8)
N(13)-C(10)	1.324(6)	C(45)-C(46)	1.393(8)
N(13)-C(6)	1.445(6)	C(46)-C(47)	1.382(7)
N(14)-C(12)	1.327(6)	C(47)-C(48)	1.382(7)
N(14)-C(19)	1.438(6)	C(47)-C(50)	1.508(7)
N(15)-C(31)	1.336(6)	C(51)-C(52)	1.511(7)
N(15)-C(27)	1.447(6)	C(52)-C(53)	1.395(7)
N(16)-C(33)	1.339(6)	C(53)-C(54)	1.390(7)
N(16)-C(40)	1.449(6)	C(54)-C(55)	1.507(8)
N(17)-C(52)	1.330(7)	C(56)-C(57)	1.379(8)
N(17)-C(48)	1.449(6)	C(56)-C(61)	1.398(8)

N(18)-C(54)	1.331(7)	C(56)-C(62)	1.519(9)
N(18)-C(61)	1.446(6)	C(57)-C(58)	1.376(10)
N(19)-C(73)	1.326(6)	C(58)-C(59)	1.381(10)
N(19)-C(69)	1.443(6)	C(59)-C(60)	1.385(8)
N(20)-C(75)	1.342(6)	C(60)-C(61)	1.395(8)
N(20)-C(82)	1.443(6)	C(60)-C(63)	1.499(9)
C(1)-C(2)	1.388(8)	C(64)-C(65)	1.374(8)
C(1)-C(6)	1.404(7)	C(64)-C(69)	1.395(8)
C(1)-C(7)	1.500(8)	C(64)-C(70)	1.511(8)
C(2)-C(3)	1.369(9)	C(65)-C(66)	1.373(9)
C(3)-C(4)	1.369(9)	C(66)-C(67)	1.367(9)
C(4)-C(5)	1.379(8)	C(67)-C(68)	1.391(8)
C(5)-C(6)	1.384(8)	C(68)-C(69)	1.382(7)
C(5)-C(8)	1.516(8)	C(68)-C(71)	1.509(9)
C(9)-C(10)	1.504(7)	C(72)-C(73)	1.514(7)
C(10)-C(11)	1.404(7)	C(73)-C(74)	1.389(7)
C(11)-C(12)	1.397(7)	C(74)-C(75)	1.403(7)
C(12)-C(13)	1.503(7)	C(75)-C(76)	1.509(7)
C(14)-C(15)	1.380(7)	C(77)-C(78)	1.374(7)
C(14)-C(19)	1.392(7)	C(77)-C(82)	1.398(7)
C(14)-C(20)	1.511(8)	C(77)-C(83)	1.503(8)
C(15)-C(16)	1.387(8)	C(78)-C(79)	1.382(8)
C(16)-C(17)	1.378(8)	C(79)-C(80)	1.377(8)
C(17)-C(18)	1.392(7)	C(80)-C(81)	1.381(7)
C(18)-C(19)	1.398(7)	C(81)-C(82)	1.398(7)
C(18)-C(21)	1.521(8)	C(81)-C(84)	1.502(8)

Angles (°)

N(1)-Cr(1)-N(14)	92.83(18)	C(14)-C(19)-N(14)	118.6(5)
N(1)-Cr(1)-N(13)	171.74(19)	C(18)-C(19)-N(14)	120.5(5)
N(14)-Cr(1)-N(13)	89.25(16)	C(23)-C(22)-C(27)	119.0(5)
N(1)-Cr(1)-N(12)	87.59(19)	C(23)-C(22)-C(28)	119.5(5)
N(14)-Cr(1)-N(12)	179.4(2)	C(27)-C(22)-C(28)	121.5(5)
N(13)-Cr(1)-N(12)	90.40(17)	C(22)-C(23)-C(24)	120.9(6)
N(3)-Cr(2)-N(15)	94.33(19)	C(25)-C(24)-C(23)	120.0(5)
N(3)-Cr(2)-N(16)	167.1(2)	C(24)-C(25)-C(26)	121.3(6)

N(15)-Cr(2)-N(16)	90.96(17)	C(25)-C(26)-C(27)	117.6(5)
N(3)-Cr(2)-N(4)	87.2(2)	C(25)-C(26)-C(29)	121.8(5)
N(15)-Cr(2)-N(4)	167.7(2)	C(27)-C(26)-C(29)	120.6(5)
N(16)-Cr(2)-N(4)	90.07(19)	C(22)-C(27)-C(26)	121.2(5)
N(18)-Cr(3)-N(7)	92.02(19)	C(22)-C(27)-N(15)	120.6(5)
N(18)-Cr(3)-N(17)	90.65(18)	C(26)-C(27)-N(15)	118.2(5)
N(7)-Cr(3)-N(17)	171.4(2)	N(15)-C(31)-C(32)	124.3(5)
N(18)-Cr(3)-N(6)	172.0(2)	N(15)-C(31)-C(30)	119.3(5)
N(7)-Cr(3)-N(6)	87.8(2)	C(32)-C(31)-C(30)	116.4(5)
N(17)-Cr(3)-N(6)	90.7(2)	C(31)-C(32)-C(33)	128.7(5)
N(20)-Cr(4)-N(9)	171.0(2)	N(16)-C(33)-C(32)	123.1(5)
N(20)-Cr(4)-N(10)	89.40(19)	N(16)-C(33)-C(34)	120.2(5)
N(9)-Cr(4)-N(10)	87.5(2)	C(32)-C(33)-C(34)	116.7(5)
N(20)-Cr(4)-N(19)	90.34(16)	C(38)-C(39)-C(40)	118.4(6)
N(9)-Cr(4)-N(19)	94.14(19)	C(38)-C(39)-C(42)	120.6(6)
N(10)-Cr(4)-N(19)	170.4(3)	C(40)-C(39)-C(42)	121.0(5)
N(2)-N(1)-Cr(1)	174.5(5)	C(39)-C(40)-C(35)	120.8(5)
N(1)-N(2)-N(3)	176.6(6)	C(39)-C(40)-N(16)	120.9(5)
N(2)-N(3)-Cr(2)	159.7(5)	C(35)-C(40)-N(16)	118.2(5)
N(5)-N(4)-Cr(2)	136.4(5)	C(44)-C(43)-C(48)	118.5(5)
N(4)-N(5)-N(6)	176.0(6)	C(44)-C(43)-C(49)	120.1(5)
N(5)-N(6)-Cr(3)	134.3(4)	C(48)-C(43)-C(49)	121.4(5)
N(8)-N(7)-Cr(3)	174.5(5)	C(45)-C(44)-C(43)	122.3(6)
N(7)-N(8)-N(9)	177.2(6)	C(44)-C(45)-C(46)	118.4(5)
N(8)-N(9)-Cr(4)	165.2(5)	C(47)-C(46)-C(45)	120.8(5)
N(11)-N(10)-Cr(4)	142.8(5)	C(46)-C(47)-C(48)	119.6(5)
N(12)-N(11)-N(10)	174.5(6)	C(46)-C(47)-C(50)	120.5(5)
N(11)-N(12)-Cr(1)	143.6(5)	C(48)-C(47)-C(50)	120.0(5)
C(10)-N(13)-C(6)	117.5(4)	C(47)-C(48)-C(43)	120.5(5)
C(10)-N(13)-Cr(1)	124.2(3)	C(47)-C(48)-N(17)	118.8(5)
C(6)-N(13)-Cr(1)	118.3(3)	C(43)-C(48)-N(17)	120.7(5)
C(12)-N(14)-C(19)	118.0(4)	N(17)-C(52)-C(53)	123.0(5)
C(12)-N(14)-Cr(1)	125.2(3)	N(17)-C(52)-C(51)	120.5(5)
C(19)-N(14)-Cr(1)	116.8(3)	C(53)-C(52)-C(51)	116.5(5)
C(31)-N(15)-C(27)	116.9(4)	C(54)-C(53)-C(52)	129.9(5)
C(31)-N(15)-Cr(2)	125.4(4)	N(18)-C(54)-C(53)	122.5(5)
C(27)-N(15)-Cr(2)	117.7(3)	N(18)-C(54)-C(55)	120.1(5)

C(33)-N(16)-C(40)	117.2(4)	C(53)-C(54)-C(55)	117.4(5)
C(33)-N(16)-Cr(2)	126.2(3)	C(57)-C(56)-C(61)	118.3(6)
C(40)-N(16)-Cr(2)	116.2(3)	C(57)-C(56)-C(62)	121.3(6)
C(52)-N(17)-C(48)	116.3(4)	C(61)-C(56)-C(62)	120.3(5)
C(52)-N(17)-Cr(3)	125.3(3)	C(58)-C(57)-C(56)	121.1(7)
C(48)-N(17)-Cr(3)	118.3(4)	C(57)-C(58)-C(59)	119.6(6)
C(54)-N(18)-C(61)	117.3(4)	C(58)-C(59)-C(60)	121.8(7)
C(54)-N(18)-Cr(3)	126.5(4)	C(59)-C(60)-C(61)	117.4(6)
C(61)-N(18)-Cr(3)	115.9(3)	C(59)-C(60)-C(63)	121.4(6)
C(73)-N(19)-C(69)	117.7(4)	C(61)-C(60)-C(63)	121.2(5)
C(73)-N(19)-Cr(4)	125.5(3)	C(60)-C(61)-C(56)	121.9(5)
C(69)-N(19)-Cr(4)	116.8(3)	C(60)-C(61)-N(18)	120.1(5)
C(75)-N(20)-C(82)	116.0(4)	C(56)-C(61)-N(18)	118.0(5)
C(75)-N(20)-Cr(4)	125.9(3)	C(65)-C(64)-C(69)	118.9(5)
C(82)-N(20)-Cr(4)	117.9(3)	C(65)-C(64)-C(70)	121.4(6)
C(2)-C(1)-C(6)	117.4(6)	C(69)-C(64)-C(70)	119.8(5)
C(2)-C(1)-C(7)	120.3(5)	C(66)-C(65)-C(64)	121.3(6)
C(6)-C(1)-C(7)	122.3(5)	C(67)-C(66)-C(65)	119.1(6)
C(3)-C(2)-C(1)	122.6(6)	C(66)-C(67)-C(68)	121.7(6)
C(2)-C(3)-C(4)	118.4(6)	C(69)-C(68)-C(67)	118.2(6)
C(3)-C(4)-C(5)	122.0(7)	C(69)-C(68)-C(71)	121.3(6)
C(4)-C(5)-C(6)	118.8(6)	C(67)-C(68)-C(71)	120.4(6)
C(4)-C(5)-C(8)	120.2(6)	C(68)-C(69)-C(64)	120.8(5)
C(6)-C(5)-C(8)	121.0(5)	C(68)-C(69)-N(19)	120.7(5)
C(5)-C(6)-C(1)	120.8(5)	C(64)-C(69)-N(19)	118.3(4)
C(5)-C(6)-N(13)	119.2(5)	N(19)-C(73)-C(74)	123.8(5)
C(1)-C(6)-N(13)	120.0(5)	N(19)-C(73)-C(72)	120.1(5)
N(13)-C(10)-C(11)	123.6(5)	C(74)-C(73)-C(72)	116.0(5)
N(13)-C(10)-C(9)	120.1(5)	C(73)-C(74)-C(75)	128.8(5)
C(11)-C(10)-C(9)	116.3(5)	N(20)-C(75)-C(74)	122.8(5)
C(12)-C(11)-C(10)	127.9(5)	N(20)-C(75)-C(76)	119.9(4)
N(14)-C(12)-C(11)	122.3(5)	C(74)-C(75)-C(76)	117.2(5)
N(14)-C(12)-C(13)	120.5(5)	C(78)-C(77)-C(82)	118.4(5)
C(11)-C(12)-C(13)	117.3(5)	C(78)-C(77)-C(83)	121.1(5)
C(15)-C(14)-C(19)	119.0(5)	C(82)-C(77)-C(83)	120.5(5)
C(15)-C(14)-C(20)	120.1(5)	C(77)-C(78)-C(79)	121.8(6)
C(19)-C(14)-C(20)	120.9(5)	C(80)-C(79)-C(78)	118.8(5)

C(14)-C(15)-C(16)	121.6(6)	C(79)-C(80)-C(81)	121.8(6)
C(17)-C(16)-C(15)	118.4(5)	C(80)-C(81)-C(82)	118.2(5)
C(16)-C(17)-C(18)	122.1(6)	C(80)-C(81)-C(84)	120.4(5)
C(17)-C(18)-C(19)	118.0(5)	C(82)-C(81)-C(84)	121.4(5)
C(17)-C(18)-C(21)	120.6(5)	C(81)-C(82)-C(77)	121.0(5)
C(19)-C(18)-C(21)	121.3(5)	C(81)-C(82)-N(20)	120.7(4)
C(14)-C(19)-C(18)	120.9(5)	C(77)-C(82)-N(20)	118.3(4)
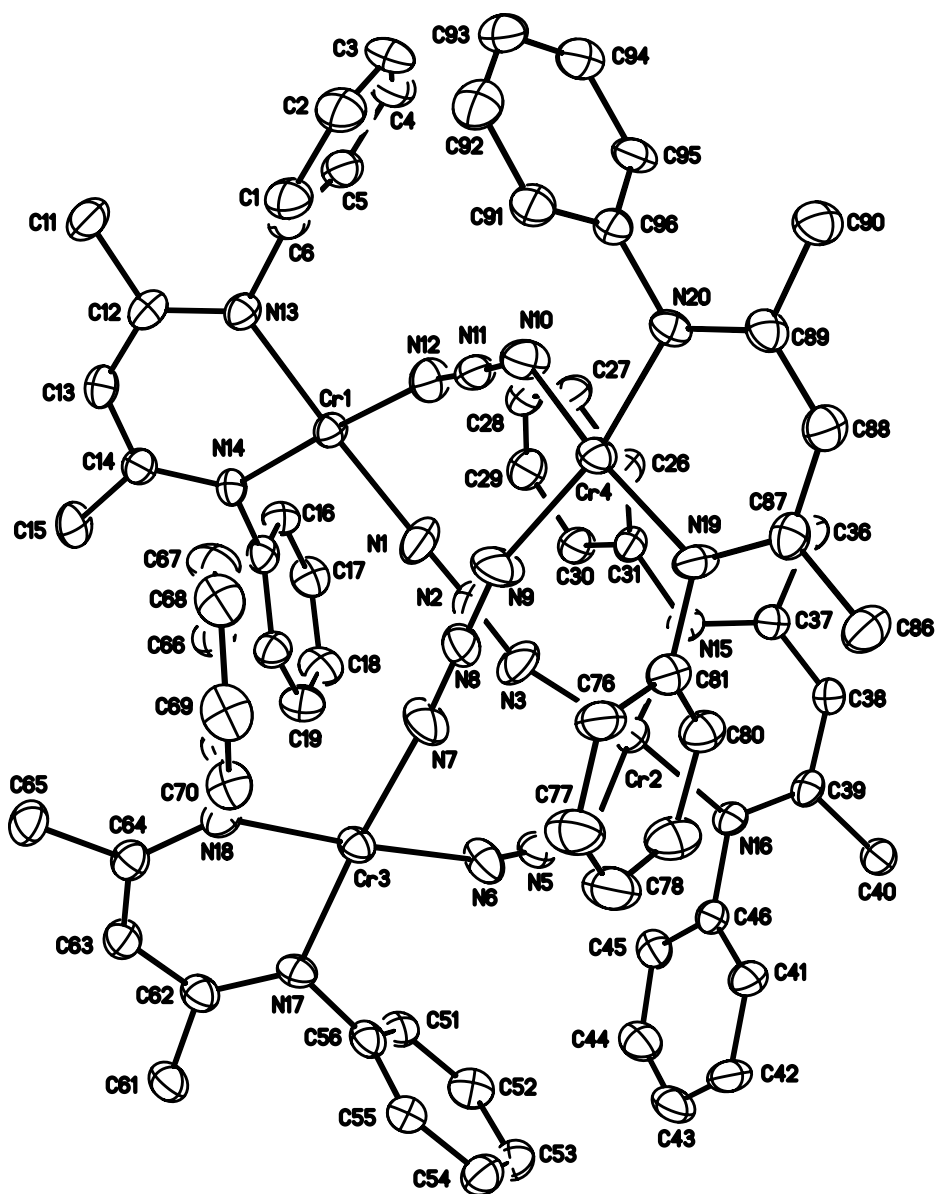
Figure 3.4   Molecular structure of $(L^{Et}Cr)_4(\mu\text{-}N_3)_4$ (**27**). Ellipsoids are drawn at the 30% probability level. Hydrogen atoms, an Et_2O molecule, and ethyl groups have been omitted for clarity.

Table 3.2   Interatomic distances (Å) and angles (°) for (L^{Et}Cr)$_4$(μ-N$_3$)$_4$ (**27**)

	Distances (Å)		
Cr(1)-N(1)	1.996(6)	C(30)-C(31)	1.425(10)
Cr(1)-N(12)	2.020(5)	C(30)-C(34)	1.476(11)
Cr(1)-N(14)	2.029(5)	C(32)-C(33)	1.428(11)
Cr(1)-N(13)	2.043(5)	C(34)-C(35)	1.482(12)
Cr(2)-N(3)	2.007(6)	C(36)-C(37)	1.529(9)
Cr(2)-N(4)	2.033(6)	C(37)-C(38)	1.373(9)
Cr(2)-N(16)	2.034(5)	C(38)-C(39)	1.398(9)
Cr(2)-N(15)	2.035(6)	C(39)-C(40)	1.530(8)
Cr(3)-N(7)	2.009(6)	C(41)-C(46)	1.381(10)
Cr(3)-N(6)	2.024(6)	C(41)-C(42)	1.415(11)
Cr(3)-N(18)	2.024(5)	C(41)-C(47)	1.516(11)
Cr(3)-N(17)	2.033(5)	C(42)-C(43)	1.381(14)
Cr(4)-N(9)	2.011(6)	C(43)-C(44)	1.333(14)
Cr(4)-N(20)	2.026(5)	C(44)-C(45)	1.370(11)
Cr(4)-N(19)	2.039(5)	C(45)-C(46)	1.416(10)
Cr(4)-N(10)	2.045(6)	C(45)-C(49)	1.495(11)
N(1)-N(2)	1.162(8)	C(47)-C(48)	1.474(12)
N(2)-N(3)	1.150(8)	C(49)-C(50)	1.497(14)
N(4)-N(5)	1.167(7)	C(51)-C(52)	1.374(10)
N(5)-N(6)	1.183(7)	C(51)-C(56)	1.385(9)
N(7)-N(8)	1.135(7)	C(51)-C(57)	1.505(10)
N(8)-N(9)	1.158(8)	C(52)-C(53)	1.384(11)
N(10)-N(11)	1.187(7)	C(53)-C(54)	1.366(11)
N(11)-N(12)	1.151(7)	C(54)-C(55)	1.397(10)
N(13)-C(12)	1.324(9)	C(55)-C(56)	1.408(10)
N(13)-C(6)	1.449(8)	C(55)-C(59)	1.521(10)
N(14)-C(14)	1.333(8)	C(57)-C(58)	1.512(11)
N(14)-C(21)	1.458(8)	C(59)-C(60)	1.426(14)
N(15)-C(37)	1.342(8)	C(61)-C(62)	1.513(9)
N(15)-C(31)	1.441(8)	C(62)-C(63)	1.399(9)
N(16)-C(39)	1.320(8)	C(63)-C(64)	1.395(9)
N(16)-C(46)	1.448(8)	C(64)-C(65)	1.508(9)
N(17)-C(62)	1.330(8)	C(66)-C(71)	1.378(9)
N(17)-C(56)	1.429(8)	C(66)-C(67)	1.390(10)

N(18)-C(64)	1.342(8)	C(66)-C(72)	1.519(11)
N(18)-C(71)	1.461(8)	C(67)-C(68)	1.358(11)
N(19)-C(87)	1.333(8)	C(68)-C(69)	1.374(11)
N(19)-C(81)	1.435(8)	C(69)-C(70)	1.377(10)
N(20)-C(89)	1.344(8)	C(70)-C(71)	1.396(10)
N(20)-C(96)	1.438(8)	C(70)-C(74)	1.526(11)
C(1)-C(2)	1.391(11)	C(72)-C(73)	1.437(12)
C(1)-C(6)	1.392(11)	C(74)-C(75)	1.498(12)
C(1)-C(7)	1.477(12)	C(76)-C(77)	1.398(11)
C(2)-C(3)	1.346(12)	C(76)-C(81)	1.408(10)
C(3)-C(4)	1.364(12)	C(76)-C(82)	1.512(11)
C(4)-C(5)	1.376(10)	C(77)-C(78)	1.362(12)
C(5)-C(6)	1.396(10)	C(78)-C(79)	1.376(12)
C(5)-C(9)	1.517(10)	C(79)-C(80)	1.409(11)
C(7)-C(8)	1.395(13)	C(80)-C(81)	1.372(10)
C(9)-C(10)	1.486(11)	C(80)-C(84)	1.482(11)
C(11)-C(12)	1.509(9)	C(82)-C(83)	1.475(13)
C(12)-C(13)	1.389(10)	C(84)-C(85)	1.418(13)
C(13)-C(14)	1.380(9)	C(86)-C(87)	1.525(10)
C(14)-C(15)	1.499(9)	C(87)-C(88)	1.390(10)
C(16)-C(17)	1.387(9)	C(88)-C(89)	1.392(10)
C(16)-C(21)	1.403(9)	C(89)-C(90)	1.502(9)
C(16)-C(22)	1.512(10)	C(91)-C(92)	1.376(10)
C(17)-C(18)	1.374(11)	C(91)-C(96)	1.385(10)
C(18)-C(19)	1.383(11)	C(91)-C(97)	1.526(10)
C(19)-C(20)	1.355(10)	C(92)-C(93)	1.379(12)
C(20)-C(21)	1.398(9)	C(93)-C(94)	1.377(11)
C(20)-C(24)	1.502(10)	C(94)-C(95)	1.382(10)
C(22)-C(23)	1.492(10)	C(95)-C(96)	1.401(9)
C(24)-C(25)	1.539(11)	C(95)-C(99)	1.516(10)
C(26)-C(27)	1.386(10)	C(97)-C(98)	1.527(11)
C(26)-C(31)	1.418(9)	C(99)-C(100)	1.534(11)
C(26)-C(32)	1.514(11)	C(101)-C(102)	1.461(15)
C(27)-C(28)	1.377(11)	C(102)-O(1)	1.355(12)
C(28)-C(29)	1.337(11)	O(1)-C(103)	1.387(12)
C(29)-C(30)	1.395(11)	C(103)-C(104)	1.471(15)

Angles (°)

N(1)-Cr(1)-N(12)	86.4(3)	C(29)-C(30)-C(34)	121.1(7)
N(1)-Cr(1)-N(14)	92.1(2)	C(31)-C(30)-C(34)	122.1(7)
N(12)-Cr(1)-N(14)	174.4(3)	C(26)-C(31)-C(30)	120.8(7)
N(1)-Cr(1)-N(13)	177.7(3)	C(26)-C(31)-N(15)	121.7(6)
N(12)-Cr(1)-N(13)	92.0(2)	C(30)-C(31)-N(15)	117.4(6)
N(14)-Cr(1)-N(13)	89.6(2)	C(33)-C(32)-C(26)	118.3(8)
N(3)-Cr(2)-N(4)	86.4(3)	C(30)-C(34)-C(35)	113.8(8)
N(3)-Cr(2)-N(16)	171.2(3)	N(15)-C(37)-C(38)	124.9(6)
N(4)-Cr(2)-N(16)	90.7(2)	N(15)-C(37)-C(36)	119.5(6)
N(3)-Cr(2)-N(15)	93.5(3)	C(38)-C(37)-C(36)	115.6(6)
N(4)-Cr(2)-N(15)	170.7(3)	C(37)-C(38)-C(39)	127.6(7)
N(16)-Cr(2)-N(15)	90.7(2)	N(16)-C(39)-C(38)	124.5(6)
N(7)-Cr(3)-N(6)	85.4(3)	N(16)-C(39)-C(40)	119.7(6)
N(7)-Cr(3)-N(18)	93.0(3)	C(38)-C(39)-C(40)	115.8(6)
N(6)-Cr(3)-N(18)	175.5(3)	C(46)-C(41)-C(42)	117.9(9)
N(7)-Cr(3)-N(17)	176.1(3)	C(46)-C(41)-C(47)	120.1(7)
N(6)-Cr(3)-N(17)	91.8(2)	C(42)-C(41)-C(47)	122.0(8)
N(18)-Cr(3)-N(17)	90.0(2)	C(43)-C(42)-C(41)	120.9(10)
N(9)-Cr(4)-N(20)	167.0(3)	C(44)-C(43)-C(42)	119.0(9)
N(9)-Cr(4)-N(19)	94.3(3)	C(43)-C(44)-C(45)	123.7(10)
N(20)-Cr(4)-N(19)	91.1(2)	C(44)-C(45)-C(46)	117.6(9)
N(9)-Cr(4)-N(10)	86.3(3)	C(44)-C(45)-C(49)	121.6(8)
N(20)-Cr(4)-N(10)	91.2(2)	C(46)-C(45)-C(49)	120.7(7)
N(19)-Cr(4)-N(10)	166.5(3)	C(41)-C(46)-C(45)	120.5(7)
N(2)-N(1)-Cr(1)	174.6(7)	C(41)-C(46)-N(16)	121.0(7)
N(3)-N(2)-N(1)	177.7(9)	C(45)-C(46)-N(16)	118.4(7)
N(2)-N(3)-Cr(2)	161.0(7)	C(48)-C(47)-C(41)	116.6(9)
N(5)-N(4)-Cr(2)	135.4(5)	C(45)-C(49)-C(50)	113.0(8)
N(4)-N(5)-N(6)	177.6(8)	C(52)-C(51)-C(56)	118.4(7)
N(5)-N(6)-Cr(3)	157.1(6)	C(52)-C(51)-C(57)	119.7(7)
N(8)-N(7)-Cr(3)	173.6(9)	C(56)-C(51)-C(57)	121.8(6)
N(7)-N(8)-N(9)	179.1(10)	C(51)-C(52)-C(53)	121.2(7)
N(8)-N(9)-Cr(4)	163.1(7)	C(54)-C(53)-C(52)	119.8(7)
N(11)-N(10)-Cr(4)	135.5(5)	C(53)-C(54)-C(55)	121.7(7)
N(12)-N(11)-N(10)	176.8(8)	C(54)-C(55)-C(56)	116.9(7)
N(11)-N(12)-Cr(1)	159.0(7)	C(54)-C(55)-C(59)	121.8(7)

C(12)-N(13)-C(6)	118.7(6)	C(56)-C(55)-C(59)	121.2(7)
C(12)-N(13)-Cr(1)	125.2(5)	C(51)-C(56)-C(55)	122.0(7)
C(6)-N(13)-Cr(1)	116.0(4)	C(51)-C(56)-N(17)	121.6(6)
C(14)-N(14)-C(21)	117.0(5)	C(55)-C(56)-N(17)	116.3(6)
C(14)-N(14)-Cr(1)	124.5(4)	C(51)-C(57)-C(58)	114.5(7)
C(21)-N(14)-Cr(1)	118.5(4)	C(60)-C(59)-C(55)	117.9(9)
C(37)-N(15)-C(31)	116.9(6)	N(17)-C(62)-C(63)	123.4(6)
C(37)-N(15)-Cr(2)	123.0(5)	N(17)-C(62)-C(61)	120.0(6)
C(31)-N(15)-Cr(2)	120.1(5)	C(63)-C(62)-C(61)	116.6(6)
C(39)-N(16)-C(46)	118.4(5)	C(64)-C(63)-C(62)	128.6(7)
C(39)-N(16)-Cr(2)	124.2(4)	N(18)-C(64)-C(63)	122.7(6)
C(46)-N(16)-Cr(2)	117.3(4)	N(18)-C(64)-C(65)	120.6(6)
C(62)-N(17)-C(56)	118.8(5)	C(63)-C(64)-C(65)	116.7(7)
C(62)-N(17)-Cr(3)	125.8(4)	C(71)-C(66)-C(67)	119.0(7)
C(56)-N(17)-Cr(3)	115.4(4)	C(71)-C(66)-C(72)	122.8(6)
C(64)-N(18)-C(71)	116.0(5)	C(67)-C(66)-C(72)	118.1(7)
C(64)-N(18)-Cr(3)	126.2(4)	C(68)-C(67)-C(66)	119.9(8)
C(71)-N(18)-Cr(3)	117.8(4)	C(67)-C(68)-C(69)	121.3(7)
C(87)-N(19)-C(81)	116.9(6)	C(68)-C(69)-C(70)	120.2(8)
C(87)-N(19)-Cr(4)	124.8(5)	C(69)-C(70)-C(71)	118.4(8)
C(81)-N(19)-Cr(4)	118.2(5)	C(69)-C(70)-C(74)	122.9(7)
C(89)-N(20)-C(96)	116.8(5)	C(71)-C(70)-C(74)	118.7(7)
C(89)-N(20)-Cr(4)	125.5(5)	C(66)-C(71)-C(70)	121.1(6)
C(96)-N(20)-Cr(4)	117.4(4)	C(66)-C(71)-N(18)	121.4(6)
C(2)-C(1)-C(6)	116.7(9)	C(70)-C(71)-N(18)	117.5(7)
C(2)-C(1)-C(7)	122.5(9)	C(73)-C(72)-C(66)	116.2(8)
C(6)-C(1)-C(7)	120.7(7)	C(75)-C(74)-C(70)	116.4(8)
C(3)-C(2)-C(1)	121.8(9)	C(77)-C(76)-C(81)	117.5(8)
C(2)-C(3)-C(4)	120.8(8)	C(77)-C(76)-C(82)	118.1(8)
C(3)-C(4)-C(5)	120.5(9)	C(81)-C(76)-C(82)	124.4(7)
C(4)-C(5)-C(6)	118.3(8)	C(78)-C(77)-C(76)	121.5(9)
C(4)-C(5)-C(9)	118.5(8)	C(77)-C(78)-C(79)	120.3(9)
C(6)-C(5)-C(9)	123.2(7)	C(78)-C(79)-C(80)	120.4(8)
C(1)-C(6)-C(5)	121.6(7)	C(81)-C(80)-C(79)	118.5(8)
C(1)-C(6)-N(13)	120.2(7)	C(81)-C(80)-C(84)	121.7(7)
C(5)-C(6)-N(13)	117.8(7)	C(79)-C(80)-C(84)	119.9(8)
C(8)-C(7)-C(1)	120.5(10)	C(80)-C(81)-C(76)	121.8(7)

C(10)-C(9)-C(5)	114.2(8)	C(80)-C(81)-N(19)	120.4(7)
N(13)-C(12)-C(13)	122.5(6)	C(76)-C(81)-N(19)	117.7(6)
N(13)-C(12)-C(11)	119.4(7)	C(83)-C(82)-C(76)	115.8(9)
C(13)-C(12)-C(11)	118.2(7)	C(85)-C(84)-C(80)	116.9(9)
C(14)-C(13)-C(12)	129.9(7)	N(19)-C(87)-C(88)	123.7(7)
N(14)-C(14)-C(13)	122.7(6)	N(19)-C(87)-C(86)	118.9(7)
N(14)-C(14)-C(15)	119.6(6)	C(88)-C(87)-C(86)	117.4(7)
C(13)-C(14)-C(15)	117.6(7)	C(87)-C(88)-C(89)	129.2(7)
C(17)-C(16)-C(21)	117.8(7)	N(20)-C(89)-C(88)	123.1(6)
C(17)-C(16)-C(22)	121.7(6)	N(20)-C(89)-C(90)	119.2(6)
C(21)-C(16)-C(22)	120.4(6)	C(88)-C(89)-C(90)	117.7(6)
C(18)-C(17)-C(16)	120.8(7)	C(92)-C(91)-C(96)	119.4(8)
C(17)-C(18)-C(19)	120.1(7)	C(92)-C(91)-C(97)	118.5(8)
C(20)-C(19)-C(18)	121.2(8)	C(96)-C(91)-C(97)	122.1(7)
C(19)-C(20)-C(21)	118.8(7)	C(91)-C(92)-C(93)	119.2(8)
C(19)-C(20)-C(24)	120.8(7)	C(94)-C(93)-C(92)	121.5(8)
C(21)-C(20)-C(24)	120.4(6)	C(93)-C(94)-C(95)	120.5(8)
C(20)-C(21)-C(16)	121.2(6)	C(94)-C(95)-C(96)	117.5(7)
C(20)-C(21)-N(14)	122.7(6)	C(94)-C(95)-C(99)	121.9(7)
C(16)-C(21)-N(14)	116.1(6)	C(96)-C(95)-C(99)	120.6(7)
C(23)-C(22)-C(16)	117.1(7)	C(91)-C(96)-C(95)	121.8(7)
C(20)-C(24)-C(25)	113.5(7)	C(91)-C(96)-N(20)	119.5(6)
C(27)-C(26)-C(31)	118.1(7)	C(95)-C(96)-N(20)	118.7(6)
C(27)-C(26)-C(32)	122.2(7)	C(91)-C(97)-C(98)	111.4(7)
C(31)-C(26)-C(32)	119.6(7)	C(95)-C(99)-C(100)	113.6(7)
C(28)-C(27)-C(26)	120.3(7)	O(1)-C(102)-C(101)	110.9(10)
C(29)-C(28)-C(27)	121.6(8)	C(102)-O(1)-C(103)	112.9(9)
C(28)-C(29)-C(30)	122.1(8)	O(1)-C(103)-C(104)	110.0(10)
C(29)-C(30)-C(31)	116.7(7)		

The highly substituted nacnac ligand *L^R (*L^R = 2,2,6,6-tetramethylheptane-3,5,N,N'-bis-2,6-R$_2$-phenyl-diketiminato),[22] has been utilized in our group to synthesize various chromium alkyl compounds.[23] In this regard, the bulkier substitution (R = isopropyl) and the less sterically hindered substitution (R = methyl) are being used, and these ligands are abbreviated as *L^{iPr} and *L^{Me}, respectively. Chromium chloride precursors, (*L^{iPr}Cr)$_2$(μ-Cl)$_2$ and (*L^{Me}Cr)$_2$(μ-Cl)$_2$, have been synthesized and well characterized previously [23] and the azido complexes were then prepared in the same manner by treating the chlorides with NaN$_3$. Schemes 3.13 and 3.14 outline the synthesis of dimeric (*L^{iPr}Cr)$_2$(μ-N$_3$)$_2$ (28) and trimeric (*L^{Me}Cr)$_3$(μ-N$_3$)$_3$ (29). The structures of 28 and 29 are shown in Figures 3.5 and 3.6.

Ar = 2,6-diisopropylphenyl

28
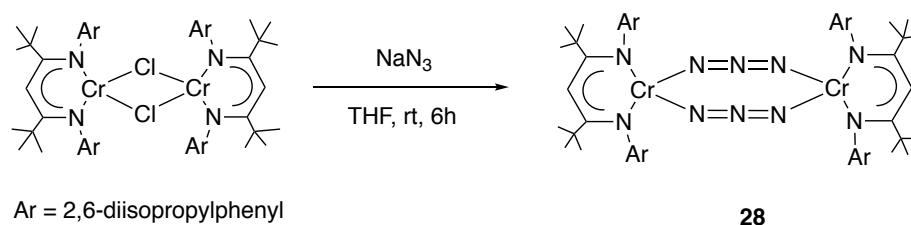
Scheme 3.13   Synthesis of (*L^{iPr}Cr)$_2$(μ-N$_3$)$_2$ (28)

Ar = 2,6-dimethylphenyl

29
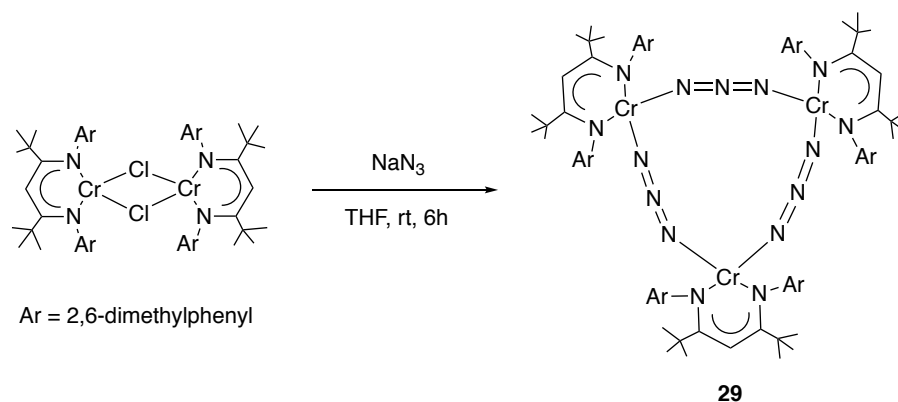
Scheme 3.14   Synthesis of (*L^{Me}Cr)$_3$(μ-N$_3$)$_3$ (29)

The binuclear complex **28** shares structural features with the reported $(L^{iPr}Cr)_2(\mu\text{-}N_3)_2$ (**24**), except for the large substituents on the backbone. The two chromium fragments are connected by two bridging azido ligands, i. e. $\mu_{1,3}\text{-}N_3$. The chromium(II) oxidation state finds expression in its preferred square planar coordination geometry. The effective magnetic moment of **28** at room temperature was measured to be 5.3(1) μ_B, identical to the value of 5.3(1) μ_B reported for **24**. The infrared spectrum of **28** exhibited azido stretching frequencies at 2126 and 2071cm^{-1}.

The formation of trinuclear complex **29** suggests that both the steric hindrance of the aryl groups and the bulk of the nacnac backbone exert an effect. Together they result in a trinuclear structure for **29**. The coordination of chromium in structure **29** is notably distorted from square planar geometry, which may be caused by the crowded nacnac fragments. The IR spectrum showed the azido ligands giving rise to three distinct stretches at 2149, 2104, and 2063 cm^{-1}. The magnetic moment of **29** was found to be 5.9(1) μ_B. The effective magnetic moment of a complex with three magnetically independent Cr(II) (S = $\frac{4}{2}$) is expected to be 8.5μ_B. The lower value of **29** indicates antiferromagnetic coupling between the metal centers.

With the successful synthesis of a family of azido compounds, the irradiation was then performed, the results are described in the following section.
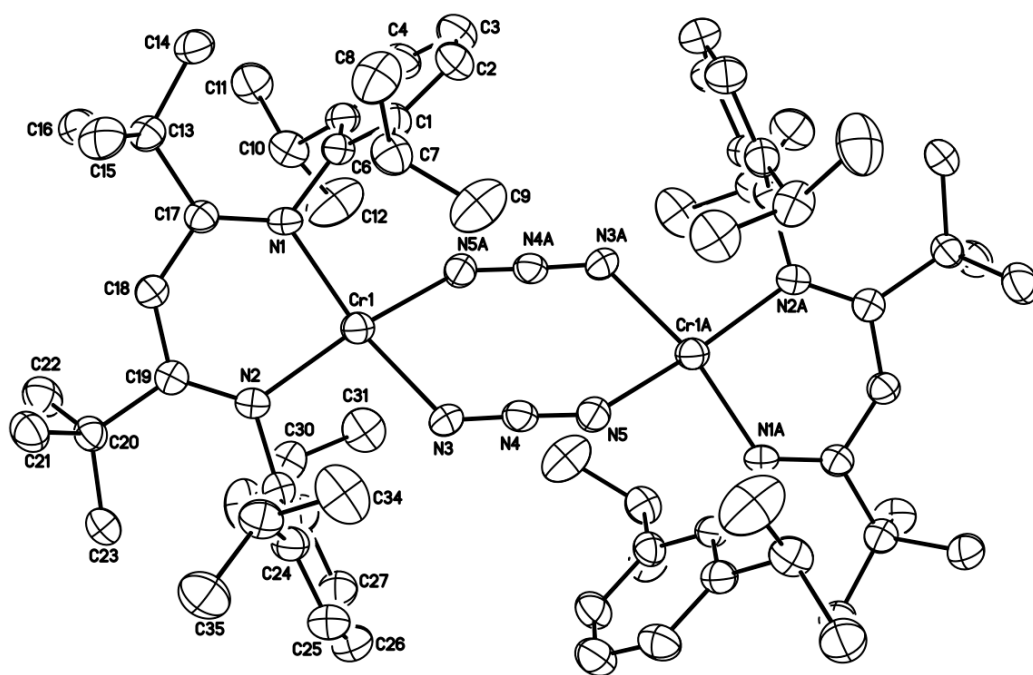
Figure 3.5   Molecular structure of (*L^{iPr}Cr)$_2$(μ-N$_3$)$_2$ (**28**). Ellipsoids are drawn at the
30% probability level. Hydrogen atoms have been omitted for clarity.

Table 3.3   Interatomic distances (Å) and angles (°) for (*L^{iPr}Cr)$_2$(μ-N$_3$)$_2$ (**28**)

Distances (Å)			
Cr(1)-N(2)	2.051(4)	C(13)-C(16)	1.524(7)
Cr(1)-N(1)	2.052(4)	C(13)-C(14)	1.534(7)
Cr(1)-N(3)	2.104(4)	C(13)-C(15)	1.539(7)
Cr(1)-N(5)A	2.105(5)	C(13)-C(17)	1.551(7)
N(1)-C(17)	1.332(6)	C(17)-C(18)	1.406(6)
N(1)-C(6)	1.443(6)	C(18)-C(19)	1.400(7)
N(2)-C(19)	1.334(6)	C(19)-C(20)	1.553(7)
N(2)-C(29)	1.448(6)	C(20)-C(23)	1.531(7)
N(3)-N(4)	1.171(6)	C(20)-C(21)	1.538(7)
N(4)-N(5)	1.157(6)	C(20)-C(22)	1.539(7)
N(5)-Cr(1)A	2.105(5)	C(24)-C(25)	1.379(8)
C(1)-C(2)	1.383(7)	C(24)-C(29)	1.398(7)
C(1)-C(6)	1.399(7)	C(24)-C(33)	1.523(7)
C(1)-C(7)	1.514(8)	C(25)-C(26)	1.378(8)
C(2)-C(3)	1.376(9)	C(26)-C(27)	1.367(9)
C(3)-C(4)	1.380(9)	C(27)-C(28)	1.397(8)
C(4)-C(5)	1.390(7)	C(28)-C(29)	1.410(7)
C(5)-C(6)	1.398(7)	C(28)-C(30)	1.508(8)
C(5)-C(10)	1.515(7)	C(30)-C(31)	1.526(9)
C(7)-C(8)	1.525(8)	C(30)-C(32)	1.534(8)
C(7)-C(9)	1.533(9)	C(33)-C(34)	1.516(8)
C(10)-C(12)	1.523(9)	C(33)-C(35)	1.523(8)
C(10)-C(11)	1.524(8)		

Angles (°)			
N(2)-Cr(1)-N(1)	91.27(16)	C(14)-C(13)-C(15)	105.4(4)
N(2)-Cr(1)-N(3)	96.63(17)	C(16)-C(13)-C(17)	110.1(4)
N(1)-Cr(1)-N(3)	156.64(18)	C(14)-C(13)-C(17)	118.4(4)
N(2)-Cr(1)-N(5)A	158.64(17)	C(15)-C(13)-C(17)	108.0(4)
N(1)-Cr(1)-N(5)A	96.21(17)	N(1)-C(17)-C(18)	120.3(4)
N(3)-Cr(1)-N(5)A	84.30(18)	N(1)-C(17)-C(13)	126.5(4)
C(17)-N(1)-C(6)	124.3(4)	C(18)-C(17)-C(13)	113.1(4)
C(17)-N(1)-Cr(1)	126.4(3)	C(19)-C(18)-C(17)	133.8(5)

C(6)-N(1)-Cr(1)	109.2(3)	N(2)-C(19)-C(18)	120.7(5)
C(19)-N(2)-C(29)	124.8(4)	N(2)-C(19)-C(20)	126.6(4)
C(19)-N(2)-Cr(1)	126.5(3)	C(18)-C(19)-C(20)	112.7(4)
C(29)-N(2)-Cr(1)	108.7(3)	C(23)-C(20)-C(21)	106.7(5)
N(4)-N(3)-Cr(1)	131.4(4)	C(23)-C(20)-C(22)	105.2(4)
N(5)-N(4)-N(3)	177.9(5)	C(21)-C(20)-C(22)	108.7(5)
N(4)-N(5)-Cr(1)A	135.1(4)	C(23)-C(20)-C(19)	118.2(4)
C(2)-C(1)-C(6)	118.0(5)	C(21)-C(20)-C(19)	109.8(4)
C(2)-C(1)-C(7)	119.6(5)	C(22)-C(20)-C(19)	107.9(4)
C(6)-C(1)-C(7)	122.4(5)	C(25)-C(24)-C(29)	117.7(5)
C(3)-C(2)-C(1)	121.4(6)	C(25)-C(24)-C(33)	119.9(5)
C(2)-C(3)-C(4)	120.2(6)	C(29)-C(24)-C(33)	122.4(5)
C(3)-C(4)-C(5)	120.5(6)	C(26)-C(25)-C(24)	121.9(6)
C(4)-C(5)-C(6)	118.5(5)	C(27)-C(26)-C(25)	119.8(6)
C(4)-C(5)-C(10)	119.6(5)	C(26)-C(27)-C(28)	121.5(6)
C(6)-C(5)-C(10)	121.9(5)	C(27)-C(28)-C(29)	117.2(5)
C(5)-C(6)-C(1)	121.4(5)	C(27)-C(28)-C(30)	120.2(5)
C(5)-C(6)-N(1)	119.1(4)	C(29)-C(28)-C(30)	122.5(5)
C(1)-C(6)-N(1)	118.7(5)	C(24)-C(29)-C(28)	121.8(5)
C(1)-C(7)-C(8)	113.0(5)	C(24)-C(29)-N(2)	119.2(4)
C(1)-C(7)-C(9)	110.3(5)	C(28)-C(29)-N(2)	118.4(5)
C(8)-C(7)-C(9)	109.6(5)	C(28)-C(30)-C(31)	111.9(5)
C(5)-C(10)-C(12)	110.3(5)	C(28)-C(30)-C(32)	112.5(6)
C(5)-C(10)-C(11)	113.0(5)	C(31)-C(30)-C(32)	108.6(5)
C(12)-C(10)-C(11)	109.6(5)	C(34)-C(33)-C(24)	111.7(5)
C(16)-C(13)-C(14)	105.6(5)	C(34)-C(33)-C(35)	109.1(5)
C(16)-C(13)-C(15)	109.0(5)	C(24)-C(33)-C(35)	112.4(5)
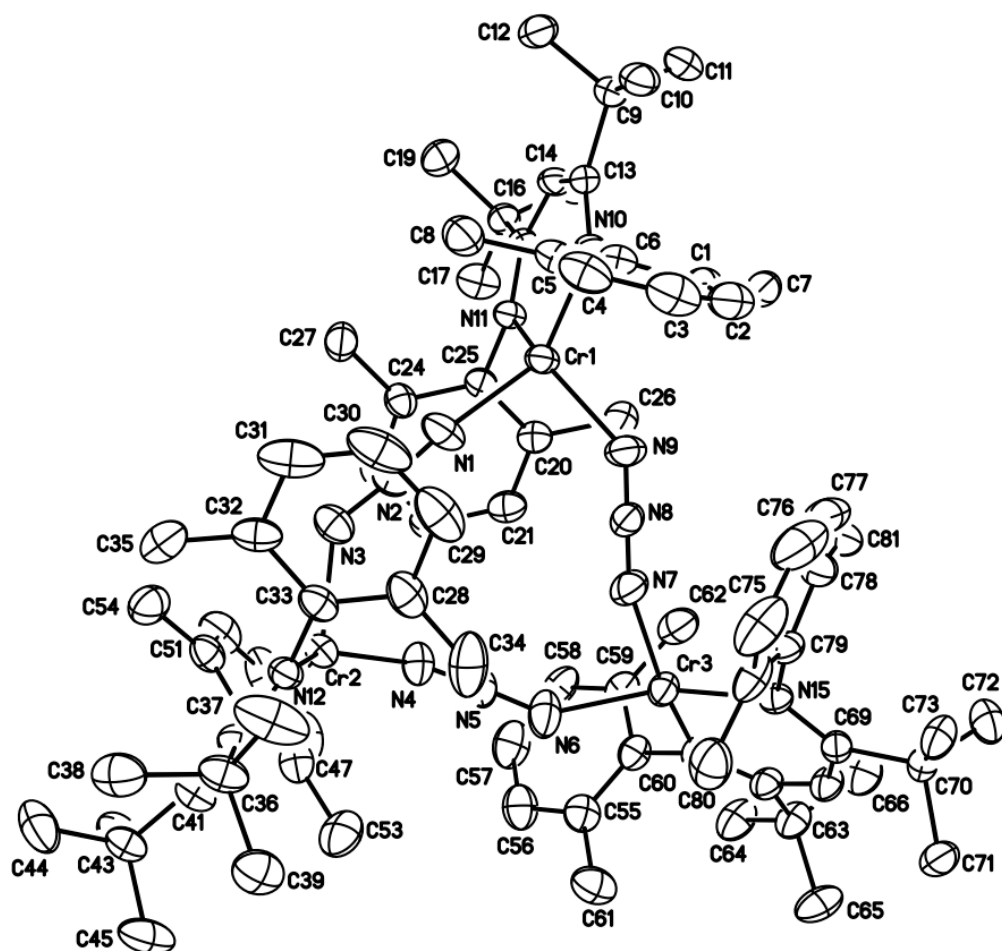
Figure 3.6   Molecular structure of (*L^Me^Cr)$_3$(μ-N$_3$)$_3$ (**29**). Ellipsoids are drawn at the 30% probability level. Hydrogen atoms have been omitted for clarity.

Table 3.4   Interatomic distances (Å) and angles (°) for (*L^{Me}Cr)$_3$(μ-N$_3$)$_3$ (**29**)

	Distances (Å)		
Cr(1)-N(10)	2.006(3)	C(24)-C(25)	1.407(6)
Cr(1)-N(11)	2.007(3)	C(24)-C(27)	1.503(6)
Cr(1)-N(1)	2.044(4)	C(28)-C(33)	1.370(6)
Cr(1)-N(9)	2.097(4)	C(28)-C(29)	1.447(8)
Cr(2)-N(13)	2.005(3)	C(28)-C(34)	1.490(8)
Cr(2)-N(12)	2.006(4)	C(29)-C(30)	1.362(9)
Cr(2)-N(3)	2.057(4)	C(30)-C(31)	1.342(9)
Cr(2)-N(4)	2.067(4)	C(31)-C(32)	1.389(7)
Cr(3)-N(15)	2.020(3)	C(32)-C(33)	1.433(6)
Cr(3)-N(7)	2.036(4)	C(32)-C(35)	1.475(7)
Cr(3)-N(6)	2.037(4)	C(36)-C(37)	1.515(7)
Cr(3)-N(14)	2.036(4)	C(36)-C(39)	1.536(7)
N(1)-N(2)	1.137(5)	C(36)-C(40)	1.557(6)
N(2)-N(3)	1.178(5)	C(36)-C(38)	1.564(7)
N(4)-N(5)	1.149(5)	C(40)-C(41)	1.399(6)
N(5)-N(6)	1.167(5)	C(41)-C(42)	1.406(6)
N(7)-N(8)	1.168(5)	C(42)-C(43)	1.553(6)
N(8)-N(9)	1.175(5)	C(43)-C(46)	1.521(7)
N(10)-C(13)	1.341(5)	C(43)-C(44)	1.527(7)
N(10)-C(6)	1.426(5)	C(43)-C(45)	1.532(7)
N(11)-C(15)	1.332(5)	C(47)-C(52)	1.385(6)
N(11)-C(25)	1.435(5)	C(47)-C(48)	1.390(8)
N(12)-C(40)	1.348(5)	C(47)-C(53)	1.507(7)
N(12)-C(33)	1.430(5)	C(48)-C(49)	1.378(9)
N(13)-C(42)	1.329(5)	C(49)-C(50)	1.341(9)
N(13)-C(52)	1.439(5)	C(50)-C(51)	1.397(7)
N(14)-C(67)	1.331(5)	C(51)-C(52)	1.382(6)
N(14)-C(60)	1.439(5)	C(51)-C(54)	1.519(7)
N(15)-C(69)	1.351(5)	C(55)-C(56)	1.389(7)
N(15)-C(79)	1.438(5)	C(55)-C(60)	1.397(6)
C(1)-C(2)	1.392(6)	C(55)-C(61)	1.504(7)
C(1)-C(6)	1.397(6)	C(56)-C(57)	1.370(8)
C(1)-C(7)	1.496(7)	C(57)-C(58)	1.360(8)
C(2)-C(3)	1.358(8)	C(58)-C(59)	1.390(7)

C(3)-C(4)	1.362(8)	C(59)-C(60)	1.386(6)
C(4)-C(5)	1.408(7)	C(59)-C(62)	1.501(7)
C(5)-C(6)	1.401(6)	C(63)-C(65)	1.532(7)
C(5)-C(8)	1.502(7)	C(63)-C(64)	1.534(6)
C(9)-C(10)	1.532(6)	C(63)-C(66)	1.558(7)
C(9)-C(11)	1.533(6)	C(63)-C(67)	1.563(6)
C(9)-C(13)	1.542(5)	C(67)-C(68)	1.399(6)
C(9)-C(12)	1.547(6)	C(68)-C(69)	1.404(6)
C(13)-C(14)	1.400(6)	C(69)-C(70)	1.556(6)
C(14)-C(15)	1.406(5)	C(70)-C(72)	1.532(6)
C(15)-C(16)	1.551(6)	C(70)-C(71)	1.541(6)
C(16)-C(17)	1.525(6)	C(70)-C(73)	1.547(6)
C(16)-C(18)	1.534(6)	C(74)-C(75)	1.383(8)
C(16)-C(19)	1.538(6)	C(74)-C(79)	1.430(7)
C(20)-C(21)	1.387(6)	C(74)-C(80)	1.487(8)
C(20)-C(25)	1.399(6)	C(75)-C(76)	1.372(10)
C(20)-C(26)	1.522(6)	C(76)-C(77)	1.351(10)
C(21)-C(22)	1.372(7)	C(77)-C(78)	1.426(8)
C(22)-C(23)	1.368(7)	C(78)-C(79)	1.357(6)
C(23)-C(24)	1.388(6)	C(78)-C(81)	1.483(8)

Angles (°)

N(10)-Cr(1)-N(11)	91.26(13)	C(24)-C(25)-N(11)	119.7(4)
N(10)-Cr(1)-N(1)	137.36(17)	C(33)-C(28)-C(29)	117.9(6)
N(11)-Cr(1)-N(1)	103.01(15)	C(33)-C(28)-C(34)	121.3(5)
N(10)-Cr(1)-N(9)	106.77(14)	C(29)-C(28)-C(34)	120.8(6)
N(11)-Cr(1)-N(9)	134.97(16)	C(30)-C(29)-C(28)	118.5(6)
N(1)-Cr(1)-N(9)	91.14(17)	C(31)-C(30)-C(29)	123.2(6)
N(13)-Cr(2)-N(12)	91.94(14)	C(30)-C(31)-C(32)	121.3(7)
N(13)-Cr(2)-N(3)	139.88(15)	C(31)-C(32)-C(33)	116.9(5)
N(12)-Cr(2)-N(3)	100.32(15)	C(31)-C(32)-C(35)	122.0(5)
N(13)-Cr(2)-N(4)	101.35(15)	C(33)-C(32)-C(35)	121.0(4)
N(12)-Cr(2)-N(4)	141.76(16)	C(28)-C(33)-N(12)	120.2(4)
N(3)-Cr(2)-N(4)	92.27(16)	C(28)-C(33)-C(32)	122.1(4)
N(15)-Cr(3)-N(7)	95.67(15)	N(12)-C(33)-C(32)	116.8(4)
N(15)-Cr(3)-N(6)	155.45(19)	C(37)-C(36)-C(39)	106.8(5)

N(7)-Cr(3)-N(6)	87.12(17)	C(37)-C(36)-C(40)	117.6(4)
N(15)-Cr(3)-N(14)	91.97(14)	C(39)-C(36)-C(40)	108.0(4)
N(7)-Cr(3)-N(14)	157.16(17)	C(37)-C(36)-C(38)	106.5(5)
N(6)-Cr(3)-N(14)	94.79(16)	C(39)-C(36)-C(38)	107.9(4)
N(2)-N(1)-Cr(1)	164.9(4)	C(40)-C(36)-C(38)	109.6(4)
N(1)-N(2)-N(3)	175.6(5)	N(12)-C(40)-C(41)	121.3(4)
N(2)-N(3)-Cr(2)	133.7(4)	N(12)-C(40)-C(36)	124.7(4)
N(5)-N(4)-Cr(2)	147.2(4)	C(41)-C(40)-C(36)	114.0(4)
N(4)-N(5)-N(6)	177.0(5)	C(40)-C(41)-C(42)	131.9(4)
N(5)-N(6)-Cr(3)	139.3(4)	N(13)-C(42)-C(41)	119.6(4)
N(8)-N(7)-Cr(3)	161.6(4)	N(13)-C(42)-C(43)	125.3(4)
N(7)-N(8)-N(9)	178.1(5)	C(41)-C(42)-C(43)	115.2(4)
N(8)-N(9)-Cr(1)	127.6(3)	C(46)-C(43)-C(44)	106.9(5)
C(13)-N(10)-C(6)	127.6(3)	C(46)-C(43)-C(45)	107.1(4)
C(13)-N(10)-Cr(1)	127.1(3)	C(44)-C(43)-C(45)	108.2(5)
C(6)-N(10)-Cr(1)	104.1(2)	C(46)-C(43)-C(42)	116.9(4)
C(15)-N(11)-C(25)	129.0(4)	C(44)-C(43)-C(42)	108.6(4)
C(15)-N(11)-Cr(1)	128.1(3)	C(45)-C(43)-C(42)	108.9(4)
C(25)-N(11)-Cr(1)	102.5(2)	C(52)-C(47)-C(48)	119.0(6)
C(40)-N(12)-C(33)	126.5(4)	C(52)-C(47)-C(53)	121.1(5)
C(40)-N(12)-Cr(2)	125.4(3)	C(48)-C(47)-C(53)	119.9(5)
C(33)-N(12)-Cr(2)	108.1(3)	C(49)-C(48)-C(47)	119.5(6)
C(42)-N(13)-C(52)	128.5(4)	C(50)-C(49)-C(48)	121.3(6)
C(42)-N(13)-Cr(2)	127.8(3)	C(49)-C(50)-C(51)	120.9(6)
C(52)-N(13)-Cr(2)	102.6(2)	C(52)-C(51)-C(50)	118.2(5)
C(67)-N(14)-C(60)	123.9(4)	C(52)-C(51)-C(54)	122.2(4)
C(67)-N(14)-Cr(3)	126.6(3)	C(50)-C(51)-C(54)	119.6(5)
C(60)-N(14)-Cr(3)	109.3(3)	C(51)-C(52)-C(47)	121.1(5)
C(69)-N(15)-C(79)	121.7(3)	C(51)-C(52)-N(13)	118.3(4)
C(69)-N(15)-Cr(3)	126.1(3)	C(47)-C(52)-N(13)	119.7(4)
C(79)-N(15)-Cr(3)	112.1(2)	C(56)-C(55)-C(60)	118.9(5)
C(2)-C(1)-C(6)	118.5(5)	C(56)-C(55)-C(61)	120.5(5)
C(2)-C(1)-C(7)	121.0(5)	C(60)-C(55)-C(61)	120.5(5)
C(6)-C(1)-C(7)	120.5(4)	C(57)-C(56)-C(55)	120.1(6)
C(3)-C(2)-C(1)	121.0(5)	C(58)-C(57)-C(56)	121.3(6)
C(2)-C(3)-C(4)	120.8(5)	C(57)-C(58)-C(59)	119.9(5)
C(3)-C(4)-C(5)	121.2(6)	C(60)-C(59)-C(58)	119.6(5)

C(6)-C(5)-C(4)	117.2(5)	C(60)-C(59)-C(62)	120.0(5)
C(6)-C(5)-C(8)	121.4(5)	C(58)-C(59)-C(62)	120.3(5)
C(4)-C(5)-C(8)	121.3(5)	C(59)-C(60)-C(55)	120.1(5)
C(1)-C(6)-C(5)	121.2(4)	C(59)-C(60)-N(14)	119.9(4)
C(1)-C(6)-N(10)	119.5(4)	C(55)-C(60)-N(14)	119.4(4)
C(5)-C(6)-N(10)	118.8(4)	C(65)-C(63)-C(64)	107.2(4)
C(10)-C(9)-C(11)	105.8(4)	C(65)-C(63)-C(66)	109.1(4)
C(10)-C(9)-C(13)	117.7(4)	C(64)-C(63)-C(66)	106.1(5)
C(11)-C(9)-C(13)	109.5(3)	C(65)-C(63)-C(67)	109.6(4)
C(10)-C(9)-C(12)	106.2(4)	C(64)-C(63)-C(67)	117.6(4)
C(11)-C(9)-C(12)	109.0(4)	C(66)-C(63)-C(67)	107.0(4)
C(13)-C(9)-C(12)	108.5(4)	N(14)-C(67)-C(68)	120.2(4)
N(10)-C(13)-C(14)	120.5(4)	N(14)-C(67)-C(63)	127.2(4)
N(10)-C(13)-C(9)	125.1(4)	C(68)-C(67)-C(63)	112.6(4)
C(14)-C(13)-C(9)	114.3(3)	C(67)-C(68)-C(69)	133.7(4)
C(13)-C(14)-C(15)	132.1(4)	N(15)-C(69)-C(68)	120.0(4)
N(11)-C(15)-C(14)	120.0(4)	N(15)-C(69)-C(70)	126.1(4)
N(11)-C(15)-C(16)	125.1(4)	C(68)-C(69)-C(70)	113.9(4)
C(14)-C(15)-C(16)	114.9(3)	C(72)-C(70)-C(71)	109.0(4)
C(17)-C(16)-C(18)	106.0(4)	C(72)-C(70)-C(73)	106.7(4)
C(17)-C(16)-C(19)	107.4(4)	C(71)-C(70)-C(73)	104.9(4)
C(18)-C(16)-C(19)	109.8(4)	C(72)-C(70)-C(69)	108.5(4)
C(17)-C(16)-C(15)	117.2(3)	C(71)-C(70)-C(69)	108.7(3)
C(18)-C(16)-C(15)	108.9(4)	C(73)-C(70)-C(69)	118.6(4)
C(19)-C(16)-C(15)	107.6(4)	C(75)-C(74)-C(79)	118.1(6)
C(21)-C(20)-C(25)	118.3(4)	C(75)-C(74)-C(80)	120.5(6)
C(21)-C(20)-C(26)	120.0(4)	C(79)-C(74)-C(80)	121.3(5)
C(25)-C(20)-C(26)	121.6(4)	C(76)-C(75)-C(74)	119.2(7)
C(22)-C(21)-C(20)	121.8(5)	C(77)-C(76)-C(75)	123.5(7)
C(23)-C(22)-C(21)	119.4(4)	C(76)-C(77)-C(78)	118.6(6)
C(22)-C(23)-C(24)	121.7(5)	C(79)-C(78)-C(77)	118.9(6)
C(23)-C(24)-C(25)	118.2(4)	C(79)-C(78)-C(81)	120.9(5)
C(23)-C(24)-C(27)	121.5(4)	C(77)-C(78)-C(81)	120.1(5)
C(25)-C(24)-C(27)	120.3(4)	C(78)-C(79)-C(74)	121.4(5)
C(20)-C(25)-C(24)	120.6(4)	C(78)-C(79)-N(15)	120.7(5)
C(20)-C(25)-N(11)	118.4(4)	C(74)-C(79)-N(15)	117.5(4)

3.2.3   Formation of nitride/dinitrogen complexes by irradiation of azides

Photolysis, with 254nm light, of the newly prepared azido complexes **26-29** led to decomposition of the azide ions, producing various nitrido and dinitrogen complexes. All the complexes that are going to be discussed were structurally characterized by X-ray diffraction analysis and some with additional spectroscopic methods.

Irradiation of $(L^{Me}Cr)_4(\mu-N_3)_4$ (**26**) in THF for 24 hours led to a color change from red to orange-brown. Upon removal of solvent, recrystallization was done in a pentane solution. Product was structurally characterized and found to be bis(μ-nitrido) complex $(L^{Me}Cr)_2(\mu-N)_2$ (**30**). **30** crystallizes in the monoclinic space group $P2_1/n$ with an inversion center located between the chromium centers. The coordination geometry for chromium is distorted tetrahedral. The bridging nitrogen atoms are bound equally between the two chromium centers with a Cr1-N3 distance of 1.784(2) Å and a Cr1-N3A distance of 1.795(2) Å. These distances fall into the range between single bonds (e.g. Cr-N_{avg} 2.068 Å in $(L^{iPr}Cr)_2(\mu-NH_2)_2$) and double bonds (e.g. Cr-N_{avg} 1.661 Å in $L^{iPr}Cr(NAd)_2$).[20] The dihedral angle between the planes defined by N1-Cr1-N2 and N3-Cr1-N3A, is 88.49°. The bond distances, tetrahedral geometry of both chromiums, as well as the centrosymmetric structure of **30** together indicate a formal oxidation state of Cr(IV) for each chromium atom. Note that this is a centrosymmetric molecule, and the geometry around the chromiums (both tetrahedral) differs from what has been observed for $(L^{iPr}Cr)_2(\mu-N)_2$ (**25**) (tetrahedral and square planar). It is interesting that two geometric forms of bis(μ-nitrido) complexes were detected. **30** was always formed in a mixture with other products (see below), making isolation of the pure compound in significant amounts exceedingly difficult.

Following the reaction pattern of photolysis of $(L^{iPr}Cr)_2(\mu\text{-}N_3)_2$ (**24**), the appearance of **30** among the products of photolysis of **26** indicated the potential formation of the corresponding dinitrogen complex upon further irradiation; however, this compound, i. e., $(L^{Me}Cr)_2(\mu\text{-}N_2)$, has not been found, even when extending the reaction time to 3 days. Notably, the known tetranuclear end-on bridged dinitrogen complex $(L^{Me}Cr)_4(\mu\text{-}N_2)_4$ (**4**) from the diazo chemistry discussed in **Chapter 1** was not among the products. Efforts have also been made to prepare a dinitrogen complex by reduction of chromium halides supported by the L^{Me} ligand, i. e., by treating $(L^{Me}Cr)_2(\mu\text{-}Cl)_2$ or $(L^{Me}Cr)_2(\mu\text{-}I)_2$ with reductants such as Li, Na, K, KC_8, Na/K, Na/Hg and Mg, either stoichiometric or in excess. These attempts did not yield the desired dinitrogen complex.

As mentioned earlier, **30** was always formed in a mixture. Crystals of $(L^{Me}Cr)_3(\mu_3\text{-}N)(\mu_2\text{-}N)(\mu_2\text{-}N_3)$ (**31**) (shown in Figure 3.8) were also obtained after irradiation of **26** for 24 hours. Additionally, another trinuclear species (**T**) was also found; unfortunately, the crystallographic structure of **T** suffered from disorder, but the structure as well as LIFDI mass spectrum (m/z: 1113.4475 [M$^+$]; calcd. m/z: 1113.4368 [M$^+$]) together support an assignment of **T** as $(L^{Me}Cr)_3(\mu_3\text{-}N)(\mu_2\text{-}N)_2$, shown in Scheme 3.15.
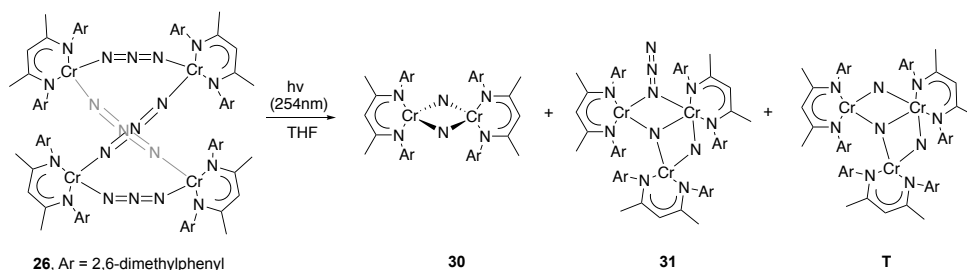
Scheme 3.15 Products formed by the irradiation of **26**

185

Figure 3.8 shows the molecular structure of **31** and Figure 3.9 shows the molecular core. Cr2 is connected to both Cr1 and Cr3 by two bridging nitrogen atoms while Cr1 and Cr3 are connected only by N10. Due to steric effects, the core is puckered, i. e., the two planes (Cr1-N10-Cr2 and Cr2-N10-Cr3) span a dihedral angle of 162.0(1) °. The coordination around each chromium center can be best described as square planar Cr1, square pyramidal Cr2 (with N3 occupying the apical position), and tetrahedral Cr3. The oxidation state assignment of each chromium center is best considered as follows. Square planar Cr1 is best described as divalent, charge-compensated by an anionic nacnac ligand and one third of nitrido N10. N10 is also bonded to Cr2 and Cr3, contributing one negative charge to each chromium. The short Cr3-N11 bond distance of 1.654(3) Å is indicative of double bond character, making Cr2 tetravalent. The net negative charge of this molecule consists of three nacnac ligands, one azido ligand and two nitrido ligands, giving **31** a possible oxidation state assignment of Cr(II)-Cr(IV)-Cr(IV). The effective magnetic moment of **31** could not be measured due to the lack of enough pure material. The structural relationship between **31** and **T** is readily apparent. It is likely that T is formed by loss of N_2 from **31**.

186
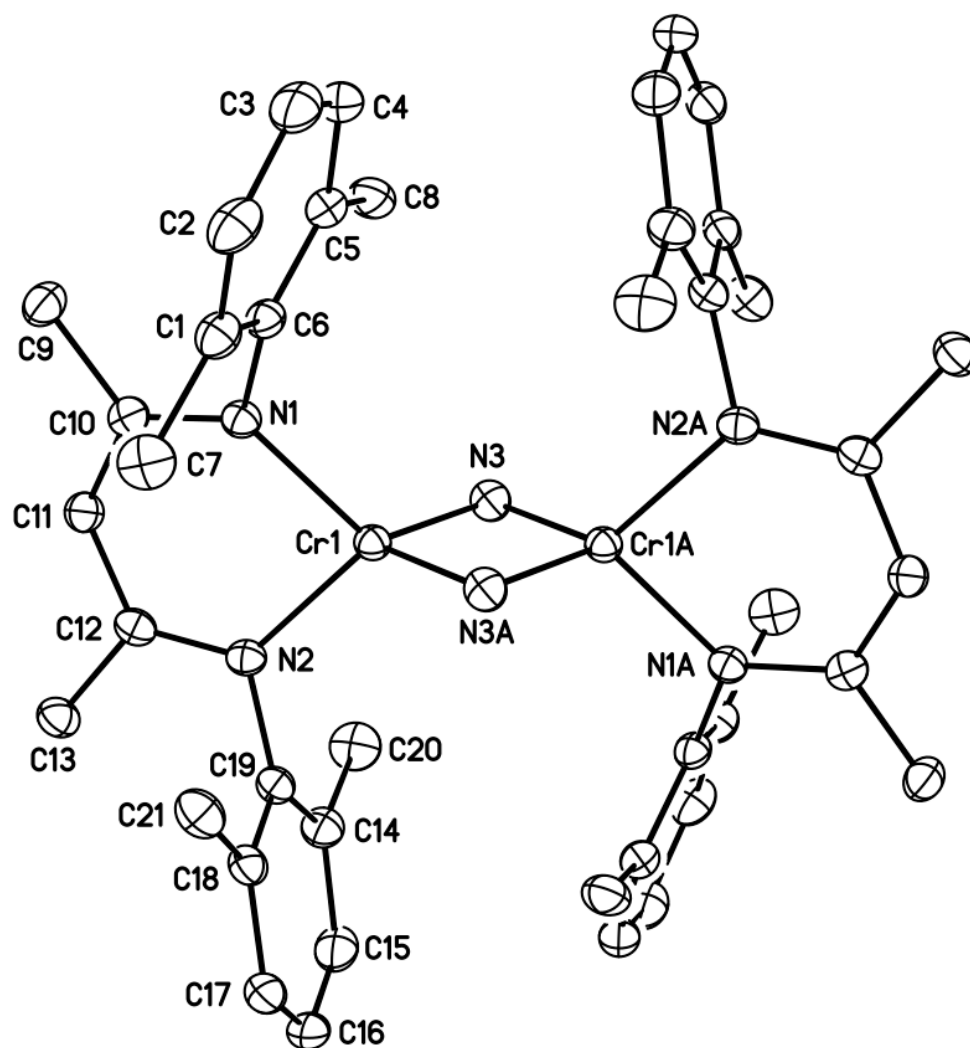
Figure 3.7   Molecular structure of $(L^{Me}Cr)_2(\mu\text{-}N)_2$ (**30**). Ellipsoids are drawn at the 30% probability level. Hydrogen atoms have been omitted for clarity.

Table 3.5   Interatomic distances (Å) and angles (°) for (L^{Me}Cr)$_2$(μ-N)$_2$ (**30**)

Distances (Å)

Cr(1)-N(3)	1.784(2)	C(4)-C(5)	1.398(4)
Cr(1)-N(3)A	1.795(2)	C(5)-C(6)	1.394(3)
Cr(1)-N(1)	1.9804(19)	C(5)-C(7)	1.497(4)
Cr(1)-N(2)	1.9846(19)	C(9)-C(10)	1.506(3)
Cr(1)-Cr(1)A	2.5004(7)	C(10)-C(11)	1.393(3)
N(1)-C(10)	1.343(3)	C(11)-C(12)	1.399(3)
N(1)-C(6)	1.446(3)	C(12)-C(13)	1.516(3)
N(2)-C(12)	1.337(3)	C(14)-C(15)	1.393(4)
N(2)-C(19)	1.444(3)	C(14)-C(19)	1.394(3)
N(3)-Cr(1)A	1.795(2)	C(14)-C(20)	1.506(4)
C(1)-C(2)	1.394(3)	C(15)-C(16)	1.369(4)
C(1)-C(6)	1.399(3)	C(16)-C(17)	1.378(4)
C(1)-C(8)	1.494(4)	C(17)-C(18)	1.394(3)
C(2)-C(3)	1.375(4)	C(18)-C(19)	1.402(3)
C(3)-C(4)	1.381(4)	C(18)-C(21)	1.501(4)

Angles (°)

N(3)-Cr(1)-N(3)A	91.36(9)	C(6)-C(5)-C(7)	121.9(2)
N(3)-Cr(1)-N(1)	119.89(8)	C(4)-C(5)-C(7)	120.5(2)
N(3)A-Cr(1)-N(1)	118.37(8)	C(5)-C(6)-C(1)	122.4(2)
N(3)-Cr(1)-N(2)	118.87(8)	C(5)-C(6)-N(1)	120.0(2)
N(3)A-Cr(1)-N(2)	120.86(8)	C(1)-C(6)-N(1)	117.5(2)
N(1)-Cr(1)-N(2)	90.39(8)	N(1)-C(10)-C(11)	123.3(2)
N(3)-Cr(1)-Cr(1)A	45.86(6)	N(1)-C(10)-C(9)	119.9(2)
N(3)A-Cr(1)-Cr(1)A	45.50(6)	C(11)-C(10)-C(9)	116.8(2)
N(1)-Cr(1)-Cr(1)A	134.16(6)	C(10)-C(11)-C(12)	126.6(2)
N(2)-Cr(1)-Cr(1)A	135.46(6)	N(2)-C(12)-C(11)	123.2(2)
C(10)-N(1)-C(6)	115.44(19)	N(2)-C(12)-C(13)	120.4(2)
C(10)-N(1)-Cr(1)	125.43(15)	C(11)-C(12)-C(13)	116.4(2)
C(6)-N(1)-Cr(1)	119.12(14)	C(15)-C(14)-C(19)	117.7(2)
C(12)-N(2)-C(19)	115.79(18)	C(15)-C(14)-C(20)	120.9(2)
C(12)-N(2)-Cr(1)	125.68(15)	C(19)-C(14)-C(20)	121.4(2)
C(19)-N(2)-Cr(1)	118.51(14)	C(16)-C(15)-C(14)	121.2(3)

Cr(1)-N(3)-Cr(1)A	88.64(9)	C(15)-C(16)-C(17)	120.8(2)
C(2)-C(1)-C(6)	117.6(2)	C(16)-C(17)-C(18)	120.2(3)
C(2)-C(1)-C(8)	121.1(2)	C(17)-C(18)-C(19)	118.2(2)
C(6)-C(1)-C(8)	121.3(2)	C(17)-C(18)-C(21)	121.2(2)
C(3)-C(2)-C(1)	121.1(3)	C(19)-C(18)-C(21)	120.5(2)
C(2)-C(3)-C(4)	120.4(2)	C(14)-C(19)-C(18)	121.8(2)
C(3)-C(4)-C(5)	120.9(3)	C(14)-C(19)-N(2)	120.6(2)
C(6)-C(5)-C(4)	117.6(2)	C(18)-C(19)-N(2)	117.6(2)
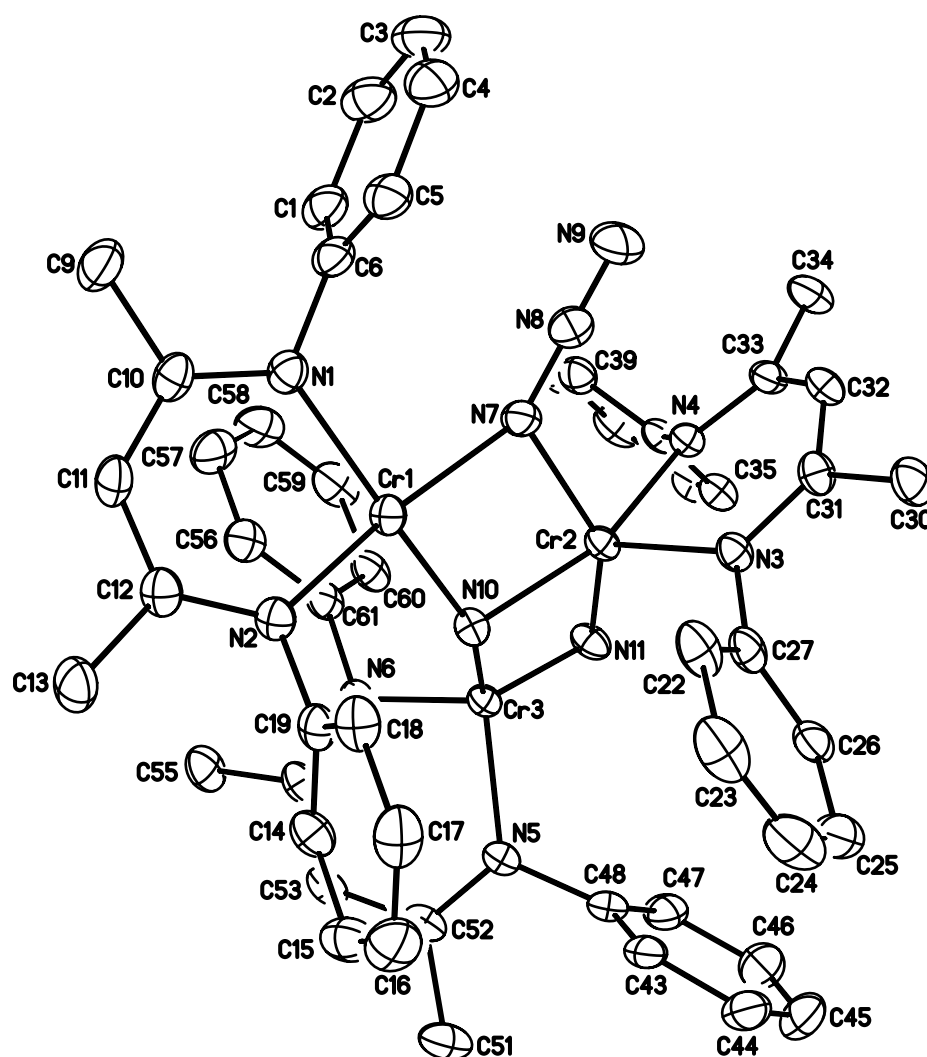
Figure 3.8   Molecular structure of $(L^{Me}Cr)_3(\mu_3\text{-}N)(\mu_2\text{-}N)(\mu_2\text{-}N_3)$ (**31**). Ellipsoids are drawn at the 30% probability level. Hydrogen atoms, an Et$_2$O molecule and methyl groups on aryls have been omitted for clarity.
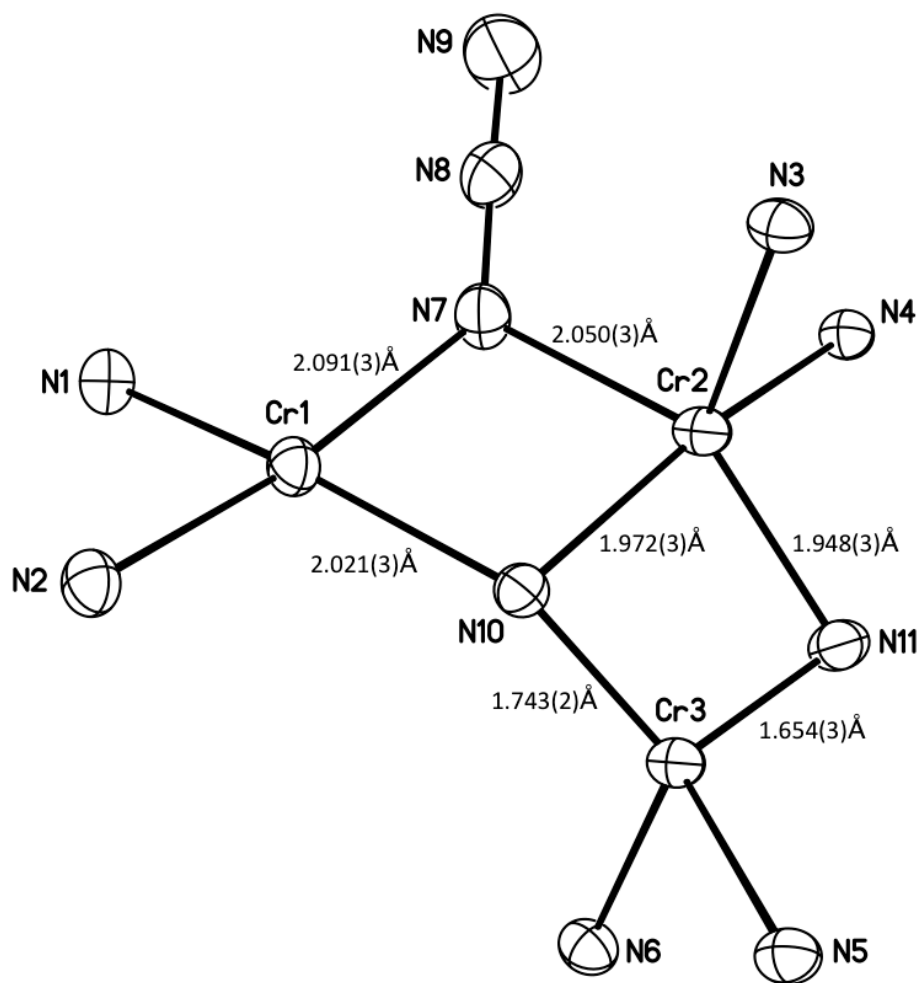
Figure 3.9   Structure of the molecular core of $(L^{Me}Cr)_3(\mu_3\text{-}N)(\mu_2\text{-}N)(\mu_2\text{-}N_3)$ (**31**). Ellipsoids are drawn at the 30% probability level.

Table 3.6   Interatomic distances (Å) and angles (°) for $(L^{Me}Cr)_3(\mu_3\text{-}N)(\mu_2\text{-}N)(\mu_2\text{-}N_3)$ (**31**)

<table>
<tr><td colspan="4" align="center">Distances (Å)</td></tr>
<tr><td>Cr(1)-N(10)</td><td>2.021(3)</td><td>C(16)-C(17)</td><td>1.371(6)</td></tr>
<tr><td>Cr(1)-N(2)</td><td>2.059(3)</td><td>C(17)-C(18)</td><td>1.398(5)</td></tr>
<tr><td>Cr(1)-N(1)</td><td>2.069(3)</td><td>C(18)-C(19)</td><td>1.410(5)</td></tr>
<tr><td>Cr(1)-N(7)</td><td>2.091(3)</td><td>C(18)-C(21)</td><td>1.502(5)</td></tr>
<tr><td>Cr(2)-N(11)</td><td>1.948(3)</td><td>C(22)-C(23)</td><td>1.392(6)</td></tr>
<tr><td>Cr(2)-N(10)</td><td>1.972(3)</td><td>C(22)-C(27)</td><td>1.406(5)</td></tr>
<tr><td>Cr(2)-N(3)</td><td>1.993(2)</td><td>C(22)-C(28)</td><td>1.489(6)</td></tr>
<tr><td>Cr(2)-N(7)</td><td>2.050(3)</td><td>C(23)-C(24)</td><td>1.372(7)</td></tr>
<tr><td>Cr(2)-N(4)</td><td>2.059(3)</td><td>C(24)-C(25)</td><td>1.367(7)</td></tr>
<tr><td>Cr(2)-Cr(3)</td><td>2.5637(7)</td><td>C(25)-C(26)</td><td>1.405(5)</td></tr>
<tr><td>Cr(3)-N(11)</td><td>1.654(3)</td><td>C(26)-C(27)</td><td>1.397(5)</td></tr>
<tr><td>Cr(3)-N(10)</td><td>1.743(2)</td><td>C(26)-C(29)</td><td>1.495(6)</td></tr>
<tr><td>Cr(3)-N(6)</td><td>1.984(3)</td><td>C(30)-C(31)</td><td>1.520(4)</td></tr>
<tr><td>Cr(3)-N(5)</td><td>1.997(3)</td><td>C(31)-C(32)</td><td>1.392(5)</td></tr>
<tr><td>N(1)-C(10)</td><td>1.340(4)</td><td>C(32)-C(33)</td><td>1.401(4)</td></tr>
<tr><td>N(1)-C(6)</td><td>1.442(4)</td><td>C(33)-C(34)</td><td>1.505(5)</td></tr>
<tr><td>N(2)-C(12)</td><td>1.335(4)</td><td>C(35)-C(36)</td><td>1.386(5)</td></tr>
<tr><td>N(2)-C(19)</td><td>1.445(4)</td><td>C(35)-C(40)</td><td>1.396(5)</td></tr>
<tr><td>N(3)-C(31)</td><td>1.339(4)</td><td>C(35)-C(41)</td><td>1.510(5)</td></tr>
<tr><td>N(3)-C(27)</td><td>1.438(4)</td><td>C(36)-C(37)</td><td>1.374(5)</td></tr>
<tr><td>N(4)-C(33)</td><td>1.323(4)</td><td>C(37)-C(38)</td><td>1.374(6)</td></tr>
<tr><td>N(4)-C(40)</td><td>1.454(4)</td><td>C(38)-C(39)</td><td>1.394(5)</td></tr>
<tr><td>N(5)-C(52)</td><td>1.329(4)</td><td>C(39)-C(40)</td><td>1.400(5)</td></tr>
<tr><td>N(5)-C(48)</td><td>1.449(4)</td><td>C(39)-C(42)</td><td>1.501(5)</td></tr>
<tr><td>N(6)-C(54)</td><td>1.336(4)</td><td>C(43)-C(48)</td><td>1.390(5)</td></tr>
<tr><td>N(6)-C(61)</td><td>1.442(4)</td><td>C(43)-C(44)</td><td>1.401(5)</td></tr>
<tr><td>N(7)-N(8)</td><td>1.251(4)</td><td>C(43)-C(49)</td><td>1.488(5)</td></tr>
<tr><td>N(8)-N(9)</td><td>1.132(4)</td><td>C(44)-C(45)</td><td>1.373(7)</td></tr>
<tr><td>C(1)-C(2)</td><td>1.394(6)</td><td>C(45)-C(46)</td><td>1.381(7)</td></tr>
<tr><td>C(1)-C(6)</td><td>1.410(5)</td><td>C(46)-C(47)</td><td>1.393(6)</td></tr>
<tr><td>C(1)-C(7)</td><td>1.500(6)</td><td>C(47)-C(48)</td><td>1.400(5)</td></tr>
<tr><td>C(2)-C(3)</td><td>1.372(6)</td><td>C(47)-C(50)</td><td>1.495(6)</td></tr>
<tr><td>C(3)-C(4)</td><td>1.378(6)</td><td>C(51)-C(52)</td><td>1.508(5)</td></tr>
</table>

C(4)-C(5)	1.395(5)	C(52)-C(53)	1.391(5)
C(5)-C(6)	1.397(5)	C(53)-C(54)	1.395(5)
C(5)-C(8)	1.505(5)	C(54)-C(55)	1.516(5)
C(9)-C(10)	1.511(5)	C(56)-C(57)	1.394(5)
C(10)-C(11)	1.388(5)	C(56)-C(61)	1.401(5)
C(11)-C(12)	1.396(5)	C(56)-C(62)	1.509(5)
C(12)-C(13)	1.517(5)	C(57)-C(58)	1.377(6)
C(14)-C(15)	1.385(5)	C(58)-C(59)	1.378(6)
C(14)-C(19)	1.400(5)	C(59)-C(60)	1.392(5)
C(14)-C(20)	1.500(5)	C(60)-C(61)	1.402(5)
C(15)-C(16)	1.375(6)	C(60)-C(63)	1.499(5)

Angles (°)

N(10)-Cr(1)-N(2)	103.15(11)	N(2)-C(12)-C(13)	120.3(3)
N(10)-Cr(1)-N(1)	159.48(11)	C(11)-C(12)-C(13)	116.3(3)
N(2)-Cr(1)-N(1)	89.06(11)	C(15)-C(14)-C(19)	118.8(3)
N(10)-Cr(1)-N(7)	77.90(10)	C(15)-C(14)-C(20)	120.1(4)
N(2)-Cr(1)-N(7)	166.98(11)	C(19)-C(14)-C(20)	121.0(3)
N(1)-Cr(1)-N(7)	93.93(11)	C(16)-C(15)-C(14)	121.4(4)
N(11)-Cr(2)-N(10)	82.94(11)	C(17)-C(16)-C(15)	119.5(4)
N(11)-Cr(2)-N(3)	120.18(12)	C(16)-C(17)-C(18)	122.1(4)
N(10)-Cr(2)-N(3)	112.75(10)	C(17)-C(18)-C(19)	117.4(4)
N(11)-Cr(2)-N(7)	144.28(12)	C(17)-C(18)-C(21)	120.8(3)
N(10)-Cr(2)-N(7)	80.00(11)	C(19)-C(18)-C(21)	121.7(3)
N(3)-Cr(2)-N(7)	95.38(11)	C(14)-C(19)-C(18)	120.8(3)
N(11)-Cr(2)-N(4)	89.15(10)	C(14)-C(19)-N(2)	121.3(3)
N(10)-Cr(2)-N(4)	157.32(10)	C(18)-C(19)-N(2)	117.9(3)
N(3)-Cr(2)-N(4)	89.61(10)	C(23)-C(22)-C(27)	117.7(4)
N(7)-Cr(2)-N(4)	94.68(11)	C(23)-C(22)-C(28)	120.4(4)
N(11)-Cr(2)-Cr(3)	40.19(8)	C(27)-C(22)-C(28)	121.9(3)
N(10)-Cr(2)-Cr(3)	42.75(7)	C(24)-C(23)-C(22)	121.5(4)
N(3)-Cr(2)-Cr(3)	126.86(8)	C(25)-C(24)-C(23)	120.1(4)
N(7)-Cr(2)-Cr(3)	116.08(8)	C(24)-C(25)-C(26)	121.3(4)
N(4)-Cr(2)-Cr(3)	126.00(7)	C(27)-C(26)-C(25)	117.7(4)
N(11)-Cr(3)-N(10)	99.64(12)	C(27)-C(26)-C(29)	120.6(3)
N(11)-Cr(3)-N(6)	115.91(12)	C(25)-C(26)-C(29)	121.7(4)

N(10)-Cr(3)-N(6)	114.65(12)	C(26)-C(27)-C(22)	121.5(3)
N(11)-Cr(3)-N(5)	107.40(12)	C(26)-C(27)-N(3)	118.6(3)
N(10)-Cr(3)-N(5)	129.35(11)	C(22)-C(27)-N(3)	119.7(3)
N(6)-Cr(3)-N(5)	90.88(11)	N(3)-C(31)-C(32)	123.8(3)
N(11)-Cr(3)-Cr(2)	49.45(9)	N(3)-C(31)-C(30)	119.4(3)
N(10)-Cr(3)-Cr(2)	50.19(8)	C(32)-C(31)-C(30)	116.8(3)
N(6)-Cr(3)-Cr(2)	131.01(8)	C(31)-C(32)-C(33)	127.5(3)
N(5)-Cr(3)-Cr(2)	136.60(8)	N(4)-C(33)-C(32)	123.0(3)
C(10)-N(1)-C(6)	115.2(3)	N(4)-C(33)-C(34)	121.0(3)
C(10)-N(1)-Cr(1)	123.8(2)	C(32)-C(33)-C(34)	116.0(3)
C(6)-N(1)-Cr(1)	120.8(2)	C(36)-C(35)-C(40)	118.4(3)
C(12)-N(2)-C(19)	115.0(3)	C(36)-C(35)-C(41)	120.9(3)
C(12)-N(2)-Cr(1)	124.4(2)	C(40)-C(35)-C(41)	120.8(3)
C(19)-N(2)-Cr(1)	120.4(2)	C(37)-C(36)-C(35)	121.4(4)
C(31)-N(3)-C(27)	115.7(3)	C(38)-C(37)-C(36)	120.0(3)
C(31)-N(3)-Cr(2)	125.2(2)	C(37)-C(38)-C(39)	120.8(4)
C(27)-N(3)-Cr(2)	119.1(2)	C(38)-C(39)-C(40)	118.5(3)
C(33)-N(4)-C(40)	115.7(3)	C(38)-C(39)-C(42)	119.7(3)
C(33)-N(4)-Cr(2)	124.3(2)	C(40)-C(39)-C(42)	121.9(3)
C(40)-N(4)-Cr(2)	119.97(19)	C(35)-C(40)-C(39)	120.9(3)
C(52)-N(5)-C(48)	115.6(3)	C(35)-C(40)-N(4)	119.2(3)
C(52)-N(5)-Cr(3)	125.4(2)	C(39)-C(40)-N(4)	119.9(3)
C(48)-N(5)-Cr(3)	118.9(2)	C(48)-C(43)-C(44)	117.5(4)
C(54)-N(6)-C(61)	116.7(3)	C(48)-C(43)-C(49)	120.7(3)
C(54)-N(6)-Cr(3)	124.9(2)	C(44)-C(43)-C(49)	121.8(4)
C(61)-N(6)-Cr(3)	118.4(2)	C(45)-C(44)-C(43)	121.3(4)
N(8)-N(7)-Cr(2)	120.3(2)	C(44)-C(45)-C(46)	119.9(4)
N(8)-N(7)-Cr(1)	137.1(2)	C(45)-C(46)-C(47)	121.1(4)
Cr(2)-N(7)-Cr(1)	98.30(12)	C(46)-C(47)-C(48)	117.7(4)
N(9)-N(8)-N(7)	177.6(5)	C(46)-C(47)-C(50)	121.3(4)
Cr(3)-N(10)-Cr(2)	87.05(11)	C(48)-C(47)-C(50)	121.0(3)
Cr(3)-N(10)-Cr(1)	151.82(15)	C(43)-C(48)-C(47)	122.3(3)
Cr(2)-N(10)-Cr(1)	103.32(11)	C(43)-C(48)-N(5)	119.5(3)
Cr(3)-N(11)-Cr(2)	90.37(12)	C(47)-C(48)-N(5)	118.0(3)
C(67)-O(1)-C(65)	114.3(5)	N(5)-C(52)-C(53)	123.3(3)
C(2)-C(1)-C(6)	118.2(4)	N(5)-C(52)-C(51)	120.1(3)
C(2)-C(1)-C(7)	121.3(4)	C(53)-C(52)-C(51)	116.6(3)

C(6)-C(1)-C(7)	120.5(4)	C(52)-C(53)-C(54)	126.7(3)
C(3)-C(2)-C(1)	121.5(4)	N(6)-C(54)-C(53)	123.9(3)
C(2)-C(3)-C(4)	119.5(4)	N(6)-C(54)-C(55)	119.9(3)
C(3)-C(4)-C(5)	121.7(4)	C(53)-C(54)-C(55)	116.0(3)
C(4)-C(5)-C(6)	118.1(4)	C(57)-C(56)-C(61)	118.1(4)
C(4)-C(5)-C(8)	120.7(4)	C(57)-C(56)-C(62)	119.9(4)
C(6)-C(5)-C(8)	121.2(4)	C(61)-C(56)-C(62)	121.9(3)
C(5)-C(6)-C(1)	121.0(4)	C(58)-C(57)-C(56)	120.7(4)
C(5)-C(6)-N(1)	119.6(3)	C(57)-C(58)-C(59)	120.6(4)
C(1)-C(6)-N(1)	119.4(3)	C(58)-C(59)-C(60)	121.0(4)
N(1)-C(10)-C(11)	123.7(3)	C(59)-C(60)-C(61)	117.9(4)
N(1)-C(10)-C(9)	120.2(3)	C(56)-C(61)-C(60)	121.7(3)
C(11)-C(10)-C(9)	115.9(3)	C(56)-C(61)-N(6)	119.7(3)
C(10)-C(11)-C(12)	128.4(3)	C(60)-C(61)-N(6)	118.6(3)
N(2)-C(12)-C(11)	123.4(3)		

Irradiation of $(L^{Et}Cr)_4(\mu\text{-}N_3)_4$ (**27**) ultimately led to the side-on bridged dinitrogen complex, with an intermediate postulated to be the corresponding bis(μ-nitrido) complex **32**. Monitoring of the reaction by ^{1}H NMR spectroscopy is depicted in Figure 3.10. ^{1}H NMR spectroscopy clearly showed some characteristic features, i. e., a broad peak at 60 ppm, which is associated with dinitrogen complex $(L^{Et}Cr)_2(\mu_2\text{-}\eta^2{:}\eta^2\text{-}N_2)$ (**33**). **33** can be independently synthesized by KC_8 reduction of $(L^{Et}Cr)_2(\mu\text{-}I)_2$; full characterization of **33** has been carried out and is included in the Experimental section. These results are in line with the results of the photolysis of $(L^{iPr}Cr)_2(\mu\text{-}N_3)_2$ (**24**). In both cases, the bis(μ-nitrido) and $(\mu_2\text{-}\eta^2{:}\eta^2\text{-}N_2)$ complexes were found, with the latter also being accessible by chemical reduction of a Cr(II) precursor.

27, Ar = 2,6-diethylphenyl   **32**   **33**
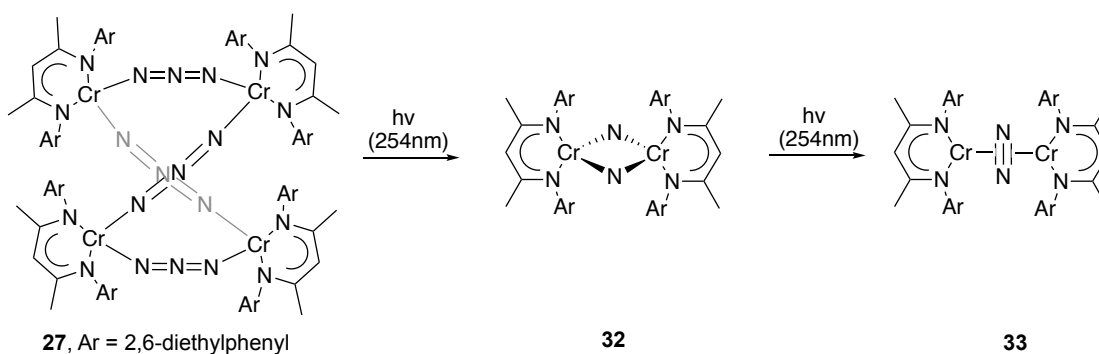
Scheme 3.16   Products formed by the irradiation of **27**
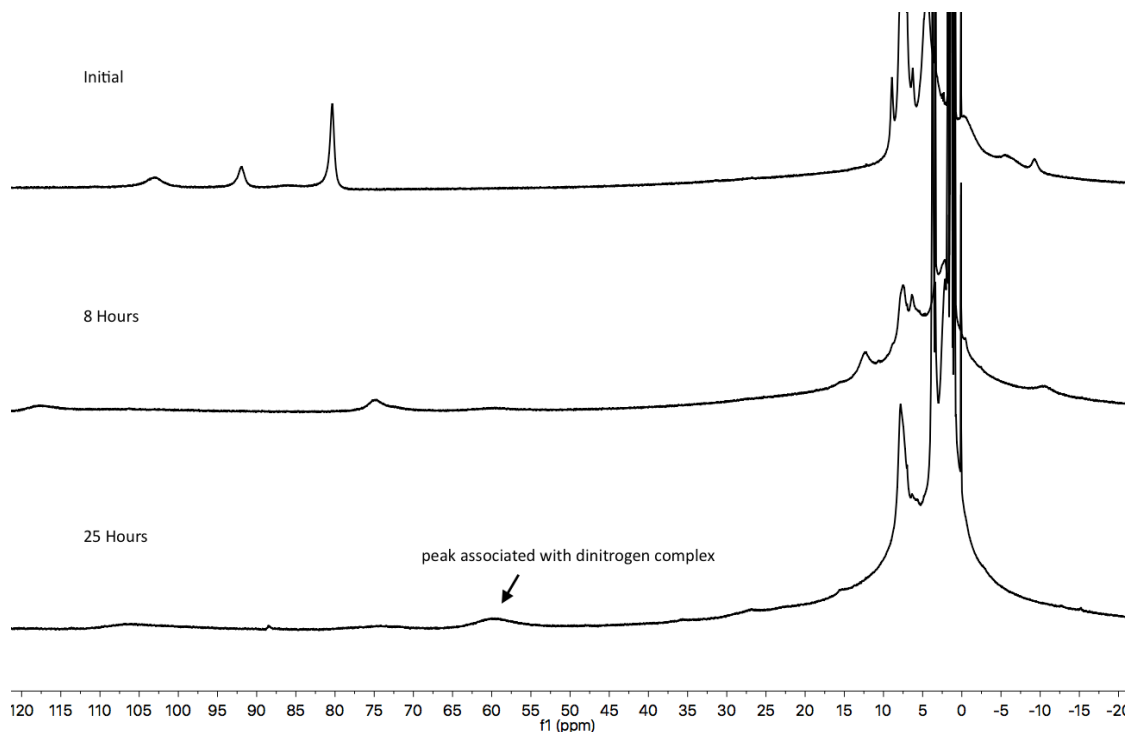
Figure 3.10 ^{1}H NMR spectra during the photolysis of **27** in C$_6$D$_{12}$, with a resonance of the dinitrogen complex identified

The structure of dinuclear nitride **32** was determined using crystals obtained after irradiation of a cyclohexane solution of **27** for 9 hours. Upon removal of solvent, **32** was recrystallized from a chilled pentane solution. The molecular structure of **32** is depicted in Figure 3.11, while the interatomic bond distances and angles are listed in Table 3.7. **32** crystallizes in the monoclinic space group *P2$_1$/n* with an inversion center located between the chromium atoms. The bridging atoms, however, were disordered over two sets of positions. The chromium centers have tetrahedral and square planar geometries to the two sets of coordinating ligands. Since the geometry of chromiums of centrosymmetric bis(μ-nitrido) (such as **30**) is tetrahedral, and the fact that the molecular ions isotope patterns in the LIFDI mass spectrum potentially correspond to

$(L^{Et}Cr)_2(\mu\text{-}N)_2$ (**32**), $(L^{Et}Cr)_2(\mu\text{-}O)_2$ and $(L^{Et}Cr)_2(\mu\text{-}OH)_2$, the disordered bridging atoms were modeled as nitrogen and oxygen atoms. The refined occupancy ratio for structure **32** is 1:1.05. Repeating the X-ray diffraction experiments on another photolytically synthesized and crystallized samples gave similarly disordered result, differing only in the occupancy ratio.[24] The appearance of oxygen in the crystallographic structure was potentially due to a reaction of **32** with adventitious dioxygen while working up the reaction.

Although the bonding information may not be entirely accurate for the disordered structure, its structural analysis is still discussed. The distance of $Cr\text{-}N_{nitride}$ (1.89(4) Å) is relatively long when compared with that in bis(μ-nitrido) **30**, in which a distance of 1.79(1) Å was observed. The centrosymmetric bis(μ-oxo) in disordered **32** is inconsistent with the reported bis(μ-oxo) complex, $(L^{iPr}Cr)_2(\mu\text{-}O)_2$. The latter bis($\mu$-oxo) has a geometrically asymmetric core with tetrahedral and square planar geometries of metal centers. If $(L^{Et}Cr)_2(\mu\text{-}OH)_2$ was considered instead of $(L^{iPr}Cr)_2(\mu\text{-}O)_2$, it might satisfy the observed centrosymmetric structure **32**. The sample was then inspected by infrared spectroscopy. However, a stretching frequency of 3750 cm^{-1} was absent for characterizing the hydroxyl group. With the combination of all of these data, the assignment for the disordered structure **32** still remains unclear.

Figure 3.11 Molecular structure of disordered $(L^{Et}Cr)_2(\mu\text{-}N)_2$ (**32**). Ellipsoids are drawn at the 30% probability level. Hydrogen atoms have been omitted for clarity.
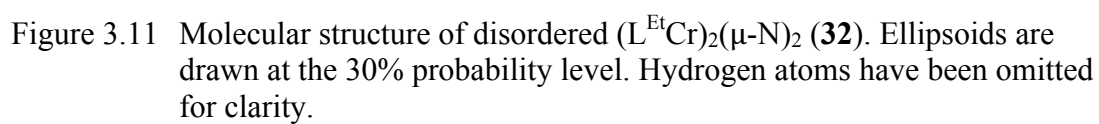
Table 3.7   Interatomic distances (Å) and angles (°) for (L^{Et}Cr)$_2$(μ-N)$_2$ (**32**)

Distances (Å)

Cr(1)-O(1)	1.849(5)	C(5)-C(6)	1.392(5)
Cr(1)-N(3)	1.862(6)	C(5)-C(9)	1.504(5)
Cr(1)-O(1)A	1.886(5)	C(7)-C(8)	1.511(5)
Cr(1)-N(3)A	1.913(6)	C(9)-C(10)	1.460(7)
Cr(1)-N(1)	2.014(3)	C(11)-C(12)	1.504(5)
Cr(1)-N(2)	2.017(3)	C(12)-C(13)	1.394(5)
Cr(1)-Cr(1)A	2.8101(13)	C(13)-C(14)	1.392(5)
N(1)-C(12)	1.335(5)	C(14)-C(15)	1.508(5)
N(1)-C(6)	1.440(4)	C(16)-C(21)	1.373(6)
N(2)-C(14)	1.328(5)	C(16)-C(17)	1.397(6)
N(2)-C(21)	1.447(4)	C(16)-C(22)	1.554(7)
O(1)-Cr(1)A	1.886(5)	C(17)-C(18)	1.354(6)
N(3)-Cr(1)A	1.913(6)	C(18)-C(19)	1.372(6)
C(1)-C(2)	1.389(4)	C(19)-C(20)	1.391(5)
C(1)-C(6)	1.402(5)	C(20)-C(21)	1.398(5)
C(1)-C(7)	1.518(5)	C(20)-C(24)	1.497(6)
C(2)-C(3)	1.377(5)	C(22)-C(23)	1.438(8)
C(3)-C(4)	1.352(5)	C(24)-C(25)	1.485(6)
C(4)-C(5)	1.400(5)		

Angles (°)

O(1)-Cr(1)-O(1)A	82.4(2)	C(3)-C(4)-C(5)	121.8(3)
N(3)-Cr(1)-N(3)A	83.8(3)	C(6)-C(5)-C(4)	117.8(3)
O(1)-Cr(1)-N(1)	174.84(16)	C(6)-C(5)-C(9)	122.2(3)
N(3)-Cr(1)-N(1)	121.81(19)	C(4)-C(5)-C(9)	120.0(3)
O(1)A-Cr(1)-N(1)	92.54(16)	C(5)-C(6)-C(1)	121.2(3)
N(3)A-Cr(1)-N(1)	119.56(18)	C(5)-C(6)-N(1)	119.3(3)
O(1)-Cr(1)-N(2)	94.64(17)	C(1)-C(6)-N(1)	119.4(3)
N(3)-Cr(1)-N(2)	122.11(19)	C(8)-C(7)-C(1)	115.9(3)
O(1)A-Cr(1)-N(2)	176.97(17)	C(10)-C(9)-C(5)	113.0(4)
N(3)A-Cr(1)-N(2)	123.1(2)	N(1)-C(12)-C(13)	122.5(3)
N(1)-Cr(1)-N(2)	90.39(12)	N(1)-C(12)-C(11)	120.4(3)
O(1)-Cr(1)-Cr(1)A	41.71(14)	C(13)-C(12)-C(11)	117.0(4)

N(3)-Cr(1)-Cr(1)A	42.59(19)	C(14)-C(13)-C(12)	128.8(4)
O(1)A-Cr(1)-Cr(1)A	40.71(14)	N(2)-C(14)-C(13)	123.4(3)
N(3)A-Cr(1)-Cr(1)A	41.19(19)	N(2)-C(14)-C(15)	120.3(3)
N(1)-Cr(1)-Cr(1)A	133.24(9)	C(13)-C(14)-C(15)	116.2(4)
N(2)-Cr(1)-Cr(1)A	136.34(9)	C(21)-C(16)-C(17)	119.5(4)
C(12)-N(1)-C(6)	116.0(3)	C(21)-C(16)-C(22)	121.2(4)
C(12)-N(1)-Cr(1)	126.9(2)	C(17)-C(16)-C(22)	119.2(4)
C(6)-N(1)-Cr(1)	117.0(2)	C(18)-C(17)-C(16)	120.5(4)
C(14)-N(2)-C(21)	115.6(3)	C(17)-C(18)-C(19)	119.8(4)
C(14)-N(2)-Cr(1)	126.4(2)	C(18)-C(19)-C(20)	121.7(4)
C(21)-N(2)-Cr(1)	118.0(3)	C(19)-C(20)-C(21)	117.6(4)
Cr(1)-O(1)-Cr(1)A	97.6(2)	C(19)-C(20)-C(24)	122.2(4)
Cr(1)-N(3)-Cr(1)A	96.2(3)	C(21)-C(20)-C(24)	120.1(3)
C(2)-C(1)-C(6)	118.0(3)	C(16)-C(21)-C(20)	120.7(3)
C(2)-C(1)-C(7)	122.5(3)	C(16)-C(21)-N(2)	119.3(3)
C(6)-C(1)-C(7)	119.5(3)	C(20)-C(21)-N(2)	120.0(3)
C(3)-C(2)-C(1)	121.3(3)	C(23)-C(22)-C(16)	114.2(5)
C(4)-C(3)-C(2)	119.9(3)	C(25)-C(24)-C(20)	117.5(4)

A dinitrogen complex supported by L^{Et} can be independently synthesized via KC$_8$ reduction of $(L^{Et}Cr)_2(\mu\text{-}I)_2$ in the presence of N$_2$ in THF/Et$_2$O. Upon removal of solvent and extraction with pentane the solution was concentrated to yield the side-on bridged dinitrogen complex $(L^{Et}Cr)_2(\mu_2\text{-}\eta^2:\eta^2\text{-}N_2)$ (**33**) in 19% crystalline yield.

Ar = 2,6-diethylphenyl

33
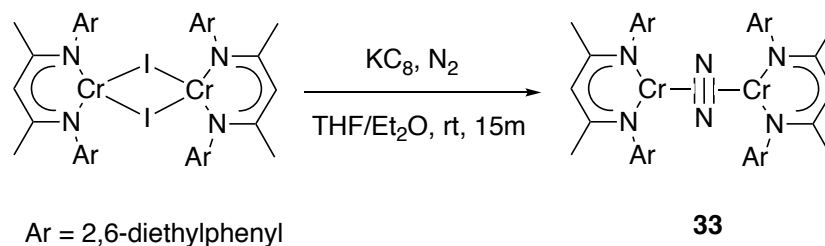
Scheme 3.17   Synthesis of $(L^{Et}Cr)_2(\mu_2\text{-}\eta^2:\eta^2\text{-}N_2)$ (**33**)

33 possesses similar features as the previously reported $(L^{iPr}Cr)_2(\mu_2\text{-}\eta^2:\eta^2\text{-}N_2)$ (**23**).[1] The former complex crystallizes in the triclinic space group $P\bar{1}$ with an inversion center located between the chromium centers. The dinitrogen fragment is bound equally between two chromium centers with a Cr-N3 distance of 2.0122(14) Å, compared to 2.0209(9) Å in **23**. The dinitrogen N-N distance was determined to be 1.244(3) Å, which is comparable to 1.249(5) Å in **23**; this long distance is indicative of partial reduction of the N$_2$ unit. The Cr-Cr separation in **33** was measured to be 3.8273(6) Å, compared to 3.844(3) Å in **23**. Due to the inversion center of **33**, the N-N stretch is IR inactive. Besides the similar structural parameters, **33** has a room temperature magnetic moment of 4.2 μ_B, which is slightly higher but comparable to the reported 3.9 μ_B in **23**.
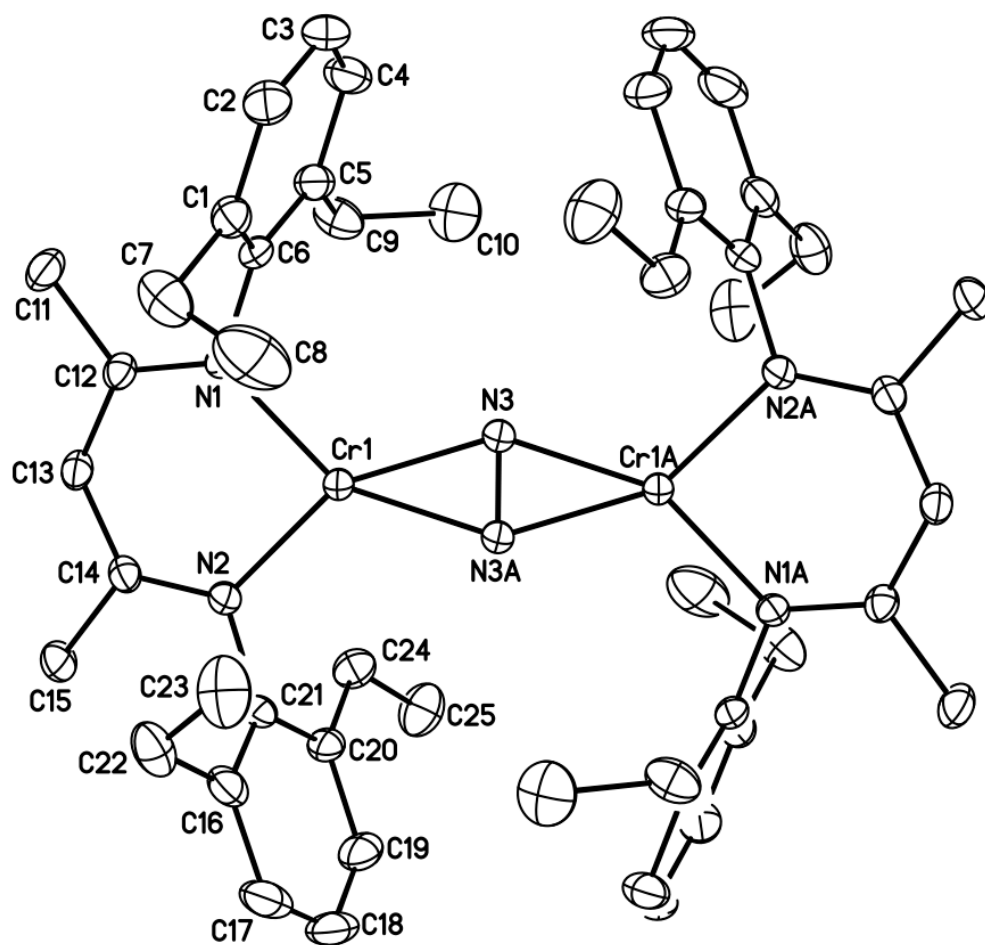
Figure 3.12   Molecular structure of $(L^{Et}Cr)_2(\mu_2\text{-}\eta^2\text{:}\eta^2\text{-}N_2)$ (**33**). Ellipsoids are drawn at the 30% probability level. Hydrogen atoms have been omitted for clarity.

Table 3.8   Interatomic distances (Å) and angles (°) for $(L^{Et}Cr)_2(\mu_2\text{-}\eta^2{:}\eta^2\text{-}N_2)$ (**33**)

Distances (Å)

Cr(1)-N(3)A	2.0120(15)	C(5)-C(9)	1.509(3)
Cr(1)-N(3)	2.0122(14)	C(7)-C(8)	1.509(4)
Cr(1)-N(1)	2.0181(14)	C(9)-C(10)	1.512(3)
Cr(1)-N(2)	2.0228(14)	C(11)-C(12)	1.510(2)
N(1)-C(12)	1.324(2)	C(12)-C(13)	1.406(2)
N(1)-C(6)	1.443(2)	C(13)-C(14)	1.397(2)
N(2)-C(14)	1.329(2)	C(14)-C(15)	1.513(2)
N(2)-C(21)	1.436(2)	C(16)-C(21)	1.399(3)
N(3)-N(3)A	1.244(3)	C(16)-C(17)	1.402(3)
N(3)-Cr(1)A	2.0121(14)	C(16)-C(22)	1.504(3)
C(1)-C(2)	1.392(3)	C(17)-C(18)	1.369(4)
C(1)-C(6)	1.400(2)	C(18)-C(19)	1.369(4)
C(1)-C(7)	1.512(3)	C(19)-C(20)	1.394(3)
C(2)-C(3)	1.372(3)	C(20)-C(21)	1.402(3)
C(3)-C(4)	1.376(3)	C(20)-C(24)	1.501(3)
C(4)-C(5)	1.394(3)	C(22)-C(23)	1.513(3)
C(5)-C(6)	1.399(2)	C(24)-C(25)	1.514(3)

Angles (°)

N(3)A-Cr(1)-N(3)	36.00(8)	C(5)-C(6)-N(1)	119.52(15)
N(3)A-Cr(1)-N(1)	152.06(6)	C(1)-C(6)-N(1)	119.58(15)
N(3)-Cr(1)-N(1)	116.26(6)	C(8)-C(7)-C(1)	112.1(2)
N(3)A-Cr(1)-N(2)	115.49(6)	C(5)-C(9)-C(10)	113.25(19)
N(3)-Cr(1)-N(2)	151.37(6)	N(1)-C(12)-C(13)	123.73(15)
N(1)-Cr(1)-N(2)	91.91(6)	N(1)-C(12)-C(11)	119.87(16)
C(12)-N(1)-C(6)	118.00(14)	C(13)-C(12)-C(11)	116.40(15)
C(12)-N(1)-Cr(1)	125.19(11)	C(14)-C(13)-C(12)	128.73(16)
C(6)-N(1)-Cr(1)	116.63(10)	N(2)-C(14)-C(13)	123.85(15)
C(14)-N(2)-C(21)	118.82(14)	N(2)-C(14)-C(15)	119.53(15)
C(14)-N(2)-Cr(1)	124.81(11)	C(13)-C(14)-C(15)	116.61(15)
C(21)-N(2)-Cr(1)	116.35(10)	C(21)-C(16)-C(17)	117.8(2)
N(3)A-N(3)-Cr(1)A	72.01(12)	C(21)-C(16)-C(22)	121.86(19)
N(3)A-N(3)-Cr(1)	71.99(12)	C(17)-C(16)-C(22)	120.3(2)

Cr(1)A-N(3)-Cr(1)	144.00(8)	C(18)-C(17)-C(16)	121.3(2)
C(2)-C(1)-C(6)	118.44(17)	C(17)-C(18)-C(19)	120.1(2)
C(2)-C(1)-C(7)	119.59(18)	C(18)-C(19)-C(20)	121.4(2)
C(6)-C(1)-C(7)	121.97(17)	C(19)-C(20)-C(21)	118.04(19)
C(3)-C(2)-C(1)	121.26(19)	C(19)-C(20)-C(24)	121.78(19)
C(2)-C(3)-C(4)	119.85(18)	C(21)-C(20)-C(24)	120.17(16)
C(3)-C(4)-C(5)	121.21(19)	C(16)-C(21)-C(20)	121.28(17)
C(4)-C(5)-C(6)	118.33(17)	C(16)-C(21)-N(2)	119.27(17)
C(4)-C(5)-C(9)	119.64(18)	C(20)-C(21)-N(2)	119.40(16)
C(6)-C(5)-C(9)	122.02(16)	C(16)-C(22)-C(23)	113.64(18)
C(5)-C(6)-C(1)	120.89(16)	C(20)-C(24)-C(25)	116.6(2)

Moving on to bulkier ligands, 24 hours of irradiation of $(*L^{iPr}Cr)_2(\mu\text{-}N_3)_2$ (**28**) in THF led to the formation of bis(μ-nitrido) complex $(*L^{iPr}Cr)_2(\mu\text{-}N)_2$ (**34**), which was isolated in 35% crystalline yield.

28, Ar = 2,6-diisopropylphenyl   **34**
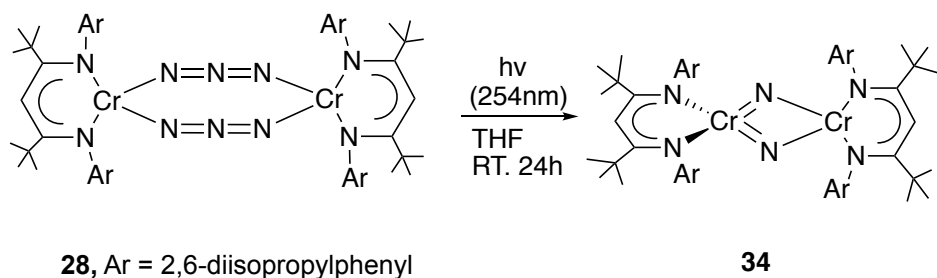
Scheme 3.18   Irradiation of **28** led to the formation of bis(μ-nitrido) complex

34 crystallizes in the monoclinic space group *C2/c*. The molecular structure is depicted in Figure 3.13. The molecular core contains two chromium atoms bridged by two nitrido ligands. The bridging nitrogen atoms were disordered over two sets of positions, with equal occupancy, shown in Figure 3.14. The N3 and N4 bridging ligands showed tetrahedral geometry around Cr1 and square planar about Cr1A. N3A and N4A were generated by crystallographic two-fold symmetry. The disordered set of bridging ligands displayed square planar with Cr1 and tetrahedral with Cr1A.

The two β-diketiminate ligand planes are essentially perpendicular to each other. The dihedral angle of the two ligand planes defined by N1, N2, Cr1 and N1A, N2A, Cr1A is 86.3°. The distances of the two bridging nitrogen atoms to Cr1 (1.627(7) Å and 1.580(8) Å) are noticeably shorter than those to Cr2 (2.124(7) Å and 2.074(8) Å). **34** is therefore described as a mixed-valent compound, like **25** $(L^{iPr}Cr)_2(\mu\text{-}N)_2$ (see p.159). The candidates for chromium formal oxidation states in **34**

are Cr(VI)-Cr(II) and Cr(V)-Cr(III). The effective magnetic moment for the former assignment (S = 0, S = $\frac{4}{2}$) is expected to be 4.8μ_B. The magnetic moment for the independent, i. e., magnetically non-interacting, Cr(V)-Cr(III) (S = $\frac{1}{2}$, S = $\frac{3}{2}$) is expected to be 4.2μ_B. A room temperature magnetic moment of **34** taken in solid state was measured to be 4.2(1) μ_B per dimer, suggested non-interacting Cr(V)-Cr(III) ions. It might, however, be unexpected for the two chromium centers to be magnetically independent under these circumstances, i. e., bridging nitride ligands.

F. Dai has previously reported a related asymmetrical structure, (L^{iPr}Cr)$_2$(μ-O)$_2$.[2] Its coordination geometries are pseudotetrahedral and square planar. The bridging oxygen atoms have significantly shorter bonds to one of the chromiums than the other. With a room temperature effective magnetic moment of 3.9(1) μ_B per dimer, it is suggested that mixed-valent complex (L^{iPr}Cr)$_2$(μ-O)$_2$ is antiferromagnetically coupled between two ions with S = $\frac{2}{2}$ (Cr^{IV}, d^2) and S = $\frac{4}{2}$ (Cr^{II}, high-spin d^4) ground states. [{(iPr$_2$N)$_2$Cr(μ-N)}$_2$] reported by C. Cummins et. al. was described that the two bridging nitrides mediate antiferromagnetic coupling of chromium centers, with a moment of 1.8 μ_B.[25]

With structure **34**, the assumption that steric hindrance interactions of the nacnac ligand affects the geometry of the bis(μ-nitrido) complex is more convincing by relating all the complexes, as shown in Scheme 3.19. The bis(μ-nitrido) **30**, with a less sterically-bulky ligand (L^{Me}), is centrosymmetric. This results in tetrahedral geometry around both chromium atoms. For **25** and **34**, the bulky isopropyl substituents break the symmetry, which give rise to a geometrically asymmetric core with tetrahedral and square planar geometries of metal centers. Ideally, the effect of the ligand bulk of **32** would provide an intermediary complex for comparison.

Unfortunately, the disordered bis(μ-nitrido) structure **32** failed to elucidate the

potential transformation.

| **30** | **32** | **25** | **34** |
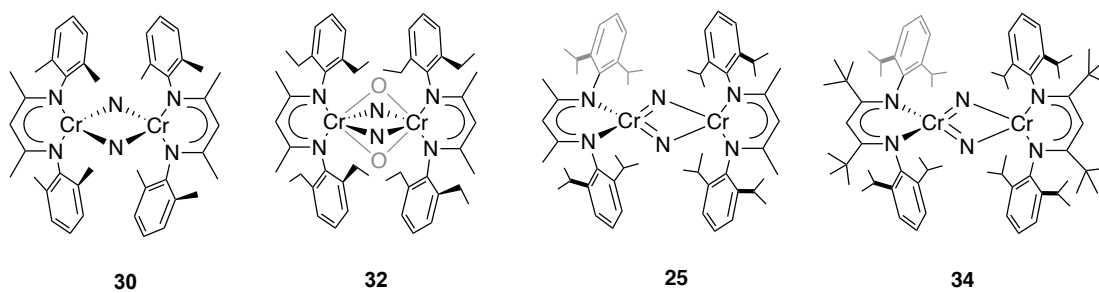
Scheme 3.19   Bis(μ-nitrido) complexes supported by various nacnac ligands. The
authenticity of structure **32** remains questionable.
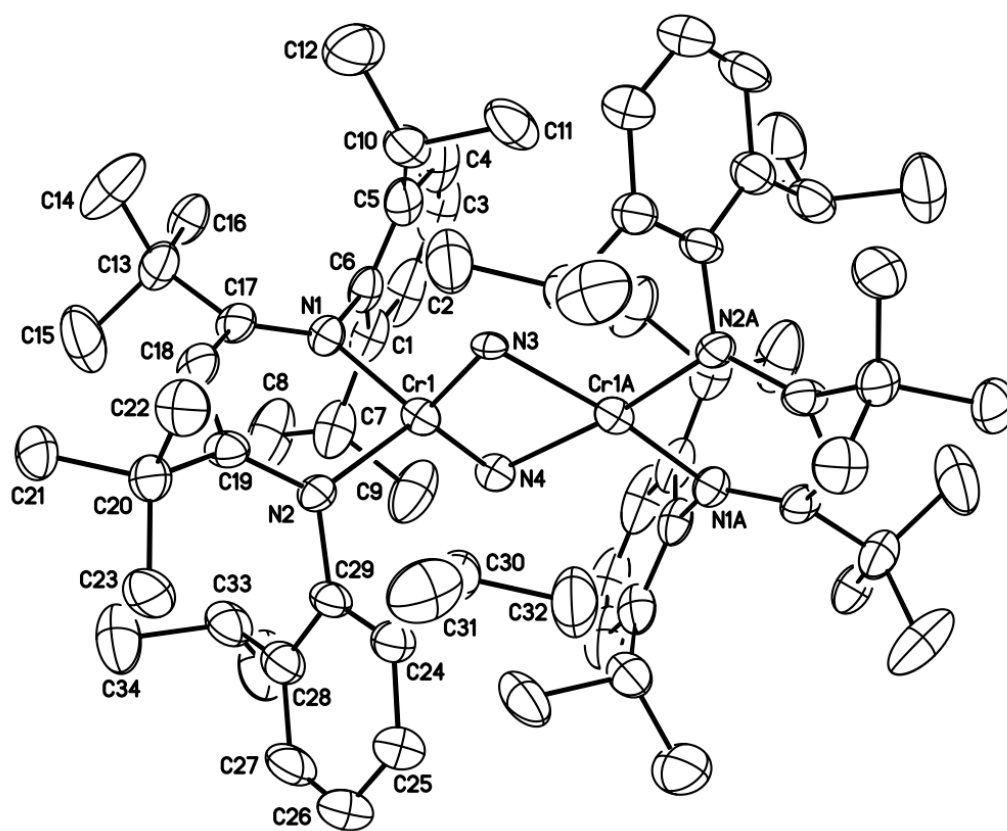
Figure 3.13   Molecular structure of (*L^{iPr}Cr)$_2$(μ-N)$_2$ (**34**). Ellipsoids are drawn at the 30% probability level. Hydrogen atoms have been omitted for clarity.
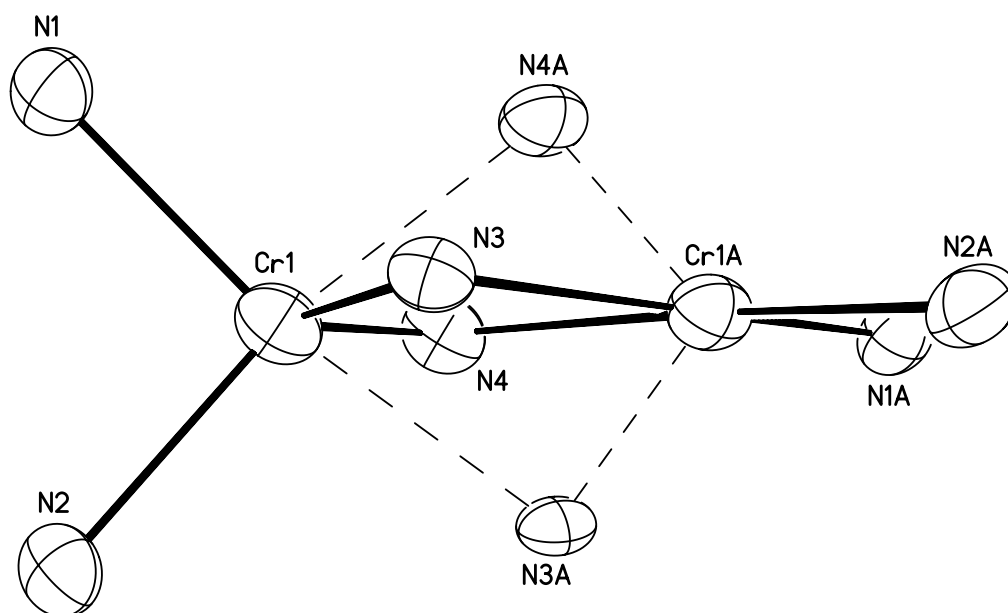
Figure 3.14 Structure of the molecular core of $(*\text{L}^{i\text{Pr}}\text{Cr})_2(\mu\text{-N})_2$ (**34**) with two sets of nitrido ligands positions. Ellipsoids are drawn at the 30% probability level.

Table 3.9   Interatomic distances (Å) and angles (°) for (*L^{iPr}Cr)$_2$(μ-N)$_2$ (**34**)

Distances (Å)

Cr(1)-N(4)	1.580(8)	C(7)-C(8)	1.539(9)
Cr(1)-N(3)	1.627(7)	C(10)-C(11)	1.538(9)
Cr(1)-N(2)	2.004(4)	C(10)-C(12)	1.539(10)
Cr(1)-N(1)	2.023(4)	C(13)-C(16)	1.529(9)
Cr(1)-N(4)A	2.074(8)	C(13)-C(14)	1.538(10)
Cr(1)-N(3)A	2.124(7)	C(13)-C(15)	1.553(10)
Cr(1)-Cr(1)A	2.6640(16)	C(13)-C(17)	1.577(8)
N(1)-C(17)	1.328(6)	C(17)-C(18)	1.431(7)
N(1)-C(6)	1.449(6)	C(18)-C(19)	1.377(7)
N(2)-C(19)	1.355(6)	C(19)-C(20)	1.569(7)
N(2)-C(29)	1.446(7)	C(20)-C(21)	1.534(8)
N(3)-N(4)A	1.838(10)	C(20)-C(23)	1.537(8)
N(3)-Cr(1)A	2.124(7)	C(20)-C(22)	1.538(8)
N(4)-N(3)A	1.838(10)	C(24)-C(25)	1.381(8)
N(4)-N(4)A	1.841(16)	C(24)-C(29)	1.401(8)
N(4)-Cr(1)A	2.074(8)	C(24)-C(30)	1.514(9)
C(1)-C(2)	1.377(10)	C(25)-C(26)	1.380(10)
C(1)-C(6)	1.398(9)	C(26)-C(27)	1.369(11)
C(1)-C(7)	1.505(10)	C(27)-C(28)	1.387(9)
C(2)-C(3)	1.400(13)	C(28)-C(29)	1.418(8)
C(3)-C(4)	1.369(13)	C(28)-C(33)	1.519(10)
C(4)-C(5)	1.406(9)	C(30)-C(31)	1.534(11)
C(5)-C(6)	1.395(9)	C(30)-C(32)	1.543(11)
C(5)-C(10)	1.508(10)	C(33)-C(35)	1.523(10)
C(7)-C(9)	1.533(10)	C(33)-C(34)	1.542(10)

Angles (°)

N(4)-Cr(1)-N(3)	103.7(4)	C(5)-C(6)-N(1)	117.8(5)
N(4)-Cr(1)-N(2)	119.0(3)	C(1)-C(6)-N(1)	119.4(6)
N(3)-Cr(1)-N(2)	114.2(3)	C(1)-C(7)-C(9)	109.1(6)
N(4)-Cr(1)-N(1)	116.2(3)	C(1)-C(7)-C(8)	113.4(7)
N(3)-Cr(1)-N(1)	109.1(3)	C(9)-C(7)-C(8)	109.8(6)
N(2)-Cr(1)-N(1)	94.76(17)	C(5)-C(10)-C(11)	111.4(7)

N(4)-Cr(1)-N(4)A	58.7(5)	C(5)-C(10)-C(12)	113.6(6)
N(3)-Cr(1)-N(4)A	58.1(3)	C(11)-C(10)-C(12)	107.3(6)
N(2)-Cr(1)-N(4)A	168.0(2)	C(16)-C(13)-C(14)	106.3(6)
N(1)-Cr(1)-N(4)A	96.6(2)	C(16)-C(13)-C(15)	106.2(6)
N(4)-Cr(1)-N(3)A	57.3(3)	C(14)-C(13)-C(15)	110.2(7)
N(3)-Cr(1)-N(3)A	67.9(4)	C(16)-C(13)-C(17)	119.5(5)
N(2)-Cr(1)-N(3)A	94.9(2)	C(14)-C(13)-C(17)	109.3(6)
N(1)-Cr(1)-N(3)A	170.2(2)	C(15)-C(13)-C(17)	105.3(6)
N(4)A-Cr(1)-N(3)A	73.8(3)	N(1)-C(17)-C(18)	120.3(5)
N(4)-Cr(1)-Cr(1)A	51.1(3)	N(1)-C(17)-C(13)	126.6(5)
N(3)-Cr(1)-Cr(1)A	52.9(2)	C(18)-C(17)-C(13)	113.1(5)
N(2)-Cr(1)-Cr(1)A	132.05(13)	C(19)-C(18)-C(17)	132.3(5)
N(1)-Cr(1)-Cr(1)A	132.92(12)	N(2)-C(19)-C(18)	121.6(5)
N(4)A-Cr(1)-Cr(1)A	36.3(2)	N(2)-C(19)-C(20)	125.0(5)
N(3)A-Cr(1)-Cr(1)A	37.63(19)	C(18)-C(19)-C(20)	112.9(5)
C(17)-N(1)-C(6)	122.5(4)	C(21)-C(20)-C(23)	105.4(5)
C(17)-N(1)-Cr(1)	121.8(4)	C(21)-C(20)-C(22)	107.8(5)
C(6)-N(1)-Cr(1)	115.6(3)	C(23)-C(20)-C(22)	107.4(5)
C(19)-N(2)-C(29)	120.5(4)	C(21)-C(20)-C(19)	113.0(5)
C(19)-N(2)-Cr(1)	119.5(3)	C(23)-C(20)-C(19)	117.8(5)
C(29)-N(2)-Cr(1)	119.6(3)	C(22)-C(20)-C(19)	105.0(4)
Cr(1)-N(3)-N(4)A	73.3(4)	C(25)-C(24)-C(29)	119.1(6)
Cr(1)-N(3)-Cr(1)A	89.5(3)	C(25)-C(24)-C(30)	117.7(6)
N(4)A-N(3)-Cr(1)A	46.3(3)	C(29)-C(24)-C(30)	123.1(5)
Cr(1)-N(4)-N(3)A	76.4(4)	C(26)-C(25)-C(24)	121.9(7)
Cr(1)-N(4)-N(4)A	74.2(4)	C(27)-C(26)-C(25)	118.8(7)
N(3)A-N(4)-N(4)A	86.5(4)	C(26)-C(27)-C(28)	122.1(7)
Cr(1)-N(4)-Cr(1)A	92.6(3)	C(27)-C(28)-C(29)	118.4(6)
N(3)A-N(4)-Cr(1)A	48.7(3)	C(27)-C(28)-C(33)	119.0(6)
N(4)A-N(4)-Cr(1)A	47.1(3)	C(29)-C(28)-C(33)	122.5(6)
C(2)-C(1)-C(6)	117.6(8)	C(24)-C(29)-C(28)	119.4(5)
C(2)-C(1)-C(7)	119.7(7)	C(24)-C(29)-N(2)	123.2(5)
C(6)-C(1)-C(7)	122.6(6)	C(28)-C(29)-N(2)	117.4(5)
C(1)-C(2)-C(3)	121.3(8)	C(24)-C(30)-C(31)	113.0(6)
C(4)-C(3)-C(2)	119.8(7)	C(24)-C(30)-C(32)	110.3(6)
C(3)-C(4)-C(5)	121.1(9)	C(31)-C(30)-C(32)	108.5(8)
C(6)-C(5)-C(4)	117.3(7)	C(28)-C(33)-C(35)	112.4(6)

C(6)-C(5)-C(10)	123.6(5)	C(28)-C(33)-C(34)	113.2(6)
C(4)-C(5)-C(10)	119.1(7)	C(35)-C(33)-C(34)	109.0(6)
C(5)-C(6)-C(1)	122.6(6)		

Even prolonged exposure of complex **34** to UV light (1 day) did not form the corresponding dinitrogen complex, $(*L^{iPr}Cr)_2(\mu_2\text{-}\eta^2\text{:}\eta^2\text{-}N_2)$. This result was unexpected, in view of the facile conversion of **25** to **23**. It is noted that a decomposition product of **34** was isolated after 24 hours of irradiation, namely $(*L^{iPr}Cr)(\mu\text{-}NAr)(\mu\text{-}NC(^tBu)CH(^tBu)CNAr)(\mu_3\text{-}Cr)$ (Ar = 2,6-diisopropylphenyl) (**35**), which was obtained in 48% yield. **35** is a binuclear complex consisting of one $*L^{iPr}Cr$ fragment, one activated nacnac ligand fragment, and a bridging aryl imido fragment between two chromium centers. The mechanism of formation of **35** from **34** is not clear and has to proceed with the loss of a nitrogen atom. A recent journal article has summarized some coordination compounds with activations involving the nacnac ligands.[26] Mindiola and co-workers observed an intramolecular, cross metathesis of metal-nitrido with the nacnac ligands.[27] This is a possible explanation for the formation of **35**. A reasonable oxidation state assignment of **35** is Cr(II)-Cr(III). The effective magnetic moment for the magnetically independent Cr(II)-Cr(III) ($S = \frac{4}{2}$, $S = \frac{3}{2}$) is expected to be 6.2 μ_B. The solution-state magnetic moment by Evans method was determined to be 3.0 μ_B. The structure of **35** is shown, further discussion is omitted as the decomposition result is not the pursuit of this study. In addition, chemical reduction (Mg, KC_8, Na) of halide precursors $(*L^{iPr}Cr)_2(\mu\text{-}X)_2$ (X = Cl and I) has been attempted, but failed to yield the corresponding dinitrogen complex, $(*L^{iPr}Cr)_2(\mu_2\text{-}\eta^2\text{:}\eta^2\text{-}N_2)$.

34, Ar = 2,6-diisopropylphenyl   **35**
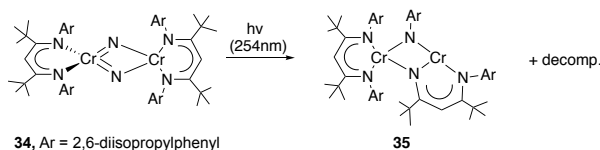
Scheme 3.20   Irradiation of **34**
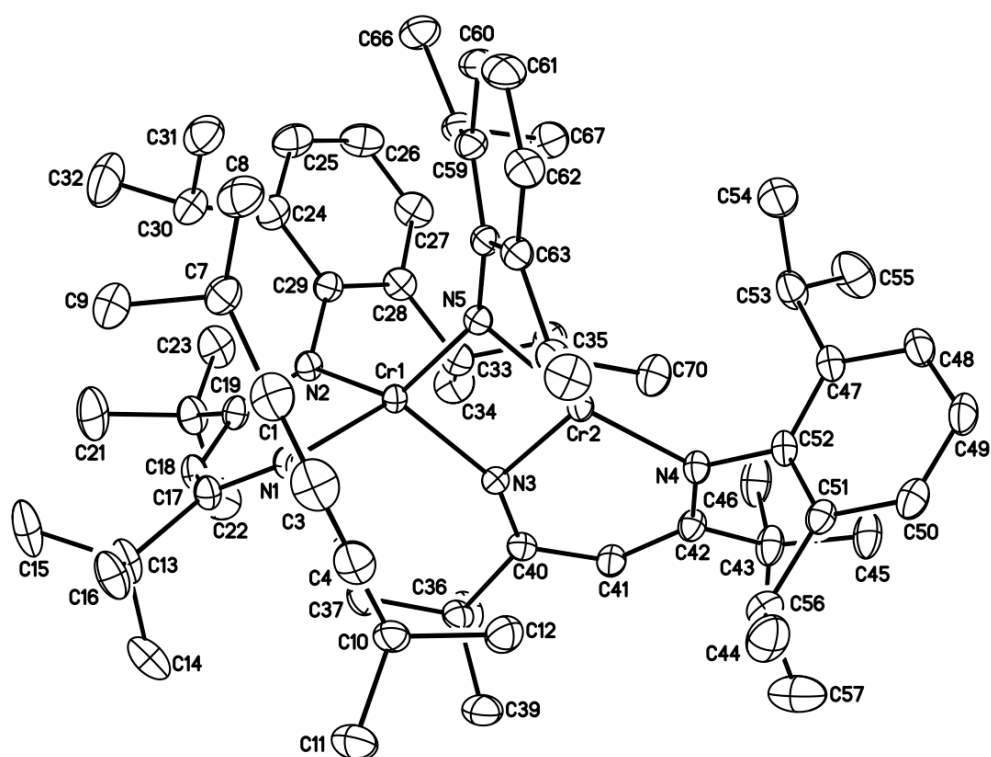
Figure 3.15 Molecular structure of (*L^{iPr}Cr)(μ-NAr)(μ-NC(^{t}Bu)CH(^{t}Bu)CNAr)(μ_3-Cr) (Ar = 2,6-diisopropylphenyl) (**35**). Ellipsoids are drawn at the 30% probability level. Hydrogen atoms have been omitted for clarity.

Table 3.10   Interatomic distances (Å) and angles (°) for (*L^{iPr}Cr)(μ-NAr)(μ-NC(^{t}Bu)CH(^{t}Bu)CNAr)(μ$_3$-Cr) (Ar = 2,6-diisopropylphenyl) (**35**)

Distances (Å)			
Cr(1)-N(5)	1.8613(18)	C(26)-C(27)	1.377(4)
Cr(1)-N(3)	1.9851(18)	C(27)-C(28)	1.398(4)
Cr(1)-N(1)	2.0355(18)	C(28)-C(29)	1.416(3)
Cr(1)-N(2)	2.0643(18)	C(28)-C(33)	1.513(4)
Cr(1)-Cr(2)	2.7044(5)	C(30)-C(31)	1.523(4)
Cr(2)-N(3)	1.9138(18)	C(30)-C(32)	1.548(4)
Cr(2)-N(5)	1.9708(18)	C(33)-C(35)	1.524(4)
Cr(2)-N(4)	2.0266(18)	C(33)-C(34)	1.547(4)
N(1)-C(17)	1.340(3)	C(36)-C(37)	1.504(3)
N(1)-C(6)	1.458(3)	C(36)-C(38)	1.534(3)
N(2)-C(19)	1.346(3)	C(36)-C(39)	1.537(4)
N(2)-C(29)	1.441(3)	C(36)-C(40)	1.557(3)
N(3)-C(40)	1.320(3)	C(40)-C(41)	1.419(3)
N(4)-C(42)	1.360(3)	C(41)-C(42)	1.384(3)
N(4)-C(52)	1.447(3)	C(42)-C(43)	1.575(3)
N(5)-C(64)	1.406(3)	C(43)-C(46)	1.534(4)
C(1)-C(2)	1.396(3)	C(43)-C(45)	1.542(4)
C(1)-C(6)	1.418(3)	C(43)-C(44)	1.542(4)
C(1)-C(7)	1.508(4)	C(47)-C(48)	1.391(3)
C(2)-C(3)	1.364(4)	C(47)-C(52)	1.397(3)
C(3)-C(4)	1.371(4)	C(47)-C(53)	1.522(4)
C(4)-C(5)	1.397(3)	C(48)-C(49)	1.378(4)
C(5)-C(6)	1.409(3)	C(49)-C(50)	1.376(4)
C(5)-C(10)	1.517(4)	C(50)-C(51)	1.397(3)
C(7)-C(8)	1.530(4)	C(51)-C(52)	1.417(3)
C(7)-C(9)	1.534(4)	C(51)-C(56)	1.524(4)
C(10)-C(12)	1.529(4)	C(53)-C(54)	1.525(4)
C(10)-C(11)	1.539(4)	C(53)-C(55)	1.535(4)
C(13)-C(14)	1.529(4)	C(56)-C(57)	1.517(4)
C(13)-C(16)	1.545(3)	C(56)-C(58)	1.521(4)
C(13)-C(15)	1.557(4)	C(59)-C(60)	1.392(3)
C(13)-C(17)	1.576(3)	C(59)-C(64)	1.432(3)
C(17)-C(18)	1.407(3)	C(59)-C(65)	1.515(3)

C(18)-C(19)	1.392(3)	C(60)-C(61)	1.373(4)
C(19)-C(20)	1.587(3)	C(61)-C(62)	1.376(4)
C(20)-C(22)	1.526(4)	C(62)-C(63)	1.395(3)
C(20)-C(23)	1.540(4)	C(63)-C(64)	1.430(3)
C(20)-C(21)	1.541(4)	C(63)-C(68)	1.509(3)
C(24)-C(25)	1.390(4)	C(65)-C(67)	1.524(4)
C(24)-C(29)	1.413(4)	C(65)-C(66)	1.533(3)
C(24)-C(30)	1.524(4)	C(68)-C(69)	1.526(3)
C(25)-C(26)	1.368(4)	C(68)-C(70)	1.535(3)

Angles (°)

N(5)-Cr(1)-N(3)	91.67(8)	C(26)-C(25)-C(24)	122.1(3)
N(5)-Cr(1)-N(1)	119.31(7)	C(25)-C(26)-C(27)	119.5(3)
N(3)-Cr(1)-N(1)	115.52(7)	C(26)-C(27)-C(28)	121.6(3)
N(5)-Cr(1)-N(2)	128.36(8)	C(27)-C(28)-C(29)	118.4(2)
N(3)-Cr(1)-N(2)	113.53(7)	C(27)-C(28)-C(33)	118.2(2)
N(1)-Cr(1)-N(2)	90.45(7)	C(29)-C(28)-C(33)	123.3(2)
N(5)-Cr(1)-Cr(2)	46.78(5)	C(24)-C(29)-C(28)	119.8(2)
N(3)-Cr(1)-Cr(2)	45.00(5)	C(24)-C(29)-N(2)	119.4(2)
N(1)-Cr(1)-Cr(2)	128.70(5)	C(28)-C(29)-N(2)	120.8(2)
N(2)-Cr(1)-Cr(2)	139.35(5)	C(31)-C(30)-C(24)	110.7(2)
N(3)-Cr(2)-N(5)	90.56(7)	C(31)-C(30)-C(32)	108.2(3)
N(3)-Cr(2)-N(4)	97.20(7)	C(24)-C(30)-C(32)	112.9(3)
N(5)-Cr(2)-N(4)	167.16(8)	C(28)-C(33)-C(35)	111.6(2)
N(3)-Cr(2)-Cr(1)	47.18(5)	C(28)-C(33)-C(34)	112.1(2)
N(5)-Cr(2)-Cr(1)	43.49(5)	C(35)-C(33)-C(34)	109.6(2)
N(4)-Cr(2)-Cr(1)	143.88(5)	C(37)-C(36)-C(38)	107.5(2)
C(17)-N(1)-C(6)	121.71(18)	C(37)-C(36)-C(39)	108.7(2)
C(17)-N(1)-Cr(1)	125.52(15)	C(38)-C(36)-C(39)	108.9(2)
C(6)-N(1)-Cr(1)	112.69(13)	C(37)-C(36)-C(40)	111.82(19)
C(19)-N(2)-C(29)	119.72(18)	C(38)-C(36)-C(40)	111.2(2)
C(19)-N(2)-Cr(1)	123.19(15)	C(39)-C(36)-C(40)	108.7(2)
C(29)-N(2)-Cr(1)	116.89(14)	N(3)-C(40)-C(41)	123.8(2)
C(40)-N(3)-Cr(2)	122.69(15)	N(3)-C(40)-C(36)	123.6(2)
C(40)-N(3)-Cr(1)	149.33(16)	C(41)-C(40)-C(36)	112.56(19)
Cr(2)-N(3)-Cr(1)	87.82(7)	C(42)-C(41)-C(40)	132.0(2)

C(42)-N(4)-C(52)	121.72(18)	N(4)-C(42)-C(41)	120.0(2)
C(42)-N(4)-Cr(2)	121.96(15)	N(4)-C(42)-C(43)	125.2(2)
C(52)-N(4)-Cr(2)	116.13(13)	C(41)-C(42)-C(43)	114.3(2)
C(64)-N(5)-Cr(1)	143.54(15)	C(46)-C(43)-C(45)	107.0(2)
C(64)-N(5)-Cr(2)	125.34(14)	C(46)-C(43)-C(44)	107.8(2)
Cr(1)-N(5)-Cr(2)	89.73(7)	C(45)-C(43)-C(44)	106.1(2)
C(2)-C(1)-C(6)	117.3(2)	C(46)-C(43)-C(42)	104.9(2)
C(2)-C(1)-C(7)	119.8(2)	C(45)-C(43)-C(42)	118.3(2)
C(6)-C(1)-C(7)	122.8(2)	C(44)-C(43)-C(42)	112.2(2)
C(3)-C(2)-C(1)	122.3(3)	C(48)-C(47)-C(52)	118.5(2)
C(2)-C(3)-C(4)	119.7(2)	C(48)-C(47)-C(53)	118.3(2)
C(3)-C(4)-C(5)	121.8(3)	C(52)-C(47)-C(53)	123.2(2)
C(4)-C(5)-C(6)	117.9(2)	C(49)-C(48)-C(47)	121.8(2)
C(4)-C(5)-C(10)	117.8(2)	C(50)-C(49)-C(48)	119.3(2)
C(6)-C(5)-C(10)	124.3(2)	C(49)-C(50)-C(51)	121.7(2)
C(5)-C(6)-C(1)	120.7(2)	C(50)-C(51)-C(52)	118.0(2)
C(5)-C(6)-N(1)	121.5(2)	C(50)-C(51)-C(56)	119.5(2)
C(1)-C(6)-N(1)	117.8(2)	C(52)-C(51)-C(56)	122.5(2)
C(1)-C(7)-C(8)	113.5(2)	C(47)-C(52)-C(51)	120.5(2)
C(1)-C(7)-C(9)	112.2(2)	C(47)-C(52)-N(4)	121.2(2)
C(8)-C(7)-C(9)	109.3(2)	C(51)-C(52)-N(4)	118.1(2)
C(5)-C(10)-C(12)	109.8(2)	C(47)-C(53)-C(54)	110.8(2)
C(5)-C(10)-C(11)	113.2(2)	C(47)-C(53)-C(55)	112.4(2)
C(12)-C(10)-C(11)	108.7(2)	C(54)-C(53)-C(55)	108.9(3)
C(14)-C(13)-C(16)	107.6(2)	C(57)-C(56)-C(58)	109.0(3)
C(14)-C(13)-C(15)	108.9(2)	C(57)-C(56)-C(51)	113.0(2)
C(16)-C(13)-C(15)	104.7(2)	C(58)-C(56)-C(51)	113.5(2)
C(14)-C(13)-C(17)	105.9(2)	C(60)-C(59)-C(64)	118.8(2)
C(16)-C(13)-C(17)	118.8(2)	C(60)-C(59)-C(65)	119.7(2)
C(15)-C(13)-C(17)	110.6(2)	C(64)-C(59)-C(65)	121.3(2)
N(1)-C(17)-C(18)	120.4(2)	C(61)-C(60)-C(59)	122.7(2)
N(1)-C(17)-C(13)	127.1(2)	C(60)-C(61)-C(62)	119.4(2)
C(18)-C(17)-C(13)	112.2(2)	C(61)-C(62)-C(63)	121.0(2)
C(19)-C(18)-C(17)	132.4(2)	C(62)-C(63)-C(64)	120.2(2)
N(2)-C(19)-C(18)	121.0(2)	C(62)-C(63)-C(68)	120.5(2)
N(2)-C(19)-C(20)	126.3(2)	C(64)-C(63)-C(68)	118.95(19)
C(18)-C(19)-C(20)	112.5(2)	N(5)-C(64)-C(63)	119.7(2)

C(22)-C(20)-C(23)	106.0(2)	N(5)-C(64)-C(59)	122.4(2)
C(22)-C(20)-C(21)	108.7(3)	C(63)-C(64)-C(59)	117.6(2)
C(23)-C(20)-C(21)	106.2(2)	C(59)-C(65)-C(67)	109.4(2)
C(22)-C(20)-C(19)	106.7(2)	C(59)-C(65)-C(66)	114.2(2)
C(23)-C(20)-C(19)	118.8(2)	C(67)-C(65)-C(66)	108.9(2)
C(21)-C(20)-C(19)	110.1(2)	C(63)-C(68)-C(69)	115.8(2)
C(25)-C(24)-C(29)	118.6(3)	C(63)-C(68)-C(70)	108.08(19)
C(25)-C(24)-C(30)	117.9(3)	C(69)-C(68)-C(70)	108.2(2)
C(29)-C(24)-C(30)	123.6(2)		

3.2.4 Explorations of synthesizing bis(μ-nitrido) 25

The photochemical conversion of bis(μ-nitrido) complex **25** to its isomer **23** has been observed. Unfortunately, this reaction made it difficult to isolate **25** in appreciable amounts. In order to study the nature of the two isomers and to explore their reactivities, a better synthesis of **25** had to be found. A number of synthetic approaches have been tried; the ideas, the experiments and the results will be briefly described in the following.

Chromium bis(μ-amido) complex $(L^{iPr}Cr)_2(\mu\text{-}NH_2)_2$ has been previously synthesized.[20] Ideally approaching **25** from $(L^{iPr}Cr)_2(\mu\text{-}NH_2)_2$ would involve four consecutive hydrogen atom abstractions. 2,4,6-tris-tert-butylphenoxy radical was selected because it has been shown to successfully convert a Mo-NH$_3$ species into a nitrido complex.[28] Applying stoichiometric to excess amounts of this radical reagent at room or elevated temperature in THF solution of $(L^{iPr}Cr)_2(\mu\text{-}NH_2)_2$ did not show any change for up to 48 hours of reaction time.

Ar = 2,6-diisopropylphenyl

25
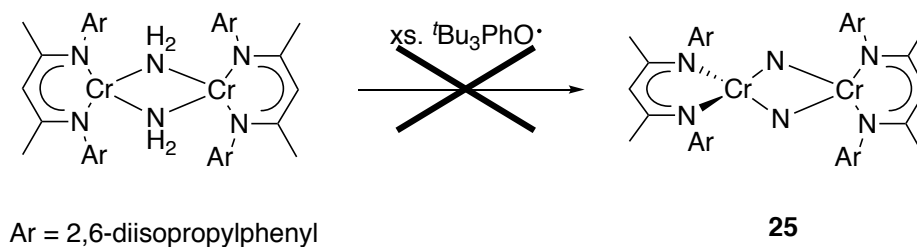
Scheme 3.21   Attempt at hydrogen abstraction from $(L^{iPr}Cr)_2(\mu\text{-}NH_2)_2$

Hill et al. showed that a nitrido complex was generated by an N-atom transfer strategy, where ammonia served as the nitrogen source.[29] A manganese chloride was mixed with iodosobenzene and NH$_3$, leading to the formation of Mn≡N in high yield.

An implication was that the Mn(O)(Cl) species was an intermediate. Following this strategy, a reaction of known $L^{iPr}Cr(O)Cl$ with NH_3 was performed.[30] The expected product was half an equivalent of **25** with the release of H_2O and HCl, which might possibly be trapped by molecular sieves and excess NH_3, respectively. However, $L^{iPr}Cr(O)_2$ was the only product detected, suggesting that byproduct H_2O might be detrimental in this reaction.

Ar = 2,6-diisopropylphenyl   **25**
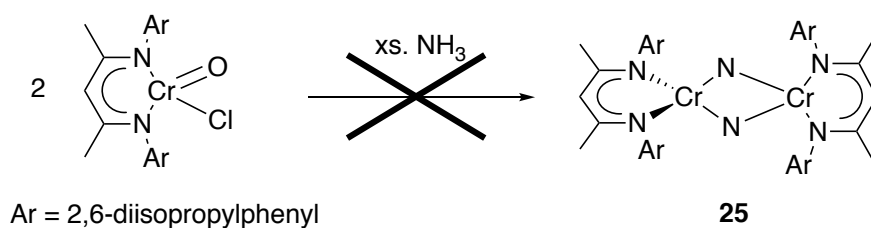
Scheme 3.22   Attempted N-atom transfer from ammonia

NaN_3 salt metathesis with $L^{iPr}Cr(O)Cl$, leading to the formation of $L^{iPr}Cr(O)N_3$ is also known.[31] Therefore, the proposed pathway to get to **25** from $L^{iPr}Cr(O)N_3$ is by irradiation of $L^{iPr}Cr(O)N_3$, followed by deoxygenation of the resulting oxo-nitrido complex. The photolysis of $L^{iPr}Cr(O)N_3$ yielded a mixture of products; resonances belonging to $L^{iPr}Cr(O)_2$ were detected in the ^1H NMR spectrum and some diamagnetic features were also observed. Both $L^{iPr}Cr^{VI}(O)N$ and free ligand are candidates for contributing the diamagnetic features. Examination of the diamagnetic resonances excluded the formation of ligands, therefore suggesting the potential formation of $L^{iPr}Cr^{VI}(O)N$. However, attempts to separate and isolate the desired product by fractional crystallization were unsuccessful, limiting characterizations and further deoxygenation process.
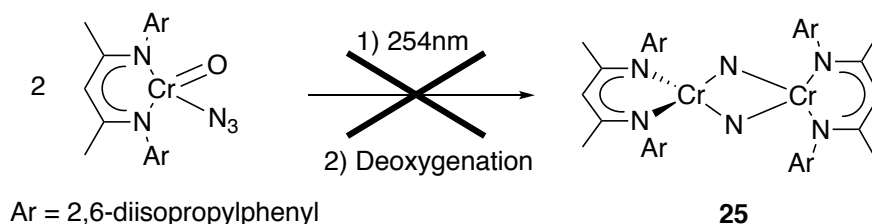
Scheme 3.23   Attempt of photolysis of oxo-azido complex followed by
deoxygenation

Another N-atom transfer reagent was tried, namely lithium anthracenyl amide
Li(dbabh) (dbabh = 2,3: 5,6-dibenzo-7-aza bicyclo[2.2.1]hepta-2,5-diene). The
synthesis has been reported [32] and the reagent has been successfully used for the
synthesis of nitrido complexes.[18, 33] Addition of Li(dbabh) to a green Et_2O solution of
$[L^{iPr}Cr(\mu\text{-}Cl)]_2$ led to the color gradually changing to red-brown over 3 hours. After
work-up, the product was crystallized from concentrated pentane solution, and
identified by X-ray diffraction as monomeric $L^{iPr}Cr(dbabh)$ (**36**), isolated in 58% yield.
Actually **36** was not the sole inorganic product; in fact, a LIFDI mass spectrum taken
of the crude products showed **36** (m/z = 661.3734) as the major component with a
minor one at m/z = 1144.6587, and the isotope pattern matched $(L^{iPr}Cr)_2(\mu\text{-}N)(\mu\text{-}$
dbabh) (calcd. m/z = 1144.6199 [M$^+$]). $(L^{iPr}Cr)_2(\mu\text{-}N)(\mu\text{-}dbabh)$ may be formed in this
reaction as well. Purification of **36** was achieved by multiple recrystallization and its
structure was determined by X-ray diffraction. **36** crystallizes in the orthorhombic
space group $Cmc2_1$ with a mirror plane running through chromium and the amide
nitrogen atom. The chromium center adopts trigonal planar geometry with the amide
nitrogen bound to chromium at a distance of 1.882(4) Å. This distance is comparable
to that in $(N(R)Ar_F)_2Cr(N)(dbabh)$ (R = ^tBu, Ar_F = 2,5-C_6H_3FMe) reported by
Cummins and co-workers ($Cr^{VI}\text{-}N_{dbabh}$ 1.814(3) Å).[33] The ^1H NMR spectrum of **36** in

C_6D_6 exhibited several isotropically shifted and broadened resonances, suggesting that **36** is paramagnetic. The effective magnetic moment of **36** in solution was measured by the Evans method, giving $\mu_{eff} = 4.6$ μ_B, consistent with chromium in the (+II) oxidation state, i. e., a high spin d^4 electronic configuration.

Ar = 2,6-diisopropylphenyl

36, 58% yield
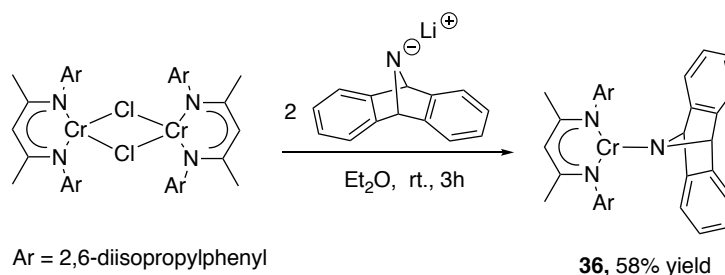
Scheme 3.24   Attempt of N-atom transfer from Li(dbabh)

Producing **25** from **36** was expected to be achievable either thermally or photolytically. Heating **36** in C_6D_6 at 60°C for 9 hours, or irradiating **36** in C_6D_6 for 3 hours were both attempted. Although a small amount of anthracene was detected by ^{1}H NMR spectroscopy, the resonances belonging to **25** were not observed.

This N-atom transfer strategy has also been used in another ligand system in our lab, as depicted in Scheme 3.25.
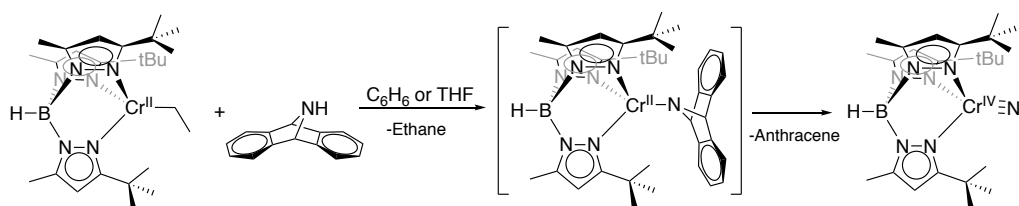
Scheme 3.25   The successful formation of chromium terminal nitride by the use of H(dbabh) as a N-atom transfer reagent

During the reaction described above, an intermediate was postulated to be Tp^{tBu,Me}Cr(dbabh), which was observed by ^{1}H NMR and UV-Vis spectroscopies. It is thus assumed that four-coordinate chromium complex is preferred in terms of eliminating anthracene from LCr(dbabh). To apply this idea, ligand donors such as pyridine and a N-heterocyclic carbene (:C{N(Ar)CH}$_2$, Ar = 2,6-diisopropylphenyl) were chosen to react with **36**. Our hope was that anthracene would be eliminated upon the addition of donor ligands. The addition of pyridine or ^{iPr}NHC to C$_6$D$_6$ solutions of **36** at 60°C for 1 and 2 days, respectively led to resonances shift, observed by ^{1}H NMR spectroscopy. However, they did not yield observable amount of anthracene, and the resonances belonging to **25** were not detected

While determining the melting point of (L^{iPr}Cr)$_2$(μ-N$_3$)$_2$ (**24**), some bubbles were observed, leading to the hypothesis that **24** was decomposing by releasing N$_2$. The melting point was measured to be 234°C. Solid state heating was then tested. Instead of directly heating **24** at its melting point, a slightly lower temperature was tried to allow slow decomposition. Some crystals of **24** were sealed in J. Young tube under vacuum and heated up to 208°C for 2.5 hours, **24** slowly melted under these conditions and C$_6$D$_6$ was then vacuum transferred into the tube. The ^{1}H NMR spectrum taken did not show the resonances associated with **25**, but ligand L^{iPr} was detected.

Solid state grinding of **24** was also tried. There was no sign of change after a period of 3 hours of grinding, as evidenced by ^{1}H NMR spectroscopy.

Figure 3.16 Molecular structure of $L^{iPr}Cr(dbabh)$ (**36**). Ellipsoids are drawn at the 30% probability level. Hydrogen atoms have been omitted for clarity.

Table 3.11   Interatomic distances (Å) and angles (°) for L^{iPr}Cr(dbabh) (**36**)

Distances (Å)

Cr(1)-N(1)	1.882(4)	C(7)-C(8)	1.377(5)
Cr(1)-N(2)	2.003(2)	C(9)-C(10)	1.395(5)
Cr(1)-N(2)A	2.003(2)	C(9)-C(14)	1.403(5)
N(1)-C(2)	1.497(6)	C(9)-C(15)	1.512(5)
N(1)-C(1)	1.500(6)	C(10)-C(11)	1.359(6)
N(2)-C(22)	1.320(4)	C(11)-C(12)	1.378(7)
N(2)-C(14)	1.441(4)	C(12)-C(13)	1.384(5)
C(1)-C(8)A	1.524(4)	C(13)-C(14)	1.399(5)
C(1)-C(8)	1.524(4)	C(13)-C(18)	1.529(5)
C(2)-C(3)	1.529(4)	C(15)-C(17)	1.513(6)
C(2)-C(3)A	1.529(4)	C(15)-C(16)	1.543(6)
C(3)-C(4)	1.365(4)	C(18)-C(19)	1.521(6)
C(3)-C(8)	1.402(5)	C(18)-C(20)	1.538(6)
C(4)-C(5)	1.385(5)	C(21)-C(22)	1.516(5)
C(5)-C(6)	1.364(6)	C(22)-C(23)	1.402(4)
C(6)-C(7)	1.395(5)	C(23)-C(22)A	1.402(4)

Angles (°)

N(1)-Cr(1)-N(2)	135.12(7)	C(3)-C(8)-C(1)	105.6(3)
N(1)-Cr(1)-N(2)A	135.12(7)	C(10)-C(9)-C(14)	118.2(3)
N(2)-Cr(1)-N(2)A	89.77(14)	C(10)-C(9)-C(15)	119.5(3)
C(2)-N(1)-C(1)	94.3(3)	C(14)-C(9)-C(15)	122.2(3)
C(2)-N(1)-Cr(1)	133.7(3)	C(11)-C(10)-C(9)	121.2(4)
C(1)-N(1)-Cr(1)	132.1(3)	C(10)-C(11)-C(12)	120.7(4)
C(22)-N(2)-C(14)	121.6(3)	C(11)-C(12)-C(13)	120.0(4)
C(22)-N(2)-Cr(1)	128.2(2)	C(12)-C(13)-C(14)	119.6(3)
C(14)-N(2)-Cr(1)	110.12(19)	C(12)-C(13)-C(18)	119.5(3)
N(1)-C(1)-C(8)A	99.6(2)	C(14)-C(13)-C(18)	120.9(3)
N(1)-C(1)-C(8)	99.6(2)	C(13)-C(14)-C(9)	120.1(3)
C(8)A-C(1)-C(8)	107.5(3)	C(13)-C(14)-N(2)	120.7(3)
N(1)-C(2)-C(3)	100.4(3)	C(9)-C(14)-N(2)	119.0(3)
N(1)-C(2)-C(3)A	100.4(3)	C(9)-C(15)-C(17)	112.2(4)
C(3)-C(2)-C(3)A	106.4(3)	C(9)-C(15)-C(16)	111.0(4)

C(4)-C(3)-C(8)	121.0(3)	C(17)-C(15)-C(16)	109.5(4)
C(4)-C(3)-C(2)	134.4(3)	C(19)-C(18)-C(13)	110.9(4)
C(8)-C(3)-C(2)	104.6(3)	C(19)-C(18)-C(20)	110.8(4)
C(3)-C(4)-C(5)	118.3(3)	C(13)-C(18)-C(20)	111.2(4)
C(6)-C(5)-C(4)	121.2(3)	N(2)-C(22)-C(23)	123.2(3)
C(5)-C(6)-C(7)	121.1(3)	N(2)-C(22)-C(21)	119.7(3)
C(8)-C(7)-C(6)	117.9(3)	C(23)-C(22)-C(21)	117.1(3)
C(7)-C(8)-C(3)	120.4(3)	C(22)A-C(23)-C(22)	127.3(4)
C(7)-C(8)-C(1)	134.0(3)		

3.2.5 Synthesis and reactivity of Cr(III) azide

Sita and co-workers have reported the successful synthesis of several bis(μ-nitrido) complexes (metal = molybdenum and tungsten). These reactions were carried out via reduction of a nitrido-chloro complex with a sodium/mercury amalgam, shown in Scheme 3.26.[10] Following this strategy, Cr(III) chloride $(L^{iPr}CrCl)_2(\mu\text{-Cl})_2$ was prepared as a precursor.[34] Addition of 2 equiv. of NaN_3 to a brown $(L^{iPr}CrCl)_2(\mu\text{-Cl})_2$ THF solution at room temperature and stirring for 6 hours resulted in a red solution, the product was characterized as $(L^{iPr}CrCl)_2(THF)(\mu\text{-N}_3)_2$ (**37**). The synthesis is depicted in Scheme 3.27 and its molecular structure has been determined by X-ray crystallography as shown in Figure 3.17; it shows a THF molecule coordinated to one of the chromium centers.

M = Mo and W

0.5% NaHg
Et₂O, 25°C

1/2
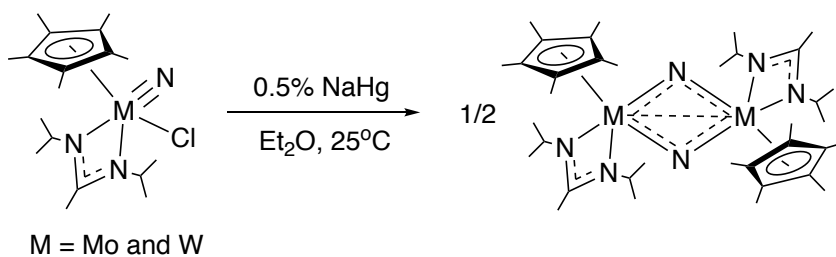
Scheme 3.26   Reductive dehalogenation of nitrido chloride to the formation of bis(μ-nitrido)

Ar = 2,6-diisopropylphenyl

2x NaN₃
THF, rt, 6h

37
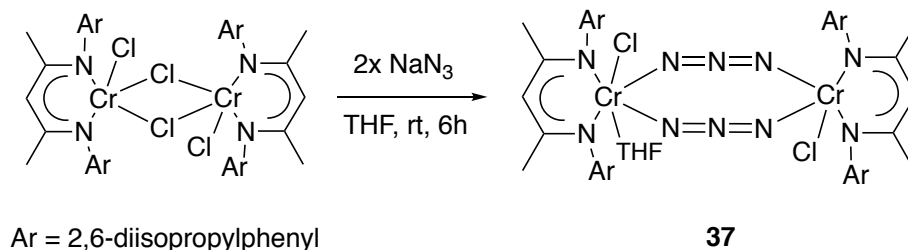
Scheme 3.27   Synthesis of $(L^{iPr}CrCl)_2(THF)(\mu\text{-N}_3)_2$ (**37**)

In **37**, six-coordinate Cr1 is octahedral and five-coordinate Cr2 adopts square pyramidal geometry with chloride in the apical position. The structural features of bridging azido groups are comparable to those reported in $(L^{iPr}Cr)_2(\mu\text{-}N_3)_2$ (**24**). The infrared spectrum of **37** also exhibited distinct azido stretching frequencies of 2117 and 2060 cm^{-1}. For a system of two non-interacting chromium(III) high spin d^3 ions, the expected magnetic moment is 5.47 μ_B. The effective magnetic moment of **37** has been measured in the solid state to be 3.3(1) μ_B, suggesting antiferromagnetic coupling between the chromium ions.
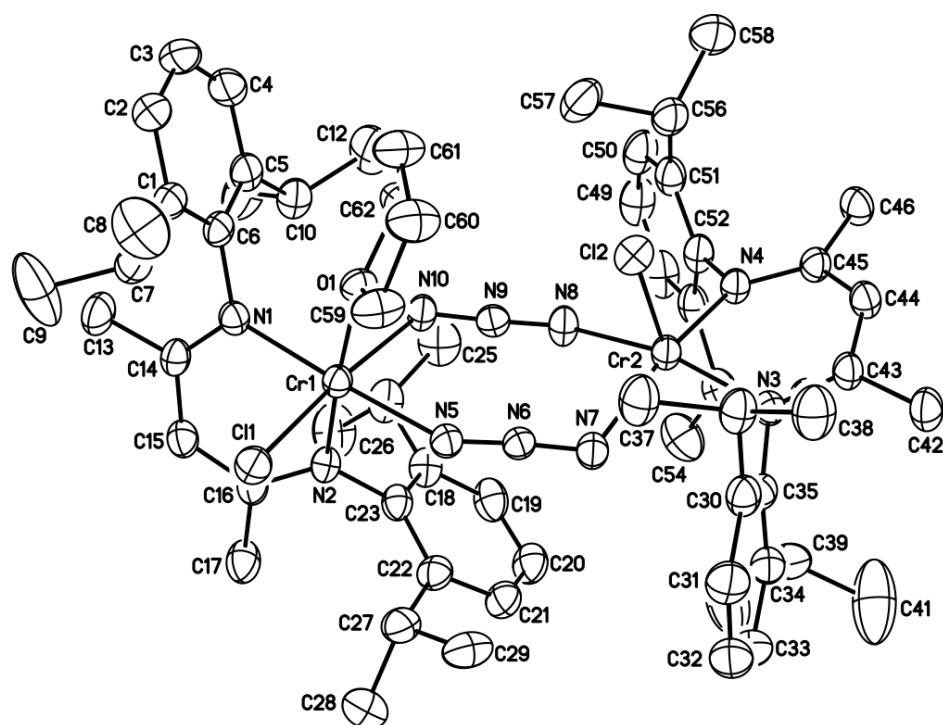
Figure 3.17 Molecular structure of $(L^{iPr}CrCl)_2(THF)(\mu\text{-}N_3)_2$ (**37**). Ellipsoids are drawn at the 30% probability level. Hydrogen atoms have been omitted for clarity.

Table 3.12   Interatomic distances (Å) and angles (º) for (L^{iPr}CrCl)$_2$(THF)(μ-N$_3$)$_2$ (**37**)

	Distances (Å)		
Cr(1)-N(2)	1.997(3)	C(18)-C(23)	1.405(5)
Cr(1)-N(1)	2.046(3)	C(18)-C(24)	1.511(6)
Cr(1)-N(10)	2.089(3)	C(19)-C(20)	1.385(6)
Cr(1)-N(5)	2.092(3)	C(20)-C(21)	1.373(6)
Cr(1)-O(1)	2.124(2)	C(21)-C(22)	1.380(5)
Cr(1)-Cl(1)	2.2888(10)	C(22)-C(23)	1.411(5)
Cr(2)-N(3)	1.988(3)	C(22)-C(27)	1.505(5)
Cr(2)-N(4)	1.990(3)	C(24)-C(25)	1.504(6)
Cr(2)-N(7)	2.046(3)	C(24)-C(26)	1.564(6)
Cr(2)-N(8)	2.080(3)	C(27)-C(29)	1.525(6)
Cr(2)-Cl(2)	2.2165(11)	C(27)-C(28)	1.551(6)
O(1)-C(62)	1.460(4)	C(30)-C(31)	1.395(5)
O(1)-C(59)	1.471(4)	C(30)-C(35)	1.410(5)
N(1)-C(14)	1.327(4)	C(30)-C(36)	1.516(6)
N(1)-C(6)	1.455(4)	C(31)-C(32)	1.374(6)
N(2)-C(16)	1.344(4)	C(32)-C(33)	1.380(6)
N(2)-C(23)	1.461(4)	C(33)-C(34)	1.402(5)
N(3)-C(43)	1.339(4)	C(34)-C(35)	1.377(5)
N(3)-C(35)	1.465(4)	C(34)-C(39)	1.524(6)
N(4)-C(45)	1.355(4)	C(36)-C(37)	1.535(5)
N(4)-C(52)	1.456(4)	C(36)-C(38)	1.558(5)
N(5)-N(6)	1.159(4)	C(39)-C(40)	1.491(6)
N(6)-N(7)	1.182(4)	C(39)-C(41)	1.533(8)
N(8)-N(9)	1.184(4)	C(42)-C(43)	1.512(5)
N(9)-N(10)	1.176(4)	C(43)-C(44)	1.394(5)
C(1)-C(2)	1.387(5)	C(44)-C(45)	1.386(5)
C(1)-C(6)	1.412(5)	C(45)-C(46)	1.498(5)
C(1)-C(7)	1.524(5)	C(47)-C(48)	1.395(6)
C(2)-C(3)	1.368(6)	C(47)-C(52)	1.411(5)
C(3)-C(4)	1.369(6)	C(47)-C(53)	1.523(6)
C(4)-C(5)	1.403(6)	C(48)-C(49)	1.377(7)
C(5)-C(6)	1.398(5)	C(49)-C(50)	1.386(7)
C(5)-C(10)	1.517(6)	C(50)-C(51)	1.387(6)
C(7)-C(9)	1.507(6)	C(51)-C(52)	1.389(5)

C(7)-C(8)	1.518(6)	C(51)-C(56)	1.511(6)
C(10)-C(12)	1.532(6)	C(53)-C(55)	1.525(6)
C(10)-C(11)	1.533(6)	C(53)-C(54)	1.531(6)
C(13)-C(14)	1.511(5)	C(56)-C(57)	1.526(6)
C(14)-C(15)	1.406(5)	C(56)-C(58)	1.545(6)
C(15)-C(16)	1.385(5)	C(59)-C(60)	1.505(5)
C(16)-C(17)	1.504(5)	C(60)-C(61)	1.508(6)
C(18)-C(19)	1.398(5)	C(61)-C(62)	1.474(6)

Angles (°)

N(2)-Cr(1)-N(1)	90.87(12)	N(2)-C(16)-C(15)	122.9(3)
N(2)-Cr(1)-N(10)	91.82(12)	N(2)-C(16)-C(17)	121.0(3)
N(1)-Cr(1)-N(10)	94.78(11)	C(15)-C(16)-C(17)	116.0(3)
N(2)-Cr(1)-N(5)	93.81(12)	C(19)-C(18)-C(23)	118.3(4)
N(1)-Cr(1)-N(5)	175.28(11)	C(19)-C(18)-C(24)	118.0(4)
N(10)-Cr(1)-N(5)	85.62(12)	C(23)-C(18)-C(24)	123.6(4)
N(2)-Cr(1)-O(1)	176.66(11)	C(20)-C(19)-C(18)	120.7(4)
N(1)-Cr(1)-O(1)	91.37(10)	C(21)-C(20)-C(19)	119.5(4)
N(10)-Cr(1)-O(1)	85.52(11)	C(20)-C(21)-C(22)	122.7(4)
N(5)-Cr(1)-O(1)	83.97(10)	C(21)-C(22)-C(23)	117.3(4)
N(2)-Cr(1)-Cl(1)	91.06(9)	C(21)-C(22)-C(27)	118.1(4)
N(1)-Cr(1)-Cl(1)	91.93(8)	C(23)-C(22)-C(27)	124.4(3)
N(10)-Cr(1)-Cl(1)	172.65(9)	C(18)-C(23)-C(22)	121.3(3)
N(5)-Cr(1)-Cl(1)	87.44(8)	C(18)-C(23)-N(2)	117.0(3)
O(1)-Cr(1)-Cl(1)	91.35(7)	C(22)-C(23)-N(2)	121.7(3)
N(3)-Cr(2)-N(4)	92.01(11)	C(25)-C(24)-C(18)	114.7(4)
N(3)-Cr(2)-N(7)	89.12(12)	C(25)-C(24)-C(26)	108.6(4)
N(4)-Cr(2)-N(7)	160.23(13)	C(18)-C(24)-C(26)	111.4(4)
N(3)-Cr(2)-N(8)	164.54(13)	C(22)-C(27)-C(29)	114.2(4)
N(4)-Cr(2)-N(8)	89.96(12)	C(22)-C(27)-C(28)	110.4(4)
N(7)-Cr(2)-N(8)	83.93(13)	C(29)-C(27)-C(28)	106.8(4)
N(3)-Cr(2)-Cl(2)	100.55(9)	C(31)-C(30)-C(35)	117.5(4)
N(4)-Cr(2)-Cl(2)	101.41(9)	C(31)-C(30)-C(36)	118.8(4)
N(7)-Cr(2)-Cl(2)	97.77(10)	C(35)-C(30)-C(36)	123.6(3)
N(8)-Cr(2)-Cl(2)	94.07(10)	C(32)-C(31)-C(30)	121.3(4)
C(62)-O(1)-C(59)	107.6(3)	C(31)-C(32)-C(33)	120.7(4)

|			
C(62)-O(1)-Cr(1)	124.6(2)	C(32)-C(33)-C(34)	119.5(4)
C(59)-O(1)-Cr(1)	121.5(2)	C(35)-C(34)-C(33)	119.5(4)
C(14)-N(1)-C(6)	115.9(3)	C(35)-C(34)-C(39)	122.7(4)
C(14)-N(1)-Cr(1)	121.6(2)	C(33)-C(34)-C(39)	117.8(4)
C(6)-N(1)-Cr(1)	122.3(2)	C(34)-C(35)-C(30)	121.4(3)
C(16)-N(2)-C(23)	117.5(3)	C(34)-C(35)-N(3)	118.4(3)
C(16)-N(2)-Cr(1)	121.8(2)	C(30)-C(35)-N(3)	120.2(3)
C(23)-N(2)-Cr(1)	120.7(2)	C(30)-C(36)-C(37)	110.7(3)
C(43)-N(3)-C(35)	116.8(3)	C(30)-C(36)-C(38)	111.8(3)
C(43)-N(3)-Cr(2)	123.1(2)	C(37)-C(36)-C(38)	109.1(3)
C(35)-N(3)-Cr(2)	119.8(2)	C(40)-C(39)-C(34)	114.0(4)
C(45)-N(4)-C(52)	116.8(3)	C(40)-C(39)-C(41)	107.5(5)
C(45)-N(4)-Cr(2)	122.7(2)	C(34)-C(39)-C(41)	111.2(4)
C(52)-N(4)-Cr(2)	120.2(2)	N(3)-C(43)-C(44)	123.1(3)
N(6)-N(5)-Cr(1)	137.0(3)	N(3)-C(43)-C(42)	121.3(3)
N(5)-N(6)-N(7)	175.6(3)	C(44)-C(43)-C(42)	115.6(3)
N(6)-N(7)-Cr(2)	123.5(3)	C(45)-C(44)-C(43)	128.6(3)
N(9)-N(8)-Cr(2)	129.0(3)	N(4)-C(45)-C(44)	122.9(3)
N(10)-N(9)-N(8)	176.1(3)	N(4)-C(45)-C(46)	120.4(3)
N(9)-N(10)-Cr(1)	130.2(2)	C(44)-C(45)-C(46)	116.6(3)
C(2)-C(1)-C(6)	118.5(4)	C(48)-C(47)-C(52)	117.1(4)
C(2)-C(1)-C(7)	118.5(4)	C(48)-C(47)-C(53)	120.7(4)
C(6)-C(1)-C(7)	123.0(3)	C(52)-C(47)-C(53)	122.2(4)
C(3)-C(2)-C(1)	121.5(4)	C(49)-C(48)-C(47)	121.6(5)
C(2)-C(3)-C(4)	119.9(4)	C(48)-C(49)-C(50)	119.5(5)
C(3)-C(4)-C(5)	121.6(4)	C(49)-C(50)-C(51)	121.7(5)
C(6)-C(5)-C(4)	117.9(4)	C(50)-C(51)-C(52)	117.6(4)
C(6)-C(5)-C(10)	122.6(4)	C(50)-C(51)-C(56)	118.9(4)
C(4)-C(5)-C(10)	119.5(4)	C(52)-C(51)-C(56)	123.4(4)
C(5)-C(6)-C(1)	120.6(4)	C(51)-C(52)-C(47)	122.4(4)
C(5)-C(6)-N(1)	119.5(3)	C(51)-C(52)-N(4)	120.7(4)
C(1)-C(6)-N(1)	119.8(3)	C(47)-C(52)-N(4)	116.9(3)
C(9)-C(7)-C(8)	108.3(4)	C(47)-C(53)-C(55)	113.0(4)
C(9)-C(7)-C(1)	113.1(4)	C(47)-C(53)-C(54)	114.1(4)
C(8)-C(7)-C(1)	112.7(4)	C(55)-C(53)-C(54)	108.7(4)
C(5)-C(10)-C(12)	111.8(4)	C(51)-C(56)-C(57)	110.4(4)
C(5)-C(10)-C(11)	111.4(4)	C(51)-C(56)-C(58)	113.1(4)

C(12)-C(10)-C(11)	109.7(4)	C(57)-C(56)-C(58)	109.3(4)
N(1)-C(14)-C(15)	123.6(3)	O(1)-C(59)-C(60)	106.1(3)
N(1)-C(14)-C(13)	121.5(3)	C(59)-C(60)-C(61)	105.7(3)
C(15)-C(14)-C(13)	114.8(3)	C(62)-C(61)-C(60)	104.3(4)
C(16)-C(15)-C(14)	128.2(3)	O(1)-C(62)-C(61)	105.1(3)

Irradiation of **37** with 254nm UV light in THF, over a course of 20 hours, caused the solution color to change from red to orange-brown. After work up, the product was collected with 42% yield, which had been structurally determined to be $(L^{iPr}CrN)_2(\mu\text{-Cl})_2$ (**38**). The byproducts had been inspected by ^1H NMR spectroscopy, and the resonances belonging to $(L^{iPr}Cr)_2(\mu\text{-Cl})_2$ were identified. It was, however, unclear how $(L^{iPr}Cr)_2(\mu\text{-Cl})_2$ was formed during the irradiation reaction.

38 crystallizes in the monoclinic space group $P2_1/n$, with an inversion center located between the chromium centers. The Cr-Cl distances average 2.35(2) Å. The $Cr\text{-}N_{nitride}$ distance is short, at 1.587(4) Å. A CSD search performed on 28 AUG 17 showed 90 structures containing terminal Cr≡N unit, with the bond distances averaging at 1.56(4) Å (range: 1.511-1.665 Å). The chromium nitride in **38** is in the range and is in good agreement with triple bond character. The infrared spectrum of **38** was compared with $(L^{iPr}Cr)_2(\mu\text{-Cl})_2$ and 1042cm^{-1} was tentatively assigned as the characteristic stretch for the terminal nitrido functionality, as compared to the reported ν_{CrN} 1046 and 1054cm^{-1} by Cummins.[33, 35]

38 is a binuclear complex and the molecular core consists of terminal nitrido and bridging chloride ligands. Complexes with the nitrido ligand favoring terminal over bridging position have precedent in the literature. A CSD search performed on 04 AUG 17 showed 3 structures containing halide and nitrido ligands, with the halide bridged between metal centers and the nitrido ligand terminally bound to the metal center. These complexes are shown in Scheme 3.28.[36-38]
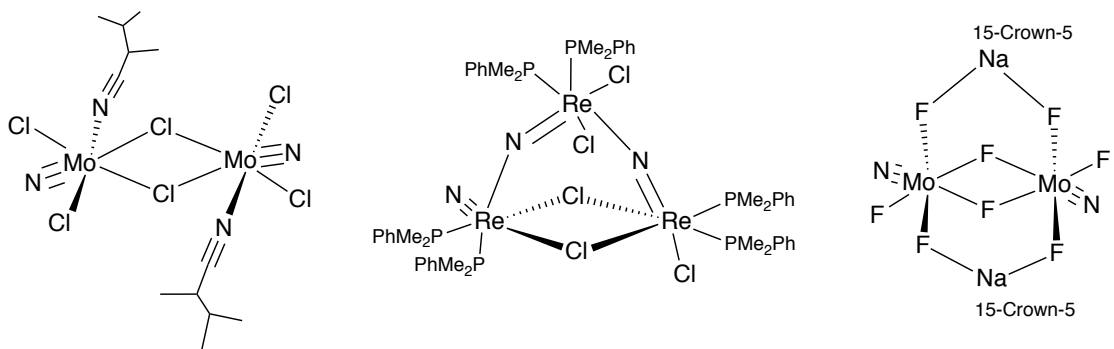
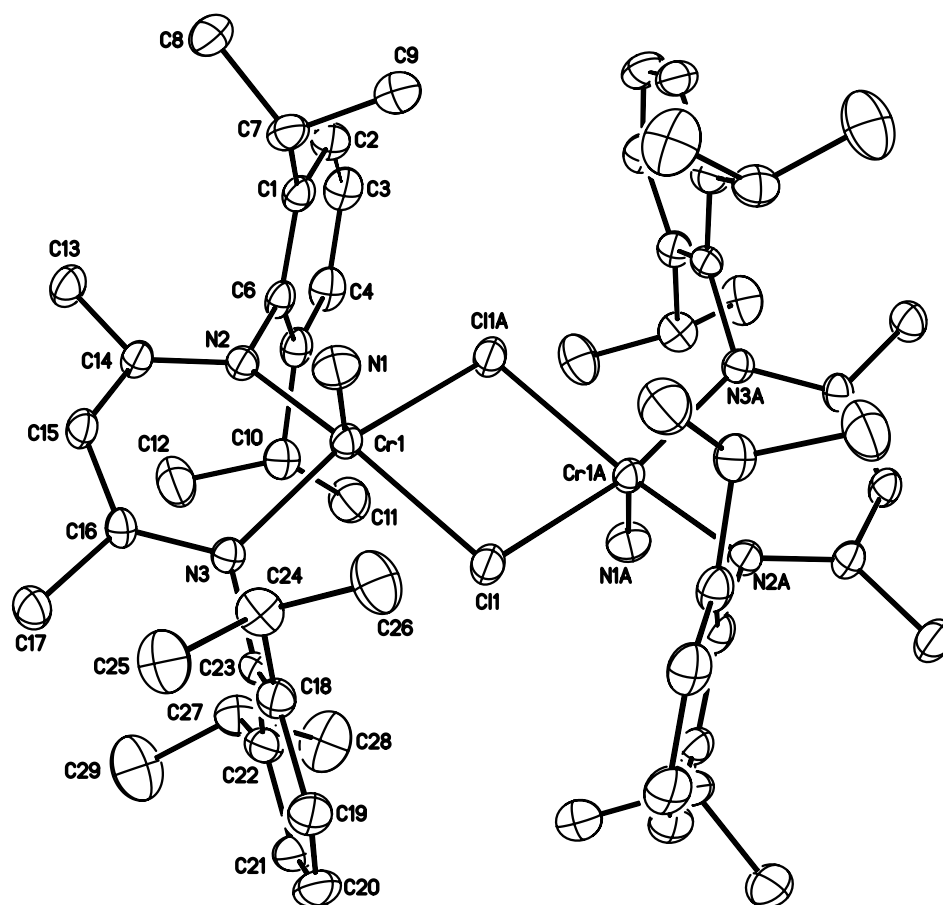Scheme 3.28   Complexes with bridging halide / terminal nitrido

Figure 3.18   Molecular structure of $(L^{iPr}CrN)_2(\mu\text{-}Cl)_2$ (**38**). Ellipsoids are drawn at the 20% probability level. Hydrogen atoms have been omitted for clarity.

Table 3.13 Interatomic distances (Å) and angles (°) for $(L^{iPr}CrN)_2(\mu\text{-Cl})_2$ (**38**)

Distances (Å)

Cr(1)-N(1)	1.587(4)	C(7)-C(8)	1.541(7)
Cr(1)-N(2)	2.016(3)	C(10)-C(12)	1.505(7)
Cr(1)-N(3)	2.036(3)	C(10)-C(11)	1.513(7)
Cr(1)-Cl(1)	2.3365(12)	C(13)-C(14)	1.493(5)
Cr(1)-Cl(1)A	2.3705(12)	C(14)-C(15)	1.393(5)
Cl(1)-Cr(1)A	2.3704(12)	C(15)-C(16)	1.402(5)
N(2)-C(14)	1.338(5)	C(16)-C(17)	1.499(5)
N(2)-C(6)	1.445(5)	C(18)-C(19)	1.399(6)
N(3)-C(16)	1.332(5)	C(18)-C(23)	1.404(6)
N(3)-C(23)	1.455(5)	C(18)-C(24)	1.510(6)
C(1)-C(2)	1.387(6)	C(19)-C(20)	1.359(7)
C(1)-C(6)	1.396(6)	C(20)-C(21)	1.353(7)
C(1)-C(7)	1.530(6)	C(21)-C(22)	1.392(6)
C(2)-C(3)	1.380(7)	C(22)-C(23)	1.392(6)
C(3)-C(4)	1.391(7)	C(22)-C(27)	1.535(6)
C(4)-C(5)	1.393(6)	C(24)-C(26)	1.502(7)
C(5)-C(6)	1.408(6)	C(24)-C(25)	1.555(7)
C(5)-C(10)	1.529(7)	C(27)-C(29)	1.516(8)
C(7)-C(9)	1.513(7)	C(27)-C(28)	1.522(7)

Angles (°)

N(1)-Cr(1)-N(2)	99.52(18)	C(9)-C(7)-C(8)	109.3(4)
N(1)-Cr(1)-N(3)	98.10(18)	C(1)-C(7)-C(8)	111.8(4)
N(2)-Cr(1)-N(3)	90.02(12)	C(12)-C(10)-C(11)	110.4(4)
N(1)-Cr(1)-Cl(1)	102.48(16)	C(12)-C(10)-C(5)	110.8(4)
N(2)-Cr(1)-Cl(1)	157.42(10)	C(11)-C(10)-C(5)	113.3(4)
N(3)-Cr(1)-Cl(1)	91.86(9)	N(2)-C(14)-C(15)	122.8(3)
N(1)-Cr(1)-Cl(1)A	101.13(16)	N(2)-C(14)-C(13)	121.7(4)
N(2)-Cr(1)-Cl(1)A	90.60(9)	C(15)-C(14)-C(13)	115.5(4)
N(3)-Cr(1)-Cl(1)A	160.38(10)	C(14)-C(15)-C(16)	127.7(4)
Cl(1)-Cr(1)-Cl(1)A	80.27(4)	N(3)-C(16)-C(15)	123.1(3)
Cr(1)-Cl(1)-Cr(1)A	99.73(4)	N(3)-C(16)-C(17)	121.2(4)
C(14)-N(2)-C(6)	116.3(3)	C(15)-C(16)-C(17)	115.6(3)

C(14)-N(2)-Cr(1)	122.1(3)	C(19)-C(18)-C(23)	116.9(4)
C(6)-N(2)-Cr(1)	121.1(2)	C(19)-C(18)-C(24)	120.4(4)
C(16)-N(3)-C(23)	116.6(3)	C(23)-C(18)-C(24)	122.7(4)
C(16)-N(3)-Cr(1)	121.4(3)	C(20)-C(19)-C(18)	121.5(4)
C(23)-N(3)-Cr(1)	121.4(2)	C(21)-C(20)-C(19)	120.7(4)
C(2)-C(1)-C(6)	118.0(4)	C(20)-C(21)-C(22)	121.4(5)
C(2)-C(1)-C(7)	118.5(4)	C(23)-C(22)-C(21)	117.8(4)
C(6)-C(1)-C(7)	123.4(4)	C(23)-C(22)-C(27)	122.2(4)
C(3)-C(2)-C(1)	121.9(5)	C(21)-C(22)-C(27)	120.0(4)
C(2)-C(3)-C(4)	119.2(4)	C(22)-C(23)-C(18)	121.7(4)
C(3)-C(4)-C(5)	121.3(5)	C(22)-C(23)-N(3)	118.5(4)
C(4)-C(5)-C(6)	117.8(5)	C(18)-C(23)-N(3)	119.8(4)
C(4)-C(5)-C(10)	120.8(4)	C(26)-C(24)-C(18)	113.0(4)
C(6)-C(5)-C(10)	121.4(4)	C(26)-C(24)-C(25)	108.8(4)
C(1)-C(6)-C(5)	121.8(4)	C(18)-C(24)-C(25)	110.3(4)
C(1)-C(6)-N(2)	120.2(4)	C(29)-C(27)-C(28)	110.9(5)
C(5)-C(6)-N(2)	118.1(4)	C(29)-C(27)-C(22)	111.2(5)
C(9)-C(7)-C(1)	110.9(4)	C(28)-C(27)-C(22)	111.5(4)

The successful formation of **38** from **37** was encouraging. The transformation depicted in Scheme 3.29 could therefore be anticipated.

38, Ar = 2,6-diisopropylphenyl   **25**
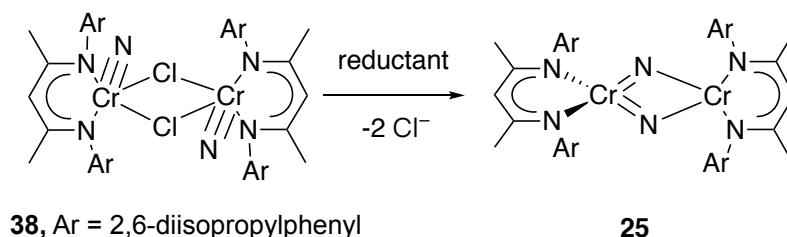
Scheme 3.29   The expected reduction of **38**

Addition of an excess of magnesium to a THF solution of **38** at room temperature effected a color change from orange to brown in 3.5 hours. After removal of solvent, the product was extracted with cold Et_2O and concentrated, cooled overnight to give a crystalline product in 62% yield. The ^1H NMR spectrum taken in C_6D_6 revealed that the resonances were identical to those observed resulting from the irradiation of **24**; the LIFDI mass spectrum supported the formation of **25** (m/z = 966.5842). The crystals collected were suitable for crystallographic analysis, therefore diffraction data was again collected for accurate structural determination (the initial crystal structure of **25** from photolysis of **24** was not of good quality). The new structure of **25** is shown in Figure 3.19 and its interatomic distances and angles are listed in Table 3.14.

25 crystallizes in the monoclinic space group $P2_1/c$. The gross structural features are of course identical to those of **25** described before (see p.159). Specifically, the two bridging nitrides are bonded unsymmetrically to the two chromium centers, just like those observed in the initial structure in Figure 3.2. With

more complete data collection, the better structure of **25** results in more precise structural information. Cr1 adopts distorted tetrahedral geometry while Cr2 is square planar (sum of the N-Cr-N angles is 360.53°). The bond distances between Cr1 and the two bridging nitrogen atoms are noticeably shorter (Cr1-N5 1.606(5) Å and Cr1-N6 1.783(6) Å) than those between Cr2 and the bridging nitrogen atoms (Cr2-N5 1.995(6) Å and Cr2-N6 2.139(5) Å). **25** is therefore described as a mixed-valent compound. The mixed-valent compound also influences the different bond distances between the chromium atoms and their coordinated nacnac ligands. These bond distances associated with the bridging $Cr_2(\mu\text{-N})_2$ core are shown in Figure 3.20.
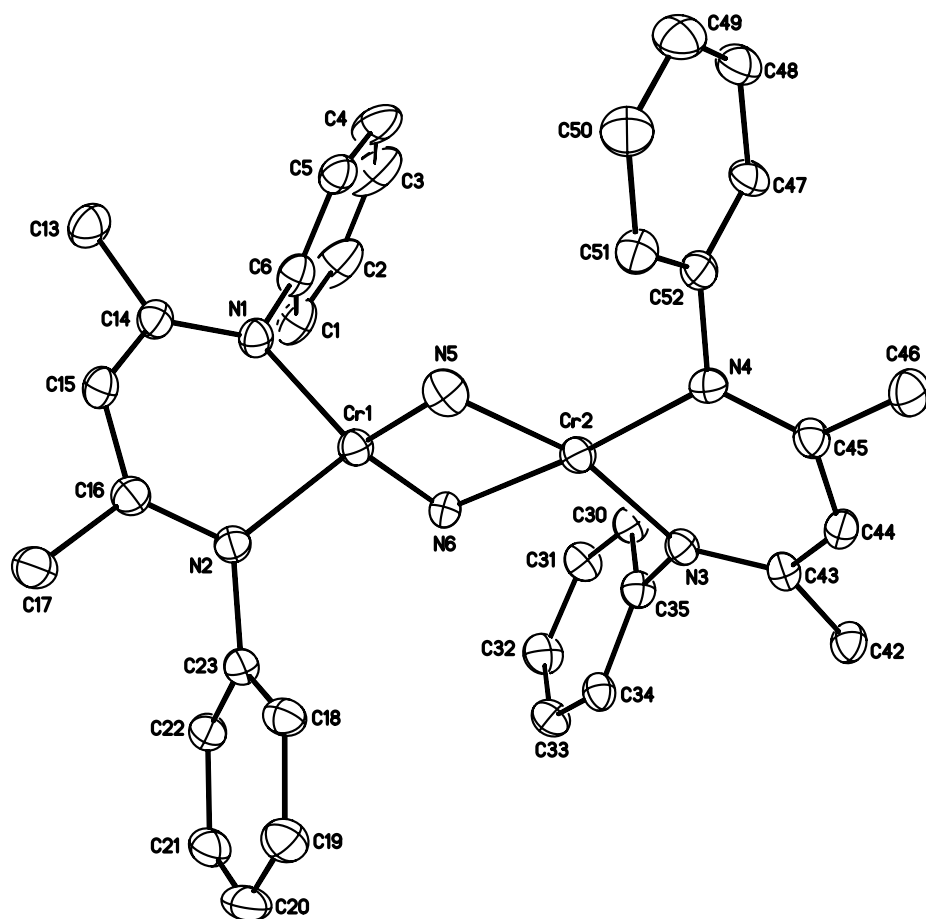
Figure 3.19 Molecular structure of $(L^{iPr}Cr)_2(\mu\text{-}N)_2$ (**25**) with better diffraction data. Ellipsoids are drawn at the 20% probability level. Hydrogen atoms and isopropyl groups have been omitted for clarity.
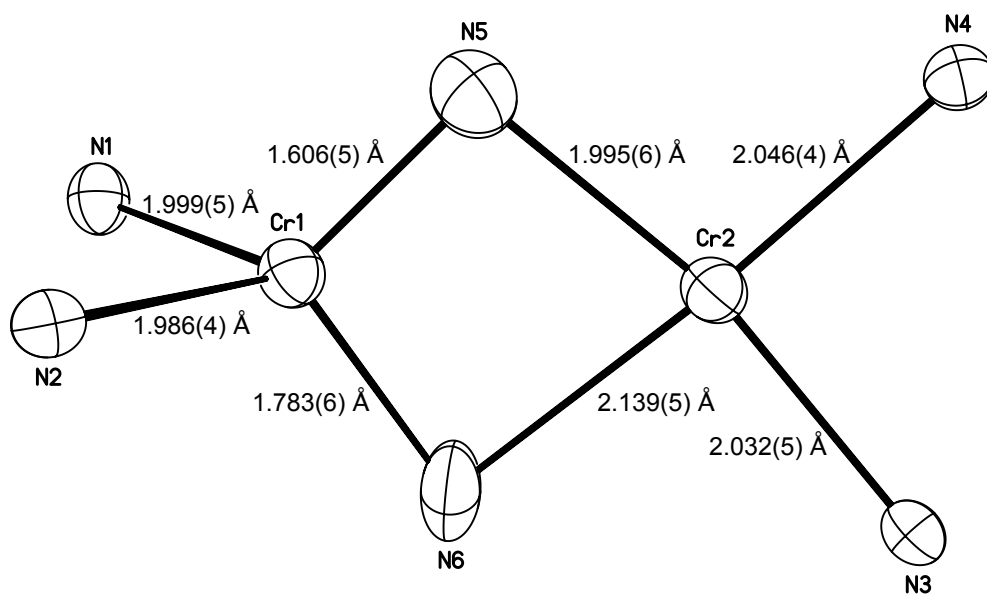
Figure 3.20 Structure of the molecule core of $(L^{iPr}Cr)_2(\mu\text{-}N)_2$ (**25**). Ellipsoids are drawn at the 20% probability level.

Table 3.14　Interatomic distances (Å) and angles (°) for $(L^{iPr}Cr)_2(\mu\text{-}N)_2$ (**25**)

Distances (Å)			
Cr(1)-N(5)	1.606(5)	C(20)-C(21)	1.373(9)
Cr(1)-N(6)	1.783(6)	C(21)-C(22)	1.385(8)
Cr(1)-N(2)	1.986(4)	C(22)-C(23)	1.411(7)
Cr(1)-N(1)	1.999(5)	C(22)-C(27)	1.522(8)
Cr(1)-Cr(2)	2.6843(12)	C(24)-C(25)	1.527(9)
Cr(2)-N(5)	1.995(6)	C(24)-C(26)	1.530(10)
Cr(2)-N(3)	2.032(5)	C(27)-C(28)	1.492(9)
Cr(2)-N(4)	2.046(4)	C(27)-C(29)	1.527(8)
Cr(2)-N(6)	2.139(5)	C(30)-C(31)	1.396(7)
N(1)-C(14)	1.329(7)	C(30)-C(35)	1.399(7)
N(1)-C(6)	1.442(7)	C(30)-C(36)	1.504(8)
N(2)-C(16)	1.348(7)	C(31)-C(32)	1.372(8)
N(2)-C(23)	1.452(7)	C(32)-C(33)	1.364(8)
N(3)-C(43)	1.321(6)	C(33)-C(34)	1.392(7)
N(3)-C(35)	1.475(6)	C(34)-C(35)	1.408(7)
N(4)-C(45)	1.346(7)	C(34)-C(39)	1.511(8)
N(4)-C(52)	1.458(7)	C(36)-C(37)	1.512(9)
C(1)-C(2)	1.402(9)	C(36)-C(38)	1.556(9)
C(1)-C(6)	1.418(8)	C(39)-C(41)	1.521(8)
C(1)-C(7)	1.519(10)	C(39)-C(40)	1.541(8)
C(2)-C(3)	1.350(12)	C(42)-C(43)	1.503(7)
C(3)-C(4)	1.391(11)	C(43)-C(44)	1.405(7)
C(4)-C(5)	1.392(9)	C(44)-C(45)	1.396(7)
C(5)-C(6)	1.397(8)	C(45)-C(46)	1.505(7)
C(5)-C(10)	1.524(9)	C(47)-C(48)	1.393(8)
C(7)-C(9)	1.522(9)	C(47)-C(52)	1.413(8)
C(7)-C(8)	1.529(9)	C(47)-C(53)	1.514(8)
C(10)-C(11)	1.524(9)	C(48)-C(49)	1.372(9)
C(10)-C(12)	1.528(9)	C(49)-C(50)	1.380(9)
C(13)-C(14)	1.513(8)	C(50)-C(51)	1.387(8)
C(14)-C(15)	1.402(8)	C(51)-C(52)	1.404(8)
C(15)-C(16)	1.385(8)	C(51)-C(56)	1.510(8)
C(16)-C(17)	1.528(8)	C(53)-C(54)	1.516(9)
C(18)-C(19)	1.388(8)	C(53)-C(55)	1.532(8)

C(18)-C(23)	1.404(8)	C(56)-C(57)	1.525(8)
C(18)-C(24)	1.499(8)	C(56)-C(58)	1.530(9)
C(19)-C(20)	1.374(8)		

Angles (°)

N(5)-Cr(1)-N(6)	100.3(3)	C(19)-C(18)-C(24)	119.6(5)
N(5)-Cr(1)-N(2)	118.6(2)	C(23)-C(18)-C(24)	123.5(5)
N(6)-Cr(1)-N(2)	116.1(2)	C(20)-C(19)-C(18)	121.9(6)
N(5)-Cr(1)-N(1)	113.2(2)	C(21)-C(20)-C(19)	120.5(6)
N(6)-Cr(1)-N(1)	114.6(2)	C(20)-C(21)-C(22)	120.7(6)
N(2)-Cr(1)-N(1)	95.01(19)	C(21)-C(22)-C(23)	117.9(6)
N(5)-Cr(1)-Cr(2)	47.7(2)	C(21)-C(22)-C(27)	119.2(5)
N(6)-Cr(1)-Cr(2)	52.65(17)	C(23)-C(22)-C(27)	122.8(5)
N(2)-Cr(1)-Cr(2)	133.90(14)	C(18)-C(23)-C(22)	122.0(5)
N(1)-Cr(1)-Cr(2)	131.03(14)	C(18)-C(23)-N(2)	120.3(5)
N(5)-Cr(2)-N(3)	166.06(19)	C(22)-C(23)-N(2)	117.8(5)
N(5)-Cr(2)-N(4)	99.15(19)	C(18)-C(24)-C(25)	110.2(6)
N(3)-Cr(2)-N(4)	91.80(17)	C(18)-C(24)-C(26)	112.3(5)
N(5)-Cr(2)-N(6)	78.0(2)	C(25)-C(24)-C(26)	109.8(6)
N(3)-Cr(2)-N(6)	91.58(19)	C(28)-C(27)-C(22)	112.0(5)
N(4)-Cr(2)-N(6)	175.39(19)	C(28)-C(27)-C(29)	108.9(5)
N(5)-Cr(2)-Cr(1)	36.54(14)	C(22)-C(27)-C(29)	111.1(6)
N(3)-Cr(2)-Cr(1)	132.09(11)	C(31)-C(30)-C(35)	117.1(5)
N(4)-Cr(2)-Cr(1)	135.67(14)	C(31)-C(30)-C(36)	119.4(5)
N(6)-Cr(2)-Cr(1)	41.50(17)	C(35)-C(30)-C(36)	123.5(5)
C(14)-N(1)-C(6)	120.1(5)	C(32)-C(31)-C(30)	121.6(6)
C(14)-N(1)-Cr(1)	119.9(4)	C(33)-C(32)-C(31)	119.8(5)
C(6)-N(1)-Cr(1)	119.7(4)	C(32)-C(33)-C(34)	122.5(6)
C(16)-N(2)-C(23)	116.8(4)	C(33)-C(34)-C(35)	116.4(5)
C(16)-N(2)-Cr(1)	118.5(4)	C(33)-C(34)-C(39)	120.0(5)
C(23)-N(2)-Cr(1)	124.7(3)	C(35)-C(34)-C(39)	123.6(5)
C(43)-N(3)-C(35)	118.6(5)	C(30)-C(35)-C(34)	122.6(5)
C(43)-N(3)-Cr(2)	124.9(3)	C(30)-C(35)-N(3)	118.5(5)
C(35)-N(3)-Cr(2)	116.5(3)	C(34)-C(35)-N(3)	118.8(5)
C(45)-N(4)-C(52)	116.6(4)	C(30)-C(36)-C(37)	111.8(6)
C(45)-N(4)-Cr(2)	122.1(3)	C(30)-C(36)-C(38)	110.0(5)

C(52)-N(4)-Cr(2)	121.3(3)	C(37)-C(36)-C(38)	110.1(6)
Cr(1)-N(5)-Cr(2)	95.8(3)	C(34)-C(39)-C(41)	112.3(5)
Cr(1)-N(6)-Cr(2)	85.8(3)	C(34)-C(39)-C(40)	111.1(5)
C(2)-C(1)-C(6)	116.1(7)	C(41)-C(39)-C(40)	108.2(5)
C(2)-C(1)-C(7)	122.5(7)	N(3)-C(43)-C(44)	122.7(5)
C(6)-C(1)-C(7)	121.5(6)	N(3)-C(43)-C(42)	121.5(5)
C(3)-C(2)-C(1)	122.8(8)	C(44)-C(43)-C(42)	115.8(5)
C(2)-C(3)-C(4)	119.8(7)	C(45)-C(44)-C(43)	129.5(5)
C(3)-C(4)-C(5)	121.5(8)	N(4)-C(45)-C(44)	123.9(5)
C(4)-C(5)-C(6)	117.2(7)	N(4)-C(45)-C(46)	120.6(5)
C(4)-C(5)-C(10)	119.3(7)	C(44)-C(45)-C(46)	115.3(5)
C(6)-C(5)-C(10)	123.5(6)	C(48)-C(47)-C(52)	117.0(6)
C(5)-C(6)-C(1)	122.7(6)	C(48)-C(47)-C(53)	118.8(5)
C(5)-C(6)-N(1)	119.3(5)	C(52)-C(47)-C(53)	124.1(5)
C(1)-C(6)-N(1)	117.9(6)	C(49)-C(48)-C(47)	122.3(6)
C(1)-C(7)-C(9)	110.9(7)	C(48)-C(49)-C(50)	119.5(6)
C(1)-C(7)-C(8)	113.1(6)	C(49)-C(50)-C(51)	121.5(7)
C(9)-C(7)-C(8)	111.3(6)	C(50)-C(51)-C(52)	118.1(6)
C(11)-C(10)-C(5)	112.5(6)	C(50)-C(51)-C(56)	118.8(6)
C(11)-C(10)-C(12)	108.8(6)	C(52)-C(51)-C(56)	123.0(5)
C(5)-C(10)-C(12)	111.8(6)	C(51)-C(52)-C(47)	121.5(5)
N(1)-C(14)-C(15)	123.4(5)	C(51)-C(52)-N(4)	120.3(5)
N(1)-C(14)-C(13)	119.9(6)	C(47)-C(52)-N(4)	118.2(5)
C(15)-C(14)-C(13)	116.7(6)	C(47)-C(53)-C(54)	110.9(6)
C(16)-C(15)-C(14)	129.0(6)	C(47)-C(53)-C(55)	112.4(5)
N(2)-C(16)-C(15)	124.7(5)	C(54)-C(53)-C(55)	111.1(6)
N(2)-C(16)-C(17)	119.2(5)	C(51)-C(56)-C(57)	111.2(5)
C(15)-C(16)-C(17)	116.0(5)	C(51)-C(56)-C(58)	113.1(6)
C(19)-C(18)-C(23)	116.8(5)	C(57)-C(56)-C(58)	110.2(6)

246

Considering the structural data provided, the candidates for formal oxidation state assignments are Cr^{VI}-Cr^{II} and Cr^{V}-Cr^{III} pairs. As discussed earlier (see p.206), the expected magnetic moments for Cr^{VI}-Cr^{II} and Cr^{V}-Cr^{III} (non-interacting ions) should be 4.8 μ_B and 4.2 μ_B respectively. The solid state effective magnetic moment of **25** taken at room temperature was measured to be 4.2μ_B, suggested the non-interacting Cr^{V}-Cr^{III} complex. This number is also consistent with that in **34**, $(*L^{iPr}Cr)_2(\mu\text{-}N)_2$, in which the solid state effective magnetic moment was measured to be 4.2 μ_B.

We then turned to X-ray photoelectron spectroscopy. It is used here to characterize the oxidation states of chromium in **25**. The XPS spectrum was obtained by irradiating **25** with an X-ray beam. By measuring the kinetic energy, the binding energy of the electrons can be determined. With these binding energies, the corresponding oxidation states can be assigned. For the Cr^{V}-Cr^{III} species, the binding energies of Cr $2p_{3/2}$ are expected to be 578 and 576 eV.[39-41] Figure 3.21 shows the Cr 2p region of **25**. The distinct peaks are at ~577 eV and ~586 eV, which are assigned to Cr $2p_{3/2}$ and Cr $2p_{1/2}$ signals respectively. The expected two signals for Cr^{V}-Cr^{III} were not clearly observed. The FWHM (full width at half maximum) of Cr $2p_{3/2}$ (~577 eV) signal was approximately 3 eV, and it was tentatively rationalized as the average of Cr^{V}-Cr^{III}.
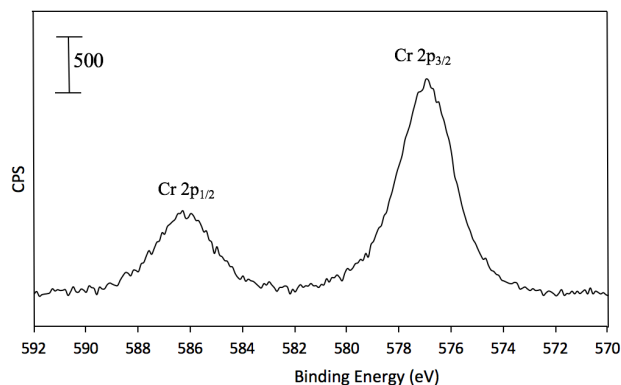
Figure 3.21 XPS investigation of the Cr 2p spectral region of **25**

To get a better understanding of the above result, additional XPS experiments were performed with a single oxidation state Cr(III) compound. As such, for $(L^{iPr}CrCl)_2(\mu\text{-}Cl)_2$, peak at ~576 eV was expected for Cr 2p$_{3/2}$. Figure 3.22 shows the result. The peak at 576 eV corresponded to the expected binding energy, but the FWHM was too large (~3 eV) for a single chemical oxidation state. This led to the speculation of the appropriate assignment for **25** (Cr^V-Cr^{III}). Therefore, the accurate assignment of mixed-valent **25** was not clearly resolved by the XPS technique.
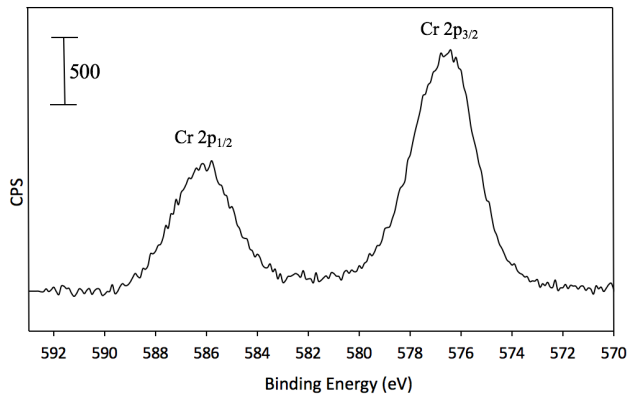

Figure 3.22 XPS investigation of the Cr 2p spectral region of $(L^{iPr}CrCl)_2(\mu\text{-}Cl)_2$

If the molecular structure of **25** in the solid state persists in solution, the ^{1}H NMR spectroscopy might show two backbone α-methyl proton signals due to the non-equivalence of the two β-diketiminate ligands. However, the ^{1}H NMR spectrum of **25** at room temperature showed one broad peak at 58 ppm, which was assigned as backbone α-methyl proton signal of β-diketiminate ligands. This observation is in line with the results obtained for the bis(μ-oxo) complex, $(L^{iPr}Cr)_2(\mu\text{-}O)_2$.[2] The molecular structure of $(L^{iPr}Cr)_2(\mu\text{-}O)_2$ also features an asymmetric core, with tetrahedral and square planar geometries of chromium centers. The bond distances between the bridging oxygen atoms to the chromiums are different, as what has been observed for **25**. It was described that a fluxional process equilibrating the two chromiums of $(L^{iPr}Cr)_2(\mu\text{-}O)_2$ was fast on the NMR time scale at room temperature. The structural observations of **25** and $(L^{iPr}Cr)_2(\mu\text{-}O)_2$ are similar. Therefore, the one set ligand signals of **25** observed at room temperature could be explained by the NMR spectroscopic results of $(L^{iPr}Cr)_2(\mu\text{-}O)_2$.[31] The proposed mechanism of fluxionality of **25** is shown in Scheme 3.30. A symmetric structure, in which all Cr-N bond distances were the same and both chromiums were tetrahedral coordinated, like those observed in **30** with L^{Me} ligand (see before, p.187), was considered as the intermediate during the molecular rearrangement.
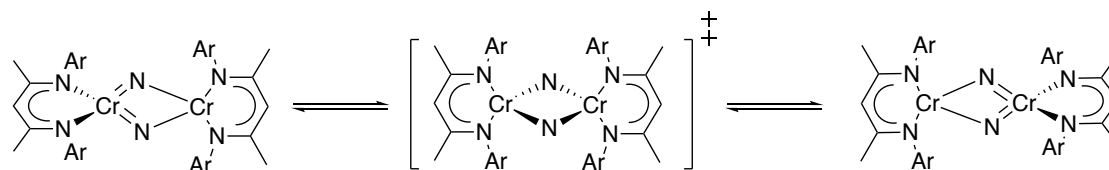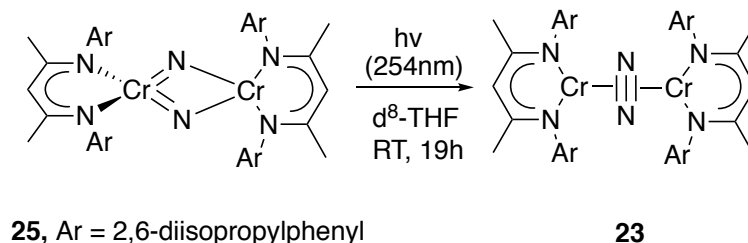

25, Ar = 2,6-diisopropylphenyl

Scheme 3.30   Proposed mechanism of the fluxionality of **25**

With a reasonable synthesis of **25** finally obtained, as depicted in Scheme 3.31, further reactivity of **25** was then explored (some included in **Appendix C**). First, **25** was irradiated in order to establish the consistency with the initial observation. Photolysis (254nm UV light) of **25** in a quartz NMR tube (with J. Young valve) in d^8-THF under vacuum led to N-N bond formation, producing the expected dinitrogen complex ($L^{iPr}Cr)_2(\mu_2-\eta^2:\eta^2-N_2)$ (**23**), quantitatively. The product was identified by ^{1}H NMR spectroscopy.[1] This transformation is illustrated in Scheme 3.32 and the spectroscopic evidence is shown in Figure 3.22. The ^{1}H NMR resonances of these two isomers bear a remarkable resemblance; one way to distinguish one from the other depends on the distinct characteristic peaks at 3.86 ppm for bis(μ-nitrido) **25** and 4.95 ppm for **23**.

Ar = 2,6-diisopropylphenyl   **37**   **38**   **25**
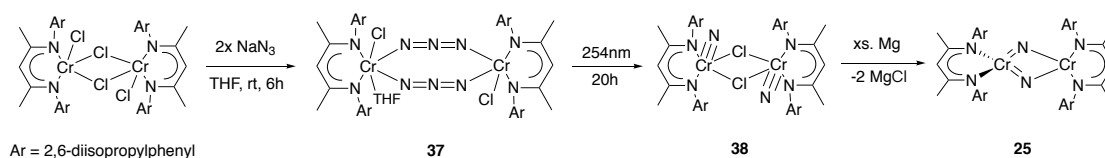
Scheme 3.31   Synthetic route to **25**

25, Ar = 2,6-diisopropylphenyl   **23**
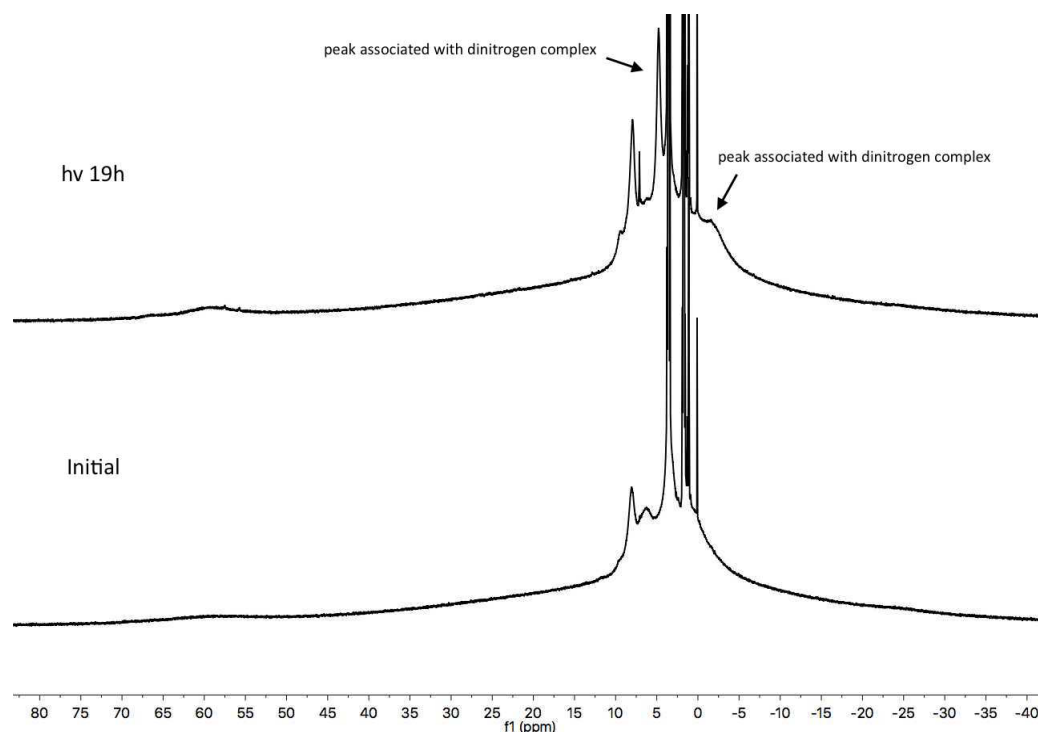
Scheme 3.32   Irradiation of **25**, producing **23**

Figure 3.22 ^{1}H NMR spectra during the photolysis of bis(μ-nitrido) complex **25** to **23** in d^8-THF, with resonances of **23** identified.

Meanwhile thermolysis of **25** (in C$_6$D$_6$) was also conducted and compared. By tracking ^{1}H NMR spectra, **25** was unchanged at 80°C for 24 hours, but it started to decompose after 24 hours heating at 110°C. The decomposition products at this point were unrecognizable; possible formation of **23** or (L^{iPr}Cr)$_2$(μ_2-η^6:η^6-C$_6$D$_6$) was ruled out by ^{1}H NMR analysis.[42] Attempts at the conversion in the opposite direction (**23** to **25**) were made. Photolysis of **23** with 254nm, 300nm or visible light for a day individually did not lead to any change by ^{1}H NMR spectroscopy. Heating **23** to 105°C for 16 hours led to decomposition, and **25** was not formed.

3.3 Conclusions

To summarize, the nitride isomer, $(L^{iPr}Cr)_2(\mu\text{-}N)_2$ (**25**), of the reported side-on bridged dinitrogen complex $(L^{iPr}Cr)_2(\mu_2\text{-}\eta^2{:}\eta^2\text{-}N_2)$ (**23**) was synthesized and characterized. The conversion from **25** to **23** was achieved by irradiating with 254nm UV lights but not thermally. Attempt to cleave the NN bond in **23** into **25** via thermal process was unsuccessful.

25, Ar = 2,6-diisopropylphenyl   **23**
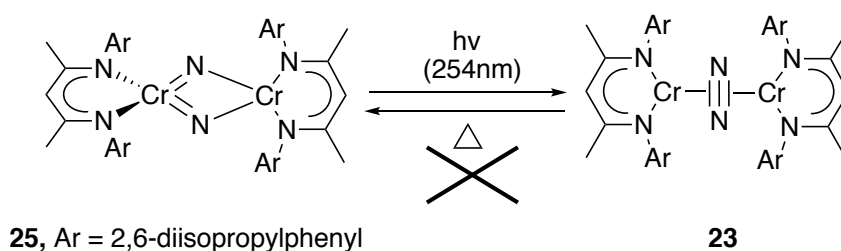
The bis(μ-nitrido) complexes supported by various nacnac ligands (L^{Me}, L^{Et}, $*L^{iPr}$) were also found along the way. Their geometrical structures provide some insights into the influence of steric factors by the substituents of nacnac ligands. The unsymmetric dichromium structure of **25** was thought due to the steric reason. The side-on bridged dinitrogen complex supported by L^{Et} ligand, $(L^{Et}Cr)_2(\mu_2\text{-}\eta^2{:}\eta^2\text{-}N_2)$ (**33**), was found during the irradiation of its chromium azido precursor. Despite the lack of observation of the conversion of **23** into **25**, it is anticipated that the groundwork laid out here could be of use for future studies of isomeric nitrogen complexes. Additionally, bis(μ-nitrido) **25** and its precursor, $(L^{iPr}Cr\equiv N)_2(\mu\text{-}Cl)_2$ (**38**), are worthy of study due to the possibility of functionalizing the nitride ligands. The preliminary reactivity studies have been carried out and are discussed in **Appendix C**. The explorations of nitrido complexes will be the focus of future studies.

3.4　Experimental

3.4.1　General Considerations

All manipulations were carried out with standard Schlenk, vacuum line, and glovebox techniques. Pentane, diethyl ether and toluene were degassed and dried by passing through activated alumina. Tetrahydrofuran was distilled from purple Na benzophenone/ketyl solutions. THF-d_8 and C_6D_6 were predried with sodium and stored under vacuum over Na/K alloy. CrI_2 was prepared according to a literature procedure.[43] $CrCl_2$ (anhydrous) was purchased from Strem Chemical Co. $CrCl_3(THF)_3$ was prepared according to a literature procedure.[44] NaN_3 was purchased from Aldrich. Lithium anthracenyl amide was synthesized according to a literature procedure.[32] All other reagents were purchased from Aldrich or Fisher/Acros and dried using standard procedures when necessary.

^{1}H NMR spectra were taken on a Bruker AVIII-400 spectrometer and were referenced to the residual protons of the solvent (C_6D_6, 7.15 ppm, THF-d_8 = 3.58 and 1.73 ppm). FT-IR spectra were obtained using a Nicolet Magna-IR 560 spectrometer with a resolution of 4 cm^{-1}. X-ray crystallographic studies were conducted at the University of Delaware X-ray Crystallography Laboratory. Elemental analyses were obtained from Robertson Microlit, Ledgewood, NJ. Mass spectra were obtained by the University of Delaware Mass Spectrometry Facility. Room temperature magnetic susceptibility measurements were carried out using a Johnson Matthey magnetic susceptibility balance. They were corrected for diamagnetism using Pascal constants and converted into effective magnetic moments.[45] Solution phase magnetic susceptibilities were determined by ^{1}H NMR spectroscopy via the Evans method [46] in C_6D_6 with C_6D_6 as an internal reference and reported after appropriate diamagnetic

corrections.[45] The photochemical reactor was a Rayonet Model RPR100, equipped with 16 14W monochromatic 254nm low-pressure mercury vapor lamps. X-ray photoelectron spectra were collected with a Thermo Scientific K-Alpha$^+$ instrument equipped with a monochromatic Al Kα source (hv = 1486.6 eV) at a takeoff angle normal to the surface and a base pressure of 5 x 10^{-9} mBar. The intense C 1s peak at 284.6 eV was used to calibrate the spectra.

3.4.2   Photochemical preparation of (L^{iPr}Cr)$_2$(μ-N)$_2$ (25)

(L^{iPr}Cr)$_2$(μ-N$_3$)$_2$ (**24**)[20] (0.20g, 0.20 mmol) was dissolved in 40 mL THF, giving a green solution. The solution was transferred into a quartz ampule and was stirred for 12 hours while being irradiated with 254nm UV light, during which time the color gradually changed to brown. The ampoule was brought back into the glovebox and the THF was removed in vacuo and the residue was extracted with pentane and concentrated, then cooled to -30°C overnight to yield red crystals of **25**.

3.4.3   Alternative preparation of (25)

(L^{iPr}Cr≡N)$_2$(μ-Cl)$_2$ (**38**) (0.10 g, 0.096 mmol) (see below) was dissolved in 15 mL THF, giving a red-orange solution. Magnesium turnings (0.023g, 0.96 mmol) were added and the solution stirred at room temperature for 3.5 hours, during which time the color gradually changed to orange-brown. The THF was then removed in vacuo and the residue was extracted with cold Et$_2$O and filtered through celite. The Et$_2$O solution was then concentrated to 4 mL and cooled to -30°C overnight to yield orange-red crystals of **25** (0.058 g, 62% yield). ^{1}H NMR (400 MHz, C$_6$D$_6$): 58.3 (br), 8.23 (br), 3.84 (br), -25.0 (br) ppm. IR (KBr): 3059 (w), 2963 (s), 2930 (s), 2867 (w), 1653 (w), 1530 (s), 1463 (s), 1437 (s), 1385 (s), 1365 (m), 1318 (s), 1255 (w), 1177 (w),

1102 (w), 1041 (w), 1021 (w), 968 (w), 936 (w), 798 (m), 760 (m) cm^{-1}. μ_{eff} (293K) = 4.2(1) μ_B. Mp: 169°C. UV/vis (THF): λ_{max} (ε) = 221 (11557), 314 (4347), 365 (5690), 420 (1314) (M^{-1}cm^{-1}). Mass Spectrum m/z (%): 966.5842 (100) [M$^+$]. Calcd. m/z: 966.5414 [M$^+$]. Anal. calcd. for C$_{70}$H$_{106}$N$_{10}$Cr$_2 \cdot$ C$_4$H$_8$O: C, 71.64; H, 8.73; N, 8.09. Found: C, 70.81; H, 8.67; N, 8.25.

3.4.4   Preparation of (L^{Me}Cr)$_4$(µ-N$_3$)$_4$ (26)

[L^{Me}Cr(THF)]$_2$(µ-Cl)$_2$ [21] (1.00 g, 1.08 mmol) was dissolved in 100 mL THF, giving a green solution. 15 equivalents of NaN$_3$ (1.05 g, 16.1 mmol) were added. The solution was stirred for 6 hours during which time the color changed to brown, and a precipitate was formed, making the solution cloudy. The THF was then removed in vacuo and the residue was extracted with pentanes and the extract filtered through celite. The resulting solution was concentrated to 10 mL and cooled to -30°C overnight to yield dark red crystals of **26** (0.352 g, 41% yield). ^{1}H NMR (400 MHz, C$_6$D$_6$): 91.2 (br), 87.5 (br), 9.16 (br), 8.21 (br), 6.37 (br), 6.09 (br), 5.72 (br), 5.19 (br), -4.6 (br), -6.6 (br) ppm. IR (KBr): 3019 (w), 2959 (m), 2920 (s), 2852 (w), 2190 (s), 2141 (s), 2110 (s), 2058 (s), 1526 (s), 1442 (s), 1388 (s), 1263 (m), 1243 (w), 1184 (s), 1096 (m), 1024 (m), 851 (m), 763 (s) cm^{-1}. μ_{eff} (293K) = 6.8(1) μ_B. Mp: 228°C. UV/vis (THF): λ_{max} (ε) = 279 (17657), 385 (19615), 488 (439), 613 (155) (M^{-1}cm^{-1}). Mass Spectrum m/z (%): 798.4797 (100) [M$^+$/2]. Calcd. m/z: 798.3032 [M$^+$/2].

3.4.5   Preparation of (L^{Et}Cr)$_4$(µ-N$_3$)$_4$ (27)

(L^{Et}Cr)$_2$(µ-Cl)$_2$ [20] (1.00 g, 1.11 mmol) was dissolved in 100 mL THF, giving a green solution. 15 equivalents of NaN$_3$ (1.09 g, 16.7 mmol) were added. The solution was stirred for 6 hours during which time the color changed to purple-brown, and a

precipitate was formed, making the solution cloudy. The THF was then removed in vacuo and the residue was extracted with pentanes and the extract filtered through celite. The resulting solution was concentrated to 10 mL and cooled to -30°C overnight to yield red crystals of **27** (0.355 g, 35% yield). ^{1}H NMR (400 MHz, C_6D_6): 103.9 (br), 91.7 (br), 84.5 (br), 80.0 (br), 9.16 (br), 7.76 (br), 6.44 (br), 4.66 (br), 3.93 (br), 0.21 (br), -3.97 (br) ppm. ^{1}H NMR (400 MHz, THF-d_8): 94.2 (br), 7.39 (br), 6.97 (br), 4.73 (br), 2.42 (br), -2.98 (br), -16.3 (br) ppm. IR (KBr): 3062 (w), 2963 (s), 2931 (s), 2874 (w), 2194 (s), 2149 (s), 2109 (s), 2056 (s), 1525 (s), 1443 (s), 1389 (s), 1327 (w), 1263 (s), 1178 (s), 1108 (m), 1023 (s), 859 (m), 803 (s), 764 (s) cm^{-1}. μ_{eff} (293K) = 7.0(1) μ_B. Mp: 204°C. UV/vis (THF): λ_{max} (ε) = 268 (29156), 379 (27989), 486 (1093), 632 (216) ($M^{-1}cm^{-1}$). Mass Spectrum m/z (%): 910.4492 (100) [M^+/2]. Calcd. m/z: 910.4285 [M^+/2]. Anal. calcd. for $C_{100}H_{132}N_{20}Cr_4$: C, 65.91; H, 7.3; N, 15.37. Found: C, 60.91; H, 6.86; N, 14.1.

3.4.6   Preparation of (*L^{iPr}Cr)$_2$(μ-N$_3$)$_2$ (28)

(*L^{iPr}Cr)$_2$(μ-Cl)$_2$ [23] (0.500 g, 0.424 mmol) was dissolved in 50 mL THF, giving a green solution. 15 equivalents of NaN$_3$ (0.413 g, 6.36 mmol) were added. The solution was stirred for 6 hours during which time the color changed to brown and a precipitate was formed, making the solution cloudy. The THF was then removed in vacuo and the residue was extracted with pentanes and the extract filtered through celite. The resulting green solution was concentrated to 8 mL and cooled to -30°C overnight to yield green crystals of **28** (0.380 g, 75% yield). ^{1}H NMR (400 MHz, THF-d_8): 7.91 (br), 1.88 (br), 1.05 (br), 0.62 (br) ppm. IR (KBr): 3059 (w), 2966 (s), 2930 (s), 2870 (w), 2126 (w), 2071 (s), 1525 (s), 1534 (w), 1482 (m), 1462 (m), 1431 (w), 1385 (m), 1346 (s), 1316 (s), 1271 (w), 1218 (w), 1136 (w), 1101 (w), 1054 (w),

956 (s), 789 (s) cm^{-1}. μ_{eff} (293K) = 5.3(1) μ_B. Mp: 203°C. UV/vis (THF): λ_{max} (ε) = 261 (31221), 404 (27170), 479 (423) (M^{-1}cm^{-1}). Mass Spectrum m/z (%): 1190.7505 (36) [M$^+$], 595.3770 (100) [M$^+$/2]. Calcd. m/z: 1190.7417 [M$^+$], 595.3707 [M$^+$/2]. Anal. calcd. for $C_{70}H_{106}N_{10}Cr_2$: C, 70.55; H, 8.97; N, 11.75. Found: C, 70.28; H, 8.84; N, 11.59.

3.4.7   Preparation of (*L^{Me}Cr)$_3$(μ-N$_3$)$_3$ (29)

(*L^{Me}Cr)$_2$(μ-Cl)$_2$ [23] (0.300 g, 0.314 mmol) was dissolved in 50 mL THF, giving a brown solution. 15 equivalents of NaN$_3$ (0.306 g, 4.71 mmol) were added. The solution was stirred for 6 hours during which time the color changed to green. The THF was then removed in vacuo and the residue was extracted with pentanes and the extract filtered through celite. The resulting solution was concentrated to 8 mL and cooled to -30°C overnight to yield green crystals of **29** (0.142 g, 47% yield). ^{1}H NMR (400 MHz, THF-d_8): 11.14 (br), 8.62 (br), 1.88 (br), -0.41 (br), -9.55 (br) ppm. IR (KBr): 3011 (w), 2959 (s), 2918 (s), 2871 (w), 2149 (s), 2104 (s), 2063 (s), 1534 (w), 1450 (s), 1467 (s), 1384 (s), 1362 (s), 1281 (m), 1216 (m), 1187 (m), 1161 (w), 1097 (w), 1030 (m), 968 (m), 766 (s) cm^{-1}. μ_{eff} (293K) = 5.9(1) μ_B. Mp: 214°C. UV/vis (THF): λ_{max} (ε) = 242 (24881), 309 (14218), 400 (15063), 512 (324) (M^{-1}cm^{-1}). Mass Spectrum m/z (%): 390.3077 (100) [*L^{Me+}]. Calcd. m/z: 390.3035. [M$^+$] was not detected.

3.4.8   Preparation of (L^{Et}Cr)$_2$(μ_2-η^2:η^2-N$_2$) (33)

(L^{Et}Cr)$_2$(μ-I)$_2$ [20] (0.20 g, 0.185 mmol) was dissolved into an Et$_2$O-THF mixture (v:v = 4:1), giving a green solution. 2.0 equivalent of KC$_8$ [47] (0.050 g, 0.37 mmol) were added piece-wise over the course of 2 minutes. The solution was stirred for 10

minutes during which time the color changed to brown. The solvents were then removed in vacuo and the residue was extracted with pentanes and the extract filtered through celite. The resulting solution was concentrated to 5 mL and cooled to -30°C overnight to yield red crystals of **33** (0.030 g, 19% yield). ^{1}H NMR (400 MHz, C_6D_6): 61.0 (br), 11.41 (br), 7.98 (br), 3.39 (br), 1.35 (br) ppm. IR (KBr): 3062 (w), 2963 (s), 2930 (s), 2874 (m), 1525 (s), 1443 (s), 1391 (s), 1328 (w), 1264 (s), 1180 (s), 1106 (m), 1024 (s), 978 (m), 851 (m), 803 (s), 764 (s), 669 (m), 598 (m) cm^{-1}. μ_{eff} (293K) = 4.2(1) μ_B. Mp: 215°C. Mass Spectrum m/z (%): 854.4266 (2) [M$^+$]. Calcd. m/z: 854.4162 [M$^+$].

3.4.9 Preparation of (*L^{iPr}Cr)$_2$(μ-N)$_2$ (34)

(*L^{iPr}Cr)$_2$(μ-N$_3$)$_2$ (**28**) (0.15 g, 0.13 mmol) was dissolved in 30 mL THF, giving a green solution. The solution was transferred into a quartz ampule and was stirred for 24 hours while being irradiated with 254nm UV light, during which time the color gradually changed to orange-brown. The ampoule was then brought back into the glovebox, where THF was removed in vacuo and the residue was extracted with pentanes and filtered through celite. The resulting solution was concentrated to 2.5 mL and 2.5 mL of diethyl ether were added (the mixture of solvents were found to be a better condition for recrystallization), then cooled to -30°C overnight to yield brown-red crystals of **34** (0.050 g, 35% yield). ^{1}H NMR (400 MHz, C_6D_6): 12.07 (br), 8.81 (br), 6.68 (br), 4.18 (br), 2.11 (br), 1.60 (br) ppm. IR (KBr): 3058 (w), 2963 (s), 2930 (s), 2870 (w), 1630 (w), 1536 (w), 1465 (s), 1431 (w), 1384 (m), 1363 (m), 1321 (w), 1256 (w), 1215 (w), 1182 (w), 1120 (w), 1097 (w), 1011(w), 902 (m), 796 (s) cm^{-1}. μ_{eff} (293K) = 4.2(1) μ_B. Mp: 163°C. UV/vis (THF): λ_{max} (ε) = 230 (27065), 327

(13188), 376 (11128), 438 (8366), 559 (1069) (M^{-1}cm^{-1}). Mass Spectrum m/z (%): 1135.7704 (100) [M$^+$]. Calcd. m/z: 1135.7317 [M$^+$].

3.4.10 Preparation of (*L^{iPr}Cr)(μ-NAr)(μ-NC(^{t}Bu)CH(^{t}Bu)CNAr)(μ$_3$-Cr) (Ar = 2,6-diisopropylphenyl) (35)

(*L^{iPr}Cr)$_2$(μ-N$_3$)$_2$ (28) (0.10 g, 0.084 mmol) was dissolved in 20 mL THF giving a green solution. The solution was transferred into a quartz ampule and was stirred for 2 days while being irradiated with 254nm UV light, during which time the color gradually changed to dark brown-red. The THF was then removed in vacuo and the residue was extracted with diethyl ether and filtered through celite. The resulting solution was concentrated to 2.5 mL then cooled to -30°C overnight to yield dark red crystals of 35 (0.045 g, 48% yield). ^{1}H NMR (400 MHz, C$_6$D$_6$): 17.2 (br), 8.69 (br), 7.73 (br), 6.80 (br), 5.67 (br), 4.32 (br), 3.93 (br), 3.15 (br), 2.64 (br), 2.08 (br), 0.56 (br), -0.04 (br) ppm. IR (KBr): 3062 (w), 2965 (s), 2922 (s), 2867 (w), 1630 (w), 1583 (w), 1544 (w), 1465 (s), 1385 (m), 1353 (m), 1318 (w), 1254 (w), 1221 (w), 1108 (w), 1058 (w), 969 (w), 933 (m), 800 (s) cm^{-1}. μ$_{eff}$ (293K) = 3.0(1) μ$_B$. Mp: 254°C. Mass Spectrum m/z: 1121.7612 [M$^+$]. Calcd. m/z: 1121.7286 [M$^+$].

3.4.11 Preparation of L^{iPr}Cr(dbabh) (36)

(L^{iPr}Cr)$_2$(μ-Cl)$_2$ [30] (0.10 g, 0.099 mmol) was dissolved in 15 mL diethyl ether giving a green solution. 2 equivalents of [Li(dbabh)(OEt$_2$)] in diethyl ether (0.054 g, 0.20 mmol) were added dropwise with stirring over 1 minute. The solution was stirred for 3 hours during which time the color changed to brown. The solvent was then removed in vacuo and the residue was extracted with pentane and the extract filtered through celite. The resulting solution was concentrated to 2 mL then cooled to -30°C overnight to yield brown crystals of 36 (0.076 g, 58% yield). ^{1}H NMR (400 MHz,

C_6D_6): 12.07 (br), 9.82 (br), 5.79 (br), -5.2 (br) ppm. IR (KBr): 3058 (w), 2962 (s), 2926 (s), 2867 (w), 1645 (w), 1528 (s), 1461 (m), 1438 (m), 1384 (s), 1319 (s), 1254 (m), 1176 (m), 1104 (w), 1019 (w), 966 (s), 935 (s), 799 (s), 761 (s), 715 (w) cm^{-1}. μ_{eff} (293K in solution state by Evans method) = 4.6(1) μ_B. Mp: 119°C. UV/vis (THF): λ_{max} (ε) = 215 (61887), 254 (11963), 309 (15987), 379 (17157), 505 (287) ($M^{-1}cm^{-1}$). Mass Spectrum m/z (%): 661.3734 (100) [M^+]. Calcd. m/z: 661.3489 [M^+].

3.4.12 Preparation of ($L^{iPr}CrCl)_2(THF)(\mu-N_3)_2$ (37)

($L^{iPr}CrCl)_2(\mu-Cl)_2$ [34] (0.500 g, 0.463 mmol) was dissolved in 30 mL THF giving a brown solution. 2 equivalents of NaN_3 (0.060 g, 0.925 mmol) were added. The solution was stirred for 6 hours during which time the color changed to dark red. The THF was then removed in vacuo and the residue was extracted with cold Et_2O and the extract filtered through celite. The resulting solution was concentrated to 8 mL then cooled to -30°C overnight to yield brown-red crystals of **37** (0.340 g, 63% yield). ^{1}H NMR (400 MHz, THF-d_8): 59.6 (br), 36.9 (br), 19.6 (br), 17.8 (br), 6.13 (br), 2.20 (br), 1.09 (br), -56.5 (br) ppm. IR (KBr): 3057 (w), 2966 (s), 2930 (s), 2868 (w), 2117 (s), 2060 (s), 1529 (s), 1463 (m), 1435 (m), 1397 (s), 1315 (s), 1253 (m), 1171 (s), 1105 (m), 1020 (s), 935 (m), 857 (m), 797 (s), 761 (m) cm^{-1}. μ_{eff} (293K) = 3.3(1) μ_B. Mp: 205°C. UV/vis (THF): λ_{max} (ε) = 288 (13432), 387 (14063), 496 (606) ($M^{-1}cm^{-1}$). Mass Spectrum m/z (%): 546.2487 (100) [(M^+-$C_4H_8O)/2$]. Calcd. m/z: 546.2456 [(M^+-$C_4H_8O)/2$].

3.4.13 Preparation of ($L^{iPr}Cr{\equiv}N)_2(\mu-Cl)_2$ (38)

($L^{iPr}CrCl)_2(THF)(\mu-N_3)_2$ (**37**) (0.15 g, 0.13 mmol) was dissolved in 30 mL THF, giving a red-orange solution. The solution was transferred into a quartz ampule

and was stirred for 20 hours while being irradiated with 254nm UV light, during which time the color gradually changed to orange-brown. The ampoule was brought back into the glovebox, where the THF was removed in vacuo and the residue was washed with cold Et_2O to remove impurities (($L^{iPr}Cr)_2(\mu-Cl)_2$ was detected in the crude Et_2O wash). The Et_2O insoluble pink-red solids collected were further redissolved in THF, concentrated to 4 mL, then cooled to -30°C overnight to yield pink crystals of **38** (0.060 g, 45% yield). ^1H NMR (400 MHz, C_6D_6): 9.02 (br), 5.83 (br), 1.38 (br), 0.58 (br) ppm. IR (KBr): 3058 (w), 2962 (s), 2927 (s), 2868 (w), 1532 (s), 1463 (w), 1437 (w), 1393 (s), 1317 (s), 1254 (w), 1176 (w), 1110 (w), 1057 (w), 1042 (w), 1024(w), 1008 (w), 937 (m), 858 (w), 796 (w), 760 (w) cm^{-1}. μ_{eff} (293K in solution state by Evans method) = 2.7(1) μ_B. Mp: >300°C. Mass Spectrum m/z (%): 518.2442 (100) $[M^+/2]$. Calcd. m/z: 518.2395 $[M^+/2]$.

Table 3.15	25 kla0915	26 kla0735	27 kla0829
Formula	$C_{58}H_{82}Cr_2N_6$	$C_{84}H_{100}Cr_4N_{20}$	$C_{104}H_{140}Cr_4N_{20}O$
Formula wt., g/mol	967.29	1597.83	1894.35
Temp, K	200(2)	200(2)	293(2)
Wavelength, Å	1.54178	1.54178	1.54178
Crystal size, mm	0.080 x 0.141 x 0.218	0.150 x 0.342 x 0.504	0.138 x 0.152 x 0.591
Color	orange-red	red	brown-purple
Crystal system	monoclinic	monoclinic	triclinic
Space group	$P\,2_1/c$	$P\,2_1/c$	$P\,\bar{1}$
a, Å	14.6304(3)	14.7105(4)	12.3062(3)
b, Å	14.0806(3)	21.0981(5)	16.2572(4)
c, Å	26.8298(6)	28.6107(7)	28.4069(6)
α, deg	90	90	97.8080(10)
β, deg	95.1280(10)	101.7800(10)	91.4980(10)
γ, deg	90	90	111.4540(10)
Volume, Å^3	5504.9(2)	8692.7(4)	5222.6(2)
Z	4	4	2
D(calcd), g/cm^3	1.167	1.221	1.205
Abs. coefficient, mm^{-1}	3.554	4.43	3.768
T_{max}/T_{min}	0.7539/0.5356	0.7538/0.4234	0.7538/0.4702
Data/restraints/params	10925/0/615	17584/0/997	20485/9/1188
GOF on F^2	1.025	1.079	1.039
Final R indices, I>2σ(I)	R1 = 0.0846, wR^2 = 0.2070	R1 = 0.0806, wR^2 = 0.1939	R1 = 0.1043, wR^2 = 0.2746
R indices (all data)	R1 = 0.1819, wR^2 = 0.2660	R1 = 0.1464, wR^2 = 0.2435	R1 = 0.1759, wR^2 = 0.3353

Table 3.16	28	29	30
	kla0864	kla0873	kla0759
Formula	$C_{70}H_{106}Cr_2N_{10}$	$C_{81}H_{111}Cr_3N_{15}$	$C_{42}H_{50}Cr_2N_6$
Formula wt., g/mol	1191.64	1450.84	742.88
Temp, K	200(2)	200(2)	200(2)
Wavelength, Å	1.54178	1.54178	0.71073
Crystal size, mm	0.153 x 0.227 x 0.230	0.104 x 0.231 x 0.258	0.144 x 0.236 x 0.371
Color	purple-green	green-brown	brown-red
Crystal system	monoclinic	triclinic	monoclinic
Space group	$P\,2_1/n$	$P\,\overline{1}$	$P\,2_1/n$
a, Å	16.0547(9)	12.2301(2)	12.9326(12)
b, Å	9.6124(5)	18.3373(3)	8.7778(8)
c, Å	23.1284(12)	20.3419(3)	17.0722(17)
α, deg	90	69.5640(10)	90
β, deg	103.865(3)	75.8680(10)	105.270(2)
γ, deg	90	83.7510(10)	90
Volume, Å^3	3465.3(3)	4144.12(12)	1869.6(3)
Z	2	2	2
D(calcd), g/cm^3	1.142	1.163	1.32
Abs. coefficient, mm^{-1}	2.926	3.564	0.62
T_{max}/T_{min}	0.7538/0.5712	0.7538/0.6104	0.7456/0.6866
Data/restraints/params	6929/0/384	15898/0/922	4310/0/232
GOF on F^2	1.087	1.023	1.046
Final R indices, I>2σ(I)	R1 = 0.0805, wR^2 = 0.2153	R1 = 0.0678, wR^2 = 0.1799	R1 = 0.0460, wR^2 = 0.1196
R indices (all data)	R1 = 0.1467, wR^2 = 0.2617	R1 = 0.1288, wR^2 = 0.2237	R1 = 0.0639, wR^2 = 0.1297

Table 3.17	31	32	33
	kla0739	**kla0866**	**kla0845**
Formula	$C_{67}H_{85}Cr_3N_{11}O$	$C_{50}H_{66}Cr_2N_{4.91}O_{1.08}$	$C_{50}H_{66}Cr_2N_6$
Formula wt., g/mol	1216.45	857.24	855.08
Temp, K	200(2)	200(2)	200(2)
Wavelength, Å	0.71073	0.71073	0.71073
Crystal size, mm	0.121 x 0.225 x 0.311	0.141 x 0.232 x 0.282	0.375 x 0.397 x 0.579
Color	brown	red-orange	red
Crystal system	triclinic	monoclinic	triclinic
Space group	$P\bar{1}$	$P2_1/n$	$P\bar{1}$
a, Å	12.4070(9)	13.496(3)	8.7893(11)
b, Å	12.5704(9)	12.003(3)	12.1991(16)
c, Å	21.9565(16)	15.258(3)	12.7037(17)
α, deg	82.2200(10)	90	61.824(2)
β, deg	73.8800(10)	109.773(4)	77.754(2)
γ, deg	81.4000(10)	90	89.187(2)
Volume, $Å^3$	3236.8(4)	2326.0(8)	1167.5(3)
Z	2	2	1
D(calcd), g/cm^3	1.248	1.224	1.216
Abs. coefficient, mm^{-1}	0.544	0.508	0.505
T_{max}/T_{min}	0.9370/0.8490	0.7456/0.6748	0.7456/0.6811
Data/restraints/params	14946/0/759	5346/22/272	5364/0/268
GOF on F^2	1.000	1.118	1.041
Final R indices, I>2σ(I)	R1 = 0.0615, wR^2 = 0.1332	R1 = 0.0679, wR^2 = 0.1778	R1 = 0.0405, wR^2 = 0.1032
R indices (all data)	R1 = 0.1117, wR^2 = 0.1595	R1 = 0.1092, wR^2 = 0.2036	R1 = 0.0512, wR^2 = 0.1117

Table 3.18	34	35	36
	kla0872	**kla0882**	**kla0862**
Formula	$C_{70}H_{106}Cr_2N_6$	$C_{70}H_{106}Cr_2N_5$	$C_{43}H_{51}CrN_3$
Formula wt., g/mol	1135.6	1121.59	661.86
Temp, K	200(2)	200(2)	200(2)
Wavelength, Å	1.54178	0.71073	0.71073
Crystal size, mm	0.238 x 0.353 x 0.366	0.477 x 0.632 x 0.853	0.270 x 0.311 x 0.476
Color	orange	red	orange-green
Crystal system	monoclinic	monoclinic	orthorhombic
Space group	$C\,2/c$	$P\,2_1/c$	$C\,m\,c\,2_1$
a, Å	23.9486(5)	17.2393(12)	18.6558(14)
b, Å	12.3153(3)	20.2173(14)	17.4768(12)
c, Å	26.1078(6)	19.7204(14)	14.6081(10)
α, deg	90	90	90
β, deg	111.4650(10)	93.8360(10)	90
γ, deg	90	90	90
Volume, Å^3	7166.0(3)	6857.8(8)	4762.9(6)
Z	4	4	4
D(calcd), g/cm^3	1.053	1.086	0.923
Abs. coefficient, mm^{-1}	2.791	0.357	0.266
T_{max}/T_{min}	0.7538/0.5206	0.7456/0.6694	0.7456/0.6940
Data/restraints/params	7112/0/375	15792/0/722	5608/1/225
GOF on F^2	0.970	1.023	1.049
Final R indices, I>2σ(I)	R1 = 0.0890, wR^2 = 0.2229	R1 = 0.0509, wR^2 = 0.1259	R1 = 0.0435, wR^2 = 0.1152
R indices (all data)	R1 = 0.1503, wR^2 = 0.2748	R1 = 0.0862, wR^2 = 0.1508	R1 = 0.0587, wR^2 = 0.1230

Table 3.19	37	38
	kla0903	**kla0917**
Formula	$C_{62}H_{90}Cl_2Cr_2N_{10}O$	$C_{58}H_{82}Cl_2Cr_2N_6$
Formula wt., g/mol	1166.33	1038.19
Temp, K	200(2)	200(2)
Wavelength, Å	1.54178	1.54178
Crystal size, mm	0.198 x 0.225 x 0.267	0.087 x 0.126 x 0.252
Color	brown-red	pink
Crystal system	monoclinic	monoclinic
Space group	$P\,2_1/n$	$P\,2_1/n$
a, Å	15.2980(3)	14.3244(4)
b, Å	21.3975(4)	13.3722(4)
c, Å	22.6653(5)	15.1893(4)
α, deg	90	90
β, deg	104.4950(10)	104.1705(19)
γ, deg	90	90
Volume, Å^3	7183.1(3)	2820.96(14)
Z	4	2
D(calcd), g/cm^3	1.079	1.222
Abs. coefficient, mm^{-1}	3.494	4.352
T_{max}/T_{min}	0.7538/0.6134	0.7538/0.6198
Data/restraints/params	14494/42/714	5611/0/317
GOF on F^2	1.071	1.076
Final R indices, I>2σ(I)	R1 = 0.0662, wR^2 = 0.1816	R1 = 0.0668, wR^2 = 0.1902
R indices (all data)	R1 = 0.1098, wR^2 = 0.2114	R1 = 0.1194, wR^2 = 0.2329

REFERENCES

1.   Monillas, W. H.; Yap, G. P. A.; MacAdams, L. A.; Theopold, K. H., *J. Am. Chem. Soc.* **2007,** *129* (26), 8090.

2.   Dai, F.; Yap, G.; Theopold, K., *J. Am. Chem. Soc.* **2013,** *135* (45), 16774.

3.   Laplaza, C.; Cummins, C., *Science* **1995,** *268* (5212), 861.

4.   Solari, E.; Da Silva, C.; Iacono, B.; Hesschenbrouck, J.; Rizzoli, C.; Scopelliti, R.; Floriani, C., *Angew. Chem. Int. Ed.* **2001,** *40* (20), 3907.

5.   Fryzuk, M.; Kozak, C.; Bowdridge, M.; Patrick, B.; Rettig, S., *J. Am. Chem. Soc.* **2002,** *124* (28), 8389.

6.   Hirotsu, M.; Fontaine, P.; Epshteyn, A.; Zavalij, P.; Sita, L., *J. Am. Chem. Soc.* **2007,** *129* (30), 9284.

7.   Curley, J.; Cook, T.; Reece, S.; Muller, P.; Cummins, C., *J. Am. Chem. Soc.* **2008,** *130* (29), 9394.

8.   Keane, A.; Yonke, B.; Hirotsu, M.; Zavalij, P.; Sita, L., *J. Am. Chem. Soc.* **2014,** *136* (28), 9906.

9.   Miyazaki, T.; Tanaka, H.; Tanabe, Y.; Yuki, M.; Nakajima, K.; Yoshizawa, K.; Nishibayashi, Y., *Angew. Chem. Int. Ed.* **2014,** *53* (43), 11488.

10.   Keane, A.; Farrell, W.; Yonke, B.; Zavalij, P.; Sita, L., *Angew. Chem. Int. Ed.* **2015,** *54* (35), 10220.

11.   Kunkely, H.; Vogler, A., *Angew. Chem. Int. Ed.* **2010,** *49* (9), 1591.

12.   Tanabe, Y.; Nishibayashi, Y., *Chem. Rec.* **2016,** *16* (3), 1549.

13.   Hirotsu, M.; Fontaine, P.; Epshteyn, A.; Zavalij, P.; Sita, L., *J. Am. Chem. Soc.* **2007,** *129* (30), 9284.

14.   Fontaine, P.; Yonke, B.; Zavalij, P.; Sita, L., *J. Am. Chem. Soc.* **2010,** *132* (35), 12273.

15. Buhr, J.; Taube, H., *Inorg. Chem.* **1979,** *18* (8), 2208.

16. Seymore, S.; Brown, S., *Inorg. Chem.* **2002,** *41* (3), 462.

17. Man, W.; Tang, T.; Wong, T.; Lau, T.; Peng, S.; Wong, W., *J. Am. Chem. Soc.* **2004,** *126* (2), 478.

18. Betley, T.; Peters, J., *J. Am. Chem. Soc.* **2004,** *126* (20), 6252.

19. Tran, B.; Pinter, B.; Nichols, A.; Konopka, F.; Thompson, R.; Chen, C.; Krzystek, J.; Ozarowski, A.; Telser, J.; Baik, M.; Meyer, K.; Mindiola, D., *J. Am. Chem. Soc.* **2012,** *134* (31), 13035.

20. Monillas, W. H. University of Delaware Ph.D. thesis, 2009.

21. Charbonneau, F.; Oguadinma, P.; Schaper, F., *Inorg. Chem. Acta.* **2010,** *363* (8), 1779.

22. Budzelaar, P.; van Oort, A.; Orpen, A., *Eur. J. Inorg. Chem.* **1998,** (10), 1485.

23. BinTaleb, A. M. University of Delaware Ph.D. thesis, 2006.

24. Another crystallographic data collection of 10 was performed, with the same crystal unit cell, giving the bridging oxygen to nitrogen atoms in a ratio of 1 to 0.37.

25. Odom, A.; Cummins, C., *Organometallics* **1996,** *15* (3), 898.

26. Camp, C.; Arnold, J., *Dalton Trans.* **2016,** *45* (37), 14462.

27. Tran, B.; Krzystek, J.; Ozarowski, A.; Chen, C.; Pink, M.; Karty, J.; Telser, J.; Meyer, K.; Mindiola, D., *Eur. J. Inorg. Chem.* **2013,** *2013* (22-23), 3916.

28. Bhattacharya, P.; Heiden, Z.; Wiedner, E.; Raugei, S.; Piro, N.; Kassel, W.; Bullock, R.; Mock, M., *J. Am. Chem. Soc.* **2017,** *139* (8), 2916.

29. Hill, C.; Hollander, F., *J. Am. Chem. Soc.* **1982,** *104* (25), 7318.

30. MacAdams, L. A. University of Delaware Ph.D. thesis, 2002.

31. Dai, F. University of Delaware Ph.D. thesis, 2012.

32. Carpino, L.; Padykula, R.; Barr, D.; Hall, F.; Krause, J.; Dufresne, R.; Thoman, C., *J. Org. Chem.* **1988,** *53* (11), 2565.

33. Mindiola, D.; Cummins, C., *Angew. Chem. Int. Ed.* **1998,** *37* (7), 945.

34. Gibson, V.; Newton, C.; Redshaw, C.; Solan, G.; White, A.; Williams, D., *Eur. J. Inorg. Chem.* **2001,** (7), 1895.

35. Odom, A.; Cummins, C.; Protasiewicz, J., *J. Am. Chem. Soc.* **1995,** *117* (24), 6613.

36. Volp, K.; Dehnicke, K.; Fenske, D., *Z. Anorg. Allg. Chem.* **1989,** *572* (5), 26.

37. Khabou, A.; Dehnicke, K.; Findeisen, K.; Fenske, D., *Z. Naturforsch.* **1988,** *43b* (12), 1616.

38. Hagenbach, A.; Strahle, J., *Z. Anorg. Allg. Chem.* **2001,** *627* (4), 726.

39. Hanafi, Z.; Ismail, F.; Mohamed, A., *Zeitschrift Fur Physikalische Chemie-International Journal of Research in Physical Chemistry & Chemical Physics* **1996,** *194*, 61.

40. Liu, R.; Conradie, J.; Erasmus, E., *J. Electron Spectrosc. Relat. Phenom.* **2016,** *206*, 46.

41. Hanafi, Z.; Ismail, F.; Mohamed, A., *Appl. Surf. Sci.* **1996,** *194*, 61.

42. Monillas, W.; Yap, G.; Theopold, K., *Angew. Chem. Int. Ed.* **2007,** *46* (35), 6692.

43. Brauer, G., *Handbook of preparative inorganic chemistry*. Second edition ed.; 1963.

44. Shamir, J., *Inorg. Chem. Acta.* **1989,** *156* (2), 163.

45. Bain, G.; Berry, J., *J. Chem. Educ.* **2008,** *85* (4), 532.

46. Evans, D., *J. Chem. Soc.* **1959**, 2003.

47. Savoia, D.; Trombini, C.; Umanironchi, A., *Pure Appl. Chem.* **1985,** *57* (12), 1887.

Appendix A

SUPPLEMENTAL INFORMATION FOR CHAPTER 1

A.1 PROPOSED MECHANISM

Chapter 1 has described the reaction of $(L^{iPr}Cr)_2(\mu\text{-H})_2$ with 1.0 equiv. of trimethylsilyl-diazomethane, and it gave the only isolable product $(L^{iPr}Cr)_2(\mu\text{-N})(\mu\text{-N(H)NC(H)SiMe}_3)$ (**9**). A re-examination of the mixture of products from the reaction with L^{Me}, mass of $(L^{Me}Cr)_2(\mu\text{-N})(\mu\text{-N(H)NC(H)SiMe}_3)$ (**9'**) was located. **9'** is therefore considered as a potential intermediate. Scheme A.1 is shown and it includes all the complexes that were found. There was no evidence for the formation of dinitrogen complexes in this reaction. The multinuclear complexes **3, 4** and **6** are grouped together for simplicity. The rest of the complexes including **9'** are grouped separately. This crude mechanism represents only one of the possibilities by which this reaction may occur.
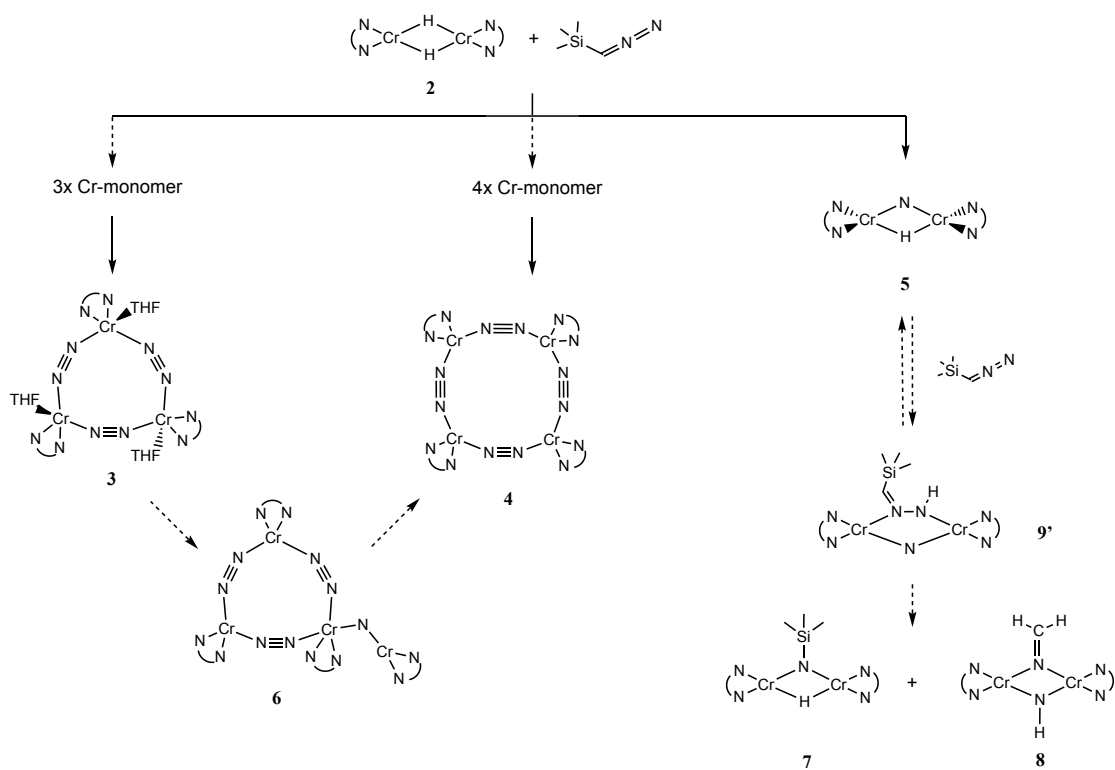
Scheme A.1   Proposed mechanism for reaction of $(L^{Me}Cr)_2(\mu\text{-}H)_2$ (**2**) with trimethylsilyl-diazomethane. Nacnac ligands have been abbreviated, and dashed arrows indicate the potential pathways from one complex to another.

A.2 ^{1}H NMR SPECTRA OF COMPLEXES 3-8

Mixture of products formed from the reaction of $(L^{iPr}Cr)_2(\mu\text{-}H)_2$ (**2**) with 1.0 equiv. of trimethylsilyl-diazomethane were separated by fractional crystallization. In this section, the ^{1}H NMR spectra of crude mixture and the individual product were shown, with their characteristic resonances identified.
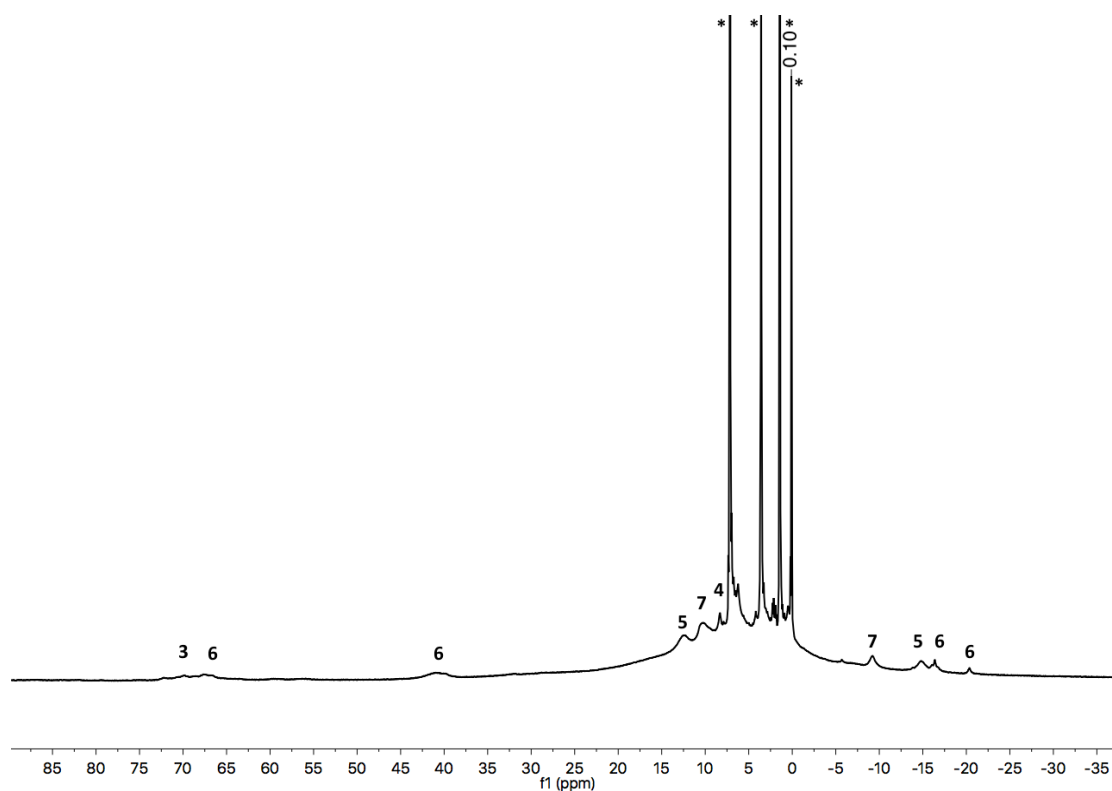
Figure A.1 ^{1}H NMR spectrum of crude products. Asterisks (*) represent solvent signals.
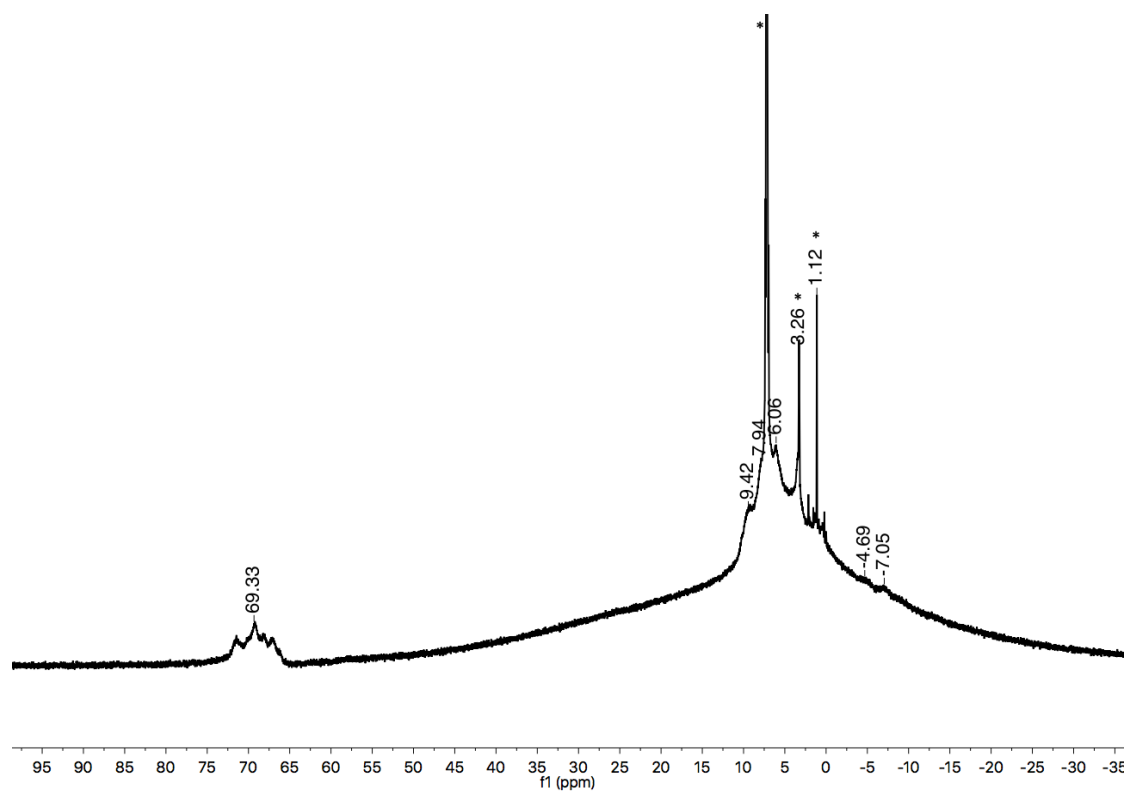
Figure A.2 ^{1}H NMR spectrum of [L^{Me}Cr(THF)]$_3$(μ-N$_2$)$_3$ (**3**). Asterisks (*) represent solvent signals.
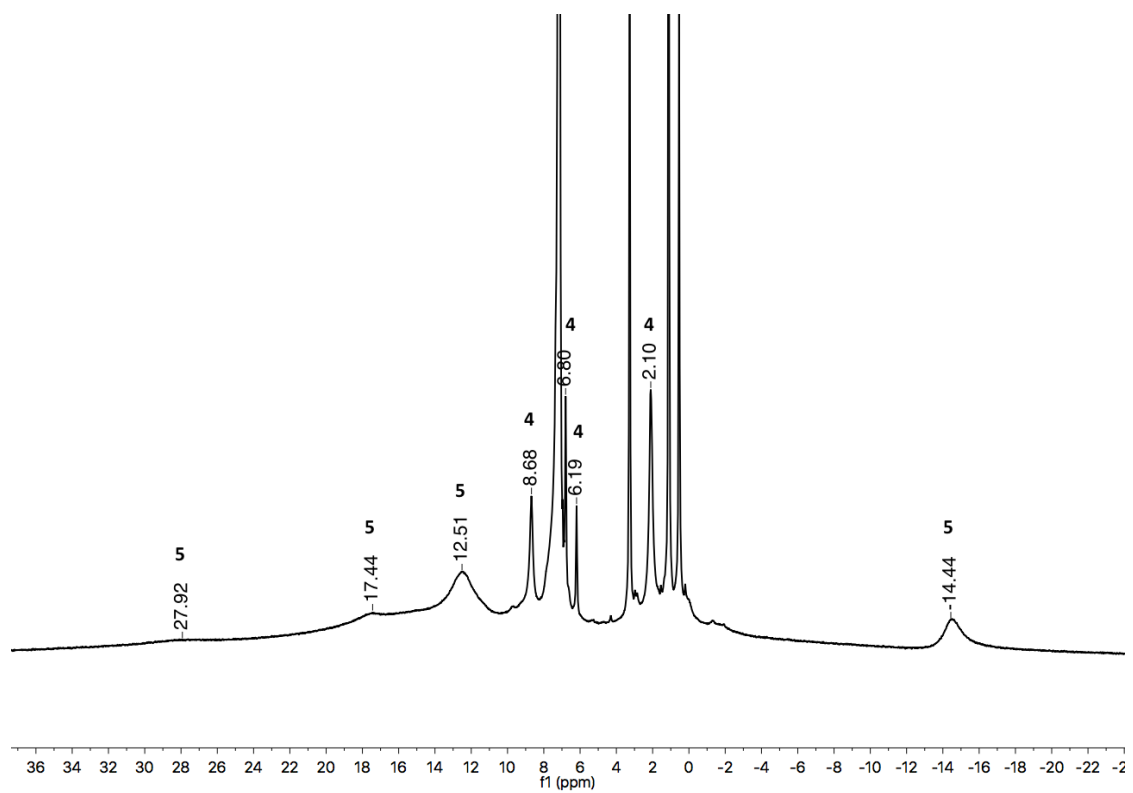
Figure A.3 ^{1}H NMR spectrum of $(L^{Me}Cr)_4(\mu\text{-}N_2)_4$ (**4**) and $(L^{Me}Cr)_2(\mu\text{-}N)(\mu\text{-}H)$ (**5**), with resonances identified.
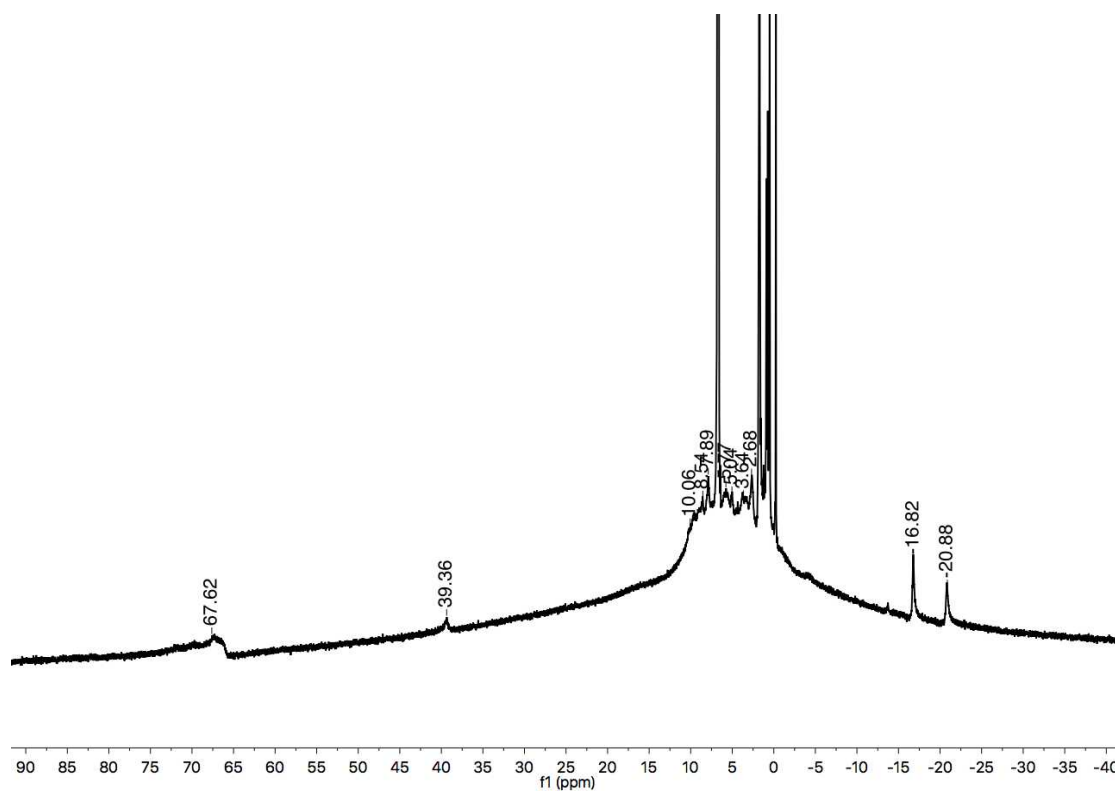
Figure A.4 ^{1}H NMR spectrum of $(L^{Me}Cr)_3(\mu-N_2)_3(\mu-N)CrL^{Me}$ (**6**).
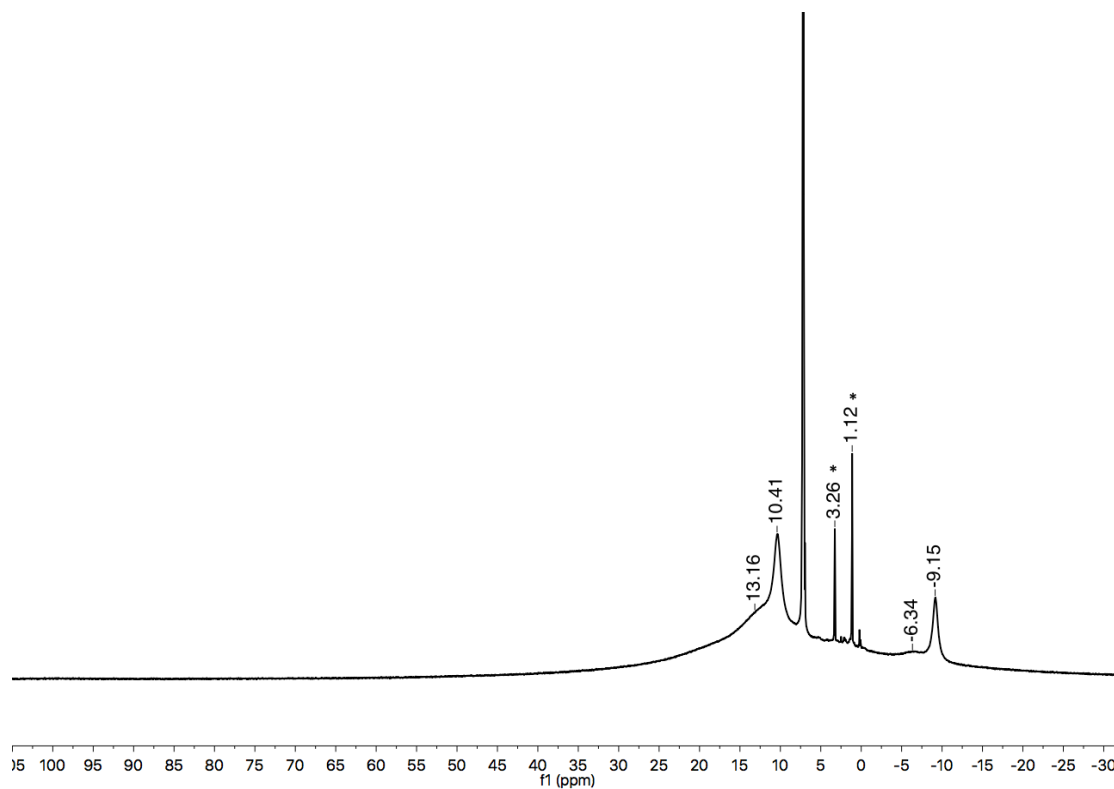
Figure A.5 ^{1}H NMR spectrum of $(L^{Me}Cr)_2(\mu\text{-}NSiMe_3)(\mu\text{-}H)$ (**7**). Asterisks (*) represent solvent signals.
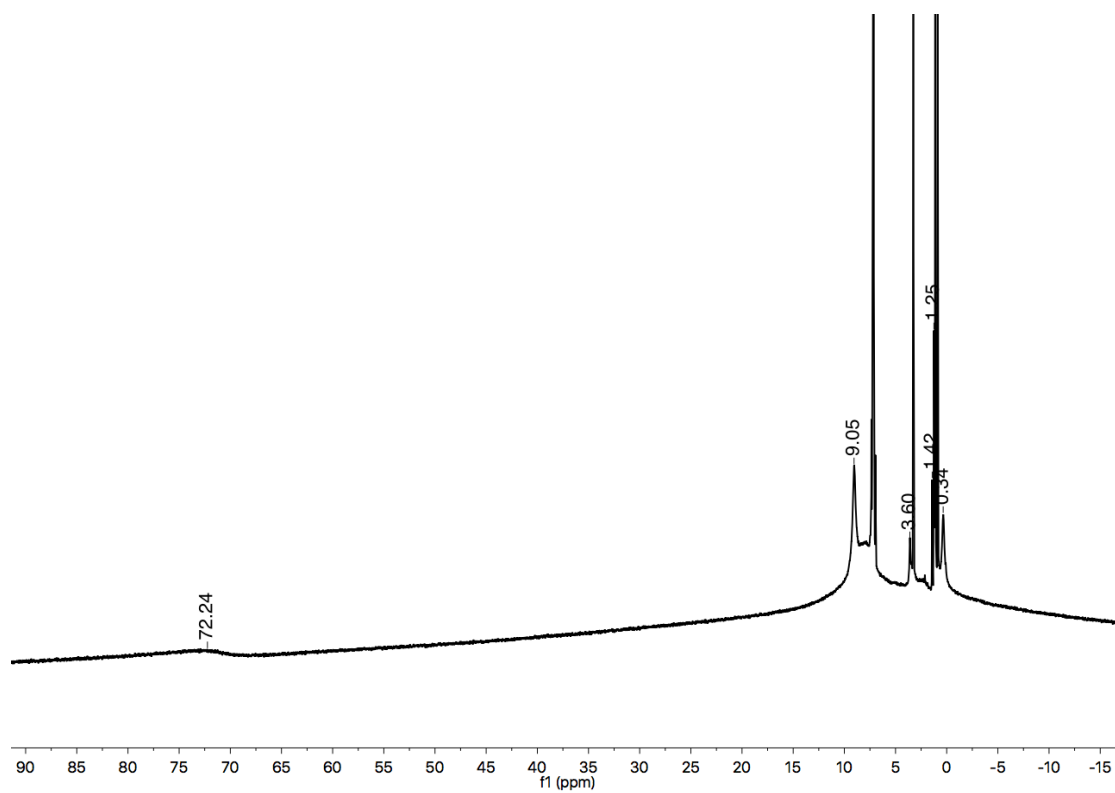
Figure A.6 ^{1}H NMR spectrum of $(L^{Me}Cr)_2(\mu\text{-}NCH_2)(\mu\text{-}NH)$ (**8**)

Appendix B

SUPPLEMENTAL INFORMATION FOR CHAPTER 2

B.1   THERMAL ACTIVATION OF CHROMIUM ALKYL HYDRIDES

To measure the rates of decomposition of chromium alkyl hydrides **1**, **16**, and **17** in benzene-d_6, ^{1}H NMR spectroscopy was employed. Characteristic peaks for alkyl hydrides at 14.7 ppm for **1**, 11.0 ppm for **16**, and 13.7 ppm for **17** represent methyl groups on the nacnac backbones. These experiments were carried out at 80°C (heating in an oil bath) and were monitored by ^{1}H NMR spectroscopy (spectra were taken at room temperature). The following figures (Figure B.1, B.2, and B.3) show ^{1}H NMR spectra of **1** (18.68 mM), **16** (19.06 mM), and **17** (18.59 mM) in benzene-d_6 heated at 80°C for the listed hours.
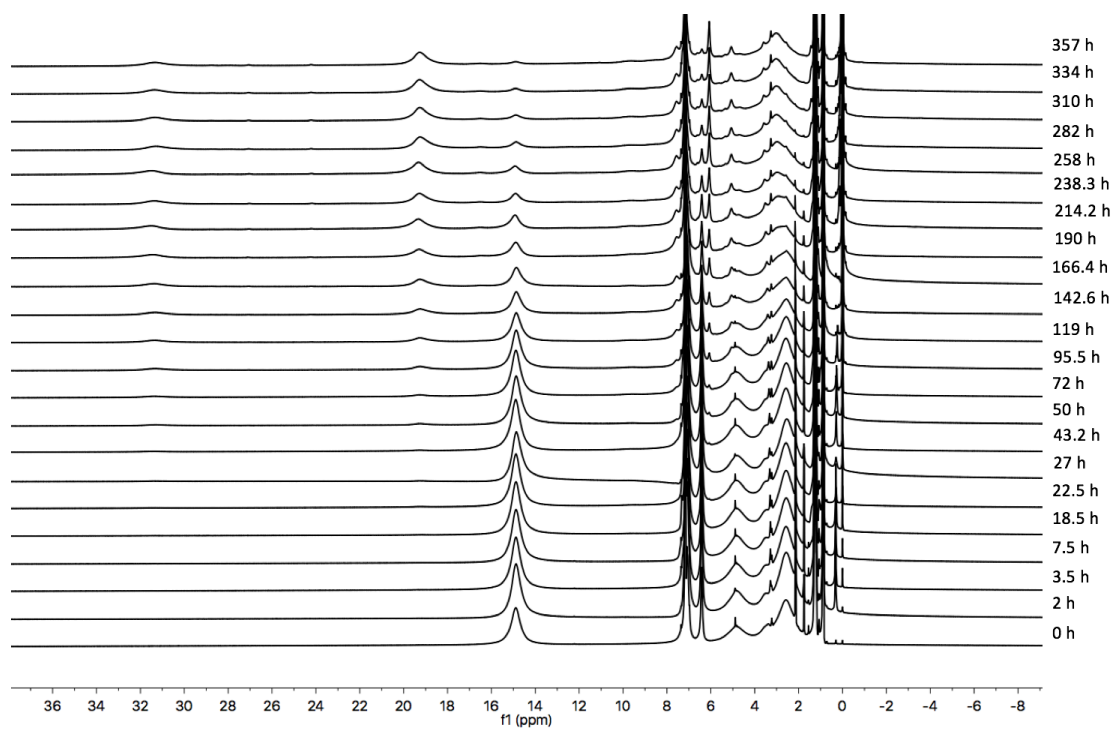
Figure B.1 ^{1}H NMR spectra of **1** in benzene-d$_6$, with the components changing over time at 80°C
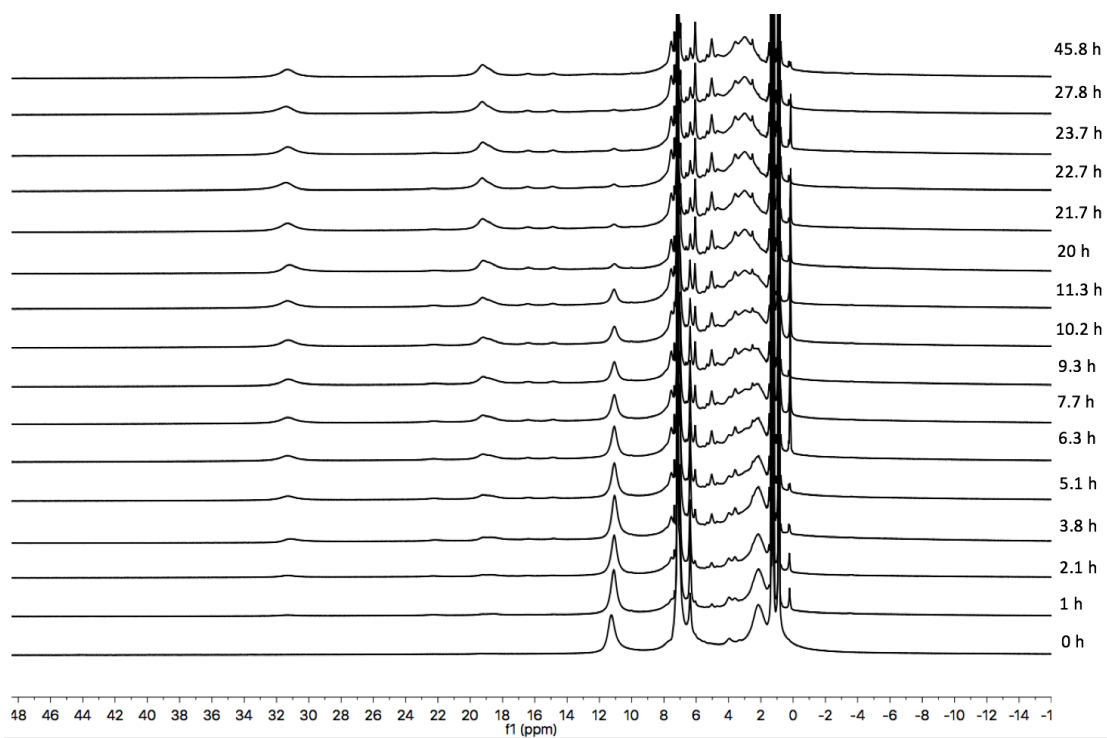
Figure B.2 ^{1}H NMR spectra of **16** in benzene-d$_6$, with the components changing over time at 80°C
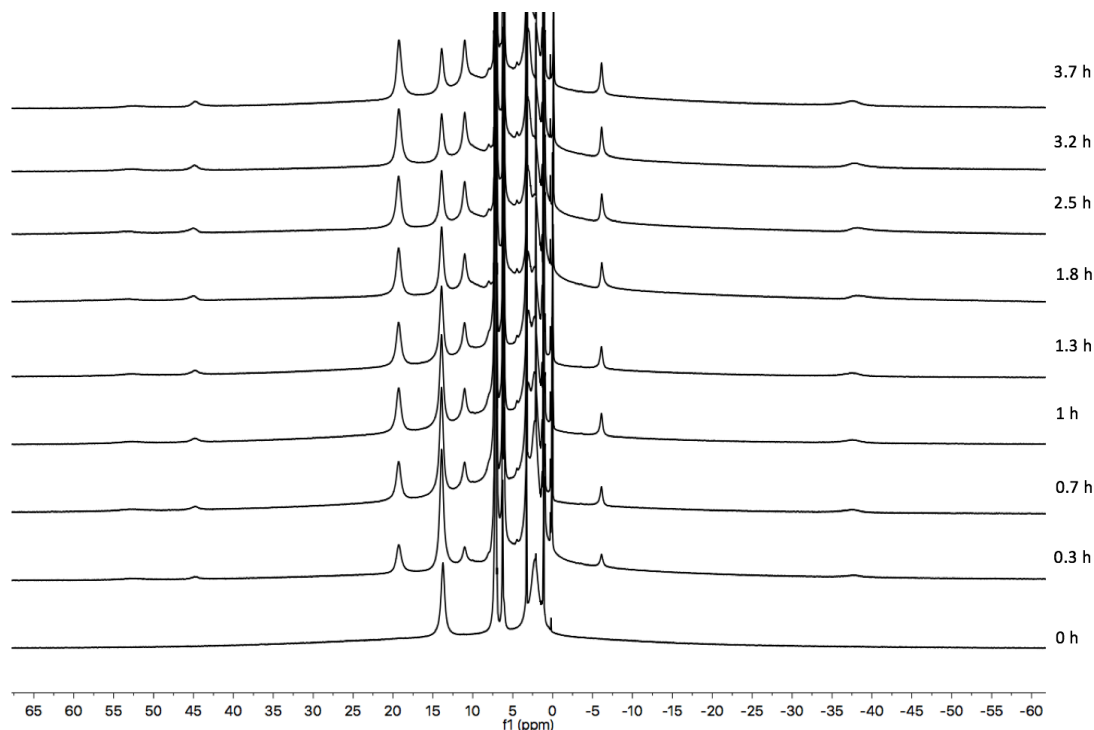
Figure B.3 ^{1}H NMR spectra of **17** in benzene-d$_6$, with the components changing over time at 80°C

By following the disappearance of the proton signals belonging to the alkyl hydride complexes, the rates of the decomposition can be determined. The integration of characteristic resonance relative to benzene-d$_6$ from ^{1}H NMR analysis was obtained. Knowledge of initial concentration was used with the initial ^{1}H NMR spectrum prior to heating; the concentration was divided by the peak area of (14.7 ppm for **1**, 11.0 ppm for **16**, and 13.7 ppm for **17**) to give a scaling factor. All subsequent integrated peak areas were multiplied by the factor to calculate the correspondent concentration. Plots of the concentration versus time were shown in the followings (Figure B.4, B.5, and B.6).
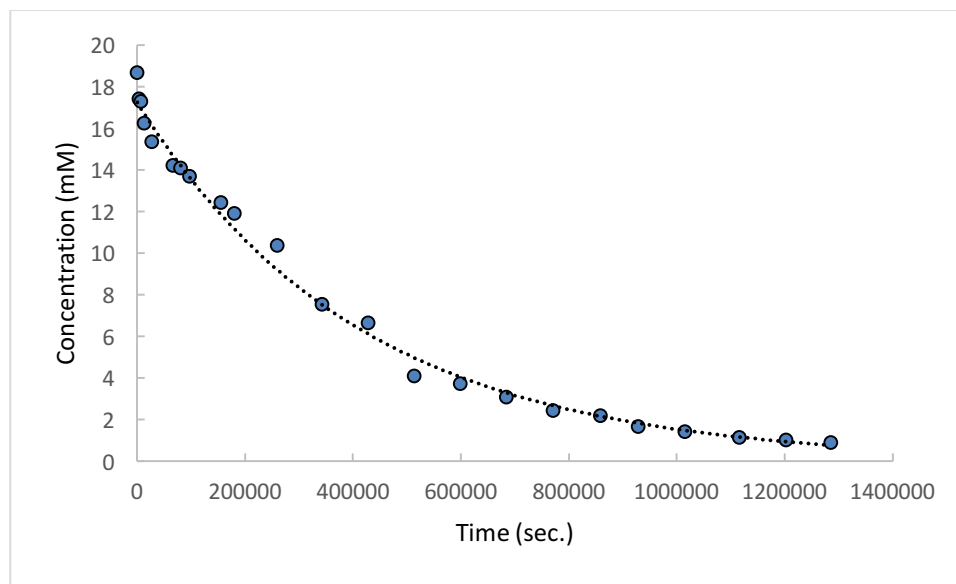
Figure B.4   Decomposition of **1** in benzene-d$_6$ at 80°C, concentration (mM) versus time (second)
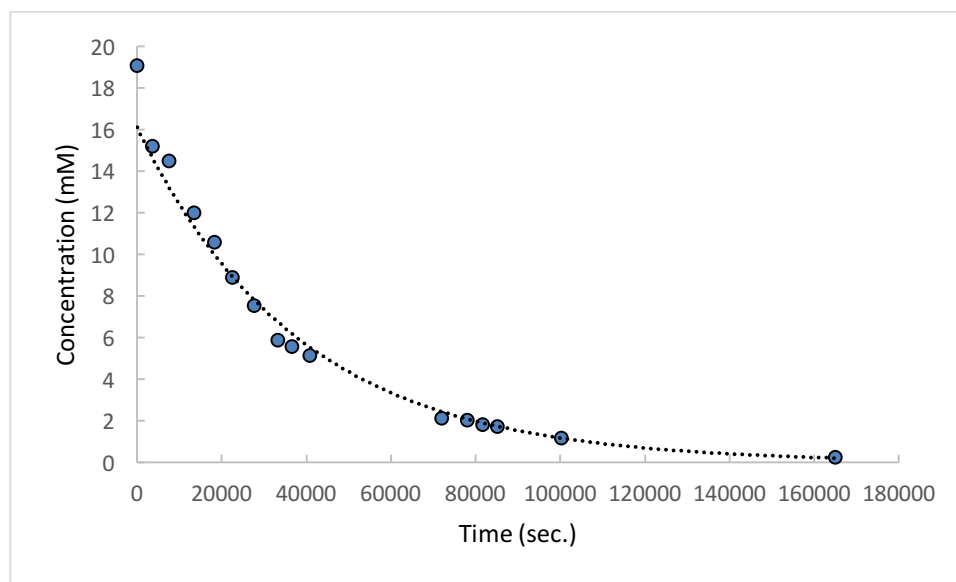
Figure B.5   Decomposition of **16** in benzene-d$_6$ at 80°C, concentration (mM) versus time (second)
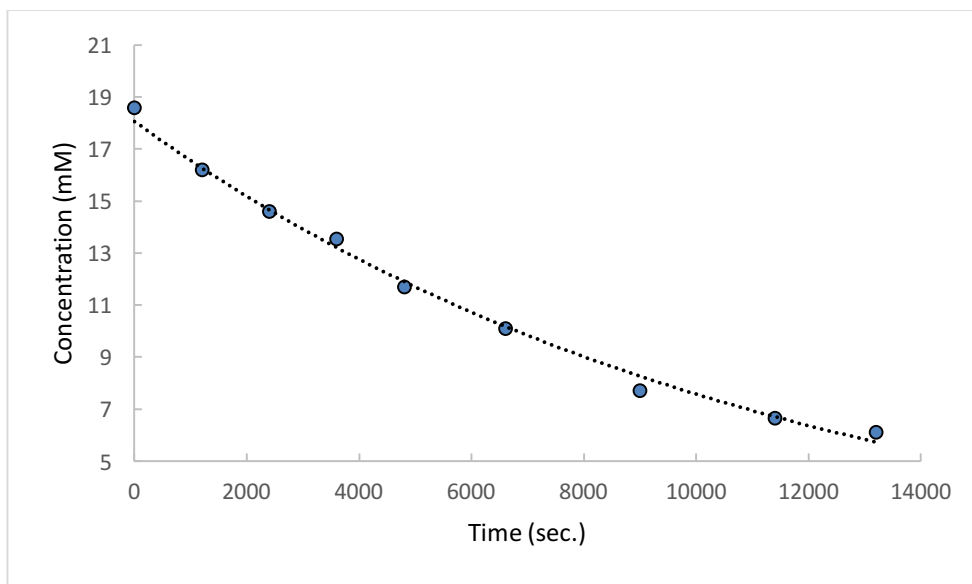
Figure B.6   Decomposition of **17** in benzene-d$_6$ at 80°C, concentration (mM) versus
            time (second)

Plots of the natural logarithm concentration versus time in seconds were shown
in the following figures (Figure B.7, B.8, and B.9). These graphs are linear with the
line of best fit equations shown. The linear relationship suggests the rate of
decomposition for the alkyl hydrides to be a first order reaction.
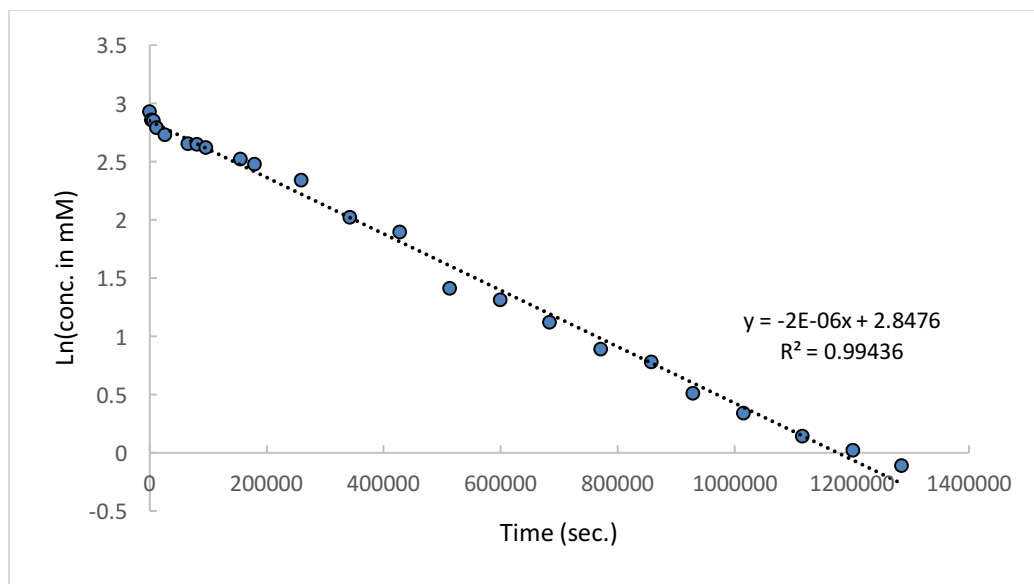
Figure B.7   The first order plot for decomposition of **1** in benzene-d$_6$ at 80°C, Ln(conc. in mM) versus time (second)
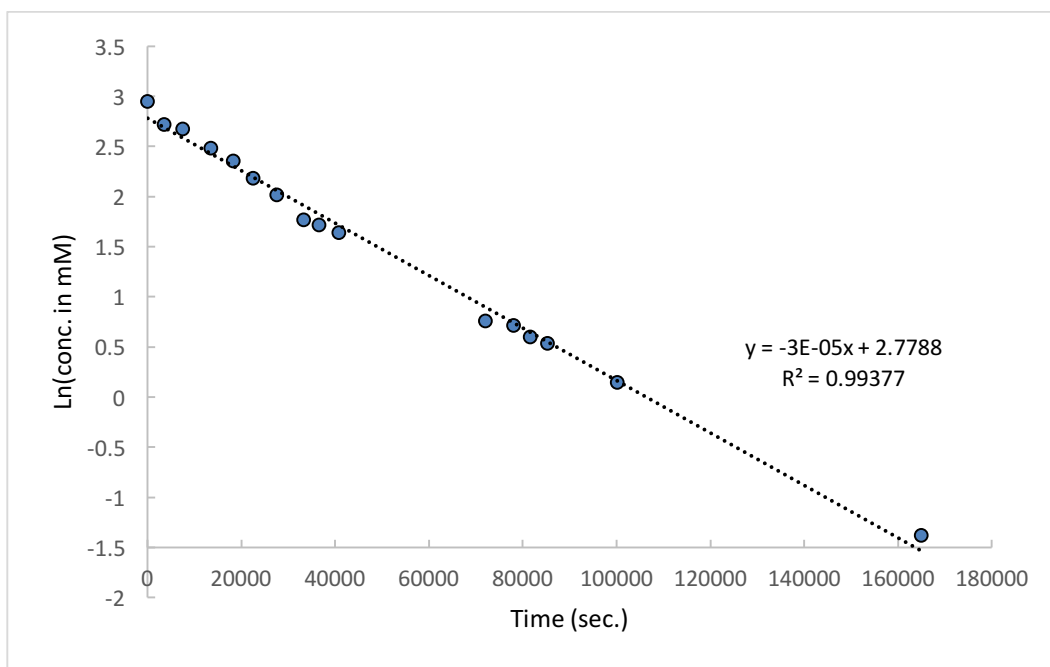
Figure B.8   The first order plot for decomposition of **16** in benzene-d$_6$ at 80°C, Ln(conc. in mM) versus time (second)
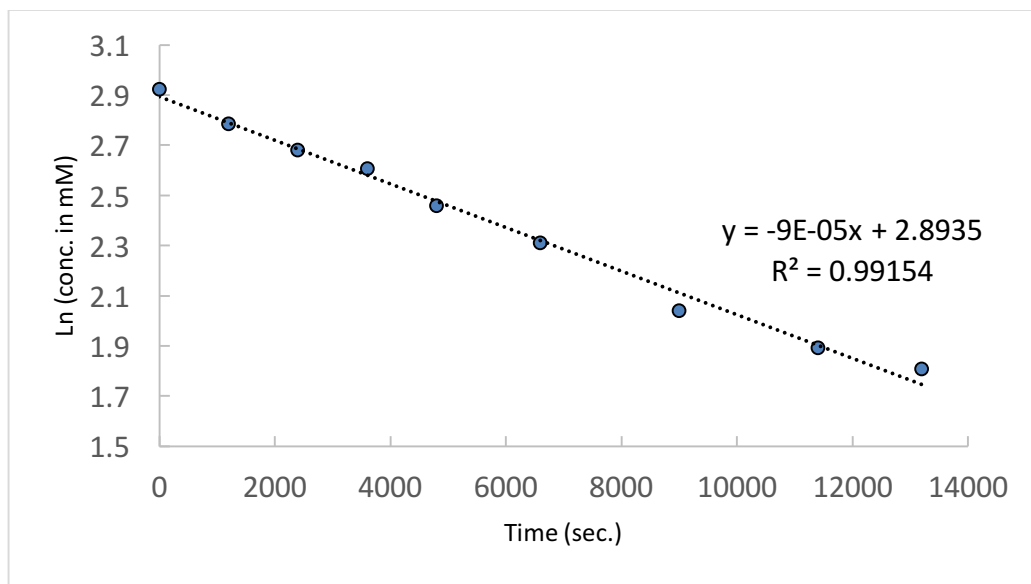
Figure B.9   The first order plot for decomposition of **17** in benzene-d_6 at 80°C, Ln(conc. in mM) versus time (second)

The table below is the comparison of reaction rate constants and half lives of benzene-d_6 reactions of **1**, **16**, and **17** at 80°C.

	1	**16**	**17**
k (s^{-1})	2.40 (5) x10^{-6}	2.62 (6) x10^{-5}	8.7 (3) x10^{-5}
$t_{1/2}$ (h)	80.2	7.3	2.2

Appendix C

SUPPLEMENTAL INFORMATION FOR CHAPTER 3

C.1 PRELIMINARY REACTIVITY STUDIES OF BIS(μ-NITRIDO) COMPLEX 25

($L^{iPr}Cr)_2(\mu\text{-N})_2$ (**25**) has been synthesized and discussed in **Chapter 3**.

Appendix C.1 will focus on preliminary reactivities of **25**. Reactivity studies of **25**

were conducted with small molecules, i. e., H_2, C_2H_4, O_2, and CO on a small scale in a

J. Young NMR tube in C_6D_6. The reactions were analyzed by ^{1}H NMR spectroscopy

and some spectroscopic methods.

Addition of 1atm. of H_2 to **25** at room temperature for 16 hours did not result

in any change, even when harsh condition was applied (80°C for 16 hours). **25** was

unreactive to 1atm. of C_2H_4 at 80°C for 16 hours. However, immediate decomposition

was detected when **25** was exposed to 1atm. of O_2 at room temperature, with the color

changing from orange-red to dark-brown. The potential decomposed products,

($L^{iPr}Cr)_2(\mu\text{-O})_2$ or $L^{iPr}Cr(O)_2$, were excluded by ^{1}H NMR spectroscopy analysis.[1, 2]

Addition of 1atm. of CO to **25** at room temperature for 1 hour had the color

changed to greenish brown. LIFDI mass spectrum taken of the crude products showed

major peaks at m/z: 1022.5573 [M$^+$] and m/z: 511.2827 [M/2$^+$], which match the

predicted isotope patterns of [**25** + 2 CO] (calcd. m/z: 1022.5313 [M$^+$]) and its

fragment, (calcd. m/z: 511.2655 [M/2$^+$]). The product was also inspected by the

infrared spectroscopy. A strong stretching frequency of 2219cm^{-1} features NCO stretching,[3, 4] suggesting the possible formation of (L^{iPr}Cr)$_2$(μ-NCO)$_2$.

In an attempt to produce the hydrogenated version of **25**, hydrogen donating reagents were tested with this complex. 2,4,6-tris-tert-butylphenol (2 equiv.) was unreactive with **25** at 80°C for 24 hours. One equivalent of 9,10-dihydroanthracene was unreactive with **25** at room temperature for 16 hours. Trifluoromethanesulfonic acid (HOTf, 2 equiv.) immediately decomposed **25**, with the color changing from red to dark brown. Hydrogen chloride solution (1M HCl in Et$_2$O) (2 equiv.) decomposed **25**. The ^{1}H NMR spectra of the reactions with HOTf and HCl only showed diamagnetic ligand resonances.

Methyl iodide (2 equiv.) was tested with **25** and the crude products were analyzed with LIFDI spectroscopy, which showed (L^{iPr}Cr)$_2$(μ-I)$_2$ (m/z: 596.5430 [M/2$^+$]) and (L^{iPr}Cr)$_2$(μ-CH$_3$)$_2$ (m/z: 968.3131 [M$^+$]). The fate of the two nitride ligands is unclear.

Tetraethylammonium chloride was tested and the expected outcome would be 0.5 equiv. of (L^{iPr}Cr)$_2$(μ-Cl)$_2$ and 1 equiv. of [L^{iPr}Cr(N)$_2$]$^-$NEt$_4^+$. However, **25** was shown to be unreactive with excess amount of NEt$_4$Cl at 65°C for 2 days.

Excess amount of trimethylsilylchloride was attempted. The reaction was stirred at 65°C for 4 days. The results were analyzed by LIFDI spectroscopy, which showed mixture of products. The mass belonging to the expected nitrido- imido- complex, L^{iPr}Cr(N)(NSiMe$_3$), was not observed.

In order to potentially form the mono-chromium terminal nitrido complex, an additional fourth coordinating ligand was tested. **25** was treated with ligand donors, i.e. pyridine and N-heterocyclic carbene. 4 equiv. of pyridine were added to a diethyl

ether solution of **25** for 16 hours at room temperature and did not lead to any change. However, stirring **25** in pure pyridine for 30 minutes at room temperature had the color changed to light orange. The ^{1}H NMR and the LIFDI mass spectra taken of the crude materials showed ligand L^{iPr} as the only recognizable product. On the other hand, 2 equiv. of ^{iPr}NHC (:C{N(Ar)CH}$_2$, Ar = 2,6-diisopropylphenyl) were added to a THF solution of **25**. The ^{1}H NMR spectrum taken did not show any change even after 24 hours heating at 80°C.

C.2   PRELIMINARY REACTIVITY STUDIES OF COMPLEX 38

With **38** in hand, alkylation was attempted. Chilled THF solutions of **38** were treated with 2 equiv. of $(CH_3)_3SiCH_2MgCl$ and $(CH_3)_3SiCH_2Li$ respectively, both of which resulted in a color change from orange-brown to red in 5 minutes and 30 minutes, respectively. After removing THF, pentane was used to extract the product. The ^1H NMR spectra of crude products of both attempts showed complicated results. Cystallization and isolation of the products were unsuccessful.

In the past, our group has been successful in producing alkylation with the nacnac chromium triflate (trifluoromethanesulfonate) complex.[5] For this reason ligand substitution was then tested, as well as the reaction between **38** and 2 equiv. of AgOTf (Scheme C.1). It resulted in a color change from red-orange to dark brown. After ten minutes, product was isolated and determined to be mononuclear $L^{iPr}Cr(N)O_2SOCF_3$ (**C1**). The molecular structure of **C1** is depicted in Figure C.1, while the corresponding interatomic distances and angles are listed in Table C.1. The Cr≡N distance of 1.546(3) Å is comparable to that in **38**, with Cr≡N 1.587(4) Å.

38, Ar = 2,6-diisopropylphenyl

C1
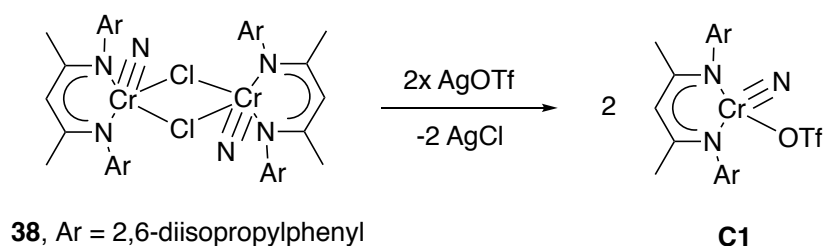
Scheme C.1   Ligand substitution of **38**

With **C1**, alkylating was then proceeded. Addition of 1 equiv. of MeLi (1.6 M in diethyl ether) to a cold Et$_2$O solution of **C1** led to a color change from green to darker green in 5 minutes. After removal of Et$_2$O, pentane was used to extract the product. Crystals were grown from concentrated pentane solution, and the molecular structure of the product (**C2**) was determined by X-ray diffraction. **C2** is a binuclear species consist of two chromiums bridged by a nitrido and a methyl imido ligand, with one methyl group on one of the metal centers. **C2** is analogous to the dimerization product of mononuclear intermediates, as illustrated in Scheme C.2.
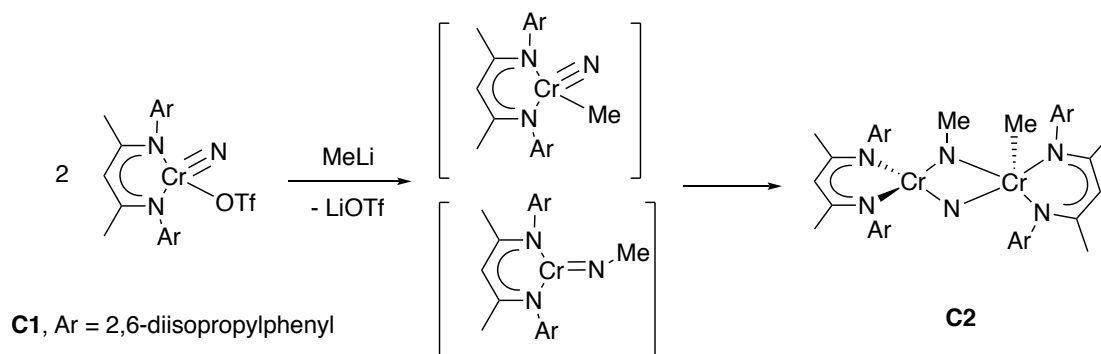
Scheme C.2   The reaction of **C1** with methyllithium

This reaction result shed some light on future focus. It has demonstrated the ability of alkylation by treating the triflate nitrido complex with an alkyl-lithium reagent. It is thus suggested that **C1** will react with an array of alkyl substrates. Migratory insertion process during the reaction was elucidated by the resulting structure **C2**. While the reaction mechanism has not been fully studied, it readily offered a preview of future synthesis.

C.3 SYNTHESIS OF BIS(μ-NITRIDO) COMPLEXES

Approaching bis(μ-nitrido) **32** with the new synthetic strategy described in **Section 3.2.5** was tried. The synthesis is analogous to those with L^{iPr}, which will be described in the experimental part. **C3**, $(L^{Et}Cr\equiv N)_2(\mu\text{-Cl})_2$, was characterized by X-ray diffraction, and is shown in Figure C.3. The $Cr\equiv N$ bond was found to be 1.587(3) Å, consistent with **38** ($Cr\equiv N$ 1.587(4) Å). Magnesium reduction on **C3** gave **32**, which was confirmed by ^1H NMR spectroscopy.

This synthesis was also tried with L^{Me}, which is included in the experimental part. **C4**, $(L^{Me}Cr\equiv N)_2(\mu\text{-Cl})_2$, was characterized and is depicted in Figure C.4. The $Cr\equiv N$ bond distance of 1.553(3) Å is consistent with those in **38** and **C3**. The following reduction on **C4** was unsuccessful with magnesium that has been used in both L^{iPr} and L^{Et} ligand systems. The bis(μ-nitrido) **30** may potentially be produced with a suitable reductant.

C.4 CRYSTAL STRUCTURES

C.4.1 Structure of $L^{iPr}Cr(N)O_2SOCF_3$ (C1)
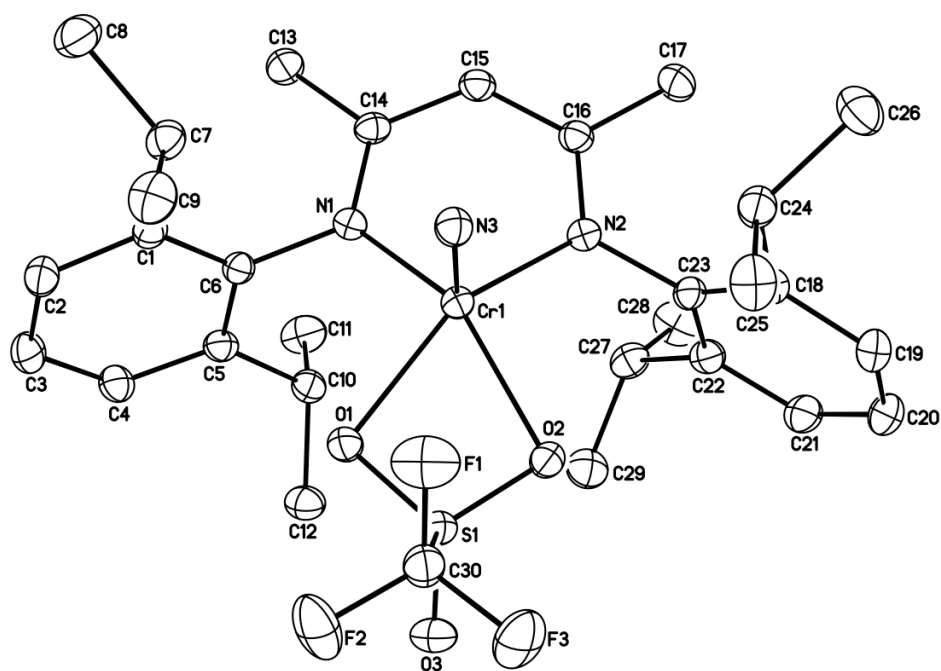
Figure C.1   Molecular structure of $L^{iPr}Cr(N)O_2SOCF_3$ (**C1**). Ellipsoids are drawn at the 20% probability level. All hydrogen atoms have been omitted for clarity.

Table C.1   Interatomic distances (Å) and angles (°) for L^{iPr}Cr(N)O$_2$SOCF$_3$ (**C1**)

Distances (Å)

Cr(1)-N(3)	1.546(3)	C(5)-C(6)	1.406(4)
Cr(1)-N(1)	1.967(3)	C(5)-C(10)	1.519(5)
Cr(1)-N(2)	1.978(3)	C(7)-C(9)	1.522(6)
Cr(1)-O(1)	2.106(2)	C(7)-C(8)	1.529(5)
Cr(1)-O(2)	2.124(2)	C(10)-C(12)	1.526(5)
Cr(1)-S(1)	2.6579(12)	C(10)-C(11)	1.534(6)
S(1)-O(3)	1.415(3)	C(13)-C(14)	1.508(4)
S(1)-O(1)	1.470(2)	C(14)-C(15)	1.399(5)
S(1)-O(2)	1.475(2)	C(15)-C(16)	1.392(5)
S(1)-C(30)	1.834(4)	C(16)-C(17)	1.513(5)
F(1)-C(30)	1.316(5)	C(18)-C(19)	1.395(5)
F(3)-C(30)	1.316(4)	C(18)-C(23)	1.403(5)
F(2)-C(30)	1.312(4)	C(18)-C(24)	1.526(5)
N(1)-C(14)	1.340(4)	C(19)-C(20)	1.378(6)
N(1)-C(6)	1.453(4)	C(20)-C(21)	1.388(6)
N(2)-C(16)	1.336(4)	C(21)-C(22)	1.391(5)
N(2)-C(23)	1.451(4)	C(22)-C(23)	1.413(4)
C(1)-C(2)	1.391(4)	C(22)-C(27)	1.520(5)
C(1)-C(6)	1.411(4)	C(24)-C(25)	1.527(5)
C(1)-C(7)	1.526(4)	C(24)-C(26)	1.533(5)
C(2)-C(3)	1.387(5)	C(27)-C(28)	1.525(6)
C(3)-C(4)	1.375(5)	C(27)-C(29)	1.531(5)
C(4)-C(5)	1.395(5)		

Angles (°)

N(3)-Cr(1)-N(1)	101.71(13)	C(6)-C(5)-C(10)	122.3(3)
N(3)-Cr(1)-N(2)	102.00(13)	C(5)-C(6)-C(1)	121.6(3)
N(1)-Cr(1)-N(2)	91.56(11)	C(5)-C(6)-N(1)	118.7(3)
N(3)-Cr(1)-O(1)	107.11(12)	C(1)-C(6)-N(1)	119.7(3)
N(1)-Cr(1)-O(1)	92.64(9)	C(9)-C(7)-C(1)	110.6(3)
N(2)-Cr(1)-O(1)	149.04(10)	C(9)-C(7)-C(8)	110.3(3)
N(3)-Cr(1)-O(2)	107.81(12)	C(1)-C(7)-C(8)	111.9(3)
N(1)-Cr(1)-O(2)	147.88(10)	C(5)-C(10)-C(12)	112.4(3)

N(2)-Cr(1)-O(2)	94.39(10)	C(5)-C(10)-C(11)	110.9(3)
O(1)-Cr(1)-O(2)	66.99(9)	C(12)-C(10)-C(11)	110.0(3)
N(3)-Cr(1)-S(1)	109.08(10)	N(1)-C(14)-C(15)	122.3(3)
N(1)-Cr(1)-S(1)	123.32(8)	N(1)-C(14)-C(13)	120.5(3)
N(2)-Cr(1)-S(1)	125.16(8)	C(15)-C(14)-C(13)	117.1(3)
O(1)-Cr(1)-S(1)	33.47(6)	C(16)-C(15)-C(14)	127.9(3)
O(2)-Cr(1)-S(1)	33.63(6)	N(2)-C(16)-C(15)	122.6(3)
O(3)-S(1)-O(1)	117.46(16)	N(2)-C(16)-C(17)	119.9(3)
O(3)-S(1)-O(2)	117.66(16)	C(15)-C(16)-C(17)	117.5(3)
O(1)-S(1)-O(2)	104.89(13)	C(19)-C(18)-C(23)	118.1(3)
O(3)-S(1)-C(30)	105.38(17)	C(19)-C(18)-C(24)	119.3(3)
O(1)-S(1)-C(30)	104.88(15)	C(23)-C(18)-C(24)	122.6(3)
O(2)-S(1)-C(30)	105.25(16)	C(20)-C(19)-C(18)	121.2(4)
O(3)-S(1)-Cr(1)	143.34(12)	C(19)-C(20)-C(21)	119.8(3)
O(1)-S(1)-Cr(1)	52.20(9)	C(20)-C(21)-C(22)	121.7(3)
O(2)-S(1)-Cr(1)	52.90(9)	C(21)-C(22)-C(23)	117.4(3)
C(30)-S(1)-Cr(1)	111.28(12)	C(21)-C(22)-C(27)	119.6(3)
S(1)-O(1)-Cr(1)	94.33(11)	C(23)-C(22)-C(27)	123.0(3)
S(1)-O(2)-Cr(1)	93.48(11)	C(18)-C(23)-C(22)	121.7(3)
C(14)-N(1)-C(6)	119.1(3)	C(18)-C(23)-N(2)	120.4(3)
C(14)-N(1)-Cr(1)	122.9(2)	C(22)-C(23)-N(2)	117.9(3)
C(6)-N(1)-Cr(1)	117.20(18)	C(18)-C(24)-C(25)	111.5(3)
C(16)-N(2)-C(23)	119.3(3)	C(18)-C(24)-C(26)	111.2(3)
C(16)-N(2)-Cr(1)	122.5(2)	C(25)-C(24)-C(26)	109.9(3)
C(23)-N(2)-Cr(1)	117.92(19)	C(22)-C(27)-C(28)	112.2(3)
C(2)-C(1)-C(6)	118.2(3)	C(22)-C(27)-C(29)	111.5(3)
C(2)-C(1)-C(7)	118.7(3)	C(28)-C(27)-C(29)	109.9(3)
C(6)-C(1)-C(7)	123.1(3)	F(2)-C(30)-F(3)	108.6(3)
C(3)-C(2)-C(1)	120.8(3)	F(2)-C(30)-F(1)	108.8(3)
C(4)-C(3)-C(2)	120.2(3)	F(3)-C(30)-F(1)	107.3(3)
C(3)-C(4)-C(5)	121.7(3)	F(2)-C(30)-S(1)	110.0(3)
C(4)-C(5)-C(6)	117.5(3)	F(3)-C(30)-S(1)	110.6(3)
C(4)-C(5)-C(10)	120.3(3)	F(1)-C(30)-S(1)	111.5(2)

C.4.2 Structure of L^{iPr}Cr(μ-NMe)(μ-N)(Me)CrL^{iPr} (C2)
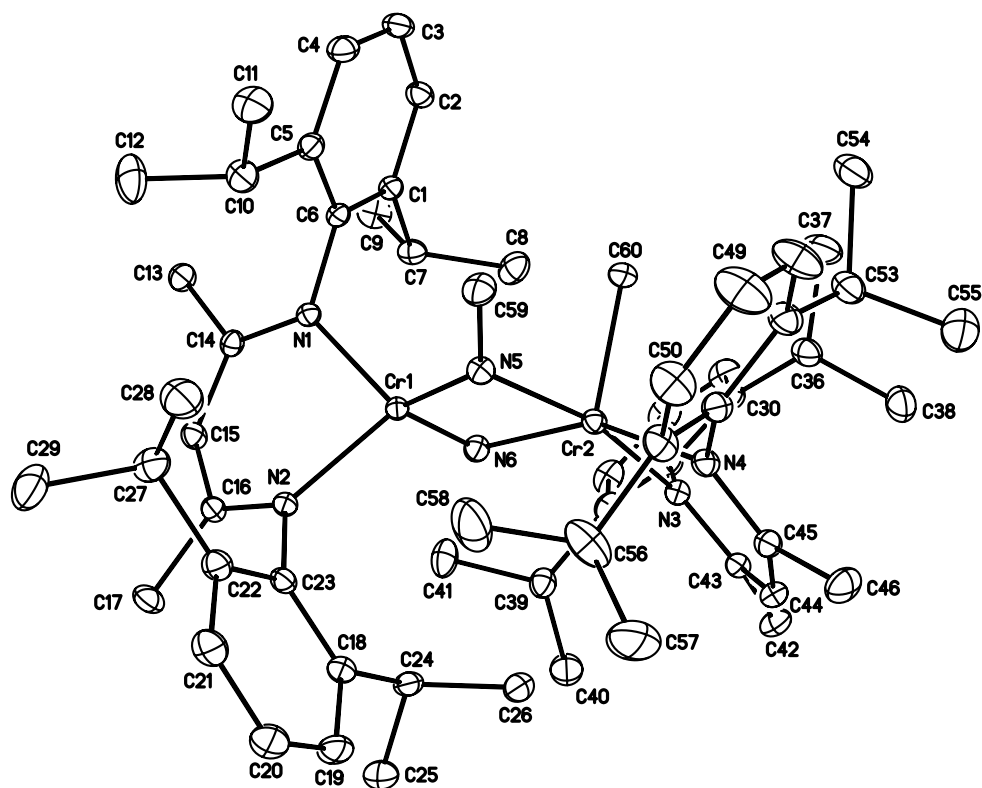
Figure C.2 Molecular structure of L^{iPr}Cr(μ-NMe)(μ-N)(Me)CrL^{iPr} (C2). Ellipsoids are drawn at the 20% probability level. All hydrogen atoms have been omitted for clarity.

Table C.2 Interatomic distances (Å) and angles (º) for $L^{iPr}Cr(\mu\text{-NMe})(\mu\text{-}N)$(Me)CrL^{iPr} (**C2**)

Distances (Å)

Cr(1)-N(6)	1.6311(15)	C(19)-C(20)	1.381(3)
Cr(1)-N(5)	1.7602(15)	C(20)-C(21)	1.376(3)
Cr(1)-N(2)	1.9940(14)	C(21)-C(22)	1.400(3)
Cr(1)-N(1)	2.0042(14)	C(22)-C(23)	1.403(3)
Cr(1)-Cr(2)	2.6707(4)	C(22)-C(27)	1.518(3)
Cr(2)-N(6)	2.0225(16)	C(24)-C(25)	1.526(3)
Cr(2)-N(5)	2.0306(16)	C(24)-C(26)	1.533(3)
Cr(2)-C(60)	2.0588(19)	C(27)-C(28)	1.524(4)
Cr(2)-N(4)	2.0970(15)	C(27)-C(29)	1.535(4)
Cr(2)-N(3)	2.1117(15)	C(30)-C(31)	1.394(3)
N(1)-C(14)	1.330(2)	C(30)-C(35)	1.410(3)
N(1)-C(6)	1.443(2)	C(30)-C(36)	1.523(3)
N(2)-C(16)	1.337(2)	C(31)-C(32)	1.381(4)
N(2)-C(23)	1.446(2)	C(32)-C(33)	1.369(4)
N(3)-C(43)	1.333(2)	C(33)-C(34)	1.401(3)
N(3)-C(35)	1.449(2)	C(34)-C(35)	1.411(3)
N(4)-C(45)	1.339(2)	C(34)-C(39)	1.518(3)
N(4)-C(52)	1.442(2)	C(36)-C(37)	1.532(3)
N(5)-C(59)	1.455(2)	C(36)-C(38)	1.534(3)
C(1)-C(2)	1.392(3)	C(39)-C(41)	1.532(3)
C(1)-C(6)	1.404(2)	C(39)-C(40)	1.539(3)
C(1)-C(7)	1.522(3)	C(42)-C(43)	1.516(3)
C(2)-C(3)	1.379(3)	C(43)-C(44)	1.396(3)
C(3)-C(4)	1.380(3)	C(44)-C(45)	1.389(3)
C(4)-C(5)	1.395(3)	C(45)-C(46)	1.523(3)
C(5)-C(6)	1.408(2)	C(47)-C(52)	1.401(3)
C(5)-C(10)	1.525(3)	C(47)-C(48)	1.403(3)
C(7)-C(8)	1.527(3)	C(47)-C(53)	1.515(3)
C(7)-C(9)	1.532(3)	C(48)-C(49)	1.371(4)
C(10)-C(11)	1.525(3)	C(49)-C(50)	1.369(4)
C(10)-C(12)	1.529(4)	C(50)-C(51)	1.391(3)
C(13)-C(14)	1.512(2)	C(51)-C(52)	1.411(3)
C(14)-C(15)	1.402(3)	C(51)-C(56)	1.516(3)

C(15)-C(16)	1.391(2)	C(53)-C(54)	1.527(3)
C(16)-C(17)	1.513(2)	C(53)-C(55)	1.529(4)
C(18)-C(19)	1.397(3)	C(56)-C(58)	1.484(5)
C(18)-C(23)	1.401(3)	C(56)-C(57)	1.522(6)
C(18)-C(24)	1.520(3)		

Angles (°)

N(6)-Cr(1)-N(5)	98.58(8)	N(2)-C(16)-C(17)	120.06(16)
N(6)-Cr(1)-N(2)	112.51(7)	C(15)-C(16)-C(17)	116.37(16)
N(5)-Cr(1)-N(2)	123.07(7)	C(19)-C(18)-C(23)	118.23(18)
N(6)-Cr(1)-N(1)	109.61(7)	C(19)-C(18)-C(24)	119.19(17)
N(5)-Cr(1)-N(1)	122.08(6)	C(23)-C(18)-C(24)	122.58(16)
N(2)-Cr(1)-N(1)	91.38(6)	C(20)-C(19)-C(18)	121.1(2)
N(6)-Cr(1)-Cr(2)	49.12(5)	C(21)-C(20)-C(19)	120.02(19)
N(5)-Cr(1)-Cr(2)	49.49(5)	C(20)-C(21)-C(22)	121.3(2)
N(2)-Cr(1)-Cr(2)	134.12(4)	C(21)-C(22)-C(23)	117.90(19)
N(1)-Cr(1)-Cr(2)	132.84(4)	C(21)-C(22)-C(27)	119.76(19)
N(6)-Cr(2)-N(5)	78.78(6)	C(23)-C(22)-C(27)	122.34(17)
N(6)-Cr(2)-C(60)	103.92(8)	C(18)-C(23)-C(22)	121.46(17)
N(5)-Cr(2)-C(60)	85.26(7)	C(18)-C(23)-N(2)	120.32(16)
N(6)-Cr(2)-N(4)	152.71(6)	C(22)-C(23)-N(2)	118.19(16)
N(5)-Cr(2)-N(4)	100.62(6)	C(18)-C(24)-C(25)	112.53(17)
C(60)-Cr(2)-N(4)	103.21(8)	C(18)-C(24)-C(26)	109.77(17)
N(6)-Cr(2)-N(3)	88.42(6)	C(25)-C(24)-C(26)	110.66(17)
N(5)-Cr(2)-N(3)	165.92(6)	C(22)-C(27)-C(28)	111.5(2)
C(60)-Cr(2)-N(3)	103.68(7)	C(22)-C(27)-C(29)	112.4(2)
N(4)-Cr(2)-N(3)	88.05(6)	C(28)-C(27)-C(29)	109.5(2)
N(6)-Cr(2)-Cr(1)	37.57(4)	C(31)-C(30)-C(35)	118.6(2)
N(5)-Cr(2)-Cr(1)	41.23(4)	C(31)-C(30)-C(36)	119.5(2)
C(60)-Cr(2)-Cr(1)	97.18(6)	C(35)-C(30)-C(36)	121.87(18)
N(4)-Cr(2)-Cr(1)	134.78(5)	C(32)-C(31)-C(30)	121.3(2)
N(3)-Cr(2)-Cr(1)	125.64(4)	C(33)-C(32)-C(31)	119.5(2)
C(14)-N(1)-C(6)	118.82(14)	C(32)-C(33)-C(34)	122.3(2)
C(14)-N(1)-Cr(1)	122.78(11)	C(33)-C(34)-C(35)	117.6(2)
C(6)-N(1)-Cr(1)	118.03(11)	C(33)-C(34)-C(39)	118.44(19)
C(16)-N(2)-C(23)	116.58(14)	C(35)-C(34)-C(39)	123.94(18)

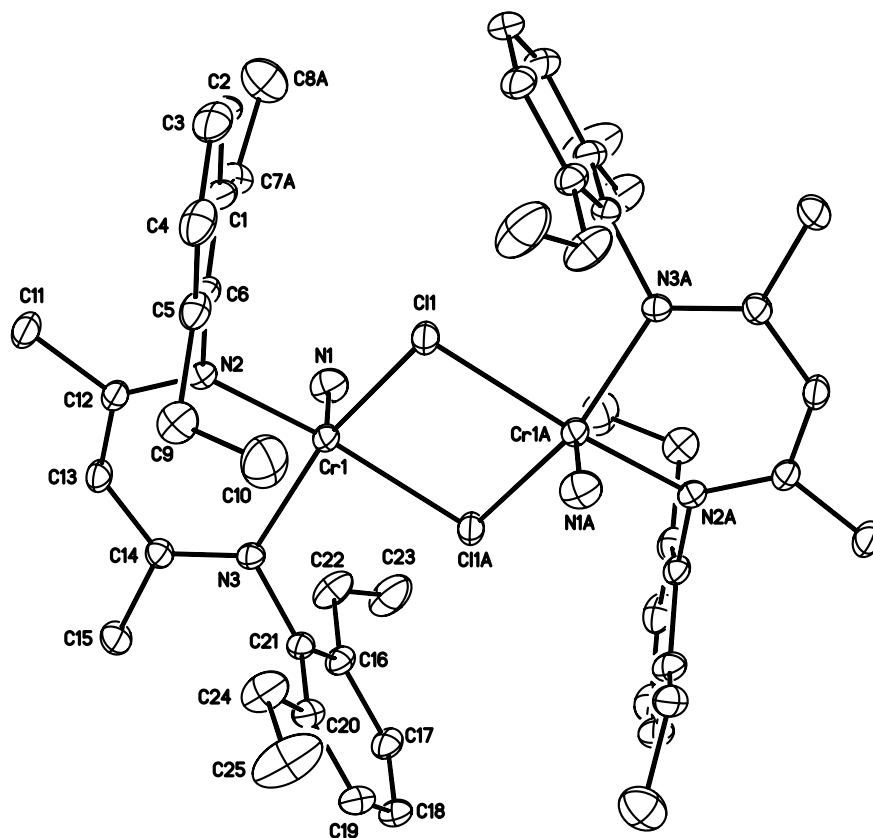|			
C(16)-N(2)-Cr(1)	121.46(12)	C(30)-C(35)-C(34)	120.72(18)
C(23)-N(2)-Cr(1)	121.71(11)	C(30)-C(35)-N(3)	117.49(17)
C(43)-N(3)-C(35)	115.37(15)	C(34)-C(35)-N(3)	121.73(17)
C(43)-N(3)-Cr(2)	123.42(13)	C(30)-C(36)-C(37)	113.1(2)
C(35)-N(3)-Cr(2)	121.20(11)	C(30)-C(36)-C(38)	111.83(18)
C(45)-N(4)-C(52)	115.77(15)	C(37)-C(36)-C(38)	108.9(2)
C(45)-N(4)-Cr(2)	123.79(13)	C(34)-C(39)-C(41)	111.82(19)
C(52)-N(4)-Cr(2)	120.30(12)	C(34)-C(39)-C(40)	111.89(19)
C(59)-N(5)-Cr(1)	134.13(13)	C(41)-C(39)-C(40)	107.63(19)
C(59)-N(5)-Cr(2)	130.40(13)	N(3)-C(43)-C(44)	123.90(17)
Cr(1)-N(5)-Cr(2)	89.29(7)	N(3)-C(43)-C(42)	121.23(17)
Cr(1)-N(6)-Cr(2)	93.32(7)	C(44)-C(43)-C(42)	114.86(16)
C(2)-C(1)-C(6)	117.85(17)	C(45)-C(44)-C(43)	128.69(17)
C(2)-C(1)-C(7)	118.10(16)	N(4)-C(45)-C(44)	124.17(17)
C(6)-C(1)-C(7)	123.99(16)	N(4)-C(45)-C(46)	121.59(18)
C(3)-C(2)-C(1)	121.52(18)	C(44)-C(45)-C(46)	114.22(17)
C(2)-C(3)-C(4)	119.92(18)	C(52)-C(47)-C(48)	117.8(2)
C(3)-C(4)-C(5)	121.31(18)	C(52)-C(47)-C(53)	122.6(2)
C(4)-C(5)-C(6)	117.81(18)	C(48)-C(47)-C(53)	119.5(2)
C(4)-C(5)-C(10)	121.16(18)	C(49)-C(48)-C(47)	121.3(2)
C(6)-C(5)-C(10)	121.00(17)	C(50)-C(49)-C(48)	120.3(2)
C(1)-C(6)-C(5)	121.56(16)	C(49)-C(50)-C(51)	121.4(3)
C(1)-C(6)-N(1)	120.01(15)	C(50)-C(51)-C(52)	118.2(2)
C(5)-C(6)-N(1)	118.43(15)	C(50)-C(51)-C(56)	118.7(2)
C(1)-C(7)-C(8)	111.75(18)	C(52)-C(51)-C(56)	123.07(19)
C(1)-C(7)-C(9)	110.65(16)	C(47)-C(52)-C(51)	121.02(19)
C(8)-C(7)-C(9)	109.58(18)	C(47)-C(52)-N(4)	119.40(19)
C(5)-C(10)-C(11)	113.34(18)	C(51)-C(52)-N(4)	119.56(17)
C(5)-C(10)-C(12)	111.7(2)	C(47)-C(53)-C(54)	113.1(2)
C(11)-C(10)-C(12)	109.4(2)	C(47)-C(53)-C(55)	111.4(2)
N(1)-C(14)-C(15)	122.93(15)	C(54)-C(53)-C(55)	109.1(2)
N(1)-C(14)-C(13)	121.32(16)	C(58)-C(56)-C(51)	114.6(3)
C(15)-C(14)-C(13)	115.75(16)	C(58)-C(56)-C(57)	107.3(3)
C(16)-C(15)-C(14)	127.91(16)	C(51)-C(56)-C(57)	112.0(3)
N(2)-C(16)-C(15)	123.55(16)		

Figure C.3   Molecular structure of (L^{Et}Cr≡N)_2(μ-Cl)_2 (**C3**). Ellipsoids are drawn at the 20% probability level. All hydrogen atoms have been omitted for clarity.

Table C.3   Interatomic distances (Å) and angles (°) for $(L^{Et}Cr\equiv N)_2(\mu\text{-}Cl)_2$ (**C3**)

Distances (Å)

Cr(1)-N(1)	1.587(3)	C(5)-C(9)	1.520(5)
Cr(1)-N(3)	2.004(2)	C(7A)-C(8A)	1.46(2)
Cr(1)-N(2)	2.014(2)	C(9)-C(10)	1.496(6)
Cr(1)-Cl(1)	2.3351(9)	C(11)-C(12)	1.509(4)
Cr(1)-Cl(1)A	2.3683(9)	C(12)-C(13)	1.392(4)
Cl(1)-Cr(1)A	2.3684(9)	C(13)-C(14)	1.390(4)
N(2)-C(12)	1.332(4)	C(14)-C(15)	1.510(4)
N(2)-C(6)	1.449(4)	C(16)-C(21)	1.398(5)
N(3)-C(14)	1.329(4)	C(16)-C(17)	1.396(4)
N(3)-C(21)	1.452(4)	C(16)-C(22)	1.509(5)
C(1)-C(7A)	1.38(2)	C(17)-C(18)	1.377(6)
C(1)-C(2)	1.400(5)	C(18)-C(19)	1.369(6)
C(1)-C(6)	1.403(5)	C(19)-C(20)	1.397(5)
C(1)-C(7B)	1.587(10)	C(20)-C(21)	1.394(5)
C(2)-C(3)	1.374(7)	C(20)-C(24)	1.509(5)
C(3)-C(4)	1.366(7)	C(22)-C(23)	1.436(6)
C(4)-C(5)	1.398(5)	C(24)-C(25)	1.447(7)
C(5)-C(6)	1.392(5)		

Angles (°)

N(1)-Cr(1)-N(3)	101.27(15)	C(5)-C(6)-C(1)	122.1(3)
N(1)-Cr(1)-N(2)	98.75(14)	C(5)-C(6)-N(2)	118.5(3)
N(3)-Cr(1)-N(2)	89.81(10)	C(1)-C(6)-N(2)	119.5(3)
N(1)-Cr(1)-Cl(1)	103.91(14)	C(1)-C(7A)-C(8A)	123.6(15)
N(3)-Cr(1)-Cl(1)	154.43(8)	C(10)-C(9)-C(5)	113.4(4)
N(2)-Cr(1)-Cl(1)	90.72(7)	N(2)-C(12)-C(13)	123.4(3)
N(1)-Cr(1)-Cl(1)A	101.60(13)	N(2)-C(12)-C(11)	120.2(3)
N(3)-Cr(1)-Cl(1)A	90.06(7)	C(13)-C(12)-C(11)	116.3(3)
N(2)-Cr(1)-Cl(1)A	159.26(8)	C(12)-C(13)-C(14)	127.3(3)
Cl(1)-Cr(1)-Cl(1)A	80.63(3)	N(3)-C(14)-C(13)	123.3(3)
Cr(1)-Cl(1)-Cr(1)A	99.37(3)	N(3)-C(14)-C(15)	119.9(3)
C(12)-N(2)-C(6)	116.7(2)	C(13)-C(14)-C(15)	116.7(3)
C(12)-N(2)-Cr(1)	122.4(2)	C(21)-C(16)-C(17)	117.2(3)

C(6)-N(2)-Cr(1)	120.28(18)	C(21)-C(16)-C(22)	121.1(3)
C(14)-N(3)-C(21)	116.7(2)	C(17)-C(16)-C(22)	121.6(3)
C(14)-N(3)-Cr(1)	123.2(2)	C(18)-C(17)-C(16)	121.4(3)
C(21)-N(3)-Cr(1)	119.64(18)	C(19)-C(18)-C(17)	119.8(3)
C(7A)-C(1)-C(2)	116.2(8)	C(18)-C(19)-C(20)	121.7(4)
C(7A)-C(1)-C(6)	125.1(8)	C(21)-C(20)-C(19)	117.2(3)
C(2)-C(1)-C(6)	117.3(4)	C(21)-C(20)-C(24)	120.2(3)
C(3)-C(2)-C(1)	121.2(4)	C(19)-C(20)-C(24)	122.6(3)
C(4)-C(3)-C(2)	120.4(3)	C(20)-C(21)-C(16)	122.6(3)
C(3)-C(4)-C(5)	121.2(4)	C(20)-C(21)-N(3)	118.1(3)
C(6)-C(5)-C(4)	117.8(4)	C(16)-C(21)-N(3)	119.3(3)
C(6)-C(5)-C(9)	122.0(3)	C(23)-C(22)-C(16)	119.7(3)
C(4)-C(5)-C(9)	120.1(3)	C(25)-C(24)-C(20)	119.6(4)

C.4.4 Structure of $(L^{Me}Cr\equiv N)_2(\mu\text{-Cl})_2$ (C4)

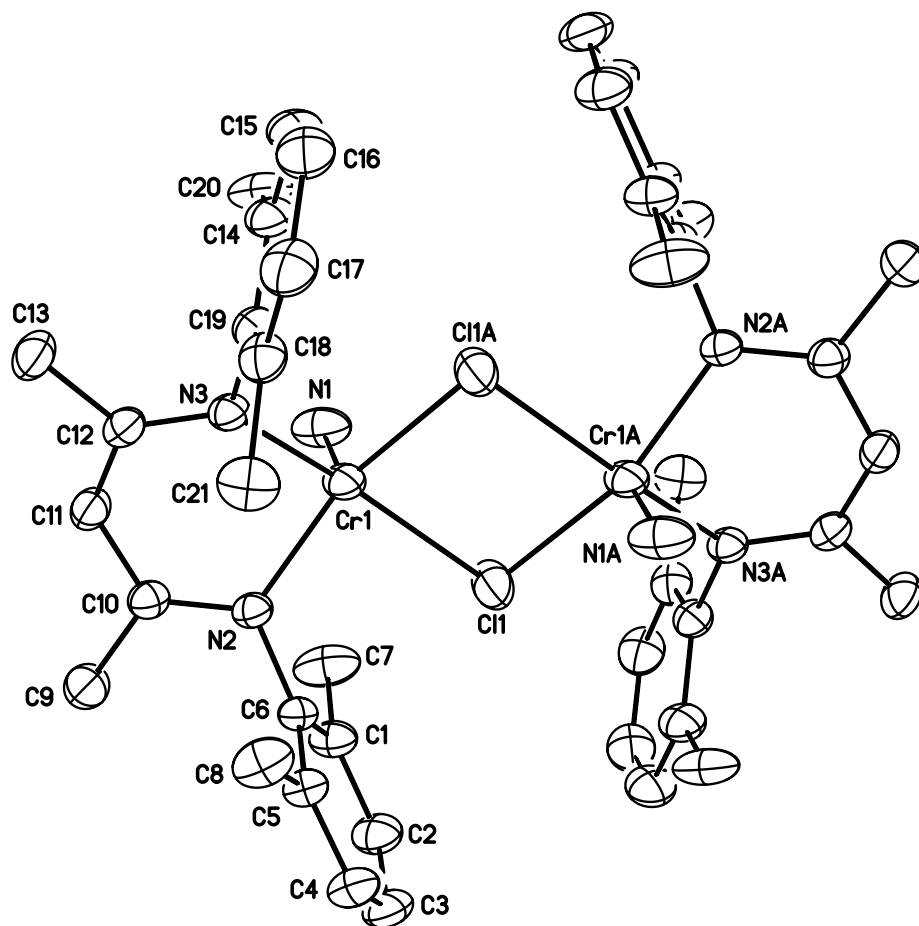
Figure C.4   Molecular structure of $(L^{Me}Cr\equiv N)_2(\mu\text{-Cl})_2$ (**C4**). Ellipsoids are drawn at the 30% probability level. All hydrogen atoms have been omitted for clarity.

Table C.4   Interatomic distances (Å) and angles (°) for (L^{Me}Cr≡N)$_2$(μ-Cl)$_2$ (**C4**)

Distances (Å)

Cr(1)-N(1)	1.553(3)	C(4)-C(5)	1.396(5)
Cr(1)-N(3)	2.000(2)	C(5)-C(6)	1.396(4)
Cr(1)-N(2)	2.002(3)	C(5)-C(8)	1.495(5)
Cr(1)-Cl(1)	2.3385(11)	C(9)-C(10)	1.505(5)
Cr(1)-Cl(1)A	2.3433(12)	C(10)-C(11)	1.404(4)
Cl(1)-Cr(1)A	2.3433(12)	C(11)-C(12)	1.403(5)
N(2)-C(10)	1.328(4)	C(12)-C(13)	1.504(4)
N(2)-C(6)	1.448(4)	C(14)-C(15)	1.398(5)
N(3)-C(12)	1.327(4)	C(14)-C(19)	1.402(5)
N(3)-C(19)	1.453(4)	C(14)-C(20)	1.502(6)
C(1)-C(6)	1.388(4)	C(15)-C(16)	1.372(6)
C(1)-C(2)	1.388(5)	C(16)-C(17)	1.370(6)
C(1)-C(7)	1.505(5)	C(17)-C(18)	1.398(5)
C(2)-C(3)	1.375(5)	C(18)-C(19)	1.383(5)
C(3)-C(4)	1.369(5)	C(18)-C(21)	1.498(5)

Angles (°)

N(1)-Cr(1)-N(3)	100.07(14)	C(4)-C(5)-C(8)	120.4(3)
N(1)-Cr(1)-N(2)	99.77(15)	C(6)-C(5)-C(8)	121.5(3)
N(3)-Cr(1)-N(2)	89.71(10)	C(1)-C(6)-C(5)	120.8(3)
N(1)-Cr(1)-Cl(1)	104.48(13)	C(1)-C(6)-N(2)	120.8(3)
N(3)-Cr(1)-Cl(1)	155.19(9)	C(5)-C(6)-N(2)	118.3(3)
N(2)-Cr(1)-Cl(1)	89.65(8)	N(2)-C(10)-C(11)	122.8(3)
N(1)-Cr(1)-Cl(1)A	104.80(14)	N(2)-C(10)-C(9)	120.8(3)
N(3)-Cr(1)-Cl(1)A	89.35(8)	C(11)-C(10)-C(9)	116.4(3)
N(2)-Cr(1)-Cl(1)A	155.19(9)	C(12)-C(11)-C(10)	126.0(3)
Cl(1)-Cr(1)-Cl(1)A	81.03(4)	N(3)-C(12)-C(11)	123.0(3)
Cr(1)-Cl(1)-Cr(1)A	98.97(4)	N(3)-C(12)-C(13)	120.0(3)
C(10)-N(2)-C(6)	117.6(2)	C(11)-C(12)-C(13)	116.9(3)
C(10)-N(2)-Cr(1)	120.2(2)	C(15)-C(14)-C(19)	117.6(4)
C(6)-N(2)-Cr(1)	121.57(19)	C(15)-C(14)-C(20)	120.6(4)
C(12)-N(3)-C(19)	116.6(2)	C(19)-C(14)-C(20)	121.9(3)
C(12)-N(3)-Cr(1)	120.9(2)	C(16)-C(15)-C(14)	121.0(4)

C(19)-N(3)-Cr(1)	121.9(2)	C(17)-C(16)-C(15)	120.4(4)
C(6)-C(1)-C(2)	118.8(3)	C(16)-C(17)-C(18)	120.9(4)
C(6)-C(1)-C(7)	121.8(3)	C(19)-C(18)-C(17)	118.1(4)
C(2)-C(1)-C(7)	119.4(3)	C(19)-C(18)-C(21)	121.2(3)
C(3)-C(2)-C(1)	121.3(3)	C(17)-C(18)-C(21)	120.7(4)
C(4)-C(3)-C(2)	119.2(3)	C(18)-C(19)-C(14)	122.0(3)
C(3)-C(4)-C(5)	121.7(3)	C(18)-C(19)-N(3)	119.0(3)
C(4)-C(5)-C(6)	118.1(3)	C(14)-C(19)-N(3)	119.0(3)

C.5 EXPERIMENTAL

C.5.1 General Considerations

All manipulations were carried out with standard Schlenk, vacuum line, and glovebox techniques. Pentane and diethyl ether were degassed and dried by passing through activated alumina. Tetrahydrofuran was distilled from purple Na benzophenone/ketyl solutions. THF-d_8 and C_6D_6 was predried with sodium and stored under vacuum over Na/K alloy. NaN_3 was purchased from Aldrich. $CrCl_3(THF)_3$ was prepared according to a literature procedure.[6] All other reagents were purchased from Aldrich or Fisher/Acros and dried using standard procedures when necessary.

^{1}H NMR spectra were taken on a Bruker AVIII-400 spectrometer and were referenced to the residual protons of the solvent (C_6D_6, 7.15 ppm, THF-d_8 = 3.58 and 1.73 ppm). FT-IR spectra were obtained using a Nicolet Magna-IR 560 spectrometer with a resolution of 4 cm^{-1}. X-ray crystallographic studies were conducted at the University of Delaware X-ray Crystallography Laboratory. Mass spectra were obtained by the University of Delaware Mass Spectrometry Facility. Solution phase magnetic susceptibilities were determined by ^{1}H NMR spectroscopy via Evans method [7] in C_6D_6 with C_6D_6 as an internal reference and reported after appropriate diamagnetic corrections. The photochemical reactor was from Rayonet Model RPR100, equipped with 16 14W monochromatic 254nm low-pressure mercury vapor lamps.

C.5.2 Preparation of L^{iPr}Cr(N)O$_2$SOCF$_3$ (C1)

(L^{iPr}Cr≡N)$_2$(μ-Cl)$_2$ (**38**) (see **Chapter 3**) (0.10g, 0.096mmol) was dissolved in 15mL THF giving a red-orange solution. Silver trifluoromethanesulfonate (0.025g, 0.192mmol) was added and the solution stirred at room temperature for 10 minutes, during which time the color gradually changed to dark brown. The THF was then removed in vacuo and the residue was extracted with cold Et$_2$O and the extract filtered through celite. The solution was then concentrated to 4mL and cooled to -30°C overnight to yield green crystals of **C1** (0.06g, 50% yield). ^{1}H NMR (400 MHz, C$_6$D$_6$): 5.94 (br), 3.57 (br), 1.49 (br), 0.29 (br) ppm. IR (KBr): 3063 (w), 2968 (s), 2927 (w), 2869 (w), 1531 (s), 1466 (m), 1440 (m), 1385 (s), 1360 (s), 1316 (s), 1256 (m), 1202 (s), 1175 (w), 1120 (m), 1104 (w), 1056 (w), 1013 (s), 1000 (s), 938 (w), 802 (m), 762 (m), 644 (m) cm^{-1}. μ_{eff} (293K in solution state by Evans method) = 1.7(1) μ_B. Mp: 190°C. Mass Spectrum m/z (%): 632.6345 (100) [M$^+$]. Calcd. m/z: 632.2227 [M$^+$].

C.5.3   Preparation of L^{iPr}Cr(μ-NMe)(μ-N)(Me)CrL^{iPr} (C2)

C1 (0.150 g, 0.237 mmol) was dissolved in 16 mL of Et$_2$O and cooled to -30°C. 0.148 mL of methyllithium (1.6 M in diethyl ether, 0.237 mmol) was added dropwise. The color of the solution gradually changed to dark green in 5 minutes. The Et$_2$O solvent was evaporated and the residue was extracted with pentane and the extract filtered through celite. The solution was concentrated to 8 mL and cooled to -30°C overnight to yield green crystals of **C2** (0.060 g, 51% yield). ^{1}H NMR (400 MHz, C$_6$D$_6$): 65.0 (br), 37.3 (br), 20.2 (br), 9.45 (br), 4.03 (br), 2.11 (br) ppm. IR (KBr): 3055 (w), 2962 (s), 2926 (w), 2868 (m), 1526 (s), 1463 (m), 1433 (m), 1384 (s), 1315 (s), 1255 (m), 1175 (m), 1103 (m), 1023 (m), 933 (m), 793 (m), 761 (m) cm^{-1}. μ_{eff}

(293K in solution state by Evans method) = 4.8(1) μ_B. Mp: 228°C. Mass Spectrum m/z (%): 996.5096 [M$^+$]. Calcd. m/z: 996.5884 [M$^+$].

C.5.4 Alternative preparation of (L^{Et}Cr)$_2$(μ-N)$_2$ (32)

Step 1. L^{Et}(H) (2.00 g, 5.52 mmol) was dissolved in 50 mL of THF and cooled to -30°C. 2.2 mL of n-butyllithium (2.5 M in hexanes, 5.52 mmol) was slowly added to this solution and allowed to stir for 1 hour. The THF solution of L^{Et}(Li) prepared *in situ* was then slowly added over 1 hour at room temperature to a slurry of CrCl$_3$(THF)$_3$ (2.07 g, 5.52 mmol) in 150 mL of THF. The color of the solution changed from purple to red-brown. After stirring at room temperature overnight, the THF was removed in vacuo and the solid was extracted with toluene and the extract filtered through celite. The toluene was then removed and the solid redissolved in THF and cooled to -30°C. A dark red powder was isolated by filtration and collected, which was L^{Et}CrCl$_2$(THF)$_2$ (2.60 g, 75%). ^{1}H NMR (400 MHz, C$_6$D$_6$): 39.4 (vb, 6H), 13.5 (br), 10.3 (br), 3.62 (b, 8H), 1.46 (b, 8H), -4.6 (br) ppm. IR (KBr): 3055 (w), 2962 (s), 2918 (w), 2864 (w), 1526 (s), 1458 (m), 1381 (s), 1261 (m), 1244 (w), 1177 (s), 1097 (w), 1018 (s), 917 (w), 880 (m), 849 (m), 763 (s) cm^{-1}. μ_{eff} (293K) = 4.4(1) μ_B. Mp: 129°C. Mass Spectrum m/z (%): 483.1376 (60) [M$^+$ - 2 THF]. Calcd. m/z: 483.1427 [M$^+$ - 2 THF].

Step 2. L^{Et}CrCl$_2$(THF)$_2$ (0.500 g, 0.795 mmol) was dissolved in 30 mL THF giving a red solution. 1 equivalent of NaN$_3$ (0.052 g) were added. The solution was stirred for 4 hours during which time the color changed to red-brown. The THF was then removed in vacuo and the residue was extracted with cold Et$_2$O and the extract filtered through celite. The resulting solution was concentrated to 8 mL then cooled to -30°C overnight to yield brown-red solids of (L^{Et}CrCl)$_2$(μ-N$_3$)$_2$ (0.277 g, 71%). ^{1}H NMR (400 MHz, C$_6$D$_6$): 35.3 (br), 28.7 (br), 13.1 (br), 11.2 (br), 10.02 (br), 3.55 (br),

2.49 (br), 1.37 (br), -1.41 (br) ppm. IR (KBr): 3058 (w), 2966 (s), 2924 (s), 2875 (w), 2145 (s), 2057 (s), 1524 (s), 1458 (m), 1442 (m), 1383 (s), 1261 (m), 1180 (s), 1098 (w), 1022 (s), 853 (s), 805 (m), 766 (s) cm^{-1}. Mass Spectrum m/z (%): 490.1999 (66) [M$^+$/2]. Calcd. m/z: 490.1830 [M$^+$/2].

Step 3. (L^{Et}CrCl)$_2$(μ-N$_3$)$_2$ (0.300 g) was dissolved in 60 mL THF giving a red-brown solution. The solution was transferred into a quartz ampule and was stirred for 20 hours while being irradiated with 254nm UV light, during which time the color gradually changed to brown. The ampoule was then brought back into glovebox where the THF solution was removed in vacuo and the residue was extracted with cold Et$_2$O and the extract filtered through celite. The resulting solution was concentrated to 6 mL, then cooled to -30°C overnight to yield dark red solids of (L^{Et}Cr≡N)$_2$(μ-Cl)$_2$ (**C3**) (0.205 g, 73% yield). ^{1}H NMR (400 MHz, C$_6$D$_6$): 10.97 (br), 8.11 (br), 5.35 (br), 3.74 (br), 0.56 (br), -1.11 (br) ppm.

Step 4. (L^{Et}Cr≡N)$_2$(μ-Cl)$_2$ (**C3**) (0.150 g, 0.162 mmol) was dissolved in 15 mL THF, giving a red-orange solution. Magnesium turnings (0.025g, 1.042 mmol) were added and the solution stirred at room temperature for 3.5 hours, during which time the color gradually changed to orange-brown. The THF was then removed in vacuo and the residue was extracted with cold Et$_2$O and filtered through celite. The Et$_2$O solution was then concentrated to 4 mL and cooled to -30°C overnight to yield red crystals of **32** (0.093 g, 67% yield). ^{1}H NMR (400 MHz, C$_6$D$_6$): 100.8 (br), 60.6 (br), 12.74 (br), 7.99 (br), 3.48 (br), 1.36 (br), -12.5 (br) ppm.

C.5.5 Preparation of (L^{Me}Cr≡N)$_2$(μ-Cl)$_2$ (C4)

Step 1. L^{Me}CrCl$_2$(THF)$_2$ [8] (0.500 g, 0.874 mmol) was dissolved in 30 mL THF giving a red solution. 1 equivalent of NaN$_3$ (0.057 g) was added. The solution was

stirred for 4 hours during which time the color changed to brown. The THF was then removed in vacuo and the residue was extracted with Et_2O and the extract filtered through celite. The resulting solution was concentrated to 10 mL then cooled to -30°C overnight to yield brown solids of $(L^{Me}CrCl)_2(\mu\text{-}N_3)_2$ (0.230 g, 61%). ^1H NMR (400 MHz, THF-d_8): 42.8 (br), 33.3 (br), 15.9 (br), 11.8 (br), 10.17 (br), 7.36 (br), -1.52 (br) ppm. IR (KBr): 3050 (w), 2965 (s), 2923 (s), 2871 (w), 2155 (s), 2062 (s), 1524 (s), 1445 (m), 1385 (s), 1261 (w), 1181 (s), 1093 (w), 1022 (s), 859 (s), 766 (s) cm^{-1}. Mass Spectrum m/z (%): 434.1248 (100) [M^+/2]. Calcd. m/z: 434.1204 [M^+/2].

Step 2. $(L^{Me}CrCl)_2(\mu\text{-}N_3)_2$ (0.300 g) was dissolved in 60 mL THF giving a red-brown solution. The solution was transferred into a quartz ampule and was stirred for 20 hours while being irradiated with 254nm UV light, during which time the color gradually changed to orange-brown. The ampoule was then brought back into glovebox where the THF solution was removed in vacuo and the residue was extracted with Et_2O and the extract filtered through celite. The resulting solution was concentrated to 8 mL, then cooled to -30°C overnight to yield red solids of $(L^{Me}Cr\equiv N)_2(\mu\text{-}Cl)_2$ (**C3**) (0.150 g, 54%). ^1H NMR (400 MHz, THF-d_8): 10.7 (br), 9.50 (br), 7.85 (br), 7.26 (br), 2.27 (br), 0.83 (br) ppm. Mass Spectrum m/z (%): 406.1225 (100) [M^+/2]. Calcd. m/z: 406.1143 [M^+/2].

Table C.5	C1	C2
	kla0933	**kla0944**
Formula	$C_{30}H_{41}CrF_3N_3O_3S$	$C_{60}H_{88}Cr_2N_6$
Formula wt., g/mol	632.72	997.36
Temp, K	200(2)	200(2)
Wavelength, Å	1.54184	1.54178
Crystal size, mm	0.161 x 0.195 x 0.250	0.460 x 0.477 x 0.545
Color	green	green
Crystal system	monoclinic	monoclinic
Space group	$P\,2_1/n$	$P\,2_1/c$
a, Å	12.462(4)	13.9635(4)
b, Å	15.016(4)	13.4640(4)
c, Å	18.286(5)	37.2965(10)
α, deg	90	90
β, deg	108.730(8)	100.0340(10)
γ, deg	90	90
Volume, $Å^3$	3240.6(17)	6904.7(3)
Z	4	4
D(calcd), g/cm^3	1.297	0.959
Abs. coefficient, mm^{-1}	3.94	2.844
T_{max}/T_{min}	0.7539/0.5947	0.7539/0.5409
Data/restraints/params	6633/0/380	14250/0/635
GOF on F^2	1.19	1.033
Final R indices, I>2σ(I)	R1 = 0.0747, wR^2 = 0.2161	R1 = 0.0456, wR^2 = 0.1301
R indices (all data)	R1 = 0.0825, wR^2 = 0.2305	R1 = 0.0496, wR^2 = 0.1334

Table C.6	C3 kla0924	C4 kla0936
Formula	$C_{50}H_{66}Cl_2Cr_2N_6$	$C_{42}H_{50}Cl_2Cr_2N_6$
Formula wt., g/mol	925.98	813.78
Temp, K	200(2)	200(2)
Wavelength, Å	0.71073	1.54178
Crystal size, mm	0.410 x 0.436 x 0.524	0.118 x 0.237 x 0.241
Color	red	red-green
Crystal system	monoclinic	triclinic
Space group	$P\,2_1/n$	$P\,\bar{1}$
a, Å	13.6667(6)	8.7099(2)
b, Å	12.7105(5)	10.9471(2)
c, Å	14.8113(6)	12.4424(3)
α, deg	90	88.2800(10)
β, deg	109.2900(10)	81.8710(10)
γ, deg	90	79.4870(10)
Volume, Å^3	2428.43(17)	1154.71(4)
Z	2	1
D(calcd), g/cm^3	1.266	1.17
Abs. coefficient, mm^{-1}	0.597	5.19
T_{max}/T_{min}	0.7456/0.6847	0.7539/0.5162
Data/restraints/params	5633/0/285	4545/0/241
GOF on F^2	1.042	1.067
Final R indices, I>2σ(I)	R1 = 0.0654, wR^2 = 0.1754	R1 = 0.0575, wR^2 = 0.1619
R indices (all data)	R1 = 0.0839, wR^2 = 0.1952	R1 = 0.0766, wR^2 = 0.1792

REFERENCES

1.   Monillas, W. H.; Yap, G. P. A.; MacAdams, L. A.; Theopold, K. H., *J. Am. Chem. Soc.* **2007,** *129* (26), 8090.

2.   Dai, F.; Yap, G.; Theopold, K., *J. Am. Chem. Soc.* **2013,** *135* (45), 16774.

3.   Duggan, D. M.; Hendrickson, D. N., *Inorg. Chem.* **1974**, 2056.

4.   Derossi, S.; Farrell, D.; Harding, C.; Mckee, V.; Nelson, J., *Dalton Trans.* **2007,** (18), 1762.

5.   Young, J.; MacAdams, L.; Yap, G.; Theopold, K., *Inorg. Chim. Acta.* **2010,** *364* (1), 138.

6.   Shamir, J., *Inorg. Chem. Acta.* **1989,** *156* (2), 163.

7.   Evans, D., *J. Chem. Soc.* **1959**, 2003.

8.   Kim, W.; Fevola, M.; Liable-Sands, L.; Rheingold, A.; Theopold, K., *Organometallics* **1998,** *17* (21), 4541.